SUPPORTING THE DEVELOPMENT OF

AN IRRIGATION STRATEGY FOR SERBIA

IRRIGATION ATLAS OF SERBIA

Prepared: Thalès de Haulleville

November 2021

Contents

Figures

Land & People

1. Topography

This section will present the topography of the Republic of Serbia: the distribution of elevation and slopes throughout the country. The data was provided by NASA / USGS / JPL-Caltech (Farr et al., 2007).

Elevation

The distribution of elevation of the Republic of Serbia is presented in Figure 1.

Figure 1 – Distribution of elevation in the Republic of Serbia.
Elevation given above sea level (a.s.l.). ***Data source:*** *NASA / USGS / JPL-Caltech (Farr et al., 2007).*

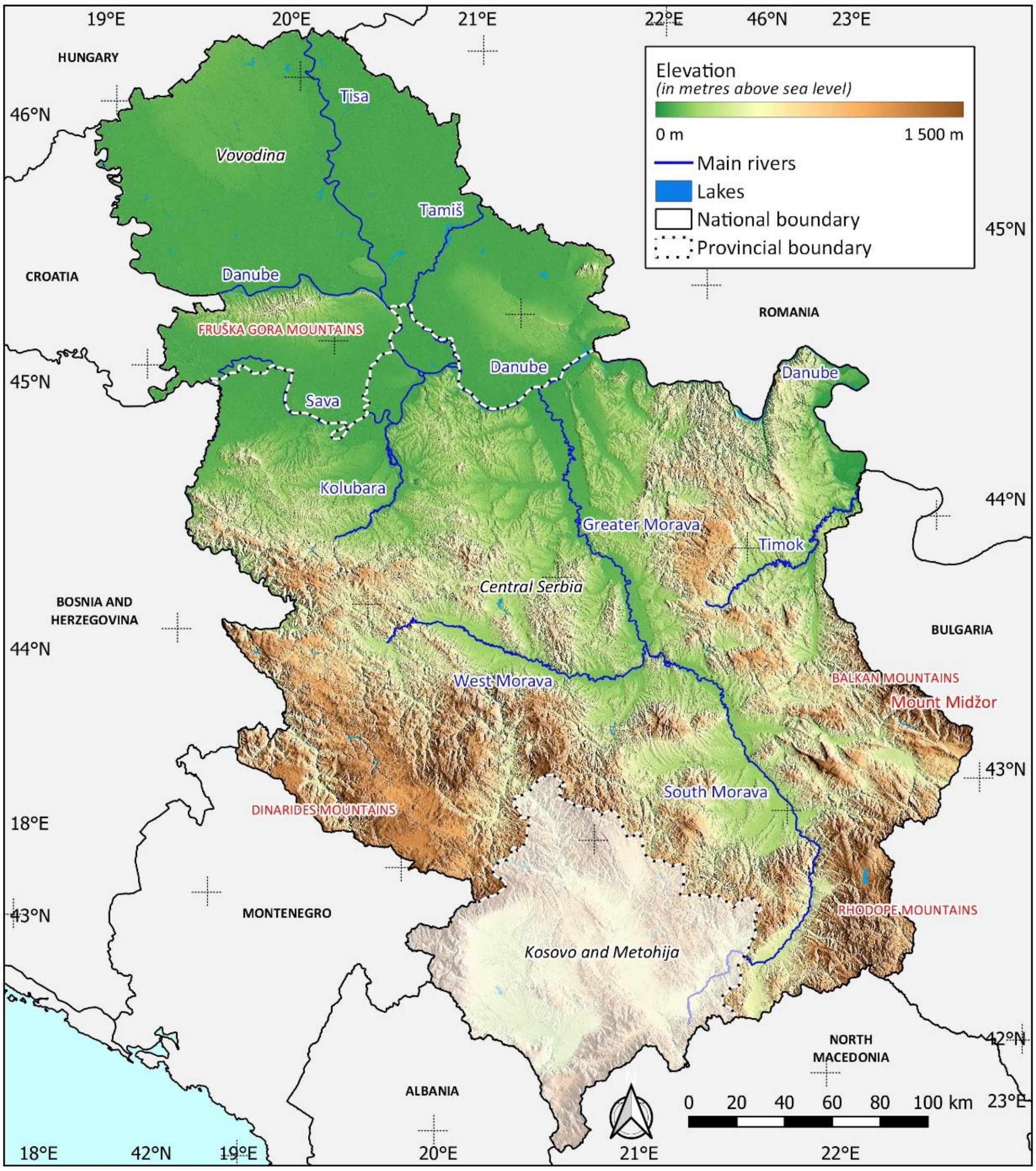

The elevation levels in the Republic of Serbia are distributed between 17 m above sea level (a.s.l.), in the plains of Vojvodina, and 2164 m a.s.l., on top of the mount Midžor, at the border with Bulgaria in the Balkan Mountain range, Southeast of the country.

The country can be divided based on its topography in two distinct regions: North of the Sava-Danube axis (around the 44.7°N parallel), lies the plains of the Vojvodina province, while South of these rivers stands the highlands of the rest of the country. In the North, the leveled topography is only broken by the Fruška Gora Mountain range, whereas the highlands of the South are cleaved by the three Morava valleys: The Greater Morava, the West Morava, and the South Morava.

Slope

The distribution of the topographic slopes of the Republic of Serbia is presented in Figure 2.

Figure 2 - Distribution of the topographic slope of the Republic of Serbia.
***Data source:** NASA / USGS / JPL-Caltech (Farr et al., 2007).*

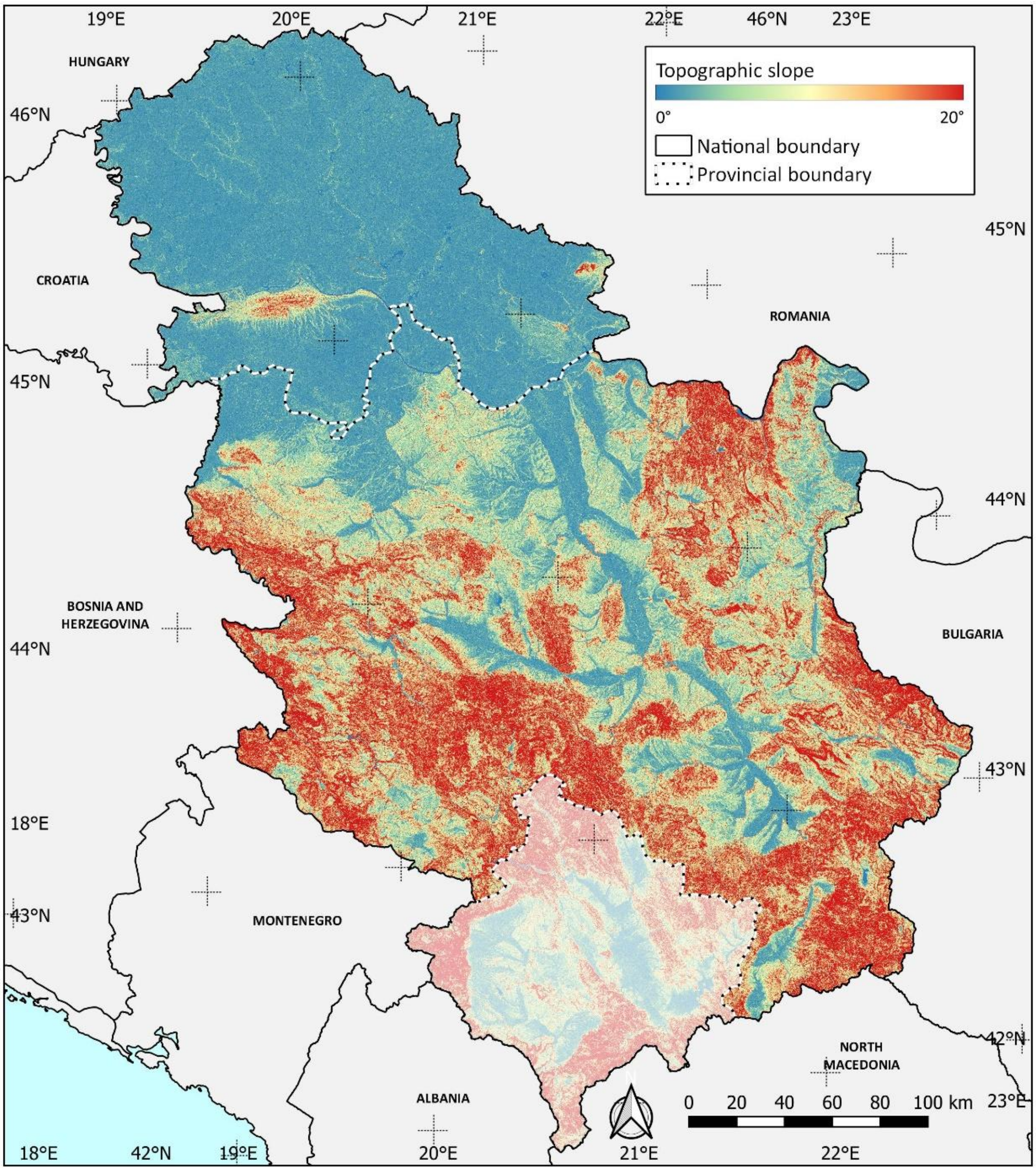

As could be expected, the distribution of the topographic slopes in the Republic of Serbia follows the same pattern than the distribution of elevation. There are very few strong topographic slopes North of the Sava-Danube axis, and most part of it lies to the South of this axis. The strongest slopes of the country are located in the Northeast of the country in the Balkan and Rhodope Mountain ranges.

2. Land cover and land use

This section will present the land cover and land use in the Republic of Serbia. It will be focused on agricultural practices.

Land cover: CORINE land census

To present a description of the distribution of land cover in the republic of Serbia, we refer to the CORINE land cover data base (Figure 3). The CORINE (coordination of information on the environment) Land Cover (CLC) inventory was initiated in 1985 to standardize data collection on land in Europe to support environmental policy development. The project is coordinated by the European Environment Agency (EEA) in the framework of the EU Copernicus program and implemented by national teams (European Environmnet Agency (EEA), 2020).

CLC uses a 44 classes nomenclature with a minimum mapping unit of 25 hectares and a minimum mapping width of 100 m. In the following map, all the classes belonging to the "Forest and semi natural areas", "Artificial surface", and "Water bodies" class groups were merged into one respective class, to give a more detailed focus on the agricultural classes.

Table 1 – Frequency distribution table for land cover classes in the Republic of Serbia.
***Data source:** Copernicus CORINE Land Cover 2018 (European Environmnet Agency (EEA), 2020)*

Class ID	*Class Description*	*Surface area (in km^2)*	*Surface area (in % of total)*
300	Forest and semi natural areas	31 027	40.04%
211	Non-irrigated arable land	22 476	29.01%
242	Complex cultivation patterns	9 824	12.68%
243	Land principally occupied by agriculture, with significant areas of natural vegetation	8 786	11.34%
100	Artificial surfaces	2 687	3.47%
231	Pastures	1 281	1.65%
500	Water bodies	810	1.05%
222	Fruit trees and berry plantations	293	0.38%
400	Inland marshes	223	0.29%
221	Vineyards	79	0.10%

According to the CLC, most of the agricultural lands in Serbia are located in Vojvodina, North of the Sava-Danube axis. This very homogenous distribution represents more than a quarter of the country area.

South of the Sava-Danube axis, the agricultural land cover is concentrated in the three Morava valleys, with a heterogeneous distribution of "non-irrigated arable land", "Complex cultivation patterns", "Land principally occupied by agriculture, with significant areas of natural vegetation", "Fruit trees and berry plantations" and "Vineyards". Together these classes represent another quarter of the country area.

There is therefore as much agricultural land North of the Sava-Danube axis than in the South of the country. But where in the North the agricultural land covers are aggregated together in large patches of the same agricultural types, in the south the agriculture is dispersed throughout the area in a heterogenous complex structure of agricultural types.

The rest of the country surface is covered for the most part by “Forest and semi natural areas” (40% of the country area) mostly located to the South of the Sava-Danube axis.

Figure 3 – Distribution of the CORINE land cover classes in the Republic of Serbia
Data source: *Copernicus CORINE Land Cover 2018 (European Environmnet Agency (EEA), 2020).*

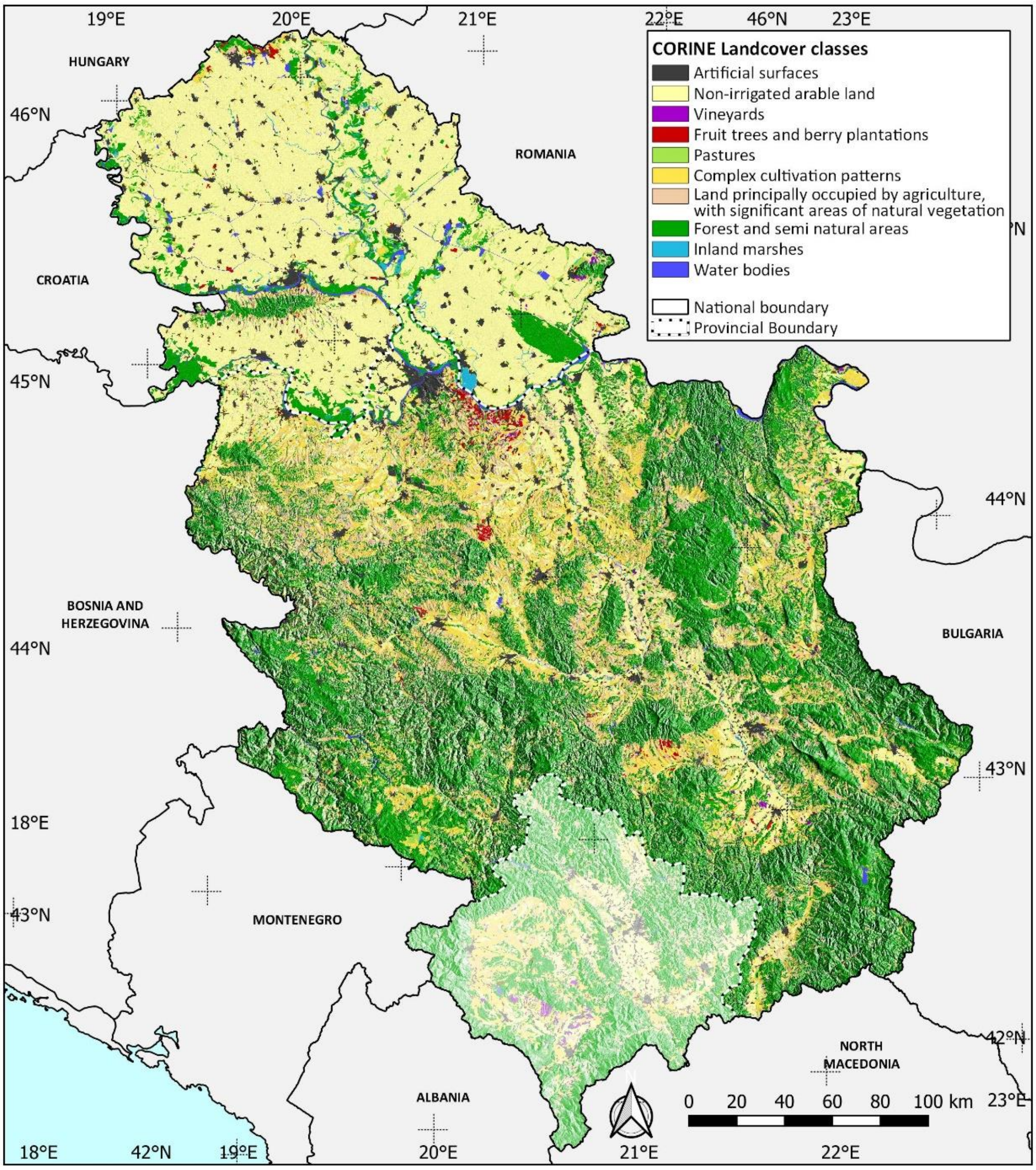

It may be noted that, according to the CLC, there are no irrigated land in the Republic of Serbia. This is however not correct as large areas of irrigated land were declared in the farm survey of 2018 (see Chapter 6). It is thus likely that these “irrigated arable lands” were simply merge to the “non-irrigated lands” class. This may have happened because the size of the irrigated crop was smaller than the analysis grid (25ha).

Land use: agricultural Census of 2012

To describe the land use of agricultural areas in the Republic of Serbia, we used the data presented in the Agricultural Census of 2012 by the Statistical Office of Serbia. This census presented a detailed image of the land use of natural land in Serbia, presenting separately meadows & pastures, forests, arable crops, forage crops, fruits plantations, vineyards, and kitchen gardens.

In the following maps the municipalities are designated by an arbitrary ID numbering system, in alphabetic order of the municipality name, for conciseness on the map (see Annex 1 - Municipality ID reference table).

Meadows & pastures

The distribution of meadow and pastures by municipality in the Republic of Serbia in 2012 is presented in Figure 4.

Figure 4 – Distribution of meadow & pasture by municipality in the Republic of Serbia in 2012
Data source: Census of Agriculture 2012 (Statistical Office of the Republic of Serbia, 2020)

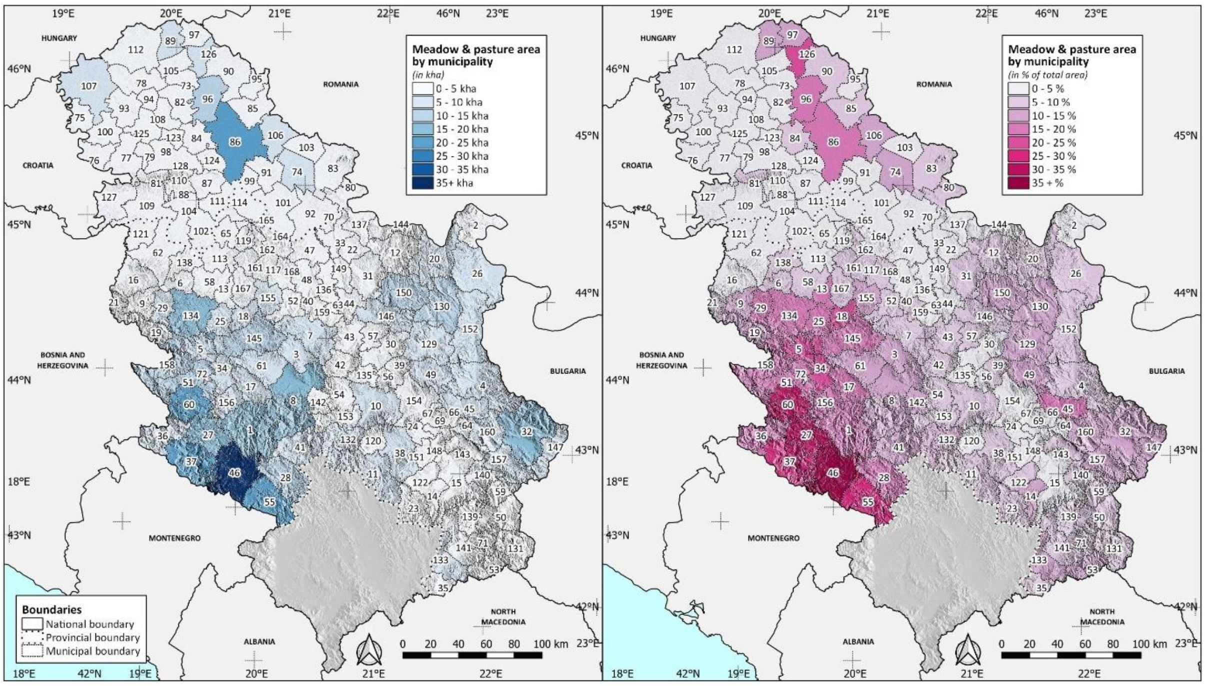

Pasture and meadows lay mostly at high altitudes, on the hills of the Southeast of the country, where it reaches 25 % of the total municipality area on average. In the flat lands and valleys, meadows and pastures a fairly rare (less than 10% of the total area in most municipalities). A few exceptions can however be noted in the Northeast of the country in the municipality of Zrenjanin (86), Novi Bečej (96) and Čoka (126), where pastures and meadows represent a bit more than 15% of the total area. Very high concentration of pasture and meadows can be found on the high altitudes of the Dinarides mountains in the southwest, in the municipalities of Čajetina (60), Sjenica (46) and Nova Varoš (27), where more than 30% of the surface area is covered by meadows and pastures. It is worth noting that the municipality of Sjenica (46) present the largest absolute surface area of pasture and meadows, more than 35 kha.

Forests

The distribution of forests by municipality in the Republic of Serbia in 2012 is presented in Ruma (104) and Pančevo (101), presenting each more than 50% of forest area.

Figure 5.

Most of Serbia's forests are located to the south of the Tisa-Danube axis. In the north of the country, the municipalities present very few forests (less than 10% of the area in most municipalities), where in the South, many municipalities have at least 10% of their areas covered by forest, with some extremes above 40% (Vrnjačka Banja (142), Kruševac (10), and Despotovac (146)). Notably, again in the South, the municipalities of Ivanjica (1) and Kraljevo (8) present each more than 40 kha of forest, and the municipality of Kruševac (10) more than 70 kha. Two exceptions can be noted as well in the North, located on the Sava-Danube axis: Ruma (104) and Pančevo (101), presenting each more than 50% of forest area.

Figure 5 - Distribution of forest cover by municipality in the Republic of Serbia in 2012.
<u>Data source:</u> Census of Agriculture 2012 (Statistical Office of the Republic of Serbia, 2020)

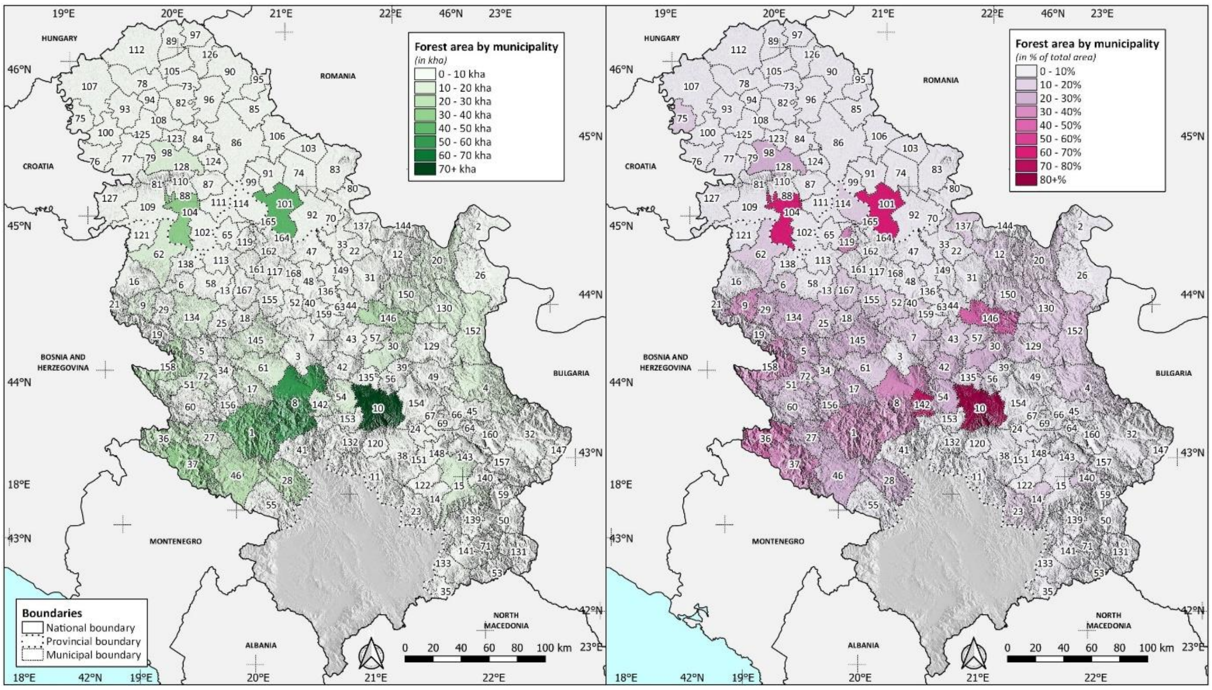

Agricultural areas

The distribution of total agricultural area (regardless of the crop type) and percentage of abandoned agricultural area by municipality in the Republic of Serbia in 2012 is presented in Figure 6.

Figure 6 – Distribution of total agricultural area and percentage of abandoned agricultural area by municipality in the Republic of Serbia in 2012.
<u>Data source:</u> Census of Agriculture 2012 (Statistical Office of the Republic of Serbia, 2020)

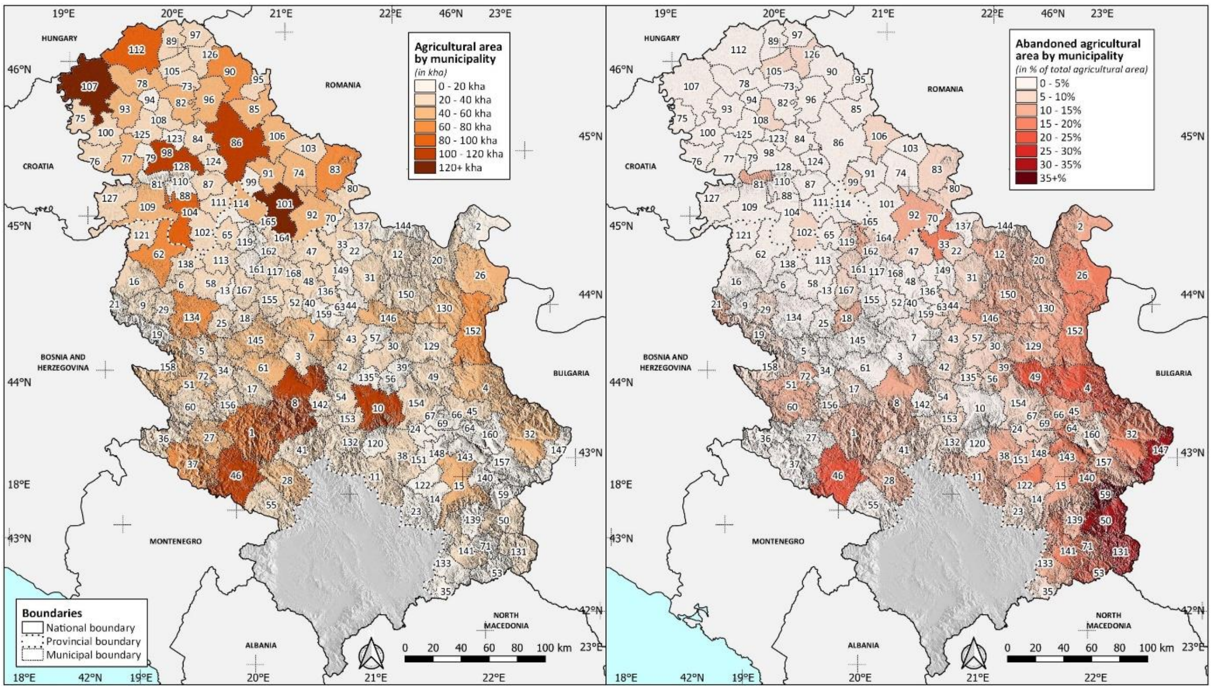

Most of the agricultural lands are located to the North of the Sava-Danube axis. There, most of the municipality present more than 20 kha of agricultural area, a large part more than 40 kha. The municipality of Zrenjanin (86), Pančevo (101), Novi Sad (98) and Sombor (107) have the highest amount of agricultural area, with more than 100 kha of agricultural land.

In the South of the country, the situation is quite different: most of the municipalities present less than 40 kha of agricultural land, with some exceptions presenting between 40 kha and 60 kha of agricultural land (Ivanjica (1), Kruševac (10), Kraljevo (8) and Sjenica (46)).

In terms of abandoned agricultural area, most of the municipalities shows an abandon ratio of their agricultural area of less than 5%. However, in the higher altitude of the South of the Sava-Danube axis, quite a few municipalities present more than 10% (sometimes more than 30%) of their declared agricultural land as abandoned. The situation is even more acute in the Rhodopes mountains, in the municipalities of Bosilegrad (131), Surdulica (50), Crna Trava (59), and Dimitrovgrad (147). There agriculture represents less than 20 kha and is abandoned at more than 80 % (less than 4kha of agricultural land is in activity in these municipalities).

Arable crops

The distribution of arable crops by municipality in the Republic of Serbia in 2012 is presented in Figure 7.

Figure 7 – Distribution of arable crops by municipality in the Republic of Serbia in 2012
Data source: Census of Agriculture 2012 (Statistical Office of the Republic of Serbia, 2020)

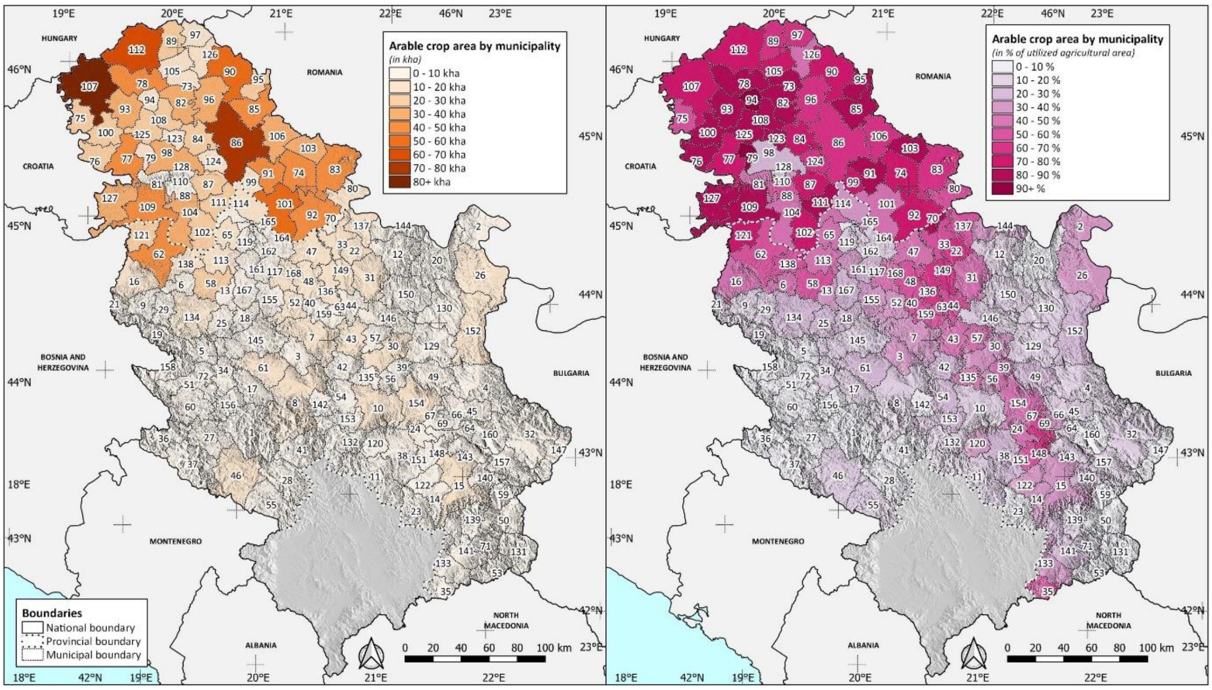

North of the Sava-Danube axis, for most municipalities (to the exception of some municipalities on the Fruška Gora range), the arable crops represent more than 60% of the total utilized agricultural area. To the South, arable crops represent often less than 20% of the municipalities utilized agricultural land, with the exceptions of the greater and south Morava valleys, where this ratio reach often more than 40%.

In term of absolute area, no municipality of the South of the country present more than 30 kha of arable crop area. In the North, most of the municipalities presents more than 30 kha and up to 70 kha of arable crops. Finally, the Largest arable crop areas are present in the municipalities of Sombor (107) and Zrenjanin (86), with more than 70 Kha of arable crop area.

Forage

The distribution of forage crops by municipality in the Republic of Serbia in 2012 is presented in Figure 8.

Figure 8 - Distribution of forage crops by municipality in the Republic of Serbia in 2012
Data source: Census of Agriculture 2012 (Statistical Office of the Republic of Serbia, 2020)

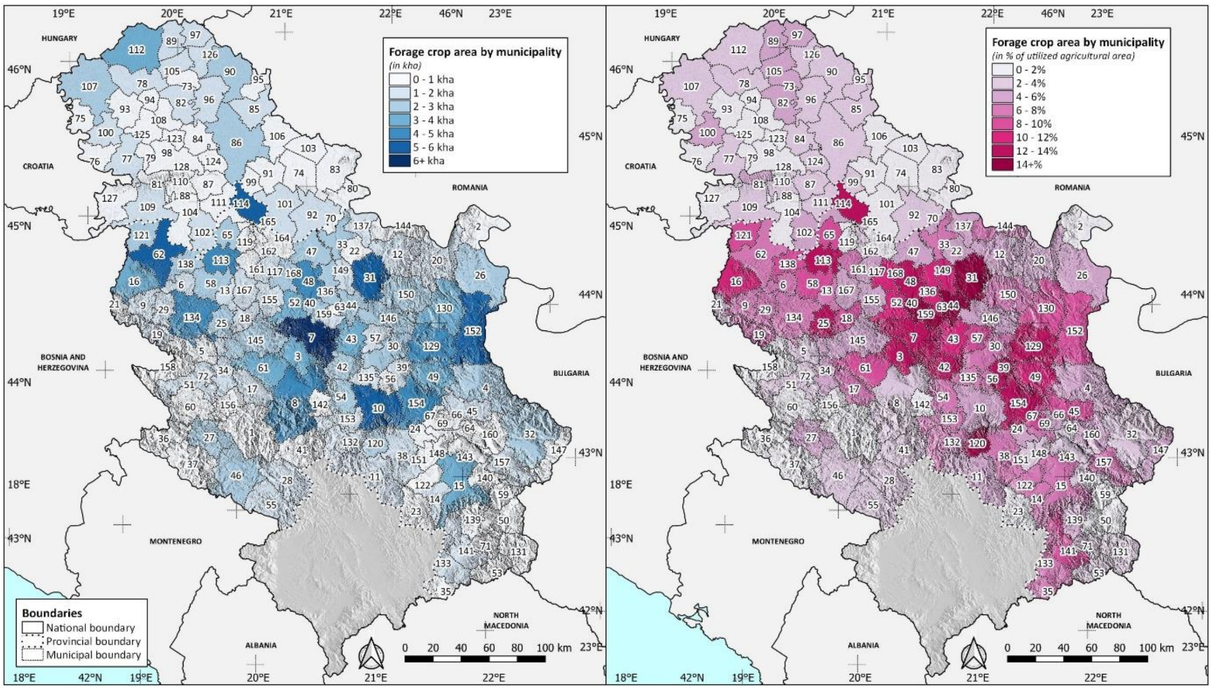

Forage crops are more represented in the South of the Sava-Danube axis. There, forage crops represent more than 6% of utilized agricultural lands for most of the municipalities, and more than 8% for many of them. The municipalities of Petrovac na Mlavi (31) Svilajnac (44), Rača (40), Lapovo (63), Batočina (159) and Blace (120) present the largest ratio of forage crops, with more than 14% of their agricultural area consisting of forage crops.

In term of absolute area, the situation is more nuanced. Most of the municipalities of Serbia present at least 1kha of forage crops. However, a certain hotspot of forage crops can be pinpointed in the center of the country with higher surface of forage crops from 2kha to 5 kha. The municipality with the largest surface area of forage crops is Kragujevac (7), with more than 6 kha of forage crops.

Fruit plantations

The distribution of fruit plantation by municipality in the Republic of Serbia in 2012 is presented in Figure 9.

Most of the fruit plantations in the republic of Serbia are located in the Dinarides mountain range, in the Southwest of the country. There, fruit plantations represent 10% to 20% of the utilized agricultural area, with 3kha to 5kha of fruit plantations per municipality. In Belgrade, in the municipalities of Grocka (164), and Zvezdara (165) more than 50 % of the utilized area consisting of fruit plantations, with more than 6kha of plantations. In the North there is almost no fruit plantations, with the noticeable exception of the municipality of Subotica (112) which presents more than 2 kha of fruit plantations.

Figure 9 - Distribution of fruit plantations by municipality in the Republic of Serbia in 2012
Data source: Census of Agriculture 2012 (Statistical Office of the Republic of Serbia, 2020)

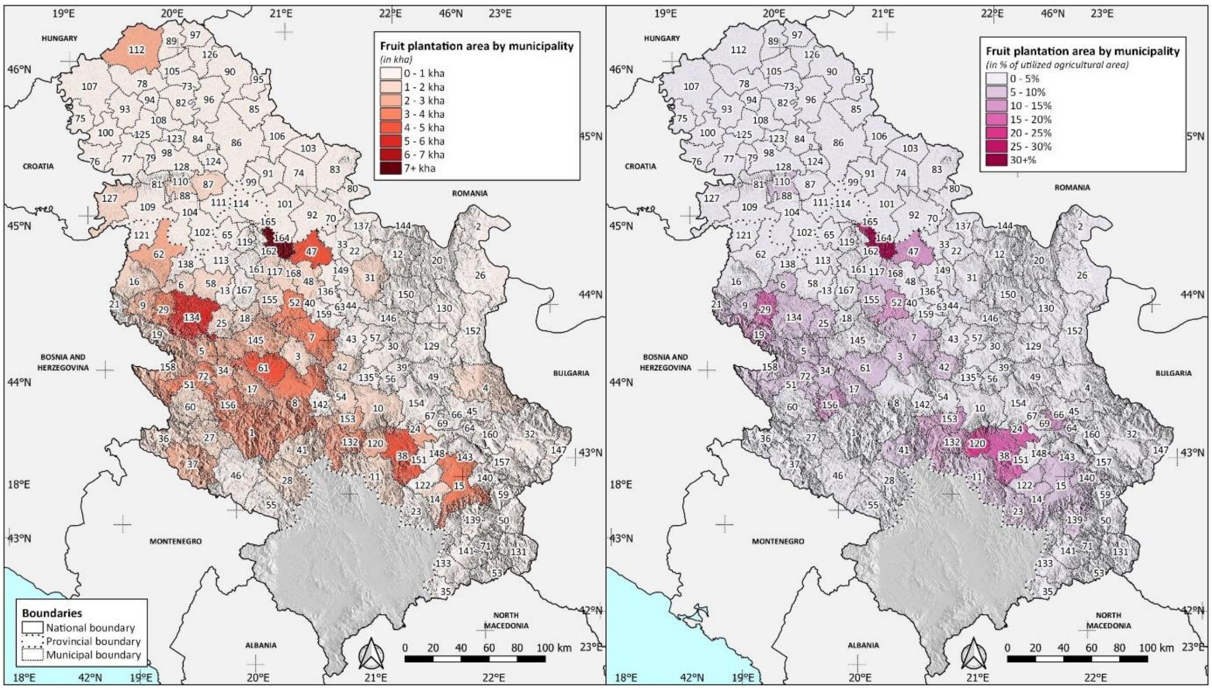

Vineyards

The distribution of vineyards by municipality in the Republic of Serbia in 2012 is presented in Figure 10.

Figure 10 - Distribution of vineyards by municipality in the Republic of Serbia in 2012
Data source: Census of Agriculture 2012 (Statistical Office of the Republic of Serbia, 2020)

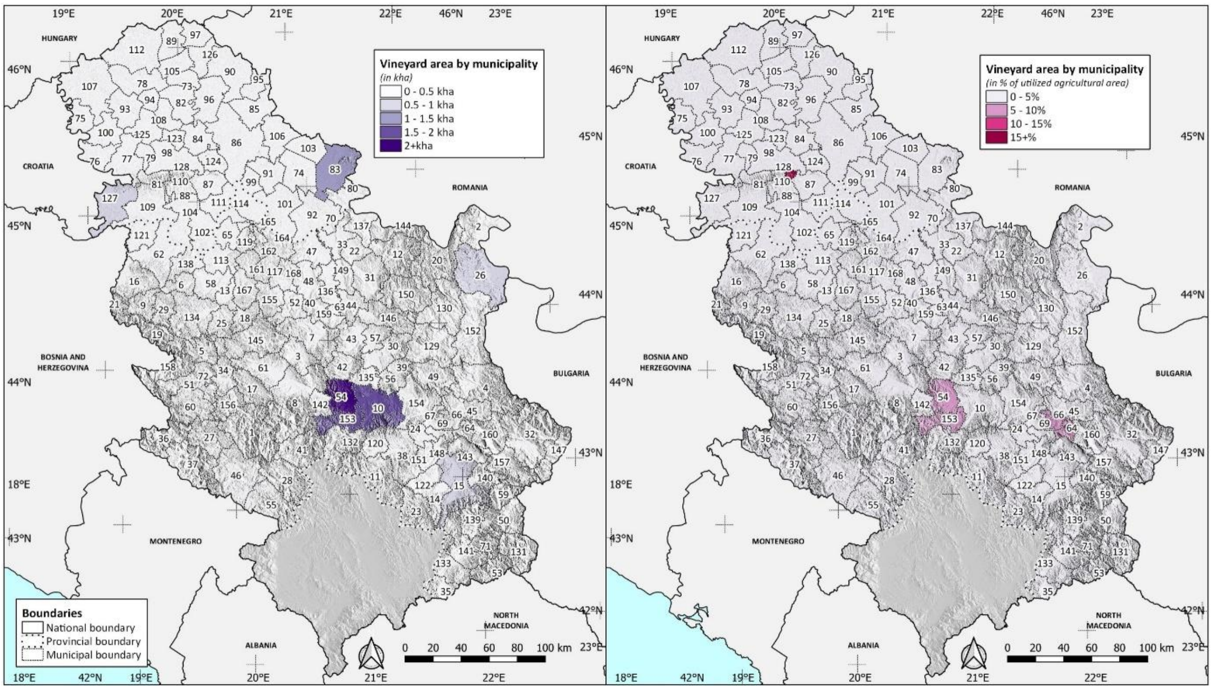

Most of the vineyards in Serbia a located in the south of the country in the municipalities of Trstenik (54), Aleksandrovac (153), and Kruševac (10), with more than 1500 ha of vineyard each. Some smaller vineyards exist in the municipality of Šid (127), Vršac (83), Negotin (26), and Leskovac (15), with a bit more than 500 ha of vineyards each.

Kitchen gardens

The distribution of kitchen garden by municipality in the Republic of Serbia in 2012 is presented in Figure 11.

Figure 11 - Distribution of kitchen garden by municipality in the Republic of Serbia in 2012
Data source: Census of Agriculture 2012 (Statistical Office of the Republic of Serbia, 2020)

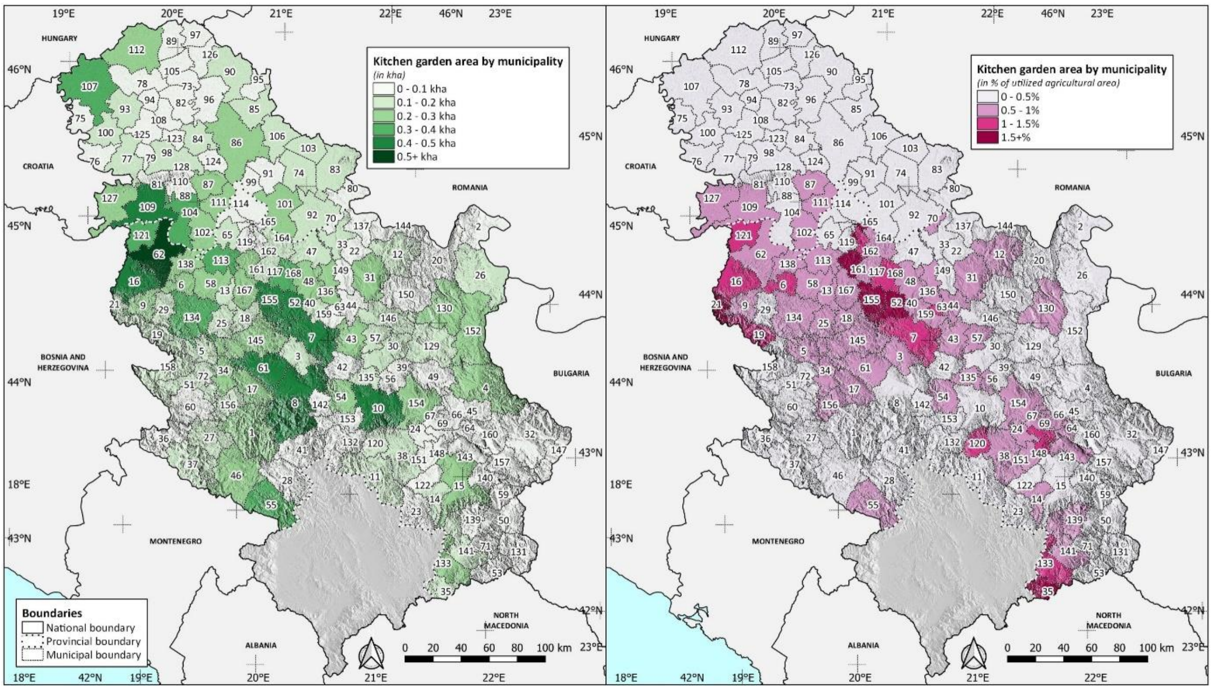

Kitchen gardens are quite common in Serbia and evenly distributed throughout the country, frequently representing more than 200 ha of land in the municipality. The practice is slightly more common in the west of the country where Kitchen Garden can represent up to 400 ha of land in the municipality. The largest concentration of kitchen garden is in Šabac (62), where they represent more than 500 ha of the municipality agricultural area.

3. Soil

This section will present the soil compositions and taxonomy in the Republic of Serbia.

Soil classification

The distribution of soil types, following the Harmonized World Soil Database (HWSD) soil taxonomy, in the Republic of Serbia is presented in Figure 12. The HWSD is the result of a collaboration between the FAO with IIASA, ISRIC-World Soil Information, Institute of Soil Science, Chinese Academy of Sciences (ISSCAS), and the Joint Research Centre of the European Commission (JRC). This data base combines existing regional and national updates of soil information worldwide with the information contained within the 1:5 000 000 scale FAO-UNESCO Soil Map of the World (Nachtergaele et al., 2010).

Figure 12 – Distribution of soil types in the Republic of Serbia following the HWSD taxonomy
Data source: *Harmonized World Soil Database* (Nachtergaele et al., 2010)

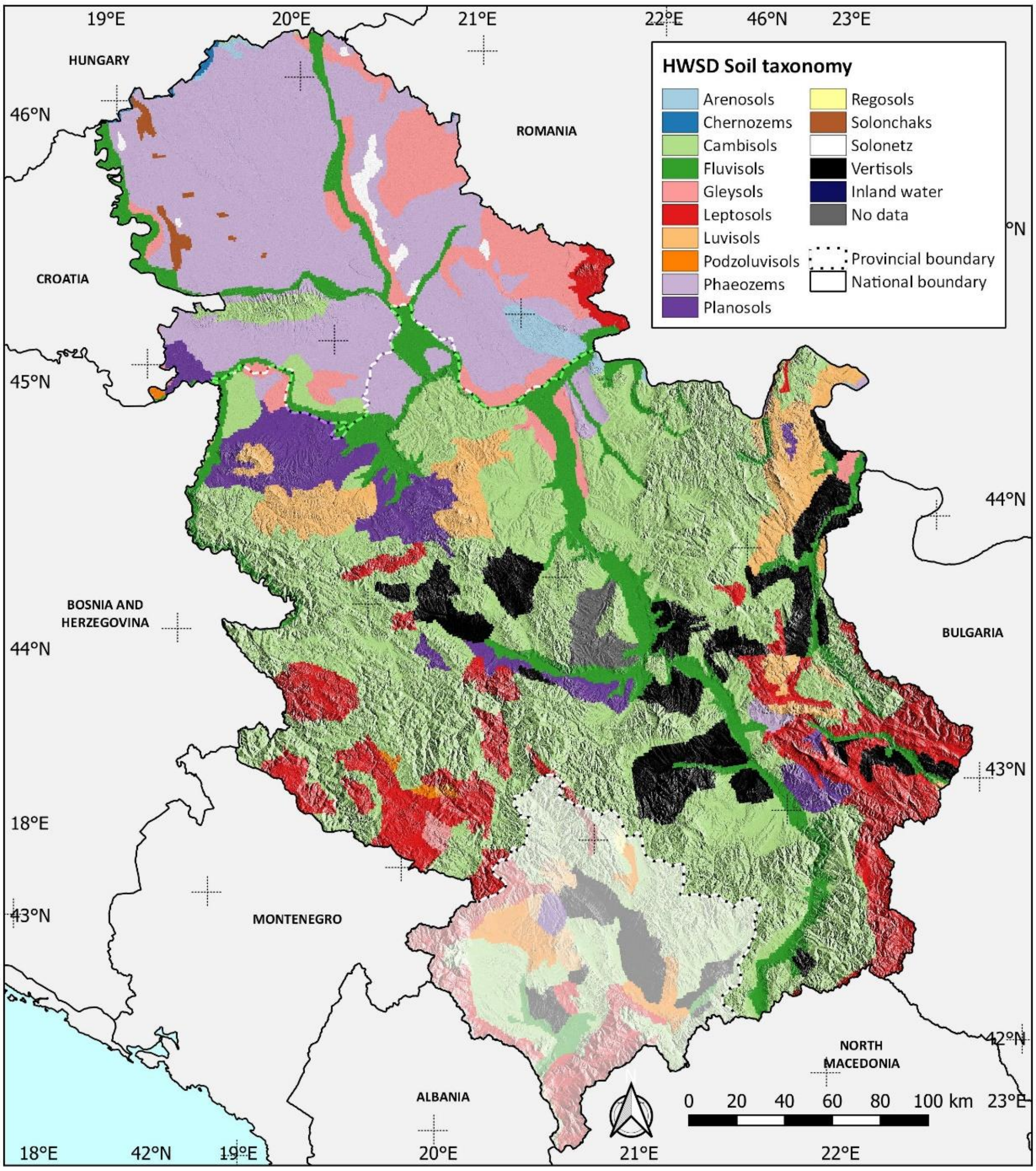

The Republic of Serbia is covered by 8 main soil types: Cambisols (38% of the total area), Phaeozems (19 % of the total area), Leptosols (10% of the total area), Fluvisols (9% of the total area), Vertisols (6% of the total area), Gleysols (5% of the total area) and Luvisols (5% of the total area) and Planosols (5% of the total area). These seven soil types represent together more than 97% of the surface of the country.

Cambisol is the most common soil in the country and can be found almost exclusively to the South of the Sava-Danube Axis, where it represents the largest part of the soil. Phaeozems on the other hand is almost exclusively found to the South of the Sava-Danube axis, where it also represents the largest part of the soil. Fluvisols are represented throughout the country, as it covers the riverbanks (Danube, Sava, Tisa, and the Morava rivers). Leptosols is found at high altitudes, in the Dinarides, Rhodopes and Balkan Mountains. Luvisols are concentrates in the Balkan Mountains and South of the Sava valley, Gleysols in the Northeast of the Country, and Planosols mainly in the West, around the Sava valley. Finally, the Vertisols are found around the three Morava valleys, and close to the Timok and in the Balkan mountains, close to the Nišava river.

Table 2 - Frequency distribution table for soil types in the Republic of Serbia following the WRB taxonomy
Data source: (Panagos et al., 2012; European Commission Joint Research Centre, March-21-2021)

Soil type	HWSD soil type ID	Surface area (in km^2)	Surface area (in % of total)
Cambisols	8	29 592	38,17%
Phaeozems	21	14 905	19,23%
Leptosols	16	7 601	9,80%
Fluvisols	9	7 328	9,45%
Vertisols	28	4 782	6,17%
Gleysols	11	4 124	5,32%
Luvisols	17	3 685	4,75%
Planosols	22	3 512	4,53%
No data	34	592	0,76%
Arenosols	4	568	0,73%
Solonetz	27	343	0,44%
Solonchaks	26	237	0,31%
Podzoluvisols	20	159	0,20%
Chernozems	6	88	0,11%
Inland water	31	3	0,00%
Regosols	25	1	0,00%

Sand, Loam and Clay content

The distribution of sand, loam, and clay in soils in the Republic of Serbia is presented in Figure 13.

Sand, loam, and soil content are close to balance (around 33% each, color close to white) in most of the country area. There is slightly less sand and clay than loam in most of the country soil. There are a few exceptions however, where sand content is higher.

Sand hot spots are ubiquitous throughout the country and can be found North and South of the Sava-Danube axis, at mid altitude, and following riverbanks. They are however more common in the Southwest of the country. Throughout the country, the sand hotspots generally reach up to 40% in sand contents. Extreme concentration of sand can however be found at the Northern tip of the country, in the Southern part of the country (around Vladičin Han (139)), in the Southwest (around Kraljevo (8)) and around Krupanj (9) and Kragujevac (7). At these extreme spots, the sand content can reach more than 50%.

Figure 13 – Distribution of soil content of sand, loam, and clay, at 30 cm depth, in the Republic of Serbia.
Top left: *sand content.* ***Top right:*** *loam content.* ***Bottom:*** *clay content.* *<u>Data source:</u> (Hengl, 2018).*

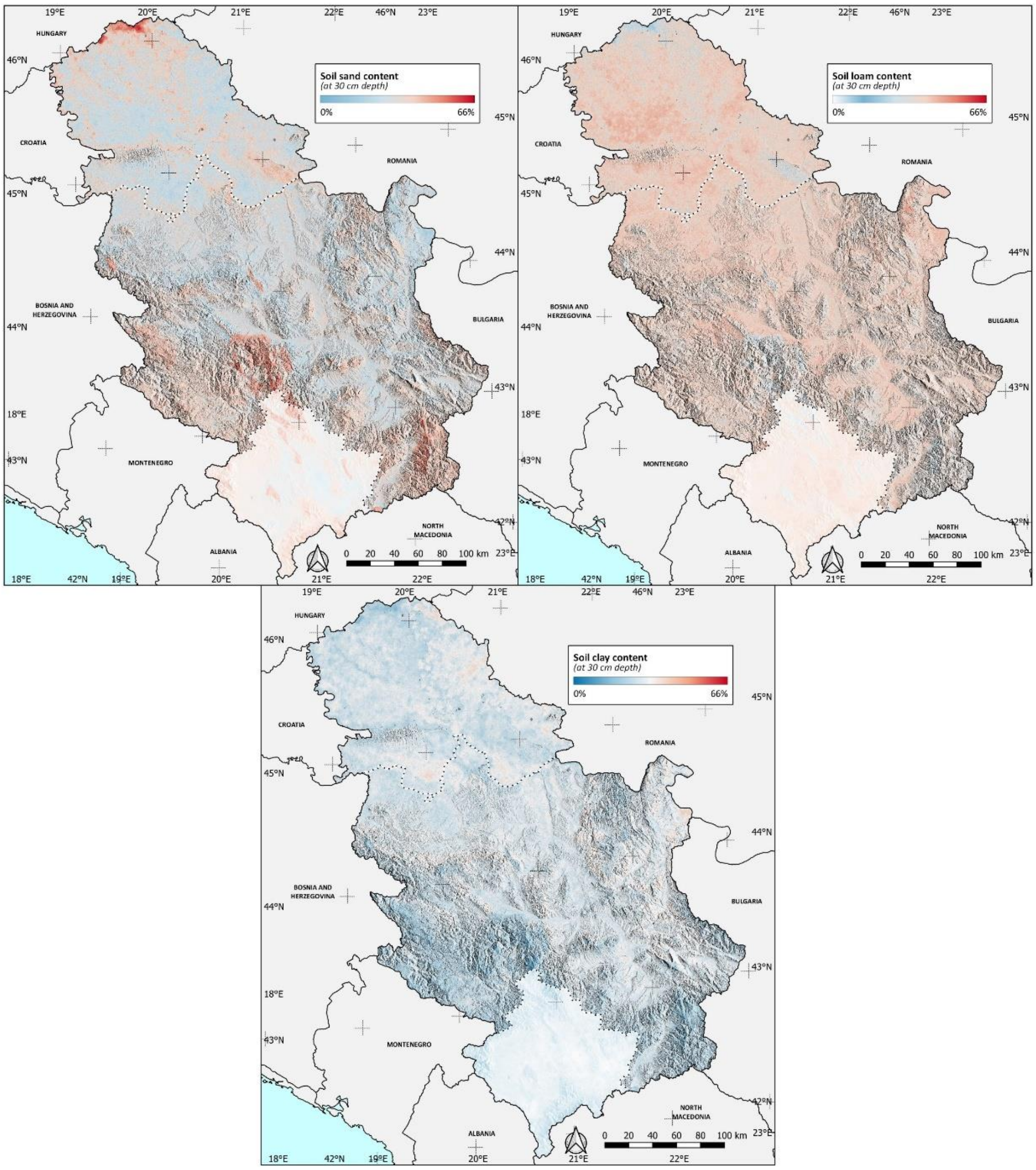

Soil water capacity

The distribution of water capacity of soils (field capacity) in the Republic of Serbia is presented in Figure 14.

Soil water capacity is roughly evenly distributed throughout Serbia (around 30%). Some lower values, around 25% can be found in the North of the country, close to Fruška Gora Mountain range and in the Northeast, close to Alibunar (74) municipality. In the South the lower values are mainly concentrated in the valleys.

Extremely high water capacity is found following the Tisa River (40% or more). On the other hand, extremely low water capacity can be found at sand hotspot (see Figure 13), around Vladičin Han (139), Kraljevo (8), Krupanj (9), and Kragujevac (7) where water capacity can be lower than 20%.

Figure 14 - Distribution of the soil water capacity at 30 cm depth in the Republic of Serbia.
Water capacity (i.e., field capacity) in volumetric percent for 33kPa and 1500kPa suctions. Data source: (Hengl et al., 2019)

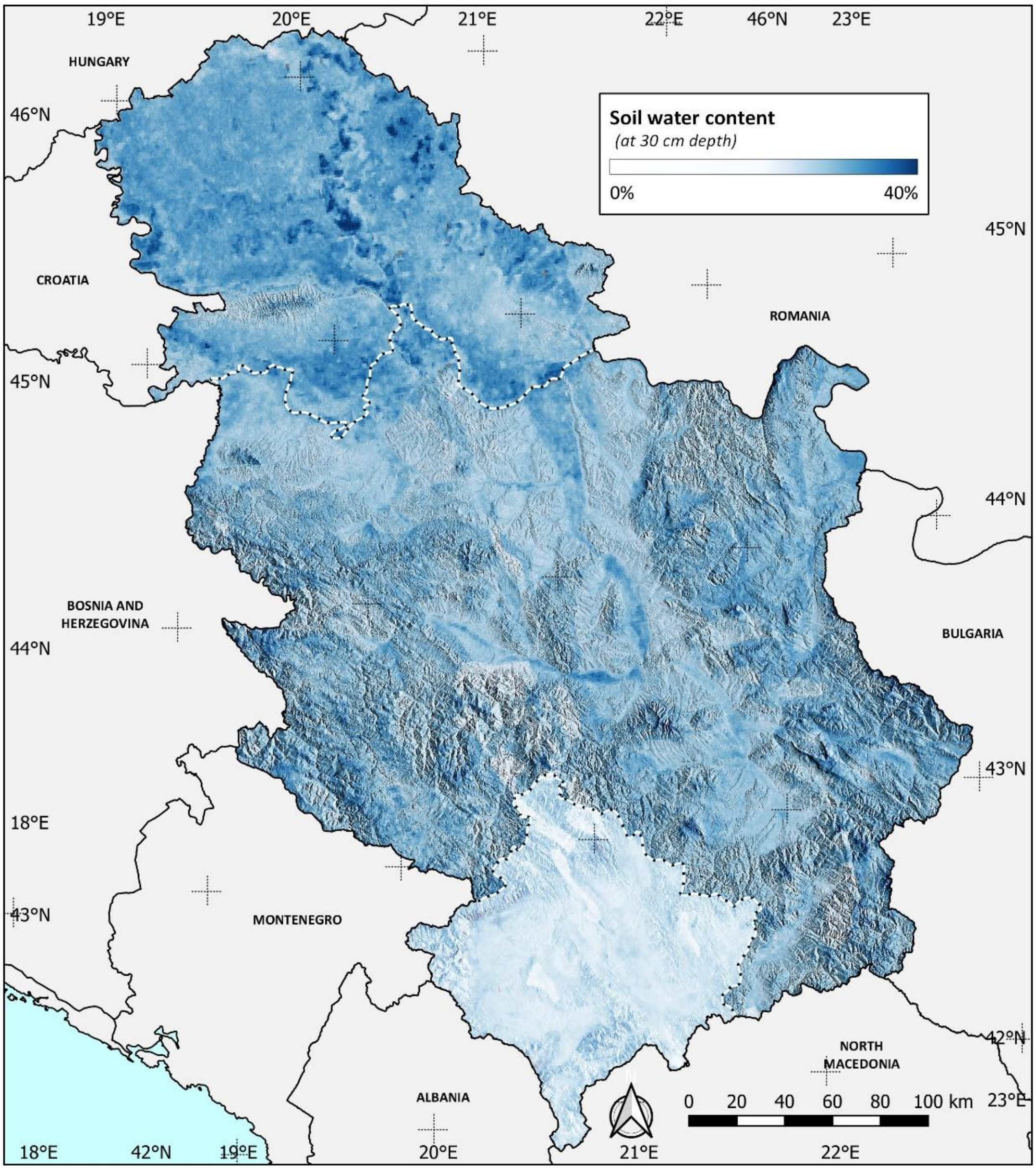

4. Demography

This section will present the distribution of population and urban centers in the Republic of Serbia.

Demographic trends

The demographic trends in the republic of Serbia are presented in Figure 15.

Figure 15 - Time series of the population in the Republic of Serbia
Time series over 1960-2020 period. ***In black:*** *total population.* ***In red:*** *urban population.* ***In green:*** *rural population.* ***In blue (dashed):*** *rural population (in % of total). Data source: World Bank (World Bank, 2020)*

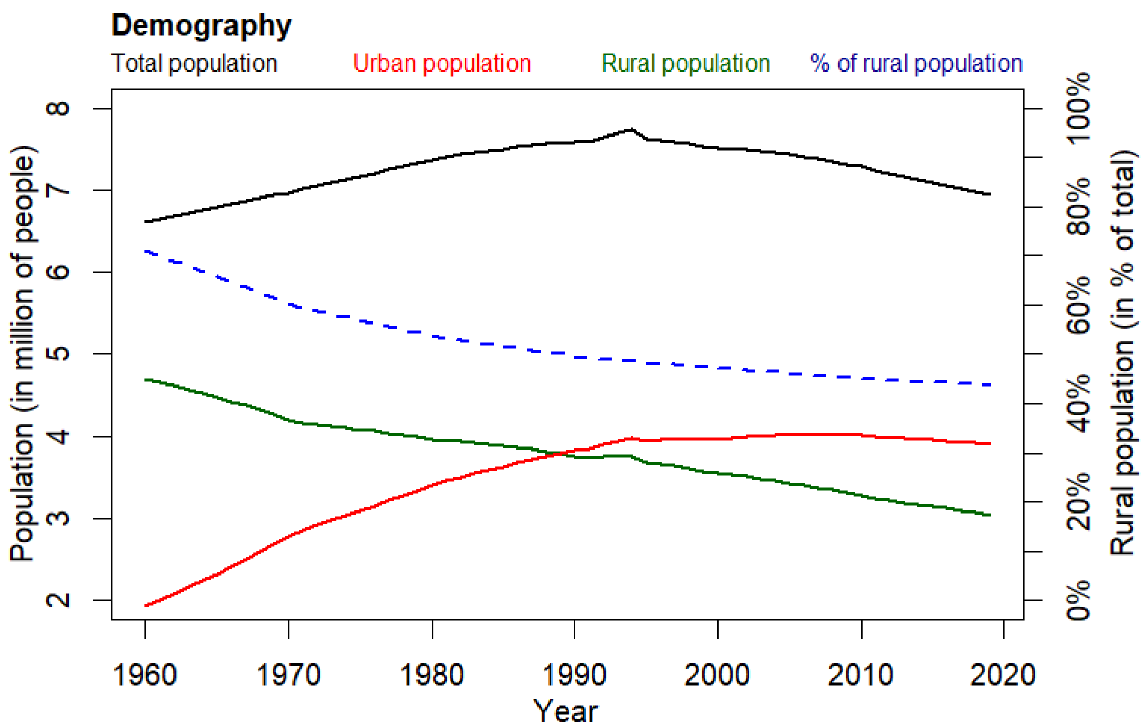

The total population of the Republic of Serbia increased until mid-1990, reaching 7.7 million in 1994. Post 1995 the populations in Serbia slowly decreased, reaching 6.9 million in 2019.

Since 1960, the rural population constantly decreased in Serbia from 4.7 million in 1960 to 3 million in 2019. Urban population on the other hand increased until mid-2000, stabilizing to around 4 million in 2007. In 2019 the urban population was 3.9 million. Because of these two tendencies, the percentage of rural population has decreased, from 71% in 1960 to 44% in 2019.

Current geographic distribution of population

The current geographic distribution of population in the Republic of Serbia is presented in Figure 16.

Figure 16 – Current geographic distribution of the population in the Republic of Serbia.
Data source: NASA SEDAC GPWv411: UN-Adjusted Population Density (Center for International Earth Science Information Network - CIESIN - Columbia University, 2018)

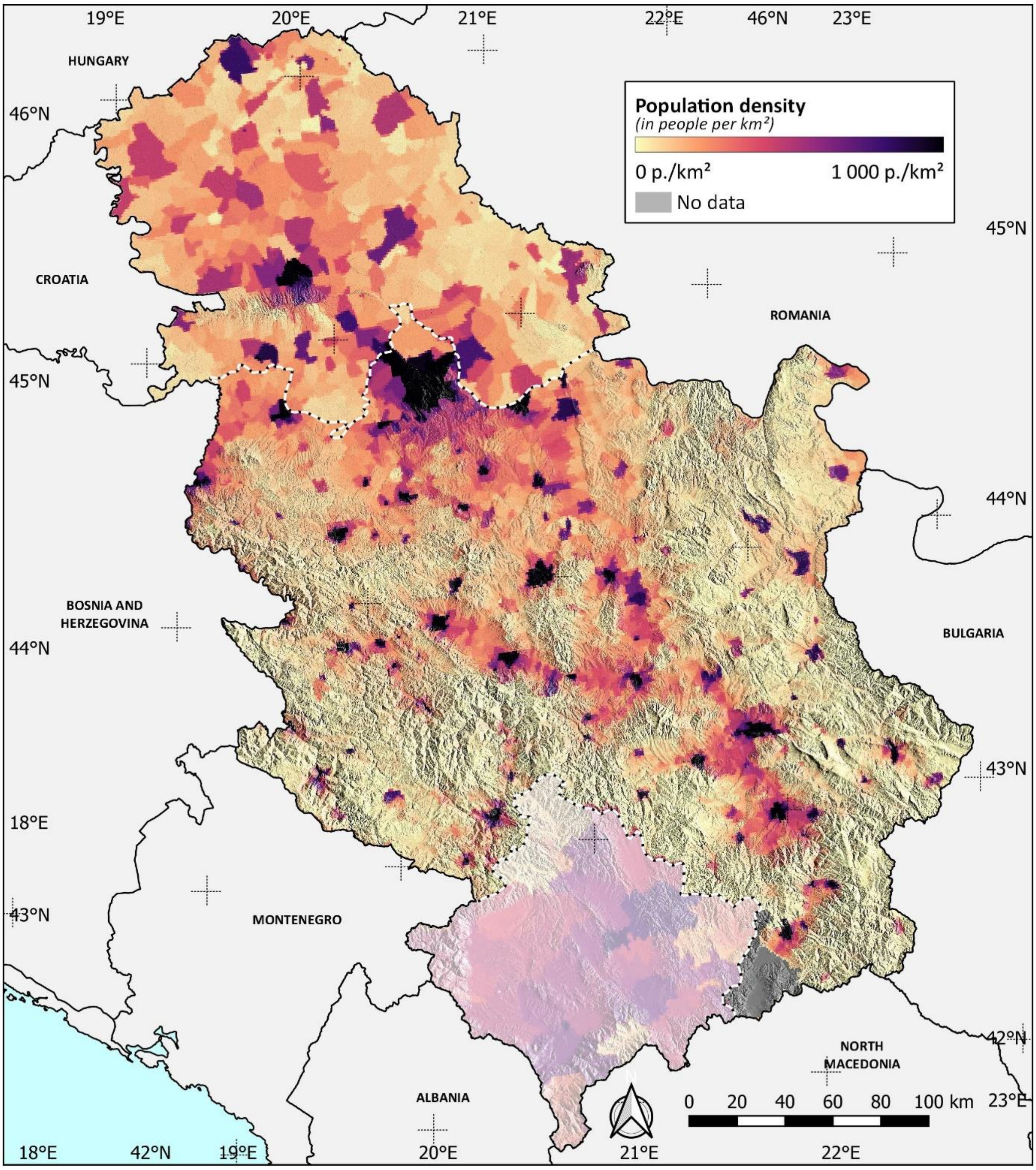

As expected from the demographic trends of the Republic of Serbia (see Figure 15), most of the Serbian population is located in the main urban center, the largest being Belgrade, Novi Sad, and Subotica in the North, and Kragujevac, Niš and Leskovac in the South. The urban center of the South of the country are for the most part located in valleys.

Outside the urban centers, the population is higher (50 to 100 people per km^2) and more evenly distributed in the flatland North of the Sava-Danube axis than in the hilly regions of the South. In the South of Serbia, most of the land outside urban center has less than 50 people per km^2.

Road distance to urban centers

To assess the quality of the road network of the Republic of Serbia, the road distance to main urban centers was calculated and presented in Figure 17.

Figure 17 - distribution of the roads distance to urban centers in the Republic of Serbia
Main urban centers were defined as areas where the population density is above 1000 people per km². Distance off-road was modeled as 10 times longer than the same distance travelled on a road. Data source: NASA SEDAC GPWv411: UN-Adjusted Population Density (Center for International Earth Science Information Network - CIESIN - Columbia University, 2018) and OpenStreetMap (OpenStreetMap Contributors, 2020).

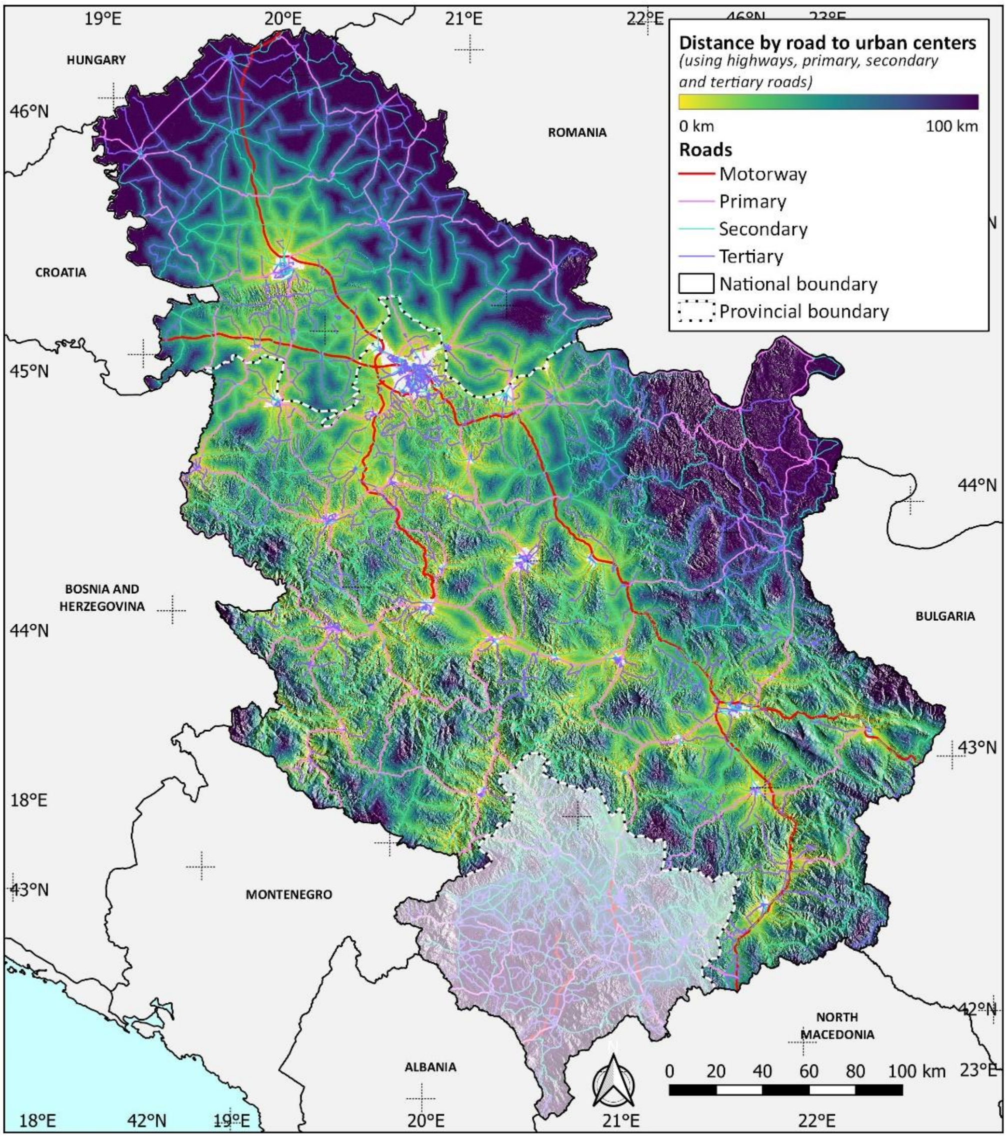

Serbia is relatively well serviced in term of road network. Indeed, the larger part of the country is less than 25 km away from an urban center.

However, there are two less well serviced area. The first is the Northern borders of the country (borders with Croatia, Hungary, and Romania). Although the region is very well serviced in term of road network, there are not very large urban centers in the area, the larger urban center being Subotica (548 people per km²). The second less well services area is in the Carpates mountains, at the Eastern border of the country. As for Northern border region, the Eastern border region is pretty much well serviced in term of road, but lacks very large urban center, the larger urban center in the area being Negotin, with only 346 people per km².

5. Water resources

This section will present the distribution of surface and ground water resources in the Republic of Serbia.

Surface water

The distribution of surface water resources for the Republic of Serbia is presented in Figure 18.

Figure 18 – Distribution of surface water in the Republic of Serbia.
In dark blue: *natural free flowing surface water.* ***In red:*** *man-made free flowing surface water.* ***In light blue:*** *still water. The width of the free-flowing surface water is proportional to the stream's water discharge. Map overlayed on a topographic map of the Republic of Serbia (data source: NASA / USGS / JPL-Caltech (Farr et al., 2007), see Figure 1). Data source: JRC Yearly Water Classification History (Pekel et al., 2016), and (Srbijavode, 2020)*

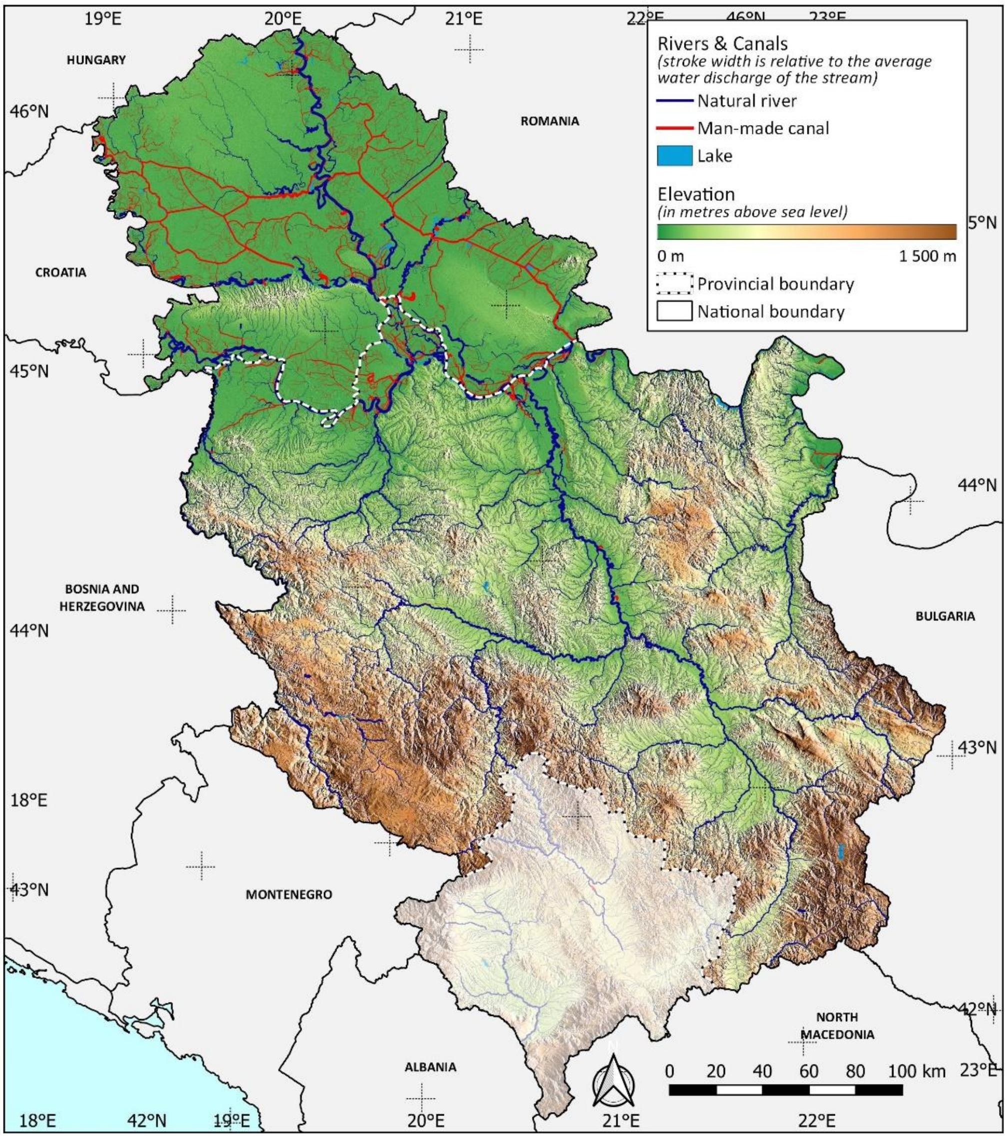

There is a clear dichotomy regarding surface water networks in the republic of Serbia, on each side of the Sava-Danube axis.

To the North of the axis, the free-flowing surface water network is very dense with natural and man-made streams, a large portion of which present very large discharge ratios. such streams are the Danube, Tisa, and Sava rivers, and the multiple canals of the Danube–Tisa–Danube (DTD) network.

In the South of the Sava-Danube axis, the free-flowing surface water network is more scattered, and mainly composed of the Morava and Ibar rivers and their affluent, the Lim River to the South-West, and the Timok river to the South-East. To the South-East, the Danube constitute the border with Romania until Negotin, where the Timok river merges with it. However, all these rivers (except the Danube) have smaller discharge ratio than the main rivers of the North of the country. Moreover, South of the Sava-Danube axis, no large-scale man-made water canal have been built.

In terms of lakes and reservoir, the South of the country is more equipped than the North of the country. We can site the Iron Gate dam on the Danube in the East of the country (at the border with Romania), Vlasina Lake on the Southern tip of Serbia, Perućac lake to the West (border with Croatia), and Gruža Lake in the center of the country, close to Knić municipality (53). To the North of the Sava-Danube axis, no very large lakes or reservoir exists. There are however a couple of bogs (Zasavica) and shallow fishponds (Ečka and Sakule).

Distance from surface water

To estimate the potential for easy water transportation in the Republic of Serbia, we calculated the cumulative slope-distance to the closest surface water source, in terms of degree-meter[1], to consider both distance and slope. The result of this analysis is presented in Figure 19.

In terms of distance to surface water, there is an even larger difference between the North and the South of Serbia. To the North of the Sava-Danube axis, because of the dense surface water network and the flat topography, a very large part of the area is less than 2000°.m from a water source, and transportation of surface water is therefore easy. To the contrary, in the North of the country, because of the more scattered surface water network and the hilly topography, there is almost no area less than 2000°.m away from a water source. The only exceptions are the three Morava and Ibar valleys, where some areas are less than 2000°.m away from the streams. Therefore, in the South of the country, water transportation of surface water may be difficult and/or costly.

[1] A degree meter (°.m) is a distance of one meter to a slope of one degree. Hence, two-degree meters can either be a distance of 2 meters at the same one degree slope, or a distance of one meter to a two degrees slope.

Figure 19 - Distribution of the distance from surface water in cumulative slope-distance in the Republic of Serbia.

Dark blue lines: *natural free flowing surface water stream.* ***Red lines:*** *man-made free flowing surface water stream.* ***In light blue:*** *still water. The width of the free-flowing surface water is proportional to the discharge of the stream.* ***Green line:*** *2 km flying distance from surface water. Data source: JRC Yearly Water Classification History (Pekel et al., 2016), (Srbijavode, 2020) and NASA / USGS / JPL-Caltech (Farr et al., 2007)*

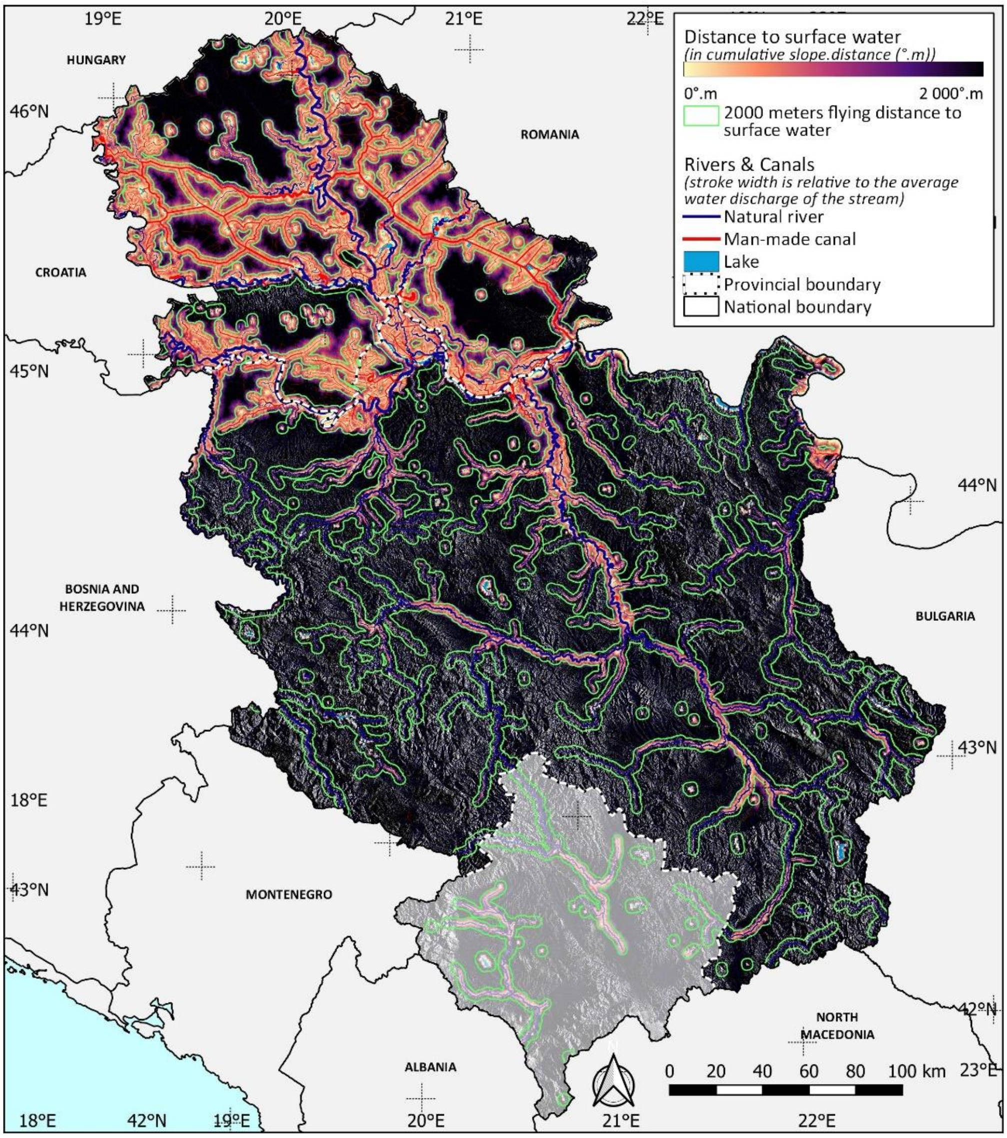

Ground Water

The distribution of aquifers in the Republic of Serbia is presented in Figure 20.

As for surface water, there is a large difference between northern and southern Serbia, in terms of aquifers. Northern Serbia is composed almost exclusively of porous aquifers, a large part of which, along the Danube and Sava rivers are highly productive.

To the South of the Sava-Danube axis, the distribution of aquifers is much more complex, with a lower proportion of highly productive aquifers. Still, three highly productive aquifers can be highlighted: the highly productive porous aquifer following the Morava and Ibar valley and two highly productive fissured aquifers in the Southeast and Southwest, around the Timok and Lim valleys. Be that as it may, these three highly productive aquifers do not represent a large portion of the surface area of the South of the country.

Figure 20 – Distribution of aquifers in the Republic of Serbia

In blue: *Highly productive aquifers.* ***In red:*** *Less than highly productive aquifers. <u>Data source:</u> International Hydrogeological Map of Europe (Duscher et al., 2015)*

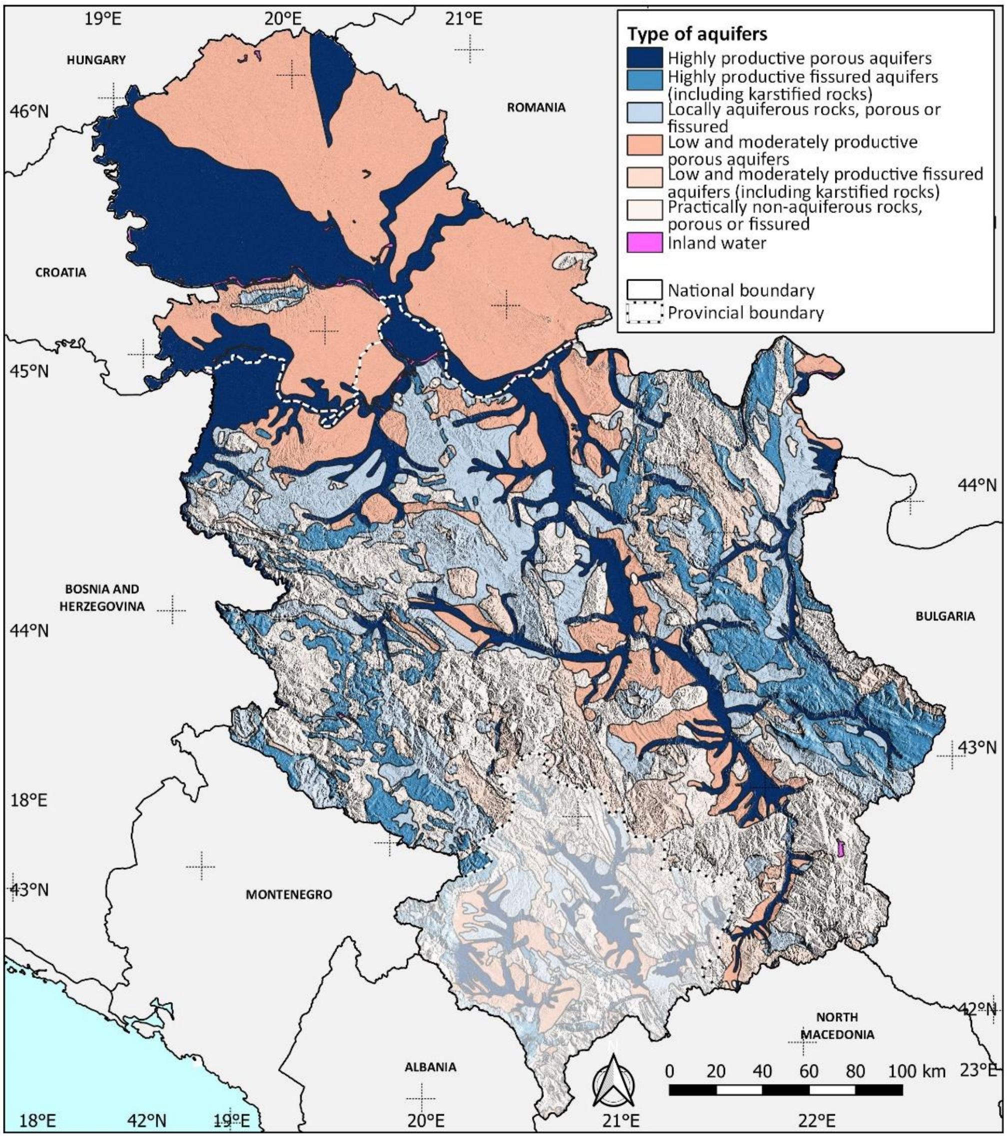

6. Irrigation practices

This section will present the current and past trends of irrigation practices in the Republic of Serbia. We will base our analysis on the data from the census of Agriculture of 2012 (Statistical Office of the Republic of Serbia, 2012) and the Farm Structures Survey of 2018 (Statistical Office of the Republic of Serbia, 2018).

Total irrigated land

The trends and distribution of irrigated crops (regardless of crop type) in the Republic of Serbia are presented in Figure 21.

Figure 21 – Trends and distribution of irrigated crop areas by municipality in the Republic of Serbia
Distribution in 2012 and 2018, and distribution of the variation between these two dates. <u>Data source:</u> Census of Agriculture 2012 (Statistical Office of the Republic of Serbia, 2012) and Farm Structures Survey 2018 (Statistical Office of the Republic of Serbia, 2018)

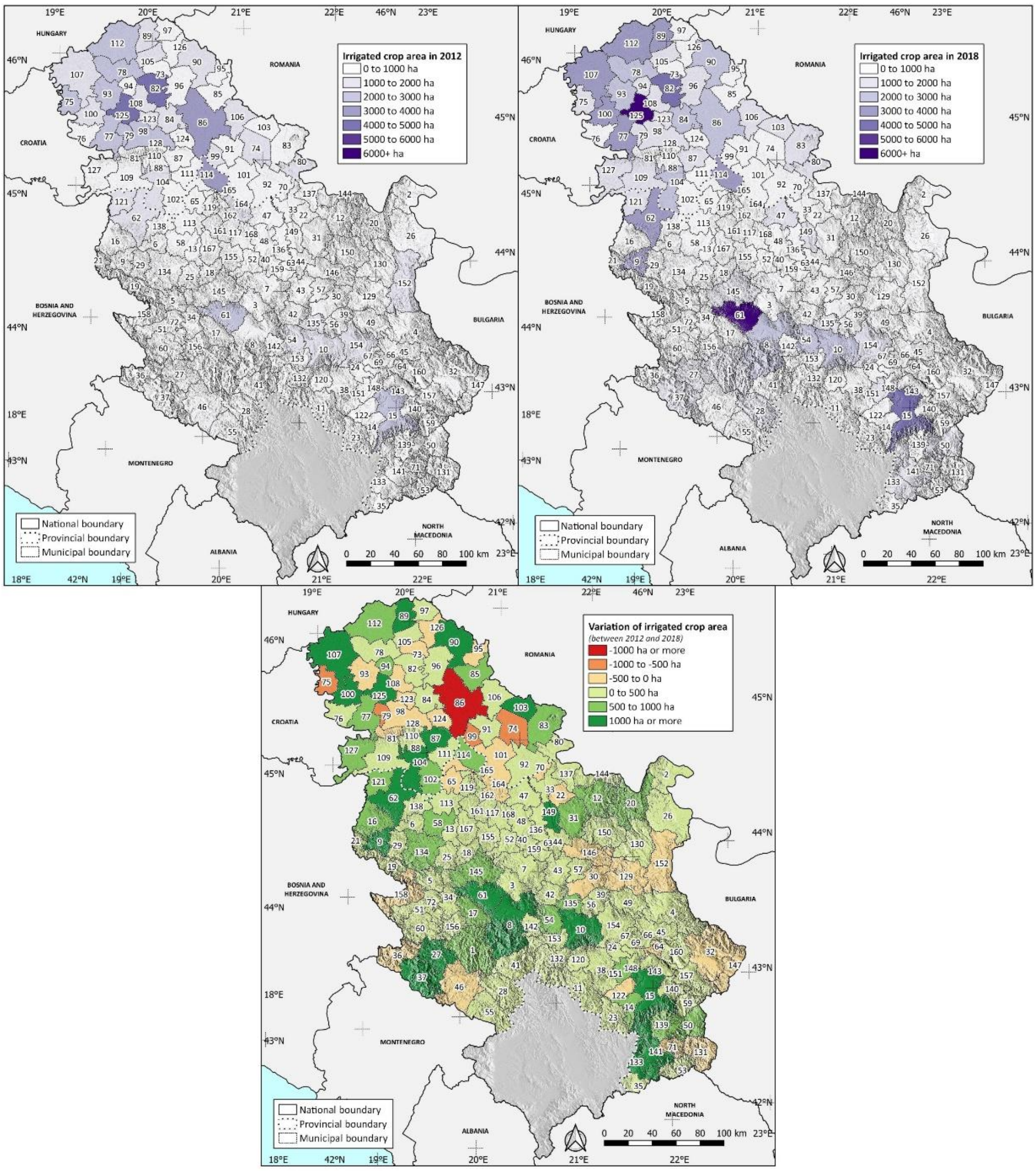

Between 2012 and 2018, irrigated crop area (regardless of crop type) increased for a large number of municipalities of the Republic of Serbia. The rest of the municipalities stayed somewhat stable in their irrigated crop area, with five notable exceptions: Apatin (75), Bački Petrovac (79), Zrenjanin (86), Opovo (99) and Alibunar (74) where the total irrigated crop area decreased. All of these five municipalities are located North of the Sava-Danube axis.

Although the increase of irrigated crops area is ubiquitous in the Republic of Serbia, the bulk of the irrigated area is located to the North of the Sava-Danube Axis (more than 3000 ha of irrigated crops area per municipality on average). in the rest of the country, most of the municipalities support less than 1000 ha of irrigated area. Things are changing rapidly however, and, in 2018, a couple of notable exception could be observed in the South: Čačak (61) (more than 6000 ha of irrigated crops), Leskovac (15) (more than 4000 ha of irrigated crops), and Kraljevo (8), Trstenik (54), and Kruševac (10) (more than 2000 ha or irrigated crops each.)

Vegetable crops

The trends and distribution of irrigated vegetable crops in the Republic of Serbia are presented in Figure 22.

Between 2012 and 2018, irrigated vegetable crops area increased in a large amount of the municipalities of the Republic of Serbia. This increased ranged between +50 ha to +150 ha and more by municipality. a few notable exceptions, Bačka Topola (78), Bečej (82), Temerin (123) can be mentioned, where the irrigated vegetable crop area decreased by more than 150 ha.

In terms of absolute value, where only 3 municipalities of the Republic of Serbia had more than 500 ha of irrigated vegetable crop area in 2012, in 2018 the number more than tripled, with a dozen municipality supporting more than 500 ha, and 3 more than 1500 ha. Although most of the municipalities supporting a large surface of irrigated vegetables crops area are located in the North of the country, the municipality presenting the largest irrigated vegetable area is located in the south: Leskovac (15), supporting more than 2000 ha of irrigated vegetable crops.

Figure 22 – Trends and distribution of irrigated vegetable crops areas by municipality in the Republic of Serbia
Distribution in 2012 and 2018, and distribution of the variation between these two dates. Data source: Census of Agriculture 2012 (Statistical Office of the Republic of Serbia, 2012) and Farm Structures Survey 2018 (Statistical Office of the Republic of Serbia, 2018)

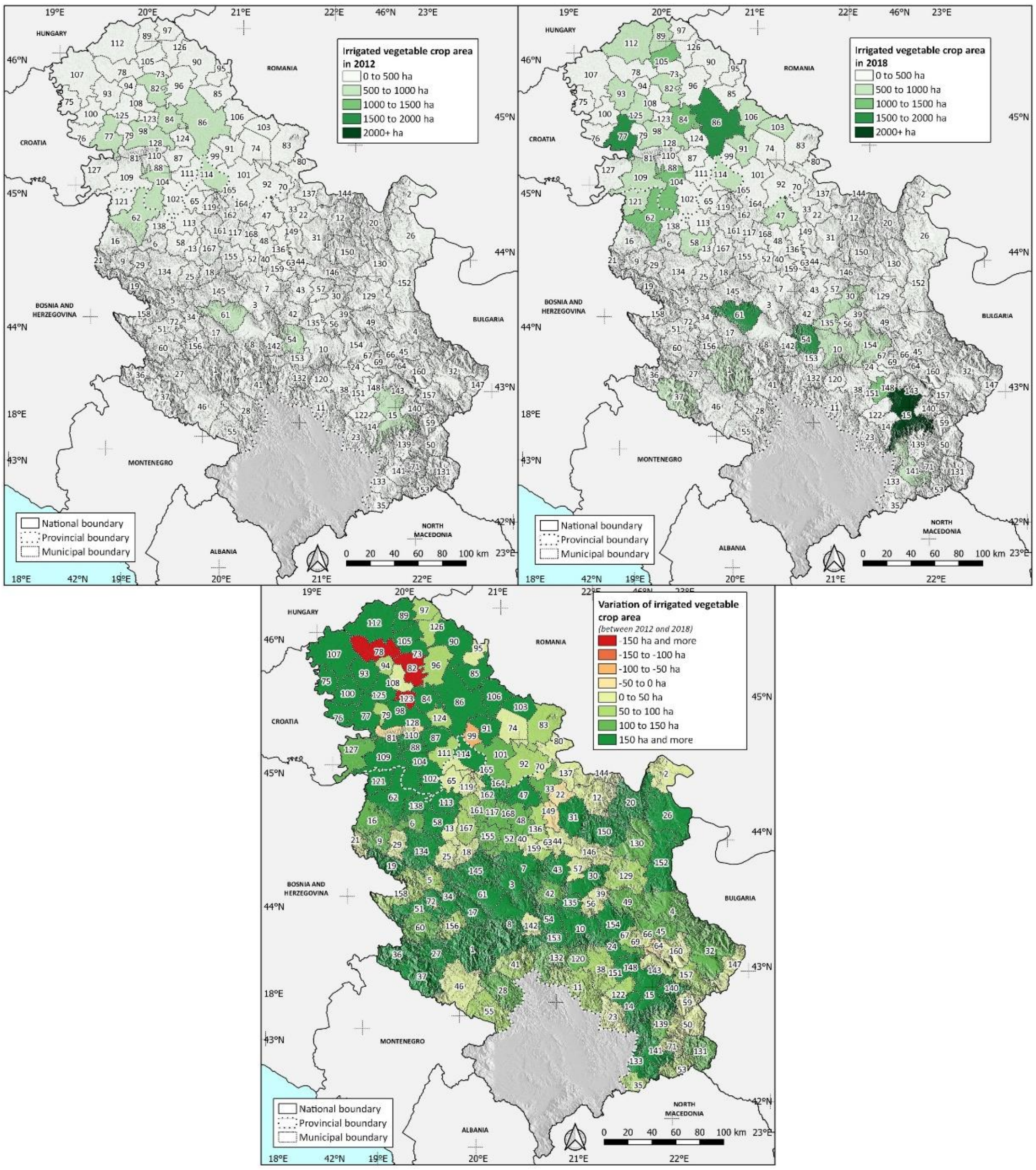

Fruits and grapes plantations

The trends and distribution of irrigated fruits and grapes plantation in the Republic of Serbia are presented in Figure 23.

Between 2012 and 2018, irrigated fruits and grapes plantations area have increased or stayed stable in Serbia. The increase is mainly located in the western municipalities, where the increase reached 200 ha to 400 ha on average. This figure decreased in only one municipality: Grocka (164) a municipality of Belgrade. There, the decrease reached more than 400 ha.

In terms of absolute values, where only 5 municipalities supported more than 600 ha of irrigated fruits and grapes plantations in 2012, in 2018, this figure more than tripled. Notably, 3 municipality presented in 2018 more than 1500 ha of irrigated fruits and grapes plantation area: Subotica (112), Šabac (62), and Čačak (61).

Figure 23 - Distribution of irrigated fruits and grapes plantations areas by municipality in the Republic of Serbia
Distribution in 2012 and 2018, and distribution of the variation between these two dates. Data source: Census of Agriculture 2012 (Statistical Office of the Republic of Serbia, 2012) and Farm Structures Survey 2018 (Statistical Office of the Republic of Serbia, 2018)

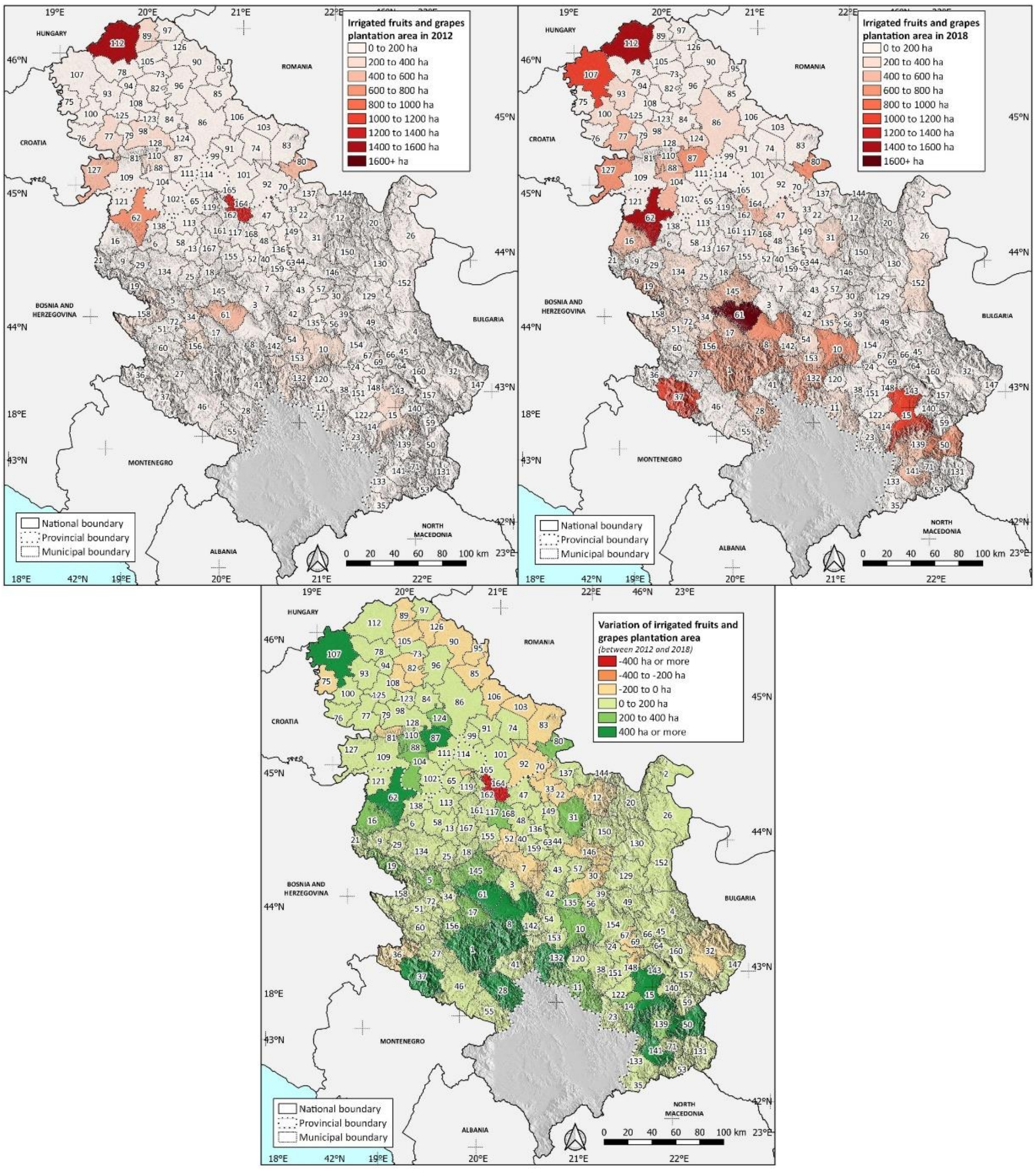

Irrigated arable & forage crop area

The trends and distribution of irrigated arable and forage crops in the Republic of Serbia are presented in Figure 24.

Most of the irrigated arable and forage crops of the Republic of Serbia were located to the North of the Sava-Danube axis in 2012 and 2018. In terms of irrigated crop area, the trends were quite stable for arable and forage crops Indeed, between 2012 and 2018, most of the municipalities in Serbia presented a stable irrigated arable and forage crop area, while a few showed a slight decrease (Zrenjanin (86), Zaječar (152), Apatin (75), Kula (93), Alibunar (74), Bački Petrovac (79), Opovo (99) and Zaječar (152)), and a few showed a slight increase (Sombor (107), Kanjiža (89), Kikinda (90), Odžaci (100), Vrbas (125), and Krupanj (9)).

Figure 24 - Distribution of irrigated arable and forage crops areas by municipality in the Republic of Serbia
Distribution in 2012 and 2018, and distribution of the variation between these two dates. <u>Data source:</u> Census of Agriculture 2012 (Statistical Office of the Republic of Serbia, 2012) and Farm Structures Survey 2018 (Statistical Office of the Republic of Serbia, 2018)

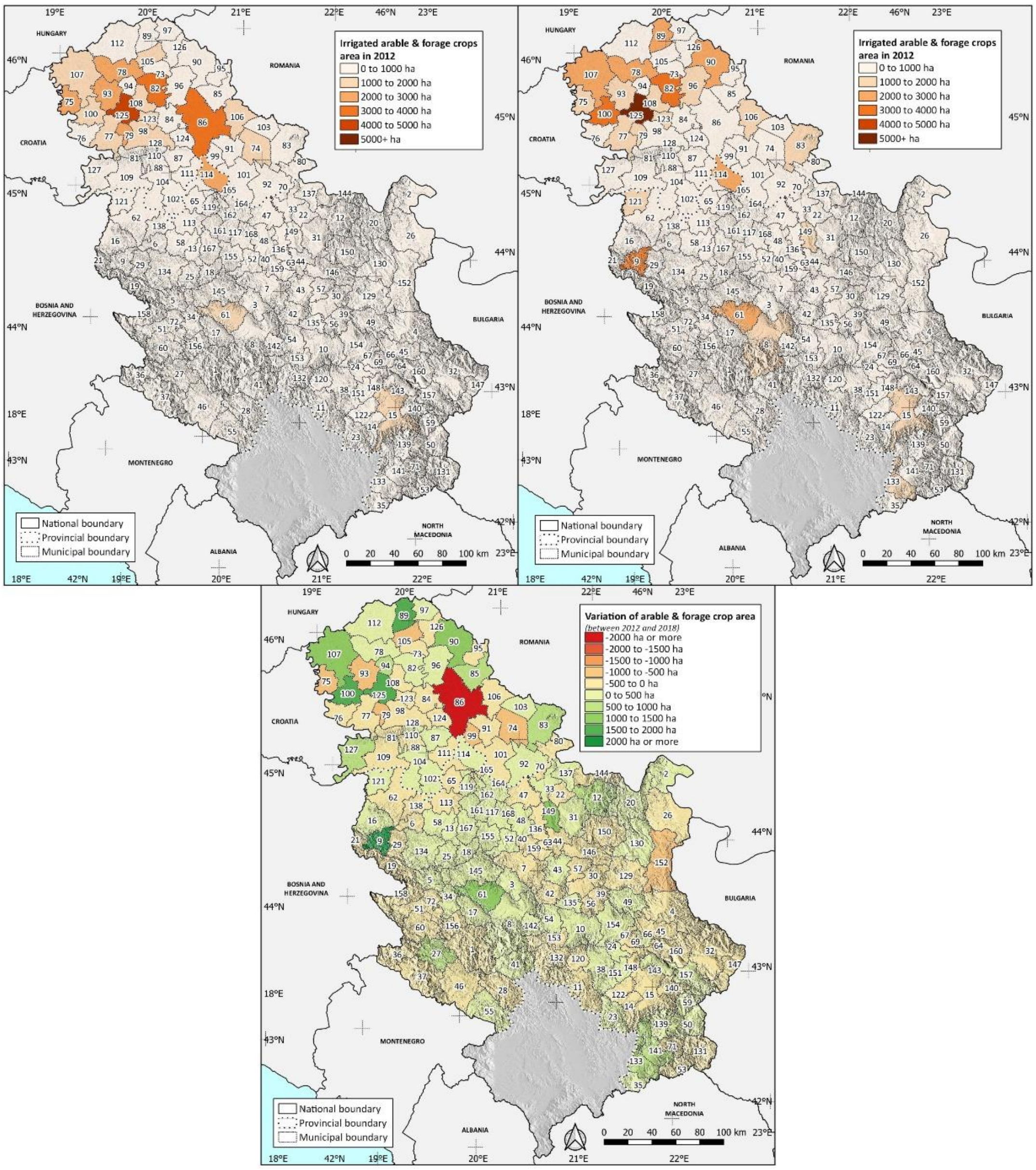

CLIMATE

7. Climate data sources

In this section, and all through this atlas, we will compare 4 sources of climatic data: 2 historical data sources, and 2 projected data sources.

Historical data sources

To characterize historical climatic conditions in Serbia we will use 3 different sources of data:

- **Local Weather Stations:** data measured by local weather stations, published in the meteorological yearbooks of the Republic Hydrometeorological Service of Serbia, Hidmet (Republic Hydrometeorological Service of Serbia, 2020). The database comprises 29 weather station throughout Serbia: *Banatski Karlovac, Belgrade, Crni Vrh, Ćuprija, Dimitrovgrad, Kikinda, Kopaonik, Kragujevac, Kraljevo, Kruševac, Kuršumlija, Leskovac, Loznica, Negotin, Niš, Palić, Požega, Rimski Šančevi, Sjenica, Smederevska Palanka, Sombor, Sremska Mitrovica, Valjevo, Veliko Gradište, Vranje, Vršac, Zaječar, Zlatibor and Zrenjanin* (see Figure 25).
  Only monthly weather station data were available. Therefore, daily, or hourly based variables (such as wet days or chill hours) could not be calculated using this source of data. These variables were thus calculated using only ERA5 data.
- **ERA5:** fifth generation ECMWF (European Centre for Medium-Range Weather Forecasts) atmospheric reanalysis of the global climate. The reanalysis combines model data with observations from across the world into a globally complete and consistent dataset (Muñoz Sabater, 2019).
- **Terra Net Evapotranspiration:** This product provides the Evapotranspiration and potential evapotranspiration data for our analysis. The algorithm used is based on the logic of the Penman-Monteith equation, which includes inputs of daily meteorological reanalysis data along with MODIS remotely sensed data products such as vegetation property dynamics, albedo, and land cover (Running et al., 2021).
- **GLDAS:** Global Land Data Assimilation System (GLDAS) will be used to provide snowfall and snow depth data for our analysis. This product ingests satellite and ground-based observational data products. Using advanced land surface modeling and data assimilation techniques, it generates optimal fields of land surface states and fluxes (Rodell et al., 2004).
- **MODIS:** MODIS database will be used to provide Leaf Area Index (LAI), Normalize Difference Vegetation Index (NDVI) and Vegetation Productivity (VP) data for our analysis. These variables are derived from MODIS products (Didan, 2015; Myneni et al., 2015)
- **European Environment Agency (EEA):** The start and the length of the growth season in Serbia was collected from the EEA database. These variables were calculated by the EEA using the Plant Phenology Index (European Environment Agency (EEA), March-21-2021).

Projected data sources

To characterize future climatic conditions in Serbia we will use 2 different sources of data:

- **NEX:** NASA Earth Exchange - Global Daily Downscaled Climate Projections (NEX – GDDP) dataset, comprising of 20 downscaled climate scenarios for the globe that are derived from the General Circulation Model runs conducted under the Coupled Model Intercomparison Project Phase 5 (CMIP5,(Taylor et al., 2012)). These models are: *BNU-ESM, CCSM4, CESM1-BGC, CNRM-CM5, CSIRO-Mk3-6-0, CanESM2, GFDL-CM3, GFDL-ESM2G, GFDL-ESM2M, IPSL-*

CM5A-LR, IPSL-CM5A-MR, MIROC-ESM-CHEM, MIROC-ESM, MIROC5, MPI-ESM-LR, MPI-ESM-MR, MRI-CGCM3, NorESM1-M, bcc-csm1-1 and inmcm4 (Thrasher et al., 2012).
Both RCP4.5 and RCP8.5 scenarios were considered for each model.

Figure 25 – Location of the 29 Weather stations considered in the atlas
Overlayed on a topographical map. Data source: Hidmet (Republic Hydrometeorological Service of Serbia, 2020) and NASA / USGS / JPL-Caltech (Farr et al., 2007).

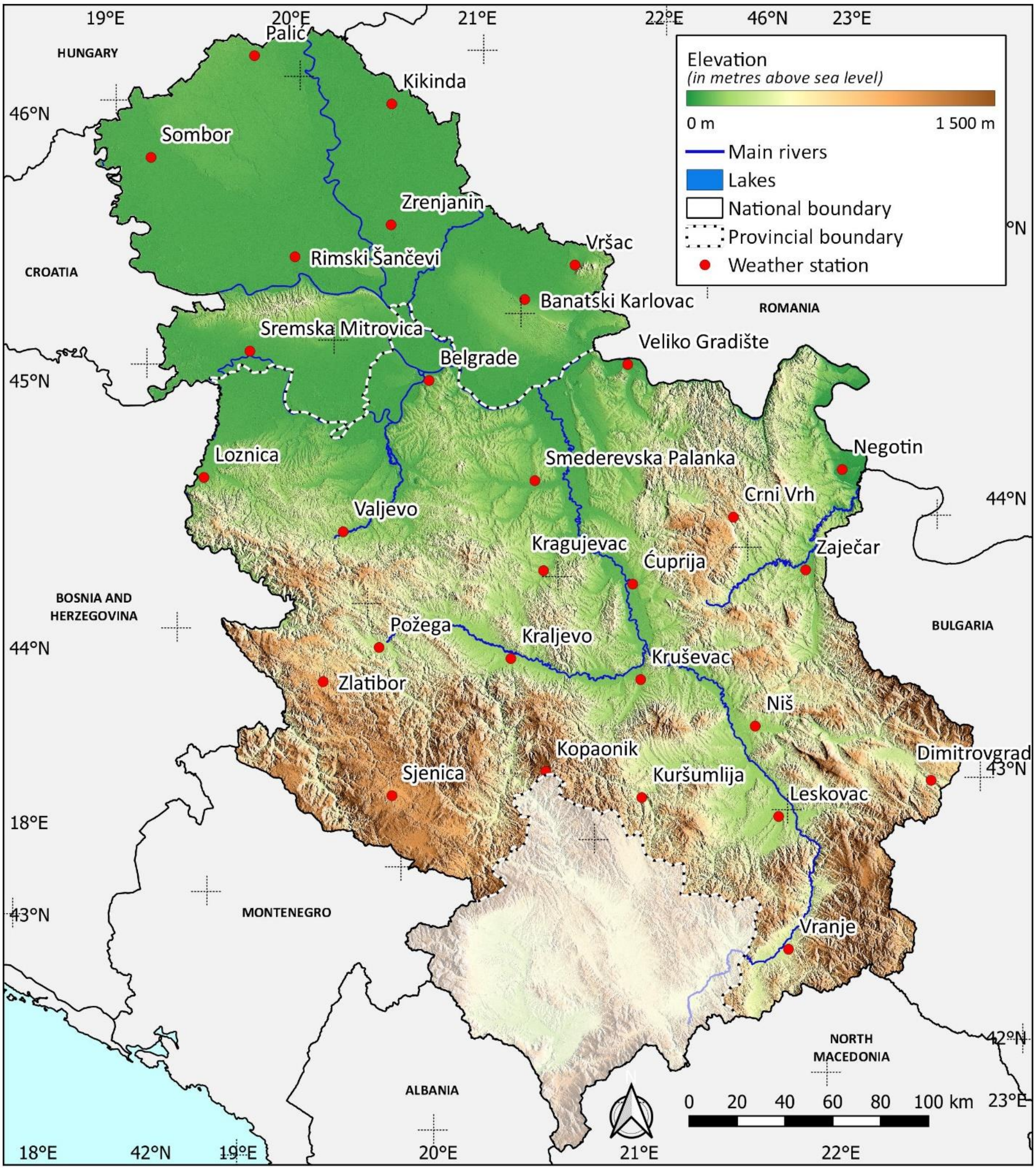

8. Average, minimum, and maximum temperature

This section will present the variation of temperatures in the Republic of Serbia, focusing on:

- Annual **average** temperature (TG_y), and monthly **average** temperature (TG_m)
- Annual **maximum** temperature (TX_y), and monthly **maximum** temperature (TX_m)
- Annual **minimum** temperature (TN_y), and monthly **minimum** temperature (TN_m)

Current seasonal variation

The current seasonal variations of the monthly average, maximum and minimum temperatures in the Republic of Serbia are presented in Figure 26. This chart presents TG_m, TX_m and TN_m, averaged over 30 years (1990 to 2019).

Figure 26 – Current monthly variations of the monthly average, minimum and maximum temperatures
*Data averaged over the 1990-2019 period. **Light dotted line**: variable value from each weather station separately. **Dark full line:** median value of the variable. **In yellow:** monthly maximum temperature. **In green:** monthly average temperature. **In blue:** monthly minimum temperature. **In red dashed line:** variable value using ERA5 database. <u>Data source:</u> Republic Hydrometeorological Service of Serbia, Hidmet (Republic Hydrometeorological Service of Serbia, 2020) and ERA5 - ECMWF / Copernicus Climate Change Service (Muñoz Sabater, 2019).*

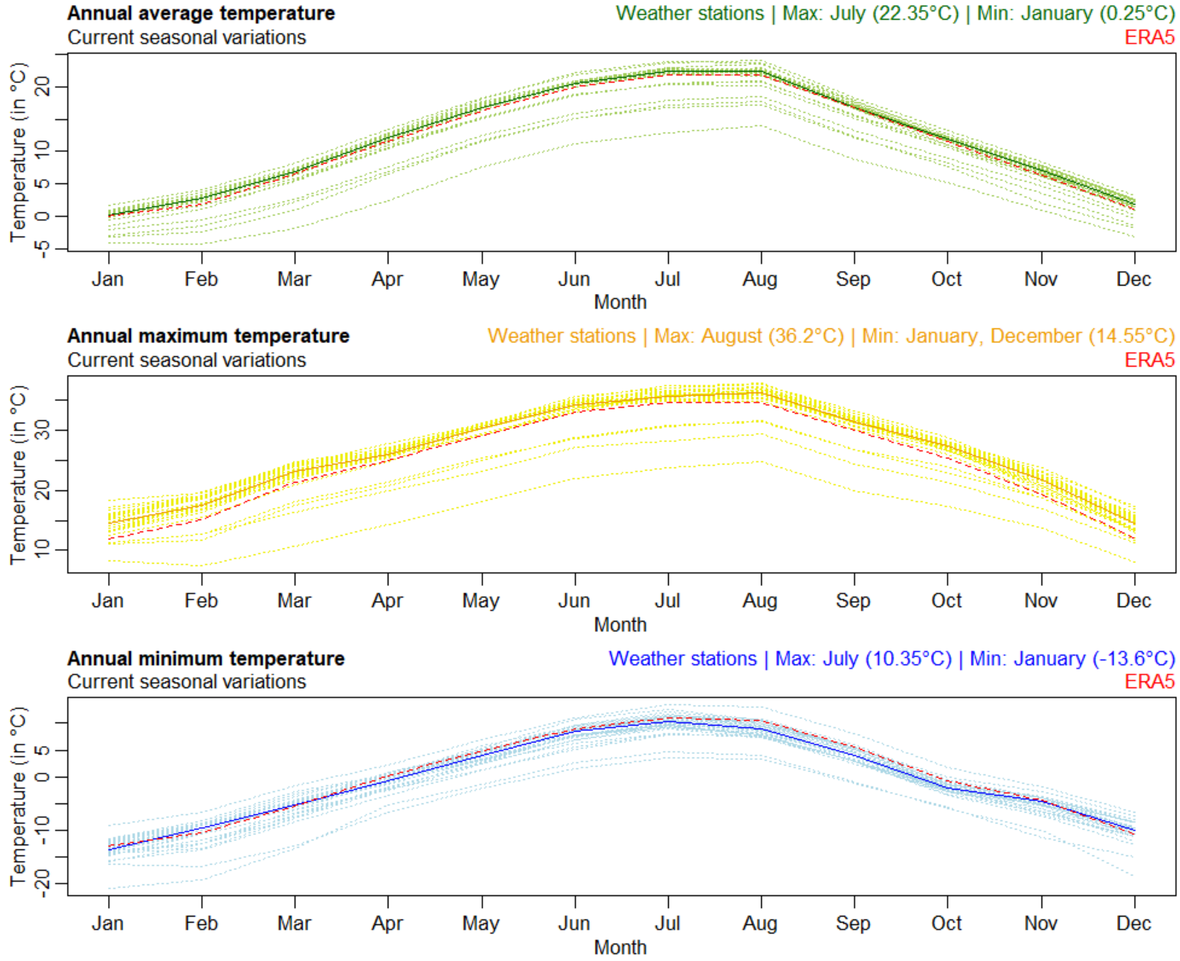

On average over the 30 years period, the monthly average, minimum and maximum temperatures followed a steady increase between a minimum in January (TG_m around 0°C, TX_m around 14°C, TN_m around -13°C) to a maximum in July and August (TG_m around 22°C, TX_m around 36°C, TN_m around 10°C), and a steady decrease from august to January.

Regarding data sources, ERA5 present a good fit to the local weather stations temperature data, with only an underestimation of TX_m and a slight overestimation of TN_m.

Spatial distribution

The current seasonal spatial distribution of temperatures throughout Serbia can be observed in Figure 27 and Figure 28. In terms of geographic distribution, average, maximum and minimum temperature presents an even distribution throughout the country all through the temperature increase period (January to July) and temperature decrease period (August to December).

Figure 27 – Current spatial distribution of monthly average temperature
Data averaged over the 1990-2019 period. Data source: ERA5 - ECMWF / Copernicus Climate Change Service (Muñoz Sabater, 2019).

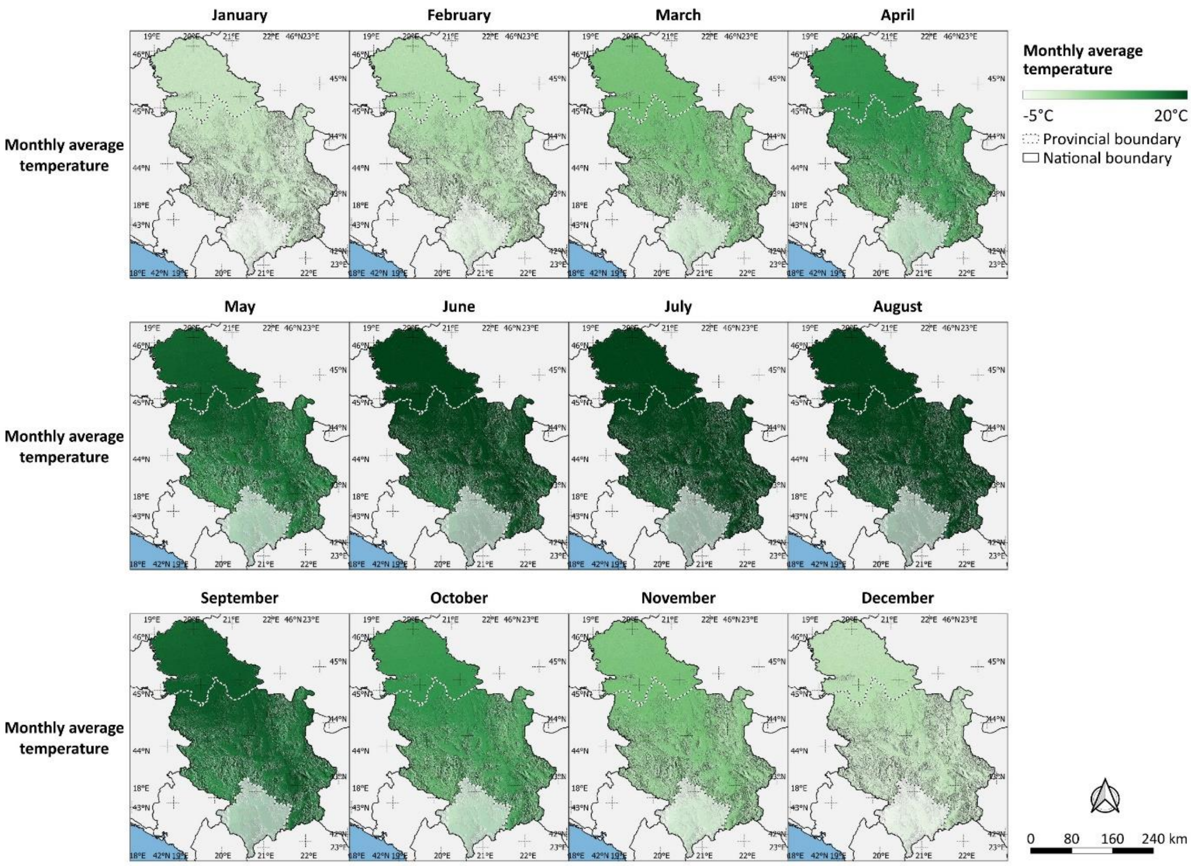

Figure 28 – current spatial distribution of monthly minimum and maximum temperatures

*Data averaged over the 1990-2019 period. **In orange:** monthly maximum temperature, **In blue:** monthly minimum temperature. <u>Data source:</u> ERA5 - ECMWF / Copernicus Climate Change Service (Muñoz Sabater, 2019).*

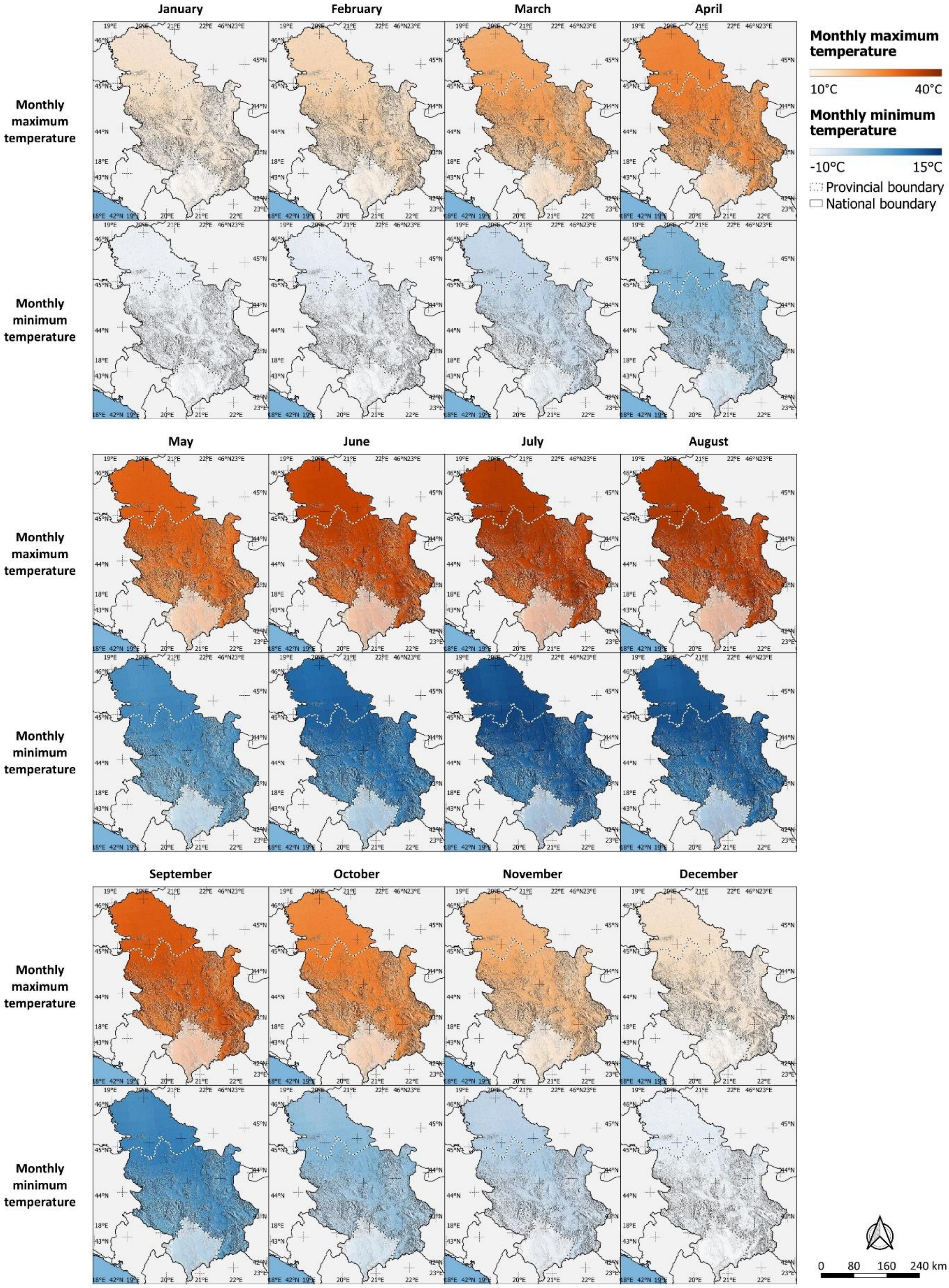

Historical monthly trends

Historical monthly trends of average, minimum and maximum temperatures can be observed in Figure 29, Figure 30, Figure 31, and Table 3.

Figure 29 – Historical time series of monthly average temperatures

Time series over 1980-2019 period. ***Light green dotted line****: variable value from each weather station separately.* ***Dark green full line:*** *median value of the variable.* ***Red dashed line:*** *variable value using ERA5 database. Data source: Republic Hydrometeorological Service of Serbia, Hidmet (Republic Hydrometeorological Service of Serbia, 2020) and ERA5 - ECMWF / Copernicus Climate Change Service (Muñoz Sabater, 2019).*

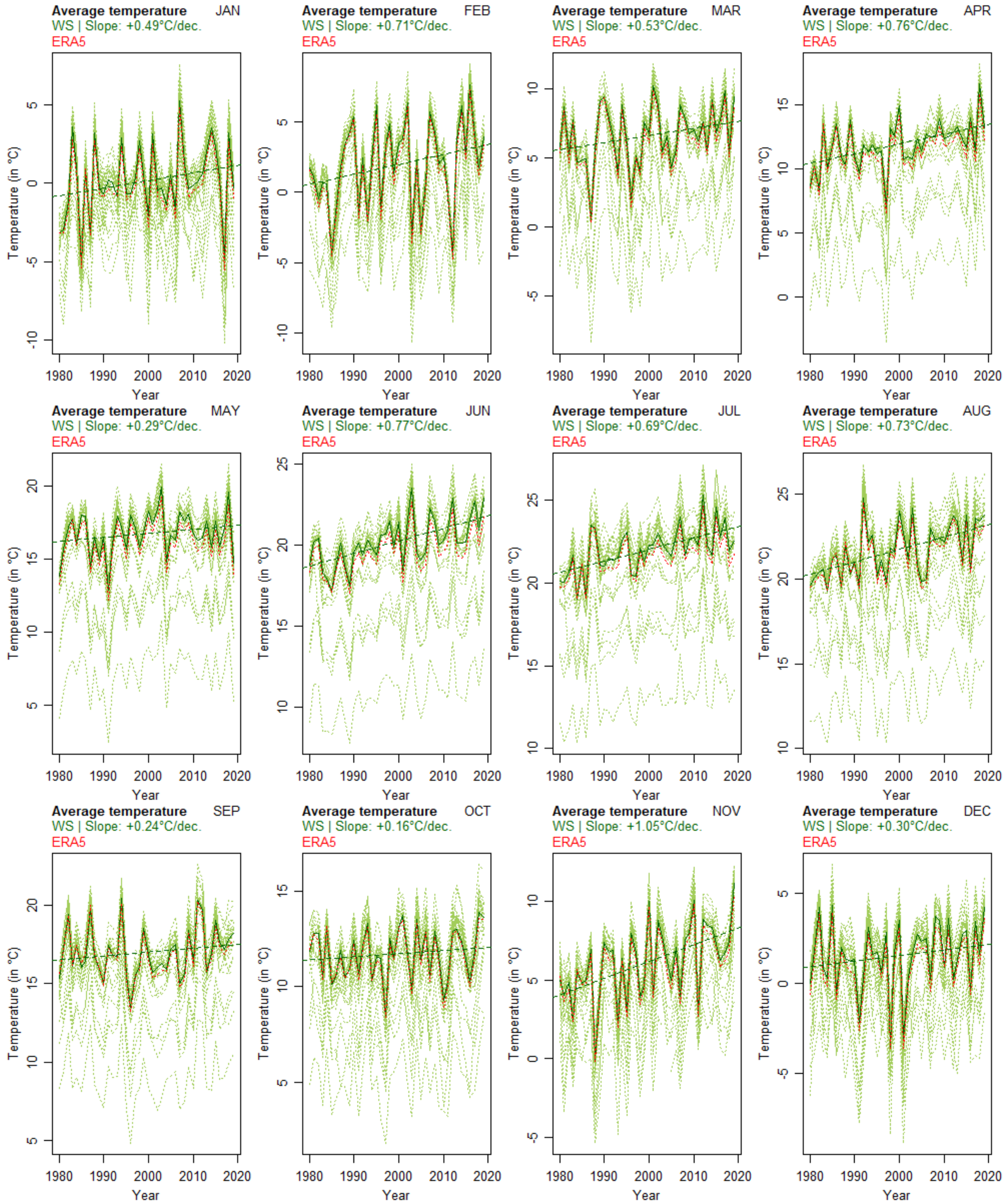

Figure 30 – Historical time series of monthly maximum temperatures

*Time series over 1980-2019 period. **Yellow dotted line**: variable value from each weather station separately. **Orange full line:** median value of the variable. **Red dashed line:** variable value using ERA5 database. Data source: Republic Hydrometeorological Service of Serbia, Hidmet (Republic Hydrometeorological Service of Serbia, 2020) and ERA5 - ECMWF / Copernicus Climate Change Service (Muñoz Sabater, 2019).*

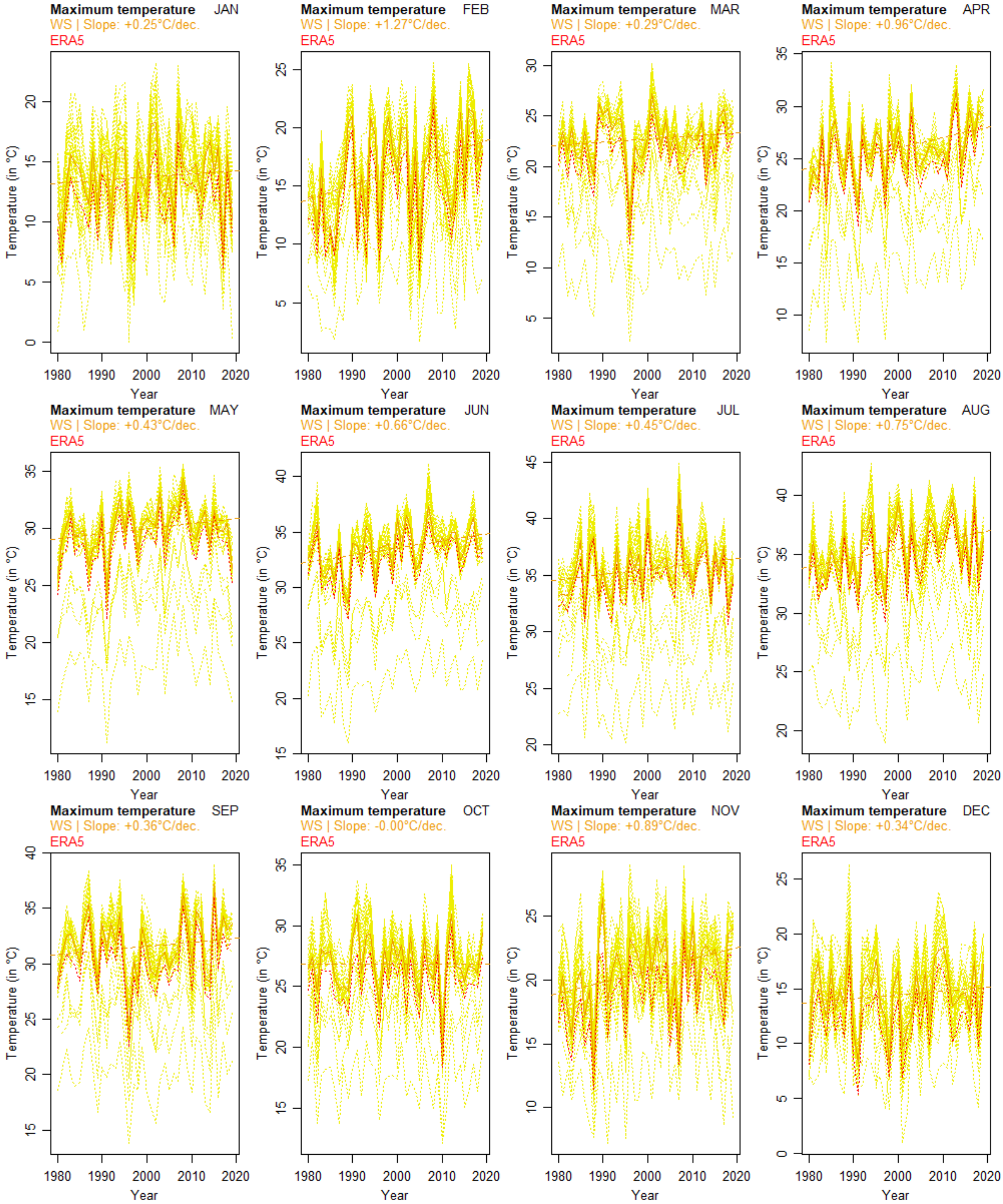

Figure 31 – Historical time series of monthly minimum temperatures

*Time series over 1980-2019 period. **Light blue dotted line**: variable value from each weather station separately. **Dark blue full line:** median value of the variable. **Red dashed line:** variable value using ERA5 database. Data source: Republic Hydrometeorological Service of Serbia, Hidmet (Republic Hydrometeorological Service of Serbia, 2020) and ERA5 - ECMWF / Copernicus Climate Change Service (Muñoz Sabater, 2019).*

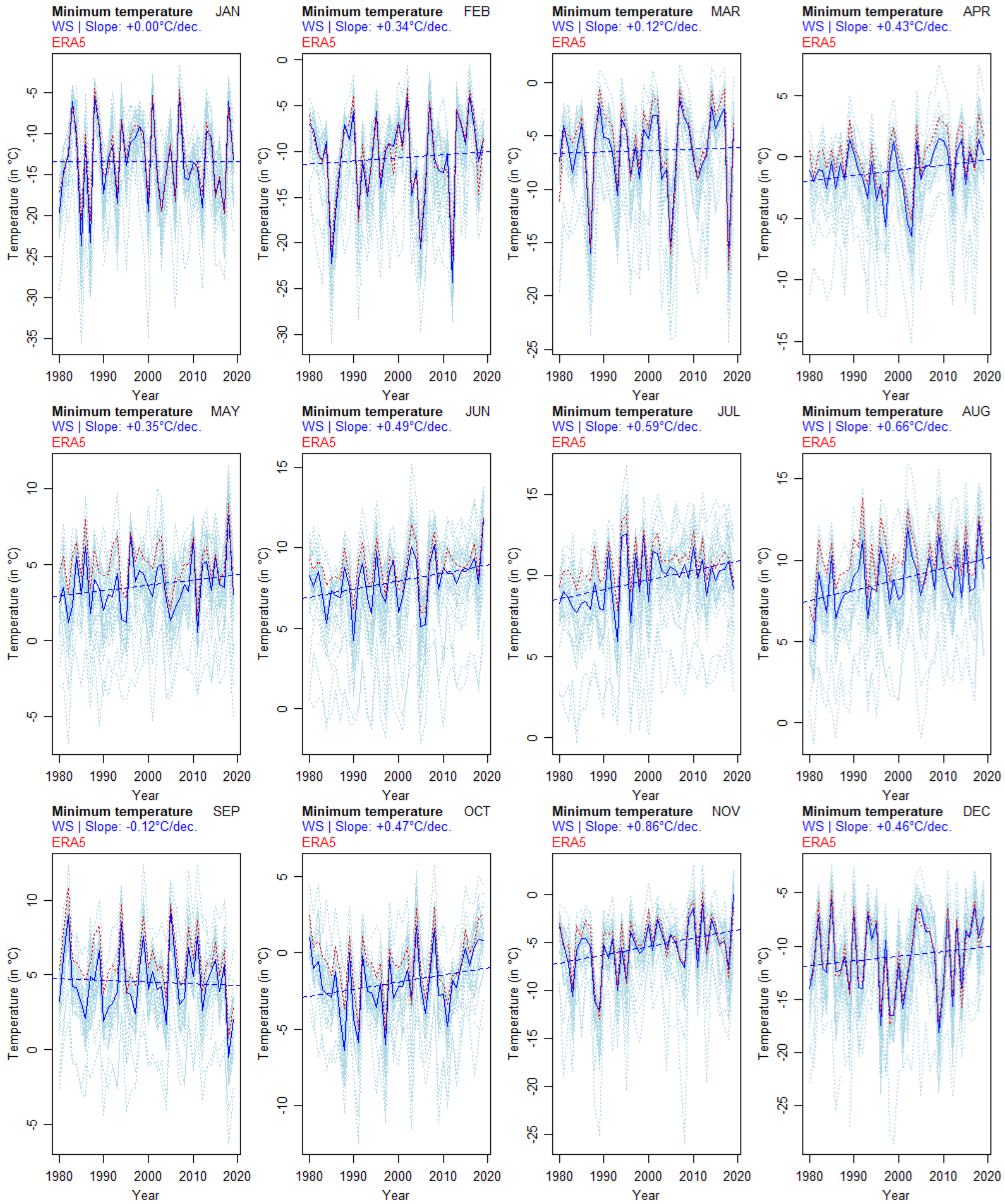

Table 3 – Characteristics of the trends from the historical time series of the monthly average, minimum and maximum temperatures (linear models)

***In green**: Monthly average temperature. **In yellow:** monthly maximum temperature. **In blue:** monthly minimum temperature. Data source: Republic Hydrometeorological Service of Serbia, Hidmet (Republic Hydrometeorological Service of Serbia, 2020).*

Variable	Month	Slope	p-value	Adjusted R^2	Average value in 1980	Average value in 2019
TG_m	January	+0.49°C/dec.	0.12	0.04	-0.79°C	1.11°C
TG_m	February	+0.71°C/dec.	0.08	0.05	0.55°C	3.33°C
TG_m	March	+0.53°C/dec.	0.07	0.06	5.55°C	7.62°C
TG_m	April	+0.76°C/dec.	0.00	0.23	10.39°C	13.36°C
TG_m	May	+0.29°C/dec.	0.16	0.03	16.19°C	17.30°C
TG_m	June	+0.77°C/dec.	0.00	0.36	18.72°C	21.73°C
TG_m	July	+0.69°C/dec.	0.00	0.35	20.64°C	23.35°C
TG_m	August	+0.73°C/dec.	0.00	0.29	20.27°C	23.12°C
TG_m	September	+0.24°C/dec.	0.27	0.01	16.51°C	17.44°C
TG_m	October	+0.16°C/dec.	0.38	-0.01	11.41°C	12.04°C
TG_m	November	+1.05°C/dec.	0.00	0.25	4.10°C	8.19°C
TG_m	December	+0.30°C/dec.	0.24	0.01	0.92°C	2.10°C
TX_m	January	+0.25°C/dec.	0.51	-0.01	13.23°C	14.21°C
TX_m	February	+1.27°C/dec.	0.01	0.13	13.82°C	18.78°C
TX_m	March	+0.29°C/dec.	0.36	0.00	22.14°C	23.29°C
TX_m	April	+0.96°C/dec.	0.01	0.16	24.10°C	27.86°C
TX_m	May	+0.43°C/dec.	0.12	0.04	29.09°C	30.77°C
TX_m	June	+0.66°C/dec.	0.01	0.13	32.23°C	34.79°C
TX_m	July	+0.45°C/dec.	0.16	0.03	34.64°C	36.39°C
TX_m	August	+0.75°C/dec.	0.02	0.11	33.91°C	36.85°C
TX_m	September	+0.36°C/dec.	0.32	0.00	30.82°C	32.24°C
TX_m	October	-0.00°C/dec.	0.99	-0.03	26.87°C	26.85°C
TX_m	November	+0.89°C/dec.	0.02	0.11	18.96°C	22.43°C
TX_m	December	+0.34°C/dec.	0.39	-0.01	13.75°C	15.09°C
TN_m	January	+0.00°C/dec.	1.00	-0.03	-13.42°C	-13.41°C
TN_m	February	+0.34°C/dec.	0.61	-0.02	-11.35°C	-10.04°C
TN_m	March	+0.12°C/dec.	0.81	-0.02	-6.63°C	-6.16°C
TN_m	April	+0.43°C/dec.	0.12	0.04	-1.97°C	-0.31°C
TN_m	May	+0.35°C/dec.	0.14	0.03	2.94°C	4.30°C
TN_m	June	+0.49°C/dec.	0.02	0.12	6.93°C	8.86°C
TN_m	July	+0.59°C/dec.	0.00	0.17	8.56°C	10.85°C
TN_m	August	+0.66°C/dec.	0.00	0.18	7.48°C	10.04°C
TN_m	September	-0.12°C/dec.	0.67	-0.02	4.76°C	4.27°C
TN_m	October	+0.47°C/dec.	0.09	0.05	-2.86°C	-1.02°C
TN_m	November	+0.86°C/dec.	0.02	0.12	-7.22°C	-3.85°C
TN_m	December	+0.46°C/dec.	0.35	0.00	-11.89°C	-10.09°C

Most of the months show an increase in monthly maximum, minimum and average temperature.

In terms of critical months, the largest increase in TG_m can be observed for the months of November (+1.0°C/decade), April (+0.8°C/decade) and June (+0.8°C/decade). For TX_m, the largest increase can be observed for the months of February (+1.3°C/decade), April (+1.0°C/decade) and November (+0.9°C/decade). Finally, for TN_m, critical months seems to be November (+0.9°C/decade), August (+0.7°C/decade) and July (+0.6°C/decade).

Overall, the month of November seem to be the month with the clearer increase for the 3 temperatures.

Historical annual trends

Historical annual trends of average, minimum and maximum temperatures can be observed in Figure 32 and Table 4.

Figure 32 – Historical time series of annual average, minimum and maximum temperatures
*Time series over 1980-2019 period. **Light dotted line**: variable value from each weather station separately. **Dark full line:** median value of the variable. **In yellow:** monthly maximum temperature. **In green:** monthly average temperature. **In blue:** monthly minimum temperature. **In red dashed line:** variable value using ERA5 database. <u>Data source:</u> Republic Hydrometeorological Service of Serbia, Hidmet (Republic Hydrometeorological Service of Serbia, 2020) and ERA5 - ECMWF / Copernicus Climate Change Service (Muñoz Sabater, 2019).*

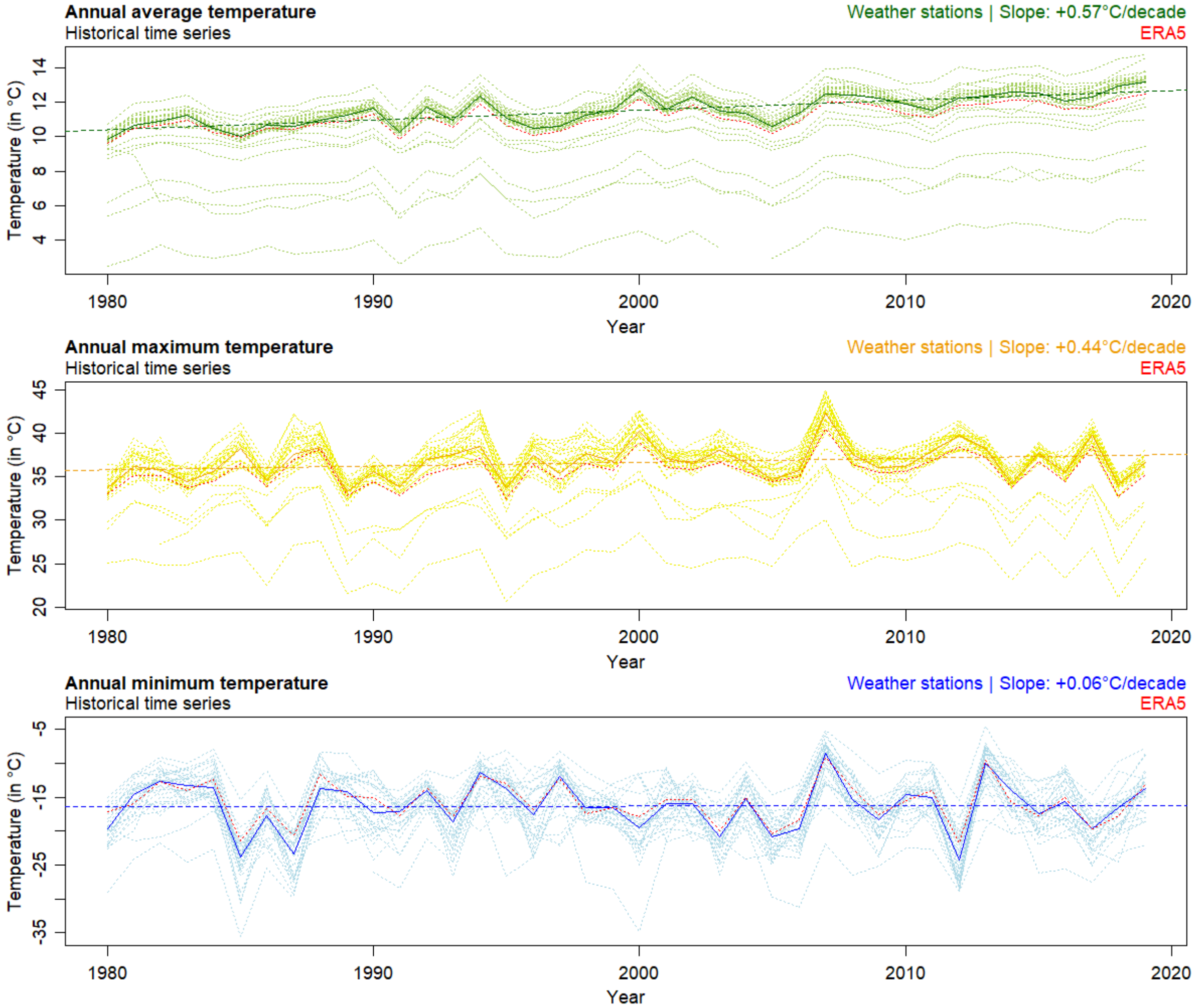

Table 4 – Characteristics of the trend of historical annual time series of average, minimum and maximum temperature (linear models)
Data source: Republic Hydrometeorological Service of Serbia, Hidmet (Republic Hydrometeorological Service of Serbia, 2020).

Variable	Slope	p-value	Adjusted R^2	Average value in 1980	Average value in 2019
TG_y	+0.57°C/decade	0.00	0.59	10.41°C	12.64°C
TX_y	+0.44°C/decade	0.10	0.04	35.79°C	37.53°C
TN_y	+0.06°C/decade	0.91	-0.03	-16.44°C	-16.21°C

Annual average temperature (TG_y) showed a clear increase in Serbia over the last 40 years (+0.6 °C/decade). TG_y presented an increase from around 10°C in 1980 to around 13°C in 2019. As can be expected of an averaged value, TG_y shows very small interannual variations ($p< 0.05$, adj. $R^2>0.5$).

The extremums were naturally more variable on a year-to-year basis, therefore presenting uncertain trends ($p>>0.05$, adjusted $R^2<<0.1$). The annual maximum temperature (TX_y) in Serbia increased (+0.4°C/decade) going from 36°C on average in 1980, to 37°C in 2019 on average. The annual minimum temperature (TN_y) stayed stable (+0.06°C/decade), staying in the vicinity of -16°C all through the 1980-2019 period.

Spatial distribution

The spatial distribution of the trends on average, minimum and maximum temperature throughout Serbia can be observed in Figure 33.

Figure 33 – Historical spatial distribution of annual average, minimum and maximum temperatures
*Data averaged over the 1980-2019 period, by decade**. In blue:** decadal averaged of the annually accumulated precipitation. **In orange:** decadal average of the annual average precipitation intensity. Data source: ERA5, ECMWF / Copernicus Climate Change Service (Muñoz Sabater, 2019).*

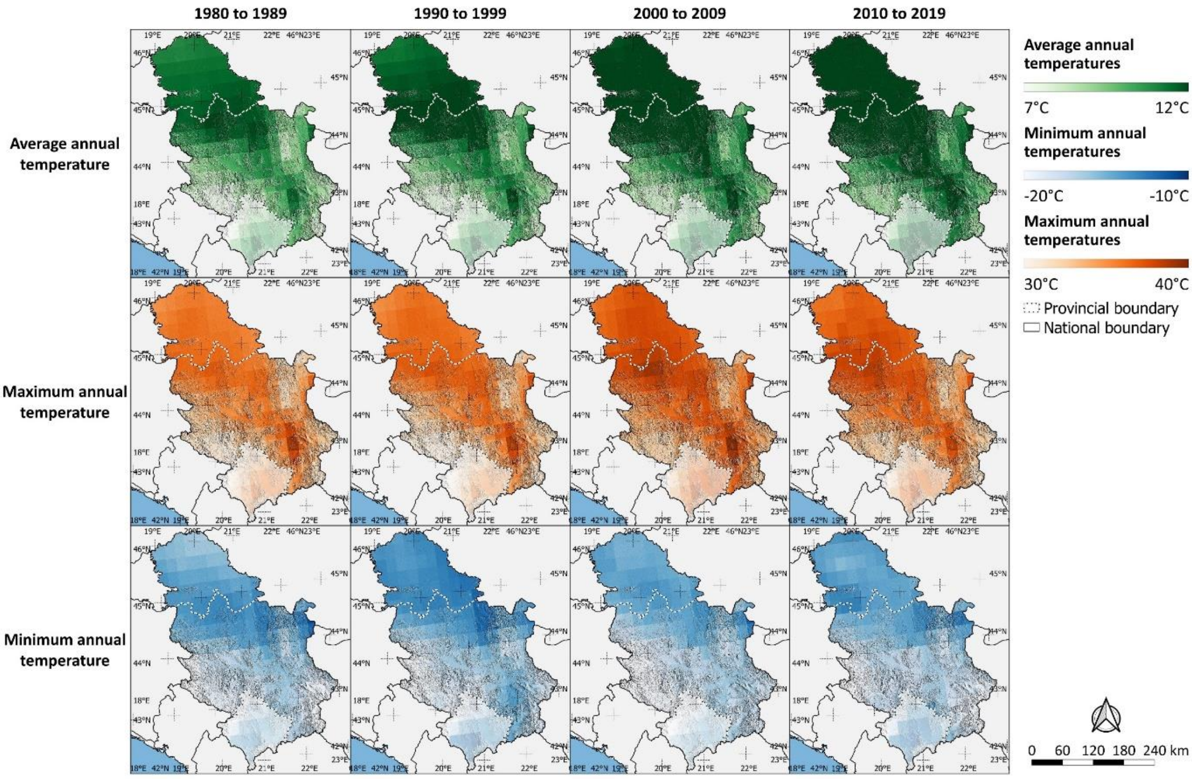

The spatial distribution is constant for average, minimum and maximum temperatures. Temperatures are higher at low altitude, in the plains of the North and the valleys of the South. This distribution is constant throughout the steady increase of temperatures.

Projected monthly trends

The monthly projected trends of average, minimum and maximum temperatures can be observed in Figure 34, Figure 35, Figure 36, Table 5 and Table 6.

Overall, most of the months are projected to increase in maximum, minimum and average temperature under both scenarios. This increase seems to be steeper under RCP8.5 scenario compared to RCP4.5 scenario.

In terms of critical months, the largest increase in TG_m can be observed for the months of August (+0.4°C/decade), September (+0.4°C/decade) and October (+0.3°C/decade) under RCP4.5 scenario, and August (+0.7°C/decade), July (+0.7°C/decade) and September (+0.6°C/decade) under RCP8.5 scenario.

For TX_m, the largest increase can be observed for the months of October (+0.5°C/decade), July (+0.5°C/decade) and June (+0.5°C/decade) under RCP4.5 scenario, and August (+0.8°C/decade), July (+0.8°C/decade) and September (+0.7°C/decade) under RCP8.5 scenario.

Finally, for TN_m, critical months seems to be September (+0.4°C/decade), March (+0.4°C/decade) and October (+0.4°C/decade) under RCP4.5 scenario, and August (+0.5°C/decade), September (+0.5°C/decade) and January (+0.5°C/decade) under RCP8.5 scenario.

Overall, it is the month at the end of the summer and the beginning of fall (July, august, September) that are projected to present the highest increase in temperatures.

Figure 34 – Projected time series of monthly average temperature

Time series over 2020-2060 period. ***Pink dotted line****: variable value for each model separately under the RCP4.5 scenario.* ***grey dotted line****: variable value for each model separately under the RCP8.5 scenario.* ***Purple full line:*** *median value of the variable under RCP4.5 scenario.* ***Black full line:*** *median value of the variable under RCP8.5 scenario. Data source: NASA Earth Exchange - Global Daily Downscaled Climate Projections (NEX – GDDP) (Thrasher et al., 2012).*

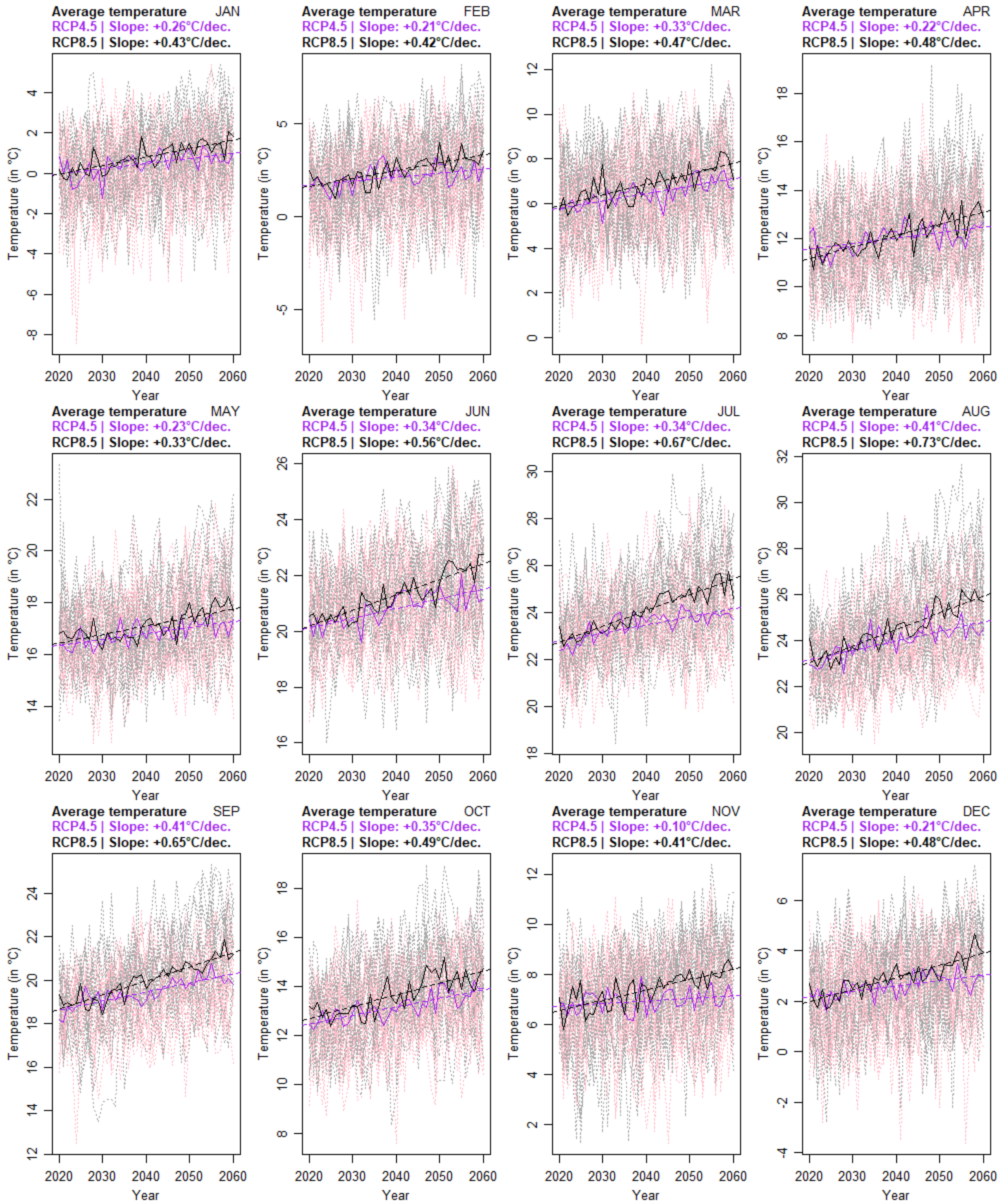

Figure 35 – Projected time series of monthly maximum temperature

Time series over 2020-2060 period. ***Pink dotted line****: variable value for each model separately under the RCP4.5 scenario.* ***grey dotted line****: variable value for each model separately under the RCP8.5 scenario.* ***Purple full line:*** *median value of the variable under RCP4.5 scenario.* ***Black full line:*** *median value of the variable under RCP8.5 scenario. Data source: NASA Earth Exchange - Global Daily Downscaled Climate Projections (NEX – GDDP) (Thrasher et al., 2012).*

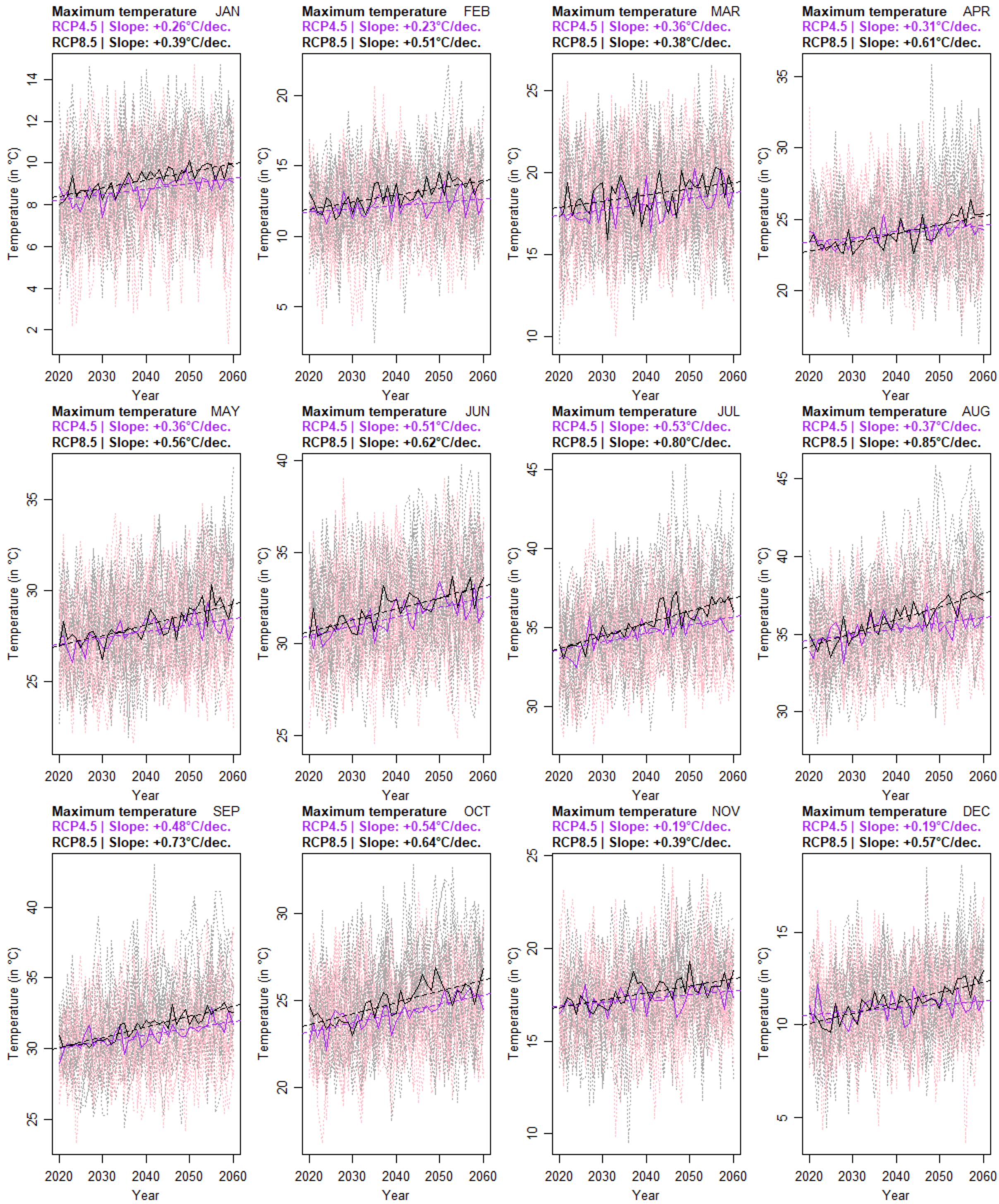

Figure 36 – Projected time series of monthly minimum temperatures

*Time series over 2020-2060 period. **Pink dotted line**: variable value for each model separately under the RCP4.5 scenario. **grey dotted line**: variable value for each model separately under the RCP8.5 scenario. **Purple full line:** median value of the variable under RCP4.5 scenario. **Black full line:** median value of the variable under RCP8.5 scenario. Data source: NASA Earth Exchange - Global Daily Downscaled Climate Projections (NEX – GDDP) (Thrasher et al., 2012).*

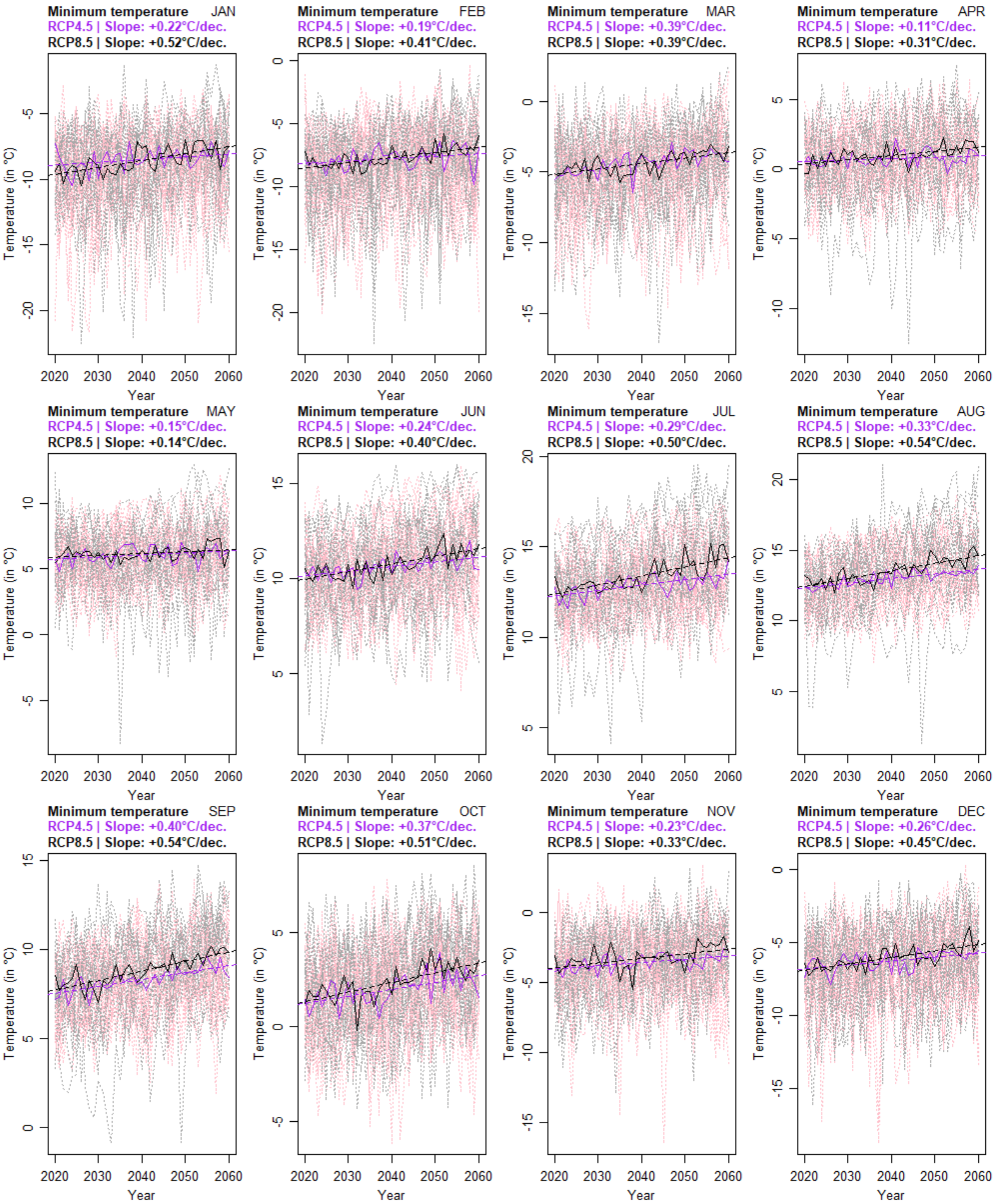

Table 5 – Characteristics of the trend from projected time series of monthly average, minimum and maximum temperature under the RCP4.5 scenario (linear models)
<u>Data source:</u> NASA Earth Exchange - Global Daily Downscaled Climate Projections (NEX – GDDP) (Thrasher et al., 2012).

RCP4.5						
Variable	**Month**	**Slope**	**p-value**	**Adj. R^2**	**Average value in 2040**	**Average value in 2060**
TG_m	January	+0.26°C/dec.	0.00	0.27	0.49°C	1.01°C
TG_m	February	+0.21°C/dec.	0.00	0.18	2.14°C	2.57°C
TG_m	March	+0.33°C/dec.	0.00	0.47	6.44°C	7.09°C
TG_m	April	+0.22°C/dec.	0.00	0.27	12.01°C	12.45°C
TG_m	May	+0.23°C/dec.	0.00	0.40	16.81°C	17.28°C
TG_m	June	+0.34°C/dec.	0.00	0.54	20.81°C	21.50°C
TG_m	July	+0.34°C/dec.	0.00	0.55	23.47°C	24.16°C
TG_m	August	+0.41°C/dec.	0.00	0.53	23.99°C	24.81°C
TG_m	September	+0.41°C/dec.	0.00	0.67	19.45°C	20.27°C
TG_m	October	+0.35°C/dec.	0.00	0.59	13.18°C	13.87°C
TG_m	November	+0.10°C/dec.	0.08	0.05	6.97°C	7.17°C
TG_m	December	+0.21°C/dec.	0.00	0.33	2.62°C	3.03°C
TX_m	January	+0.26°C/dec.	0.00	0.35	8.75°C	9.27°C
TX_m	February	+0.23°C/dec.	0.01	0.13	12.21°C	12.68°C
TX_m	March	+0.36°C/dec.	0.00	0.18	18.09°C	18.81°C
TX_m	April	+0.31°C/dec.	0.00	0.34	23.98°C	24.59°C
TX_m	May	+0.36°C/dec.	0.00	0.38	27.75°C	28.48°C
TX_m	June	+0.51°C/dec.	0.00	0.45	31.45°C	32.48°C
TX_m	July	+0.53°C/dec.	0.00	0.51	34.61°C	35.66°C
TX_m	August	+0.37°C/dec.	0.00	0.27	35.35°C	36.08°C
TX_m	September	+0.48°C/dec.	0.00	0.50	30.95°C	31.91°C
TX_m	October	+0.54°C/dec.	0.00	0.60	24.25°C	25.32°C
TX_m	November	+0.19°C/dec.	0.01	0.15	17.29°C	17.68°C
TX_m	December	+0.19°C/dec.	0.02	0.11	10.92°C	11.31°C
TN_m	January	+0.22°C/dec.	0.03	0.09	-8.50°C	-8.06°C
TN_m	February	+0.19°C/dec.	0.07	0.06	-7.76°C	-7.38°C
TN_m	March	+0.39°C/dec.	0.00	0.40	-4.38°C	-3.60°C
TN_m	April	+0.11°C/dec.	0.13	0.03	0.74°C	0.95°C
TN_m	May	+0.15°C/dec.	0.06	0.06	6.06°C	6.35°C
TN_m	June	+0.24°C/dec.	0.00	0.28	10.63°C	11.11°C
TN_m	July	+0.29°C/dec.	0.00	0.37	12.87°C	13.45°C
TN_m	August	+0.33°C/dec.	0.00	0.58	13.01°C	13.67°C
TN_m	September	+0.40°C/dec.	0.00	0.57	8.30°C	9.11°C
TN_m	October	+0.37°C/dec.	0.00	0.29	1.97°C	2.71°C
TN_m	November	+0.23°C/dec.	0.00	0.24	-3.55°C	-3.09°C
TN_m	December	+0.26°C/dec.	0.00	0.23	-6.25°C	-5.72°C

Table 6 – Characteristics of the trend from projected time series of monthly average, minimum and maximum temperature under the RCP8.5 scenario (linear models)
<u>Data source:</u> NASA Earth Exchange - Global Daily Downscaled Climate Projections (NEX – GDDP) (Thrasher et al., 2012).

RCP8.5						
Variable	**Month**	**Slope**	**p-value**	**Adj. R^2**	**Average value in 2040**	**Average value in 2060**
TG_m	January	+0.43°C/dec.	0.00	0.61	0.81°C	1.66°C
TG_m	February	+0.42°C/dec.	0.00	0.51	2.48°C	3.32°C
TG_m	March	+0.47°C/dec.	0.00	0.57	6.84°C	7.79°C
TG_m	April	+0.48°C/dec.	0.00	0.63	12.13°C	13.08°C
TG_m	May	+0.33°C/dec.	0.00	0.52	17.11°C	17.77°C
TG_m	June	+0.56°C/dec.	0.00	0.76	21.29°C	22.40°C
TG_m	July	+0.67°C/dec.	0.00	0.84	24.06°C	25.40°C
TG_m	August	+0.73°C/dec.	0.00	0.81	24.48°C	25.93°C
TG_m	September	+0.65°C/dec.	0.00	0.82	19.97°C	21.26°C
TG_m	October	+0.49°C/dec.	0.00	0.59	13.66°C	14.64°C
TG_m	November	+0.41°C/dec.	0.00	0.53	7.41°C	8.24°C
TG_m	December	+0.48°C/dec.	0.00	0.72	2.96°C	3.92°C
TX_m	January	+0.39°C/dec.	0.00	0.64	9.18°C	9.96°C
TX_m	February	+0.51°C/dec.	0.00	0.44	12.95°C	13.96°C
TX_m	March	+0.38°C/dec.	0.00	0.18	18.65°C	19.42°C
TX_m	April	+0.61°C/dec.	0.00	0.53	23.99°C	25.21°C
TX_m	May	+0.56°C/dec.	0.00	0.57	28.10°C	29.22°C
TX_m	June	+0.62°C/dec.	0.00	0.63	31.91°C	33.15°C
TX_m	July	+0.80°C/dec.	0.00	0.73	35.26°C	36.86°C
TX_m	August	+0.85°C/dec.	0.00	0.75	35.91°C	37.61°C
TX_m	September	+0.73°C/dec.	0.00	0.81	31.53°C	32.98°C
TX_m	October	+0.64°C/dec.	0.00	0.58	24.90°C	26.19°C
TX_m	November	+0.39°C/dec.	0.00	0.46	17.62°C	18.40°C
TX_m	December	+0.57°C/dec.	0.00	0.66	11.20°C	12.33°C
TN_m	January	+0.52°C/dec.	0.00	0.41	-8.56°C	-7.51°C
TN_m	February	+0.41°C/dec.	0.00	0.37	-7.68°C	-6.86°C
TN_m	March	+0.39°C/dec.	0.00	0.40	-4.39°C	-3.60°C
TN_m	April	+0.31°C/dec.	0.00	0.32	0.95°C	1.57°C
TN_m	May	+0.14°C/dec.	0.04	0.08	6.17°C	6.46°C
TN_m	June	+0.40°C/dec.	0.00	0.48	10.74°C	11.55°C
TN_m	July	+0.50°C/dec.	0.00	0.55	13.37°C	14.36°C
TN_m	August	+0.54°C/dec.	0.00	0.63	13.54°C	14.62°C
TN_m	September	+0.54°C/dec.	0.00	0.66	8.80°C	9.87°C
TN_m	October	+0.51°C/dec.	0.00	0.49	2.35°C	3.36°C
TN_m	November	+0.33°C/dec.	0.00	0.23	-3.24°C	-2.58°C
TN_m	December	+0.45°C/dec.	0.00	0.50	-6.02°C	-5.13°C

Projected annual trends

The projected trends of annual average, minimum and maximum temperatures can be observed in Figure 37 and Table 7.

Figure 37 – Projected time series of the annual average, minimum and maximum temperatures
Time series over 2020-2060 period. Time series over 2020-2060 period. ***Pink dotted line****: variable value for each model separately under the RCP4.5 scenario.* ***grey dotted line****: variable value for each model separately under the RCP8.5 scenario.* ***Purple full line:*** *median value of the variable under RCP4.5 scenario.* ***Black full line:*** *median value of the variable under RCP8.5 scenario. Data source: NASA Earth Exchange - Global Daily Downscaled Climate Projections (NEX – GDDP) (Thrasher et al., 2012).*

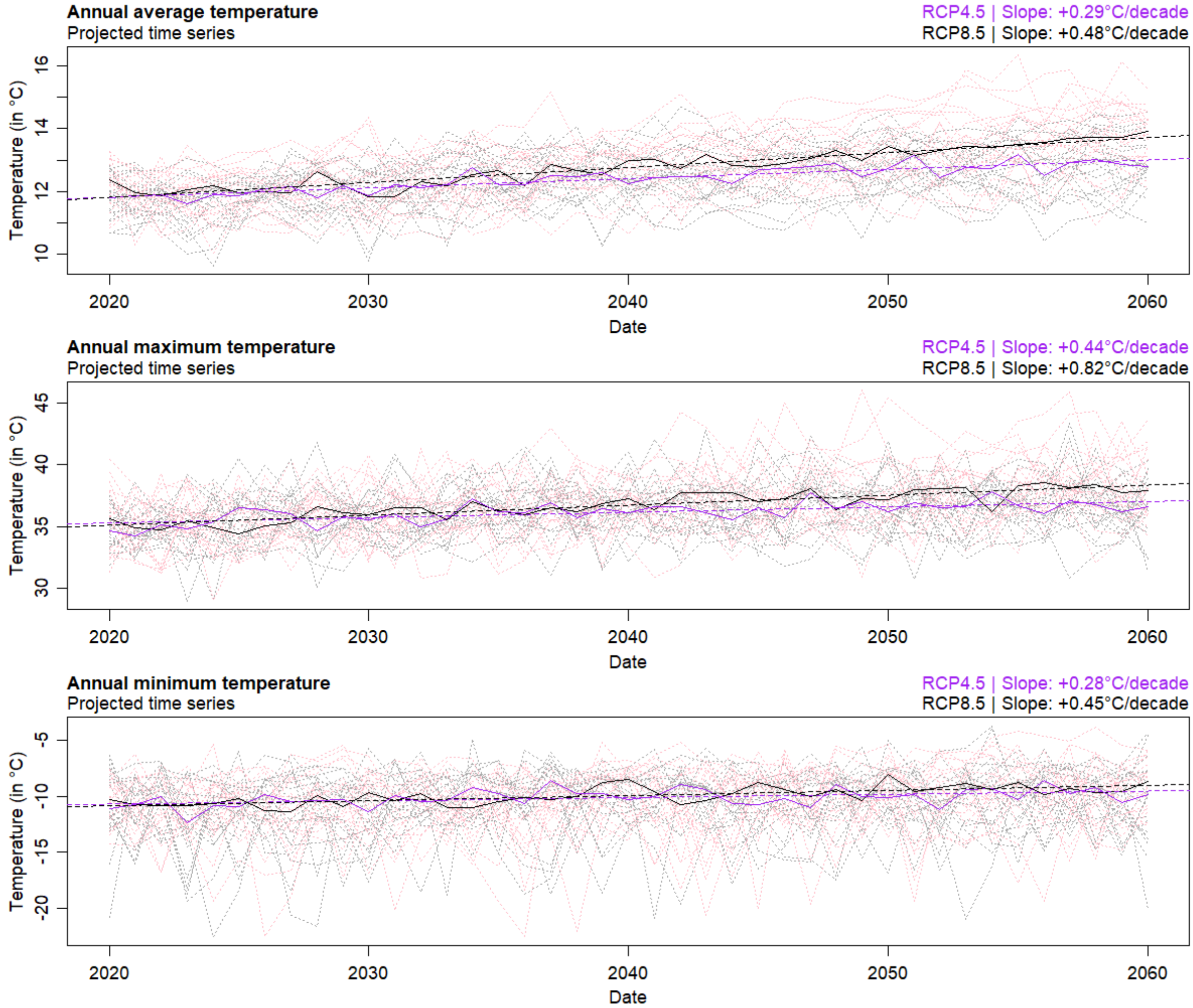

Table 7 – Characteristics of the trend from projected time series of monthly average, minimum and maximum temperature under the RCP8.5 scenario (linear models)
Data source: Republic Hydrometeorological Service of Serbia, Hidmet (Republic Hydrometeorological Service of Serbia, 2020).

RCP4.5					
Variable	**Slope**	**p-value**	**Adjusted R^2**	**Average value in 2040**	**Average value in 2060**
TG_y	+0.29°C/decade	0.00	0.76	12.42°C	13.00°C
TX_y	+0.44°C/decade	0.00	0.41	36.16°C	37.03°C
TN_y	+0.28°C/decade	0.01	0.16	-10.14°C	-9.58°C
RCP8.5					
Variable	**Slope**	**p-value**	**Adjusted R^2**	**Average value in 2040**	**Average value in 2060**
TG_y	+0.48°C/decade	0.00	0.87	12.77°C	13.73°C
TX_y	+0.82°C/decade	0.00	0.74	36.72°C	38.37°C
TN_y	+0.45°C/decade	0.00	0.43	-9.93°C	-9.02°C

As for historical data, the projected data present a steady increase of average, maximum and minimum temperature, under both RCP4.5 and RCP8.5 scenarios. RCP8.5 presents a steeper rate of increase than RCP4.5, for all temperatures.

TG_y is expected to increase at a rate of about +0.3°C/decade under RCP4.5 scenario, and +0.5°C/decade under RCP8.5 scenario. Therefore, TG_y is expected to increase from around 12.4°C in 2040 to 13.00°C on average in 2060 under the RCP4.5 scenario, and from around 12.8°C in 2040 to 13.7°C in 2060 under the RCP8.5 scenario.

TN_y is expected to increase at a rate of about +0.3°C/decade under RCP4.5 scenario, and +0.4°C/decade under RCP8.5 scenario. Therefore, TN_y is expected to increase from around -10.1°C in 2040 to -9.6°C on average in 2060 under the RCP4.5 scenario, and from around -9.9°C in 2040 to -9.0°C in 2060 under the RCP8.5 scenario.

Conclusion

The current average temperature in Serbia varies from 0°C in January to 21°C in August, with monthly maximum and minimum temperature following the same trends.

The year-to-year variations on temperatures (average, minimum and maximum) for both historical and projected data is quite low. All the temperatures increased for the last 40 years, to a rate of +0.4°C to +0.5°C per decade and they are expected to continue to increase for the next 40 years, to a rate of +0.3°C to +0.58°C per decade. This increase is expected to be mainly driven by late summer months.

9. Accumulated precipitation and precipitation intensity

This section will present the variations of precipitation in the Republic of Serbia, focusing on:

- Annually **accumulated precipitation** (RR_y) and **monthly accumulated precipitation** (RR_m)
- Annual **average precipitation intensity** (RRx_y) and monthly **average precipitation intensity** (RRx_m). Precipitation intensity is defined as the average amount of precipitation occurring on a rainy day. It is calculated as the accumulated precipitation over a period, divided by the number of rainy days (= wet days) during that period. Daily data on precipitation were not available from the local weather stations. The analysis of historical trends of RRx was thus conducted using ERA5 data only.

Current seasonal variation

The current seasonal variation of monthly accumulated precipitation and average precipitation intensity in the Republic of Serbia are presented in Figure 38. This chart presents RR_m and RRx_m averaged over 30 years (1990 to 2019).

Figure 38 – Current monthly variations of accumulated precipitation and average precipitation intensity
Data averaged over the 1990-2019 period. ***In light blue:*** *accumulated precipitation for each weather station.* ***In dark blue full line:*** *median value of accumulated precipitation, calculated over all weather stations.* ***In red:*** *variable calculated with ERA5 data. Data source: ERA5 - ECMWF / Copernicus Climate Change Service (Muñoz Sabater, 2019) and Republic Hydrometeorological Service of Serbia, Hidmet (Republic Hydrometeorological Service of Serbia, 2020).*

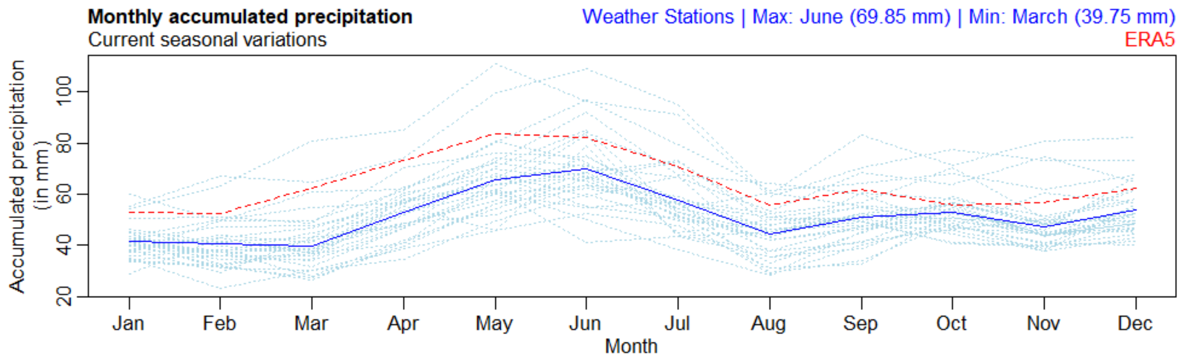

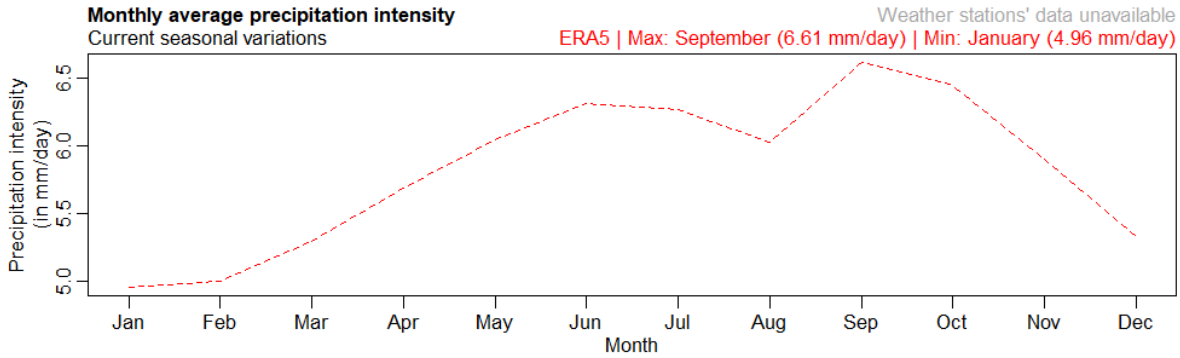

Serbia presents a rainy season from April to July, peaking in May-June showing a monthly accumulated precipitation (RR_m) around 70 mm per month. The rest of the year (August to March), the country shows a baseline monthly accumulated precipitation between 40 to 50 mm per month.

Precipitation intensity presents a steady increase from 5 mm/day in January to 6.2 mm/day in June. It is then more or less stable from June to August and increases again up to 6.6 mm/day during the months of September and October, before steadily decreasing until January. September and October are thus prone to less accumulated precipitation than during the rainy season (May-June) but tend to present more intense precipitations.

Comparing the data sources, ERA5 overestimates the local weather station RR_m by 10 to 20 mm from January to May, and from June to October.

Spatial distribution

The monthly spatial distribution of accumulated precipitation and average precipitation intensity throughout Serbia can be observed in Figure 39.

RR_m and RRx_m are more pronounced on the hills of the South of Serbia than on the flatland of the North. This is particularly noticeable during the rainy season (from April to July).

Figure 39 – Current spatial distribution of monthly accumulated precipitation and average precipitation intensity

Data averaged over the 1990-2019 period. ***In blue:*** *monthly accumulated precipitation.* ***In red:*** *monthly average precipitation intensity.* *<u>Data source:</u> ERA5 - ECMWF / Copernicus Climate Change Service (Muñoz Sabater, 2019).*

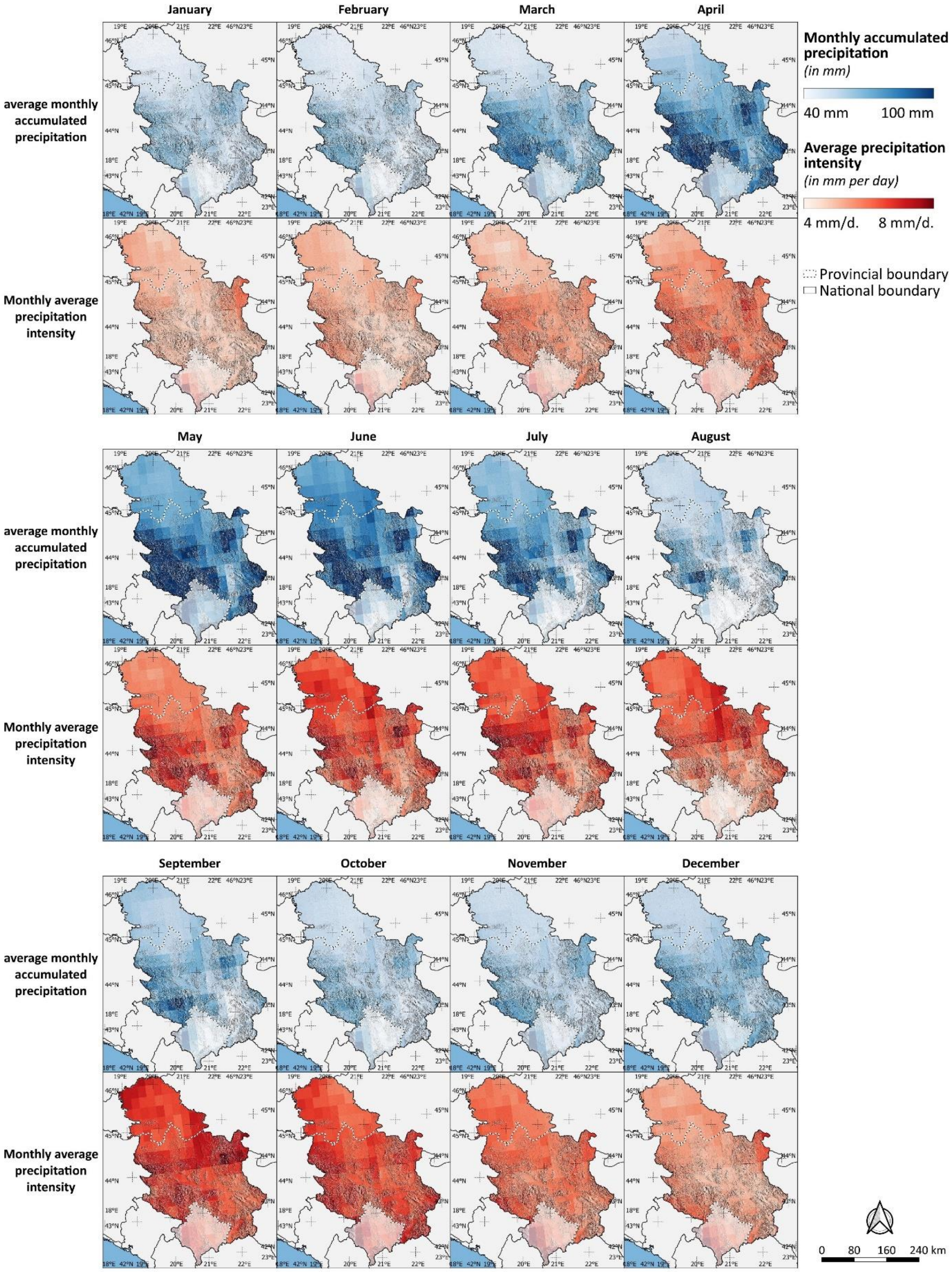

Historical monthly trends

The historical trends of monthly accumulated precipitation and monthly average precipitation intensity can be observed in Figure 40 and Figure 41 and Table 8.

Figure 40 – Historical monthly time series of accumulated precipitation

Time series over 1980-2019 period. ***Light blue dotted line****: variable value from each weather station separately.* ***Dark blue full line:*** *median value of the variable.* ***Red dashed line:*** *variable value using ERA5 database. Data source: Republic Hydrometeorological Service of Serbia, Hidmet (Republic Hydrometeorological Service of Serbia, 2020) and ERA5 - ECMWF / Copernicus Climate Change Service (Muñoz Sabater, 2019).*

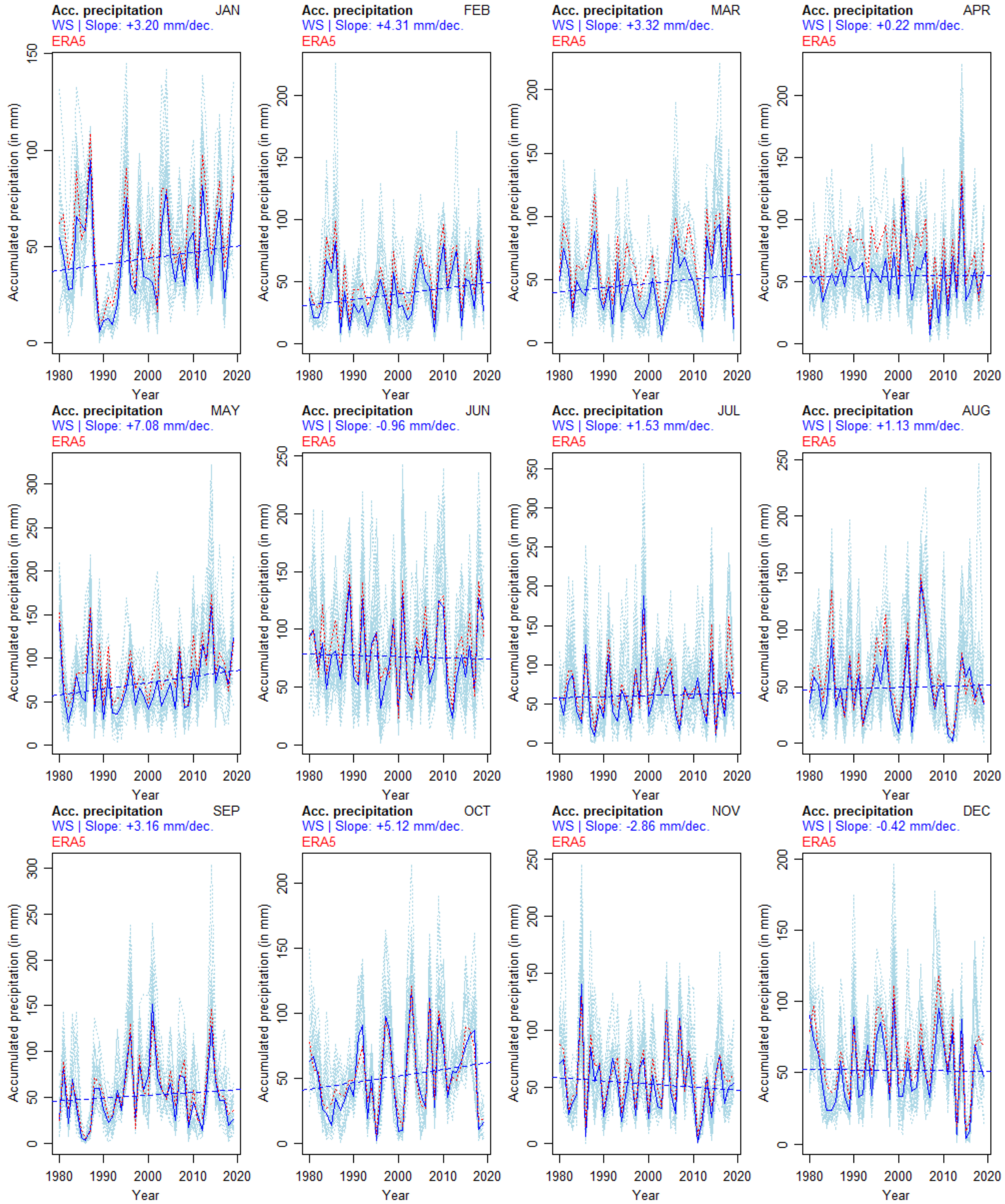

Figure 41 – Historical monthly time series of average precipitation intensity

Time series over 1980-2019 period. ***Red dashed line:*** *variable value using ERA5 database.* <u>*Data source:*</u> *ERA5 - ECMWF / Copernicus Climate Change Service (Muñoz Sabater, 2019).*

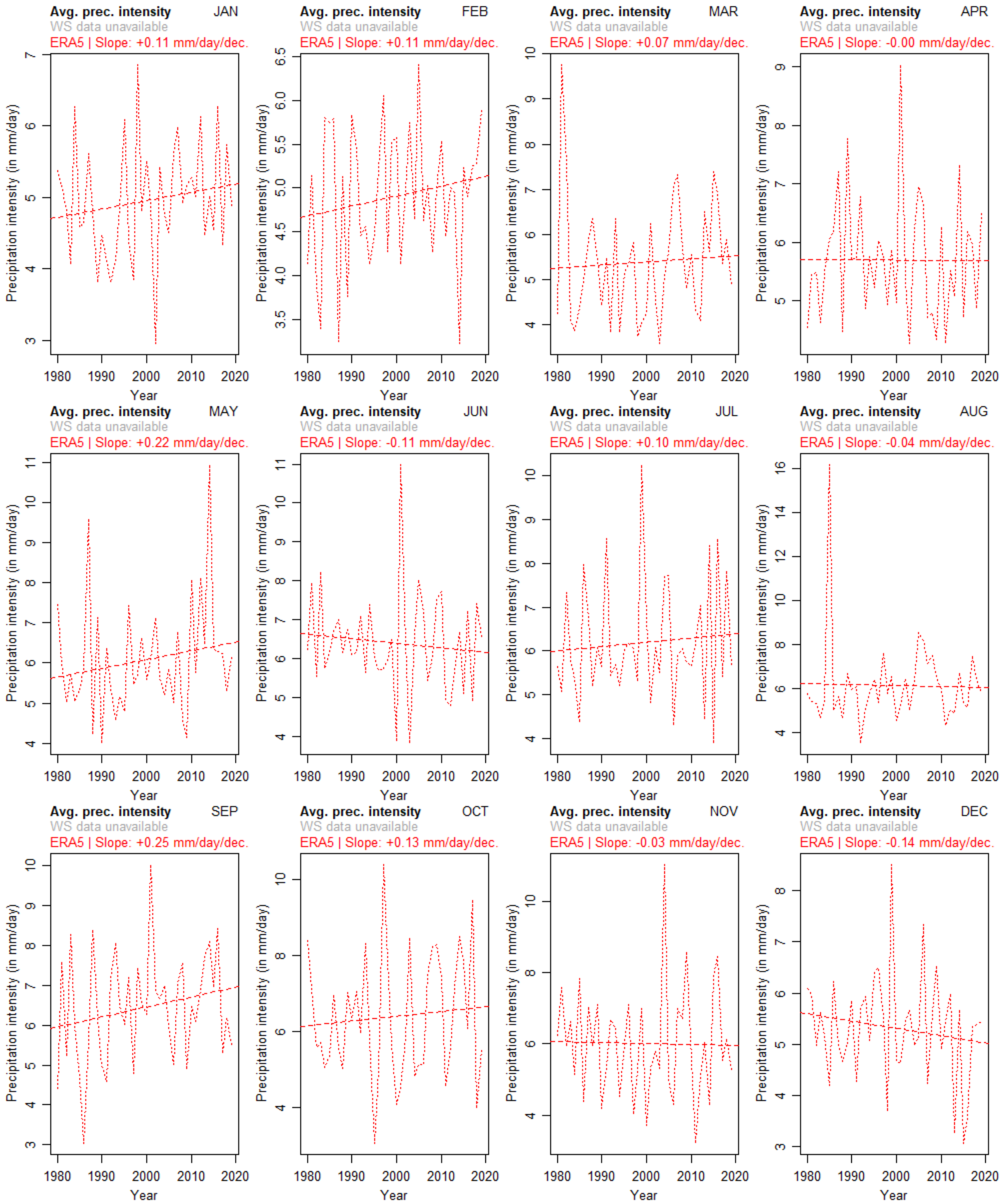

Table 8 – Characteristics of the trends from the historical time series of the monthly accumulated precipitation and monthly average precipitation intensity (linear models)
Data source: Republic Hydrometeorological Service of Serbia, Hidmet (Republic Hydrometeorological Service of Serbia, 2020) and ERA5 - ECMWF / Copernicus Climate Change Service (Muñoz Sabater, 2019).

Variable	Month	Slope	p-value	Adj. R^2	Average value in 1980	Average value in 2019
RR_m	January	+3.20 mm/dec.	0.29	0.00	37.64 mm	50.12 mm
RR_m	February	+4.31 mm/dec.	0.13	0.03	31.59 mm	48.42 mm
RR_m	March	+3.32 mm/dec.	0.33	0.00	40.35 mm	53.31 mm
RR_m	April	+0.22 mm/dec.	0.94	-0.03	53.52 mm	54.38 mm
RR_m	May	+7.08 mm/dec.	0.12	0.04	57.40 mm	85.02 mm
RR_m	June	-0.96 mm/dec.	0.82	-0.02	78.64 mm	74.89 mm
RR_m	July	+1.53 mm/dec.	0.76	-0.02	57.50 mm	63.46 mm
RR_m	August	+1.13 mm/dec.	0.78	-0.02	46.79 mm	51.18 mm
RR_m	September	+3.16 mm/dec.	0.49	-0.01	46.38 mm	58.72 mm
RR_m	October	+5.12 mm/dec.	0.23	0.01	41.37 mm	61.34 mm
RR_m	November	-2.86 mm/dec.	0.48	-0.01	58.30 mm	47.15 mm
RR_m	December	-0.42 mm/dec.	0.91	-0.03	52.59 mm	50.94 mm
RRx_m	January	+0.11 mm/day/dec.	0.31	0.00	4.72 mm/day	5.17 mm/day
RRx_m	February	+0.11 mm/day/dec.	0.30	0.00	4.68 mm/day	5.12 mm/day
RRx_m	March	+0.07 mm/day/dec.	0.70	-0.02	5.25 mm/day	5.52 mm/day
RRx_m	April	-0.00 mm/day/dec.	0.98	-0.03	5.71 mm/day	5.69 mm/day
RRx_m	May	+0.22 mm/day/dec.	0.27	0.01	5.64 mm/day	6.49 mm/day
RRx_m	June	-0.11 mm/day/dec.	0.52	-0.01	6.62 mm/day	6.17 mm/day
RRx_m	July	+0.10 mm/day/dec.	0.60	-0.02	6.00 mm/day	6.38 mm/day
RRx_m	August	-0.04 mm/day/dec.	0.88	-0.03	6.22 mm/day	6.05 mm/day
RRx_m	September	+0.25 mm/day/dec.	0.20	0.02	5.96 mm/day	6.92 mm/day
RRx_m	October	+0.13 mm/day/dec.	0.58	-0.02	6.13 mm/day	6.62 mm/day
RRx_m	November	-0.03 mm/day/dec.	0.89	-0.03	6.08 mm/day	5.96 mm/day
RRx_m	December	-0.14 mm/day/dec.	0.33	0.00	5.59 mm/day	5.04 mm/day

Overall, most of the months showed a mild increase of RR_m with slopes lower than 5 mm per decade, and large interannual and geographic variation, up to 200 and 300 mm of variation range. The trends qualities are thus very poor (adj. R^2 <<0.5, p-value >>0.05) and should be observed with circumspection.

In terms of critical months, the largest increase in RR_m can be observed for the months of May (+7 mm/decade), October (+5 mm/decade) and February (+ 4 mm/decade) for local weather stations.

A very large interannual variation (up to 10 mm/day) can be observed in the monthly analysis of precipitation intensity. The trends qualities are thus very poor (adj. R^2 <<0.5, p-value >>0.05) and should be observed with circumspection. Be that as it may, a mild increase in RRx_m can be observed for most of the months.

In terms of critical months, the largest increase in RRx_m can be observed for the months of September (+0.25 mm/day/decade), May (+0.22 mm/day/decade) and December (+ 0.14 mm/day/decade).

In terms of critical months, the largest increase in RR_m can be observed for the months of May (+7 mm/decade), October (+5 mm/decade) and February (+ 4 mm/decade) for local weather stations.

Historical annual trends

Historical annual trends on accumulated precipitation can be observed in Figure 42 and Table 9.

Figure 42 – Historical annual time series of accumulated precipitation and average precipitation intensity
*Time series over 1980-2019 period. **In light blue:** variable for each weather station. **In dark blue full line:** median value of the variable, calculated over all weather stations. **In dark blue dashed line:** minimum and maximum values of the variable, calculated over all weather stations. **In red:** variable calculated with ERA5 data. Data source: ERA5, ECMWF / Copernicus Climate Change Service (Muñoz Sabater, 2019), Republic Hydrometeorological Service of Serbia, Hidmet (Republic Hydrometeorological Service of Serbia, 2020).*

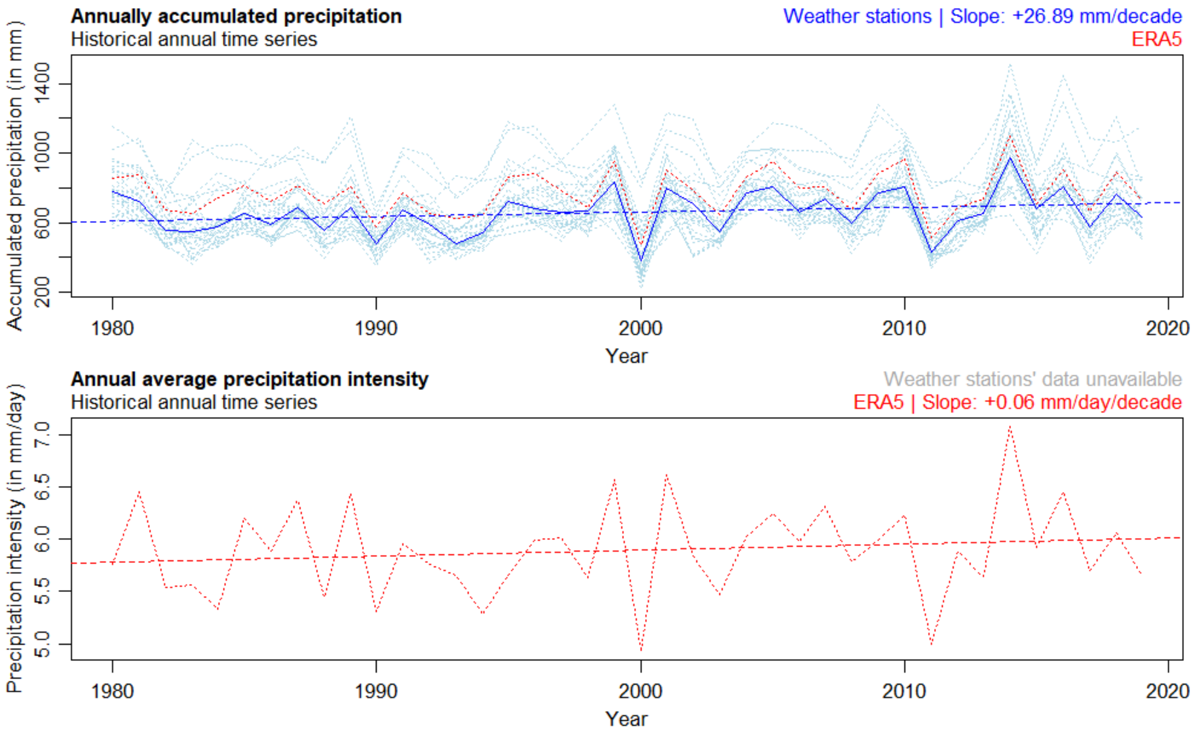

Table 9 – Characteristics of the trend from historical annual times series of accumulated precipitation and average precipitation intensity (linear models)
Data source: ERA5, ECMWF / Copernicus Climate Change Service (Muñoz Sabater, 2019), Republic Hydrometeorological Service of Serbia, Hidmet (Republic Hydrometeorological Service of Serbia, 2020).

Variable	Slope	p-value	Adj. R^2	Average value in 1980	Average value in 2019
RR_y	+26.89 mm/dec.	0.11	0.04	606.62 mm	711.47 mm
RRx_y	+0.06 mm/day/dec.	0.37	0.00	5.78 mm/day	6.00 mm/day

RR_y in Serbia presented a very large range of variability during the last 40 years: RR_y varied from about 300 mm in 2000 to 1100 mm in 2014. Between these two dates RR_y almost quadrupled. RRx_y varied as well during the last 40 years, although to a lesser extent: from 5 mm/day in 2000 to 7 mm/day in 2014. This (very) heavy variation makes RR_y and RRx_y very difficult to model, which therefor yields very high level of uncertainty ($p>>0.05$; Adj. R^2 close to 0). All the following trends should therefore be observed with the highest level of circumspection.

Be that as it may, RR_y showed an increase in Serbia over the last 40 years (+27 mm/decade). As for RR_m, ERA5 tended to overestimate the RR_y presented by local weather stations by about 100 mm per year. RR_y thus seemed to present an increase from around 607 mm in 1980 to 711 mm in 2019.

Although presenting a very strong year to year variation (see above), RRx_y's yearly variation seemed to stay, on average, stable around 6 mm/ day.

Spatial distribution

The historical spatial distribution of annually accumulated precipitation and annual average precipitation intensity throughout Serbia can be observed in Figure 43.

The spatial distribution seems to be constant for RR_y and RRx_y. The precipitation and precipitation intensity are higher in the high lands of the south especially on mountain tops, and lower in the plains of the North and valleys of the South.

Figure 43 – Historical spatial distribution of annually accumulated precipitation and annual average precipitation intensity
*Data averaged over the 1980-2019 period, by decade. **In blue:** decadal averaged of the annually accumulated precipitation. **In red:** decadal average of the annual average precipitation intensity. Data source: ERA5, ECMWF / Copernicus Climate Change Service (Muñoz Sabater, 2019)*

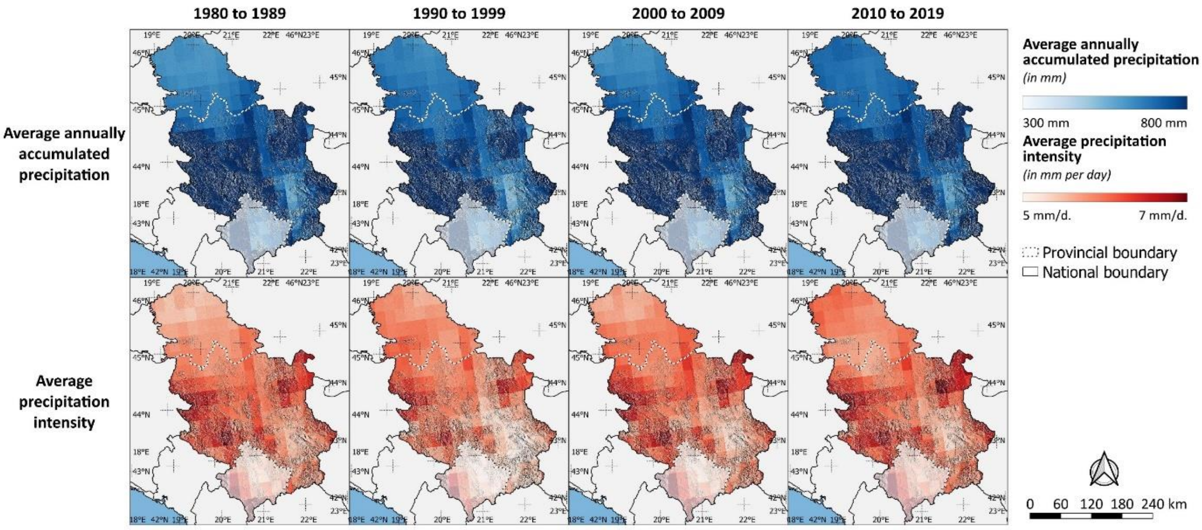

Projected monthly trends

The projected trends of monthly accumulated precipitation and average precipitation intensity can be observed in Figure 46, Figure 47, Table 10 and Table 11.

Figure 44 – Projected time series of monthly accumulated precipitation

Time series over 2020-2060 period. ***Pink dotted line****: variable value for each model separately under the RCP4.5 scenario.* ***grey dotted line****: variable value for each model separately under the RCP8.5 scenario.* ***Purple full line:*** *median value of the variable under RCP4.5 scenario.* ***Black full line:*** *median value of the variable under RCP8.5 scenario. Data source: NASA Earth Exchange - Global Daily Downscaled Climate Projections (NEX – GDDP) (Thrasher et al., 2012).*

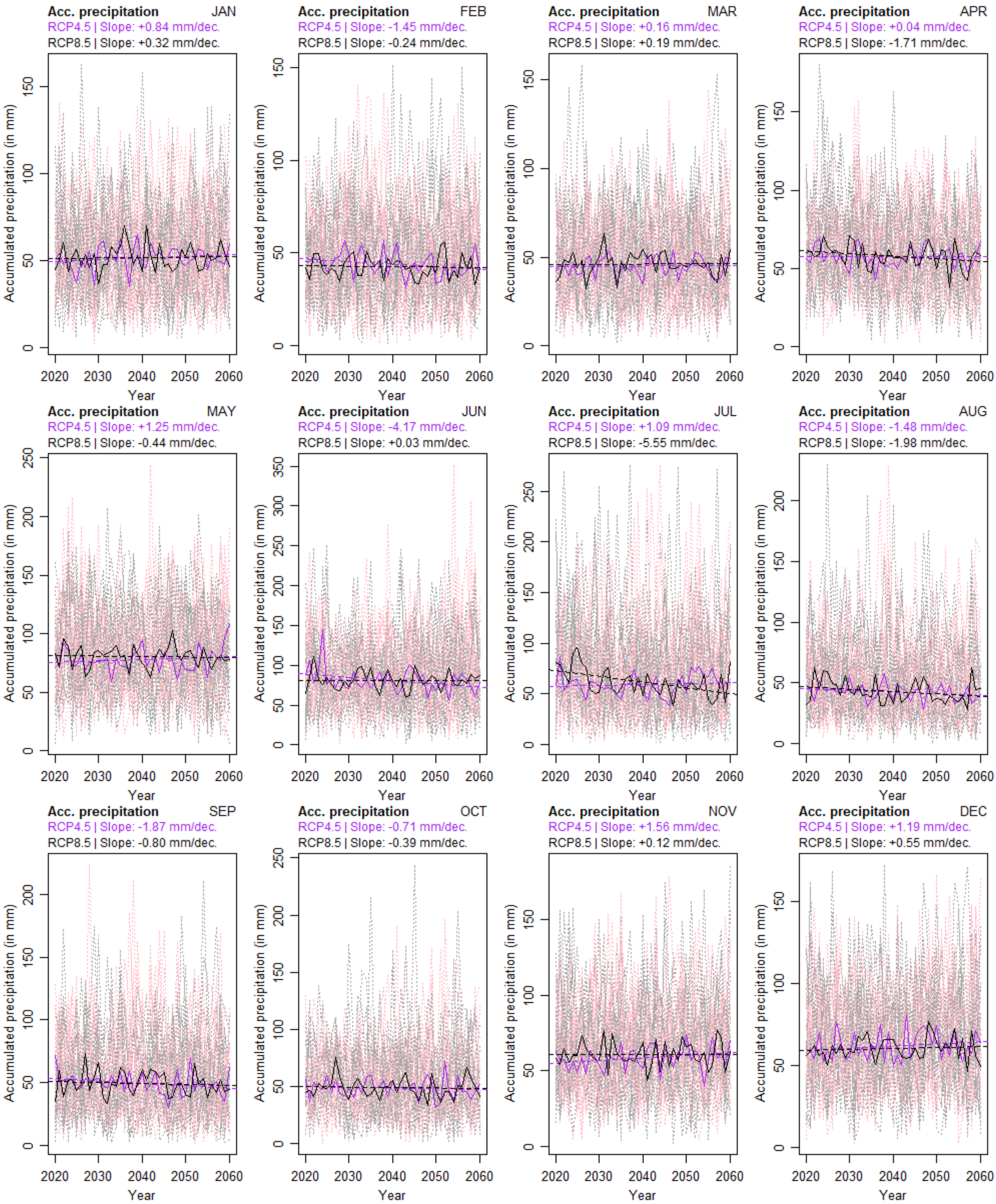

Figure 45 – Projected time series of monthly average precipitation intensity

*Time series over 2020-2060 period. **Pink dotted line**: variable value for each model separately under the RCP4.5 scenario. **grey dotted line**: variable value for each model separately under the RCP8.5 scenario. **Purple full line:** median value of the variable under RCP4.5 scenario. **Black full line:** median value of the variable under RCP8.5 scenario. <u>Data source:</u> NASA Earth Exchange - Global Daily Downscaled Climate Projections (NEX – GDDP) (Thrasher et al., 2012).*

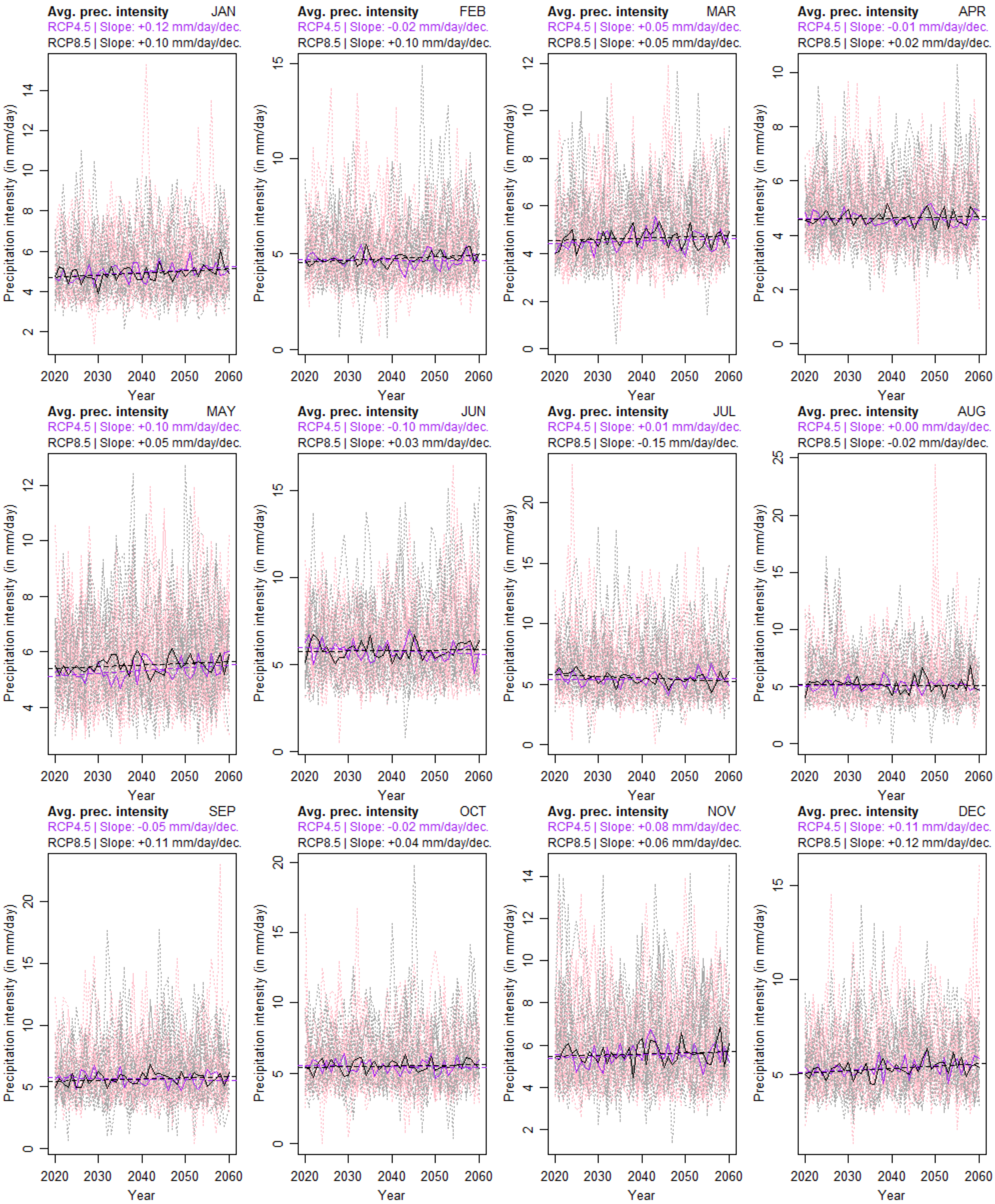

Table 10 – Characteristics of the trend from projected time series of monthly accumulated precipitation and monthly average precipitation intensity under the RCP4.5 scenario (linear models)
<u>Data source:</u> NASA Earth Exchange - Global Daily Downscaled Climate Projections (NEX – GDDP) (Thrasher et al., 2012).

RCP4.5						
Variable	**Month**	**Slope**	**p-value**	**Adj. R^2**	**Average value in 2040**	**Average value in 2060**
RR_m	January	+0.84 mm/dec.	0.34	0.00	51.33 mm	53.00 mm
RR_m	February	-1.45 mm/dec.	0.08	0.05	44.10 mm	41.20 mm
RR_m	March	+0.16 mm/dec.	0.83	-0.02	44.80 mm	45.11 mm
RR_m	April	+0.04 mm/dec.	0.97	-0.03	57.44 mm	57.52 mm
RR_m	May	+1.25 mm/dec.	0.34	0.00	77.63 mm	80.13 mm
RR_m	June	-4.17 mm/dec.	0.03	0.09	81.29 mm	72.96 mm
RR_m	July	+1.09 mm/dec.	0.43	-0.01	59.10 mm	61.28 mm
RR_m	August	-1.48 mm/dec.	0.09	0.05	42.58 mm	39.62 mm
RR_m	September	-1.87 mm/dec.	0.10	0.04	49.30 mm	45.57 mm
RR_m	October	-0.71 mm/dec.	0.51	-0.01	49.01 mm	47.59 mm
RR_m	November	+1.56 mm/dec.	0.12	0.04	58.45 mm	61.57 mm
RR_m	December	+1.19 mm/dec.	0.29	0.00	61.84 mm	64.23 mm
RRx_m	January	+0.12 mm/day/dec.	0.01	0.13	4.95 mm/day	5.19 mm/day
RRx_m	February	-0.02 mm/day/dec.	0.73	-0.02	4.68 mm/day	4.65 mm/day
RRx_m	March	+0.05 mm/day/dec.	0.37	0.00	4.51 mm/day	4.61 mm/day
RRx_m	April	-0.01 mm/day/dec.	0.76	-0.02	4.60 mm/day	4.58 mm/day
RRx_m	May	+0.10 mm/day/dec.	0.02	0.10	5.33 mm/day	5.54 mm/day
RRx_m	June	-0.10 mm/day/dec.	0.16	0.03	5.79 mm/day	5.59 mm/day
RRx_m	July	+0.01 mm/day/dec.	0.86	-0.02	5.43 mm/day	5.46 mm/day
RRx_m	August	+0.00 mm/day/dec.	0.94	-0.03	5.08 mm/day	5.09 mm/day
RRx_m	September	-0.05 mm/day/dec.	0.42	-0.01	5.63 mm/day	5.52 mm/day
RRx_m	October	-0.02 mm/day/dec.	0.75	-0.02	5.48 mm/day	5.45 mm/day
RRx_m	November	+0.08 mm/day/dec.	0.21	0.02	5.53 mm/day	5.69 mm/day
RRx_m	December	+0.11 mm/day/dec.	0.04	0.08	5.34 mm/day	5.57 mm/day

Under the RCP4.5 scenario, most of the months are predicted to present a very mild variation of RR_m (between +2 mm/ decade to -2 mm/decade). The only exception is predicted to be June, with -4 mm/decade. Under the RCP8.5 scenario, trends are somewhat similar, with variations between +2 mm/ decade to -2 mm/decade. The exception is however predicted to be July under RCP8.5 scenario, with -6 mm/decade.

Looking into RRx_m, and under both scenario, most of the months are predicted to present a very mild variation (between +0.1 mm per wet day/ decade to -0.2 mm per wet day/decade).

Table 11 – Characteristics of the trend from projected time series of monthly accumulated precipitation and monthly average precipitation intensity under the RCP8.5 scenario (linear models)
Data source: NASA Earth Exchange - Global Daily Downscaled Climate Projections (NEX – GDDP) (Thrasher et al., 2012).

RCP8.5						
Variable	**Month**	**Slope**	**p-value**	**Adj. R^2**	**Average value in 2040**	**Average value in 2060**
RR_m	January	+0.32 mm/dec.	0.74	-0.02	51.78 mm	52.43 mm
RR_m	February	-0.24 mm/dec.	0.76	-0.02	42.48 mm	41.99 mm
RR_m	March	+0.19 mm/dec.	0.82	-0.02	46.23 mm	46.62 mm
RR_m	April	-1.71 mm/dec.	0.09	0.05	57.95 mm	54.54 mm
RR_m	May	-0.44 mm/dec.	0.70	-0.02	80.27 mm	79.40 mm
RR_m	June	+0.03 mm/dec.	0.99	-0.03	80.98 mm	81.03 mm
RR_m	July	-5.55 mm/dec.	0.00	0.22	61.50 mm	50.40 mm
RR_m	August	-1.98 mm/dec.	0.11	0.04	43.22 mm	39.26 mm
RR_m	September	-0.80 mm/dec.	0.53	-0.02	49.23 mm	47.63 mm
RR_m	October	-0.39 mm/dec.	0.74	-0.02	48.96 mm	48.18 mm
RR_m	November	+0.12 mm/dec.	0.91	-0.03	60.70 mm	60.94 mm
RR_m	December	+0.55 mm/dec.	0.55	-0.02	60.25 mm	61.35 mm
RRx_m	January	+0.10 mm/day/dec.	0.03	0.09	4.90 mm/day	5.10 mm/day
RRx_m	February	+0.10 mm/day/dec.	0.01	0.16	4.75 mm/day	4.95 mm/day
RRx_m	March	+0.05 mm/day/dec.	0.34	0.00	4.63 mm/day	4.73 mm/day
RRx_m	April	+0.02 mm/day/dec.	0.48	-0.01	4.63 mm/day	4.68 mm/day
RRx_m	May	+0.05 mm/day/dec.	0.16	0.03	5.52 mm/day	5.63 mm/day
RRx_m	June	+0.03 mm/day/dec.	0.64	-0.02	5.83 mm/day	5.88 mm/day
RRx_m	July	-0.15 mm/day/dec.	0.02	0.12	5.51 mm/day	5.21 mm/day
RRx_m	August	-0.02 mm/day/dec.	0.83	-0.02	5.15 mm/day	5.11 mm/day
RRx_m	September	+0.11 mm/day/dec.	0.08	0.05	5.65 mm/day	5.86 mm/day
RRx_m	October	+0.04 mm/day/dec.	0.46	-0.01	5.53 mm/day	5.61 mm/day
RRx_m	November	+0.06 mm/day/dec.	0.39	-0.01	5.59 mm/day	5.71 mm/day
RRx_m	December	+0.12 mm/day/dec.	0.02	0.11	5.30 mm/day	5.55 mm/day

Projected annual trends

Projected annual trends on annually accumulated precipitation and annual average precipitation intensity can be observed in Figure 46 and Table 12.

Figure 46 – Projected time series of the annual accumulated precipitation and average precipitation intensity
Time series over 2020-2060 period. Time series over 2020-2060 period. ***Pink dotted line****: variable value for each model separately under the RCP4.5 scenario.* ***grey dotted line****: variable value for each model separately under the RCP8.5 scenario.* ***Purple full line:*** *median value of the variable under RCP4.5 scenario.* ***Black full line:*** *median value of the variable under RCP8.5 scenario. Data source: NASA Earth Exchange - Global Daily Downscaled Climate Projections (NEX – GDDP) (Thrasher et al., 2012).*

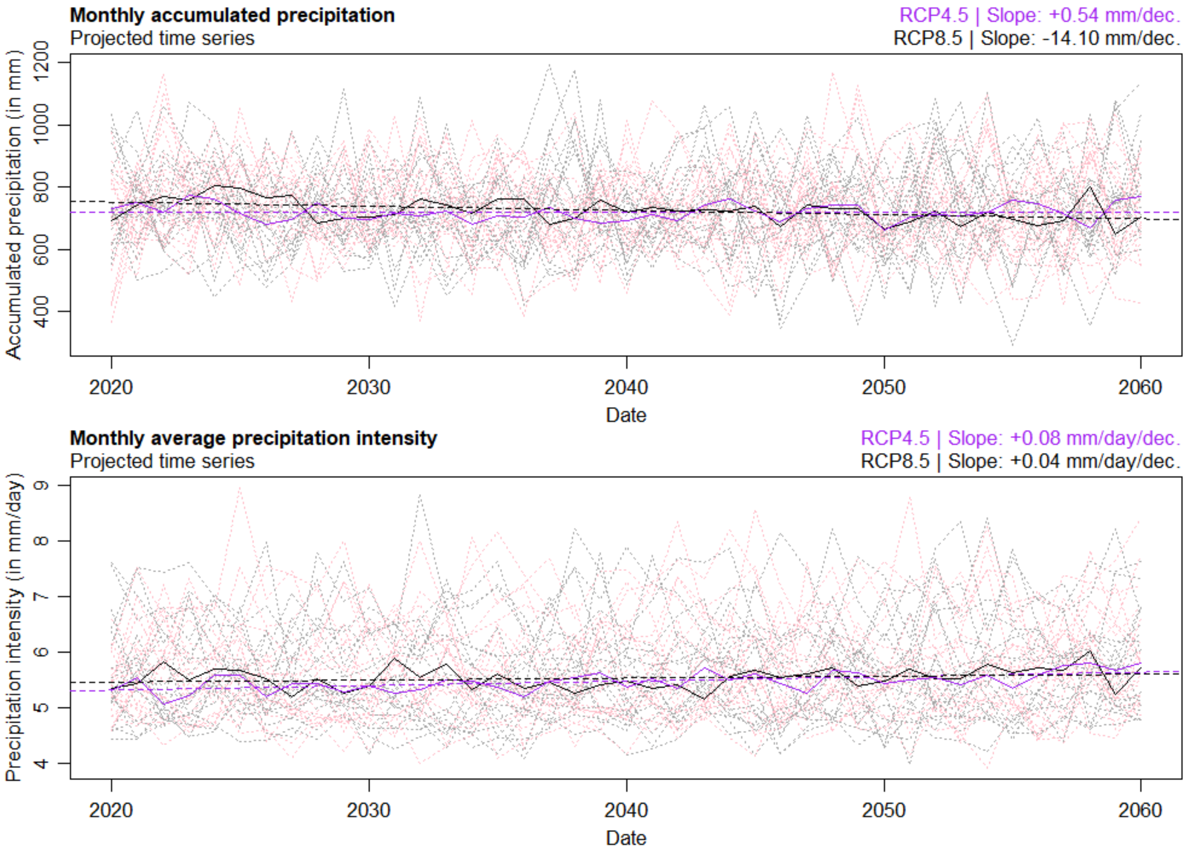

Table 12 – Characteristics of the trend from projected time series of monthly accumulated precipitation and average precipitation intensity under the RCP4.5 and RCP8.5 scenario (linear models)
Data source: NASA Earth Exchange - Global Daily Downscaled Climate Projections (NEX – GDDP) (Thrasher et al., 2012)

RCP4.5					
Variable	**Slope**	**p-value**	**Adjusted R^2**	**Average value in 2040**	**Average value in 2060**
RR_y	+0.54 mm/dec.	0.89	-0.03	719.85 mm	720.92 mm
RRx_y	+0.08 mm/day/dec.	0.00	0.30	5.47 mm/day	5.64 mm/day
RCP8.5					
Variable	**Slope**	**p-value**	**Adjusted R^2**	**Average value in 2040**	**Average value in 2060**
RR_y	-14.10 mm/dec.	0.00	0.17	725.63 mm	697.42 mm
RRx_y	+0.04 mm/day/dec.	0.17	0.02	5.53 mm/day	5.60 mm/day

Looking into variation of RR_y, under the RCP4.5 scenario the NEX median models does not seem to predict any relevant variation (+0.1 mm/decade), the same model under the RCP8.5 scenario predicts a decrease in precipitation (-14 mm/decade). Therefore, where the NEX median model under the RCP4.5 scenario expect the RR_y to stay stable (720 mm on average in 2040 and 721 mm on average in

2060), the same model under the RCP8.5 scenario expects a decrease from 726 mm on average in 2040 to 697 mm on average in 2060.

For RRx_y, decadal variation is predicted by the NEX median model under both scenarios to remain stable for the next 40 years, around 5,5 mm/wet days/decade.

Conclusion

The accumulated precipitation, and in a lesser extent, average precipitation intensity, are, in Serbia, subject to very strong interannual variations and their monthly and annual trends are unclear and must be observed with circumspection.

Serbia presents a rainy season from April to July, with a monthly accumulated precipitation rate of about 70 mm. The rest of the year presents a baseline precipitation of 40 to 50 mm. The precipitation intensity rises during the rainy season to about 6.2 mm per wet day, but peaks after the rainy season, in September and October, to around 6.6 mm per wet day. September and October are thus prone to less accumulated precipitation than during the rainy season but tend to present more intense precipitations. In January the precipitation is less intense (5 mm per wet day).

Regarding year-to-year variation, the accumulated precipitation, both historical and projected, are extremely variable, and can almost quadruple between years. Although the accumulated precipitation seemed to slightly increase during the last 40 years, it is expected to stay stable or even decrease during the next 40 years. Moreover, if a decrease happens, this trend is expected to be driven by a decrease in precipitation during the summer months.

The precipitation intensity presents a quite large interannual variation as well but did not show any strong variation during the last 40 years. The NEX projections seems to confirm this historical trend for the next 40 years.

10. Wet days, very wet days, and duration of the longest dry spell

This section will present the variations of wet days, very wet days, and the duration of the longest dry spell in the Republic of Serbia, using the following variables:

- Annually **accumulated wet days** (WD_y) and monthly **accumulated wet days** (WD_m). Accumulated wet days are define as the number of days over a given period, when the accumulated precipitation is greater than 1 mm.
- Annually **accumulated very wet days** (VWD_y) and monthly **accumulated very wet days** (VWD_m). Accumulated very wet days are define as the number of days over a given period, when the accumulated precipitation is greater than the 95th quantile of the daily accumulated precipitations over the period.
- Duration of the **longest dry spell** of the year (DS_y) and duration of the **longest dry spell** of the month (DS_m). The duration of the **longest dry spell** is defined as the largest number of consecutive days over a given period where the daily accumulated precipitation is below 1 mm.

Because wet days, very wet days and the duration of the longest dry spell are calculated at a daily level, and because daily data from weather stations were not available, this section will only present ERA5 data for historical trends.

Current seasonal variations

The current seasonal variations of wet days, very wet days, and duration of the longest dry spell can be observed in Figure 47. This chart presents the WD_m, VWD_m and DS_m averaged over 30 years (1990 to 2019).

As could be expected, WD_m and VWD_m follow the increasing pattern of the monthly accumulated precipitation from January (WD_m: 10.5 days, VWD_m: 0.2 days) until the rainy season, in May-June, reaching 13 wet days and 0.8 very wet days per month. Both indices than decrease from June to August. In September and October, while WD_m continues its decrease below its January level (reaching around 9 wet days), VWD_m start to re increase. This highlights the fact that September and October present less accumulated wet days, but the wet days that occur during these two months are more intense (=very wet days), confirming the increase of precipitation intensity observed in Figure 39. After October, VWD_m decreases and WD_m increases to reach their respective January levels.

DS_m is at its lowest (around 7 days) during the wet season. It increases sharply until August, reaching 11 days, and stays stable until October (around 10-11 days), further confirming the fact that September and October present fewer wet days but more intense one. In November, DS_m steadily decreases until April.

Figure 47 – Current monthly variation of accumulated wet days, accumulated very wet days, and the duration of the longest dry spell.

*Data averaged over the 1990-2019 period. **In green:** monthly accumulated wet days. **In blue:** monthly accumulated very wet days. **In red:** duration of the longest dry spell of the month. Data source: ERA5 - ECMWF / Copernicus Climate Change Service (Muñoz Sabater, 2019).*

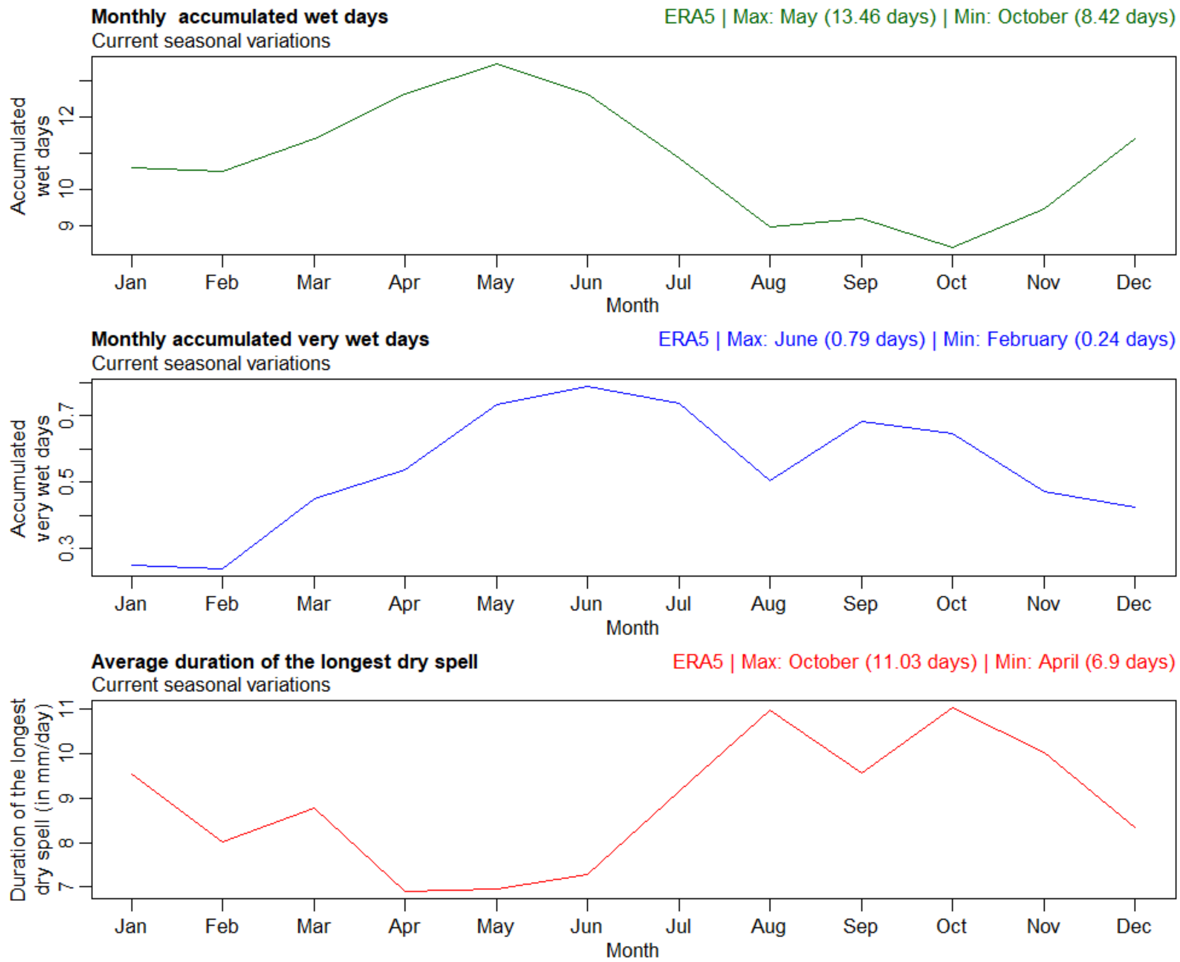

Spatial distribution

The current seasonal spatial distribution of wet days and very wet days and the duration of the longest try spell of the month throughout Serbia can be observed in Figure 48 and Figure 49.

As for RR_m and RRx_m, WD_m and VWD_m are more common on the hills of the South of Serbia than on the flatland of the North. This is particularly noticeable during the wet season (from April to July). Interestingly, at the peak of the wet season, very wet days start to be more common in the flatland of the North of the country than in the valleys of the south. The hilltop of the south however maintains a large number of very wet days.

The spatial distribution of DS_m is somewhat inverse than the spatial distribution of WD_m and VWD_m: dry spells are longer in the flatland of the North and in the valley of the South than on the Hilltops of the south of the country.

Figure 48 – Current spatial distribution of monthly accumulated wet days and very wet days

*Data averaged over the 1990-2019 period. **In green:** monthly accumulated wet days. **In blue:** monthly accumulated very wet days. <u>Data source:</u> ERA5 - ECMWF / Copernicus Climate Change Service (Muñoz Sabater, 2019).*

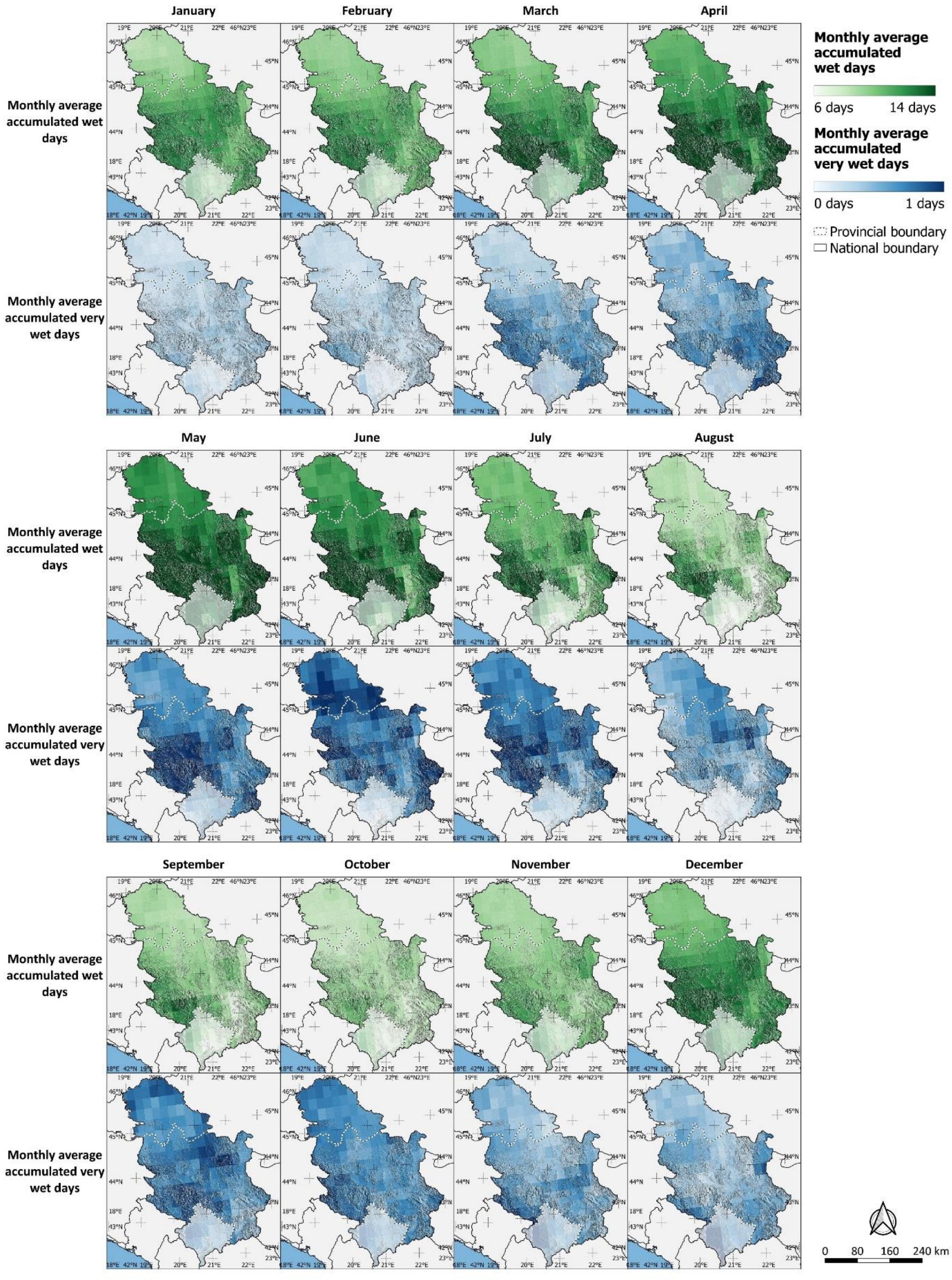

Figure 49 – Current spatial distribution of the duration of the longest dry spell of the month
Data averaged over the 1990-2019 period. ***Data source:*** *ERA5 - ECMWF / Copernicus Climate Change Service (Muñoz Sabater, 2019).*

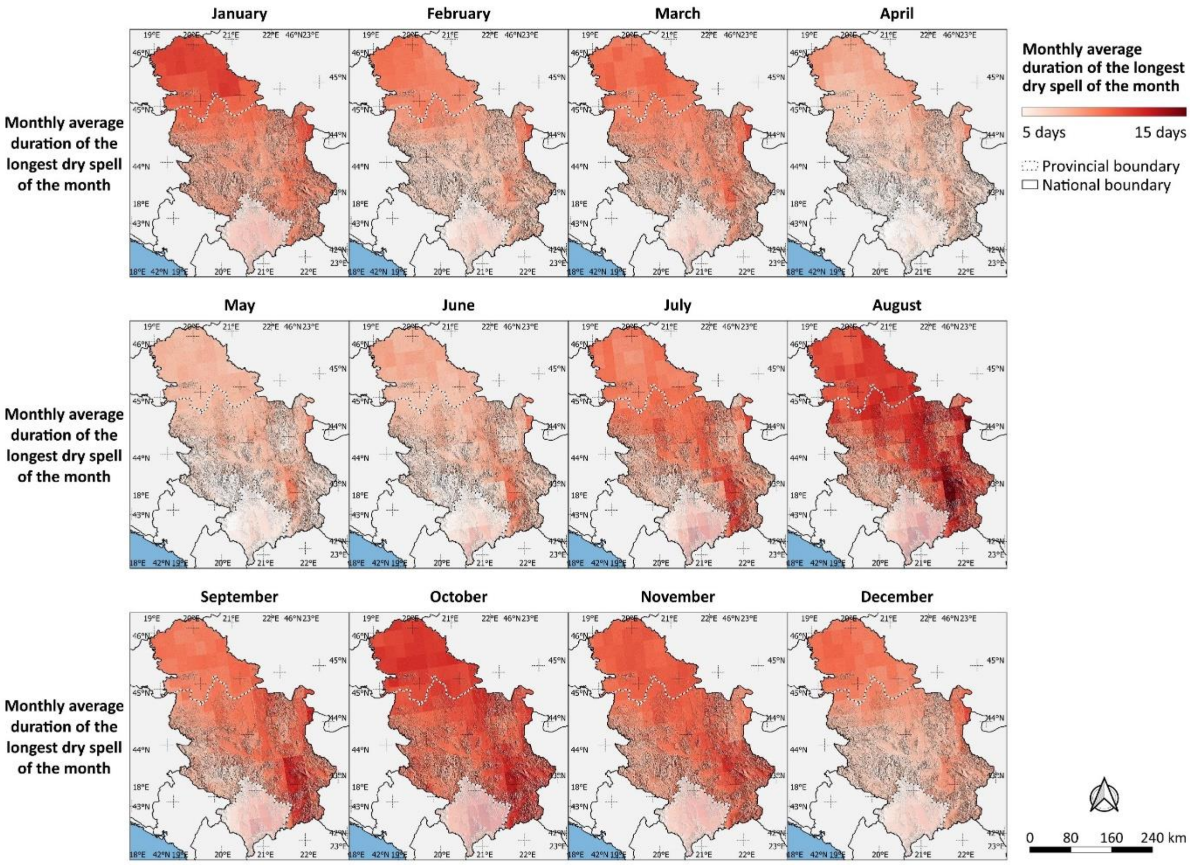

Historical monthly trends

The monthly historical trends on accumulated wet days, accumulated very wet days and the duration of the longest dry spell at a monthly scale can be observed in Figure 50, Figure 51, Figure 52 and Table 13 .

Overall, although a large interannual variation, most of the monthly values remained stable on average. WD_m showed a variation between -0.6 days/decade to +0.7 days/ decade, VWD_m a variation between -0.1 days/decade to +0.1 days/decade and DS_m a variation between -1 day/decade and -1 day /decade.

Figure 50 – Historic time series of the monthly accumulated wet days

Time series over 1980-2019 period. Data source: ERA5, ECMWF / Copernicus Climate Change Service (Muñoz Sabater, 2019), Republic Hydrometeorological Service of Serbia.

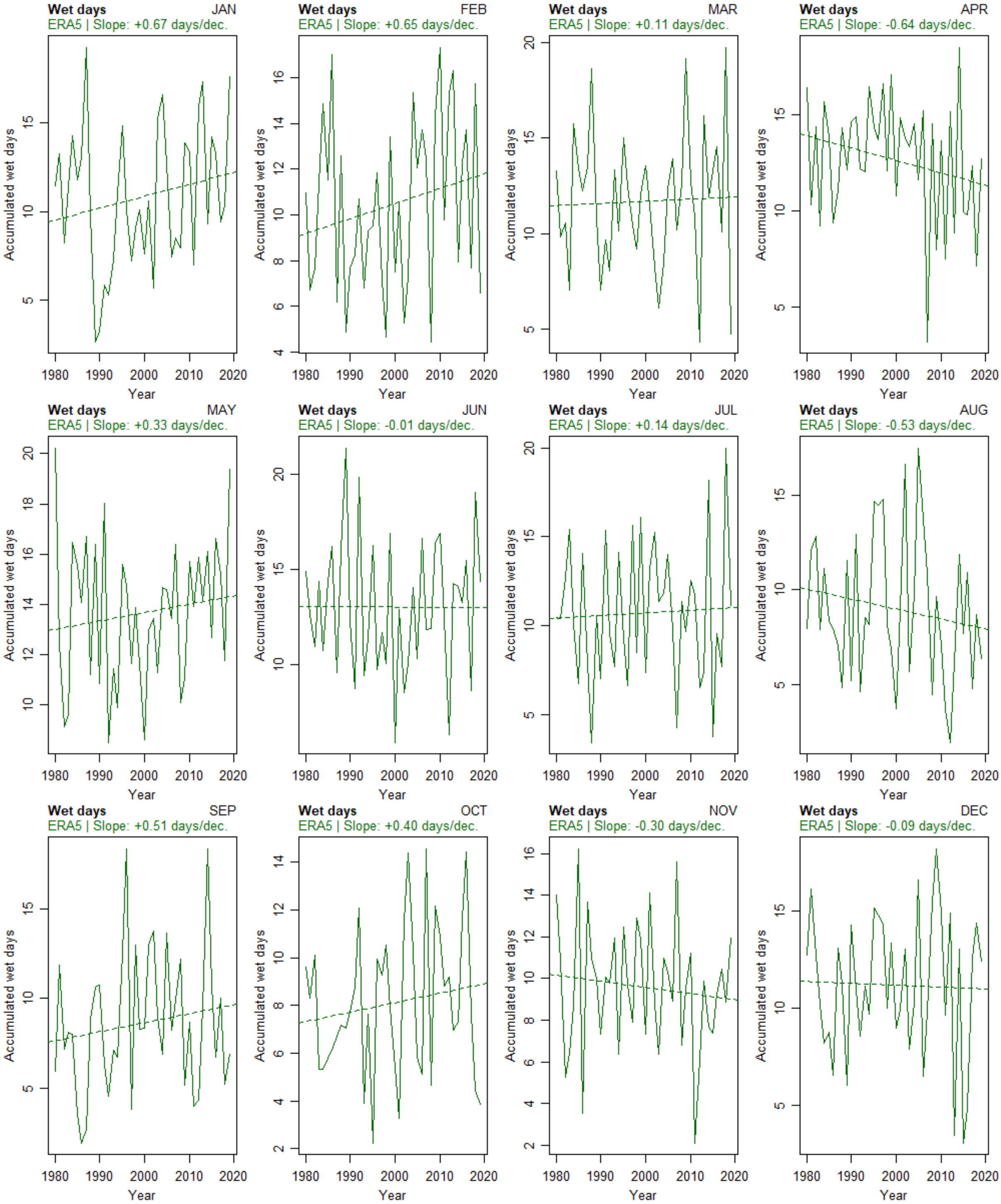

Figure 51 – Historic time series of the monthly accumulated very wet days

Time series over 1980-2019 period. Data source: ERA5, ECMWF / Copernicus Climate Change Service (Muñoz Sabater, 2019), Republic Hydrometeorological Service of Serbia

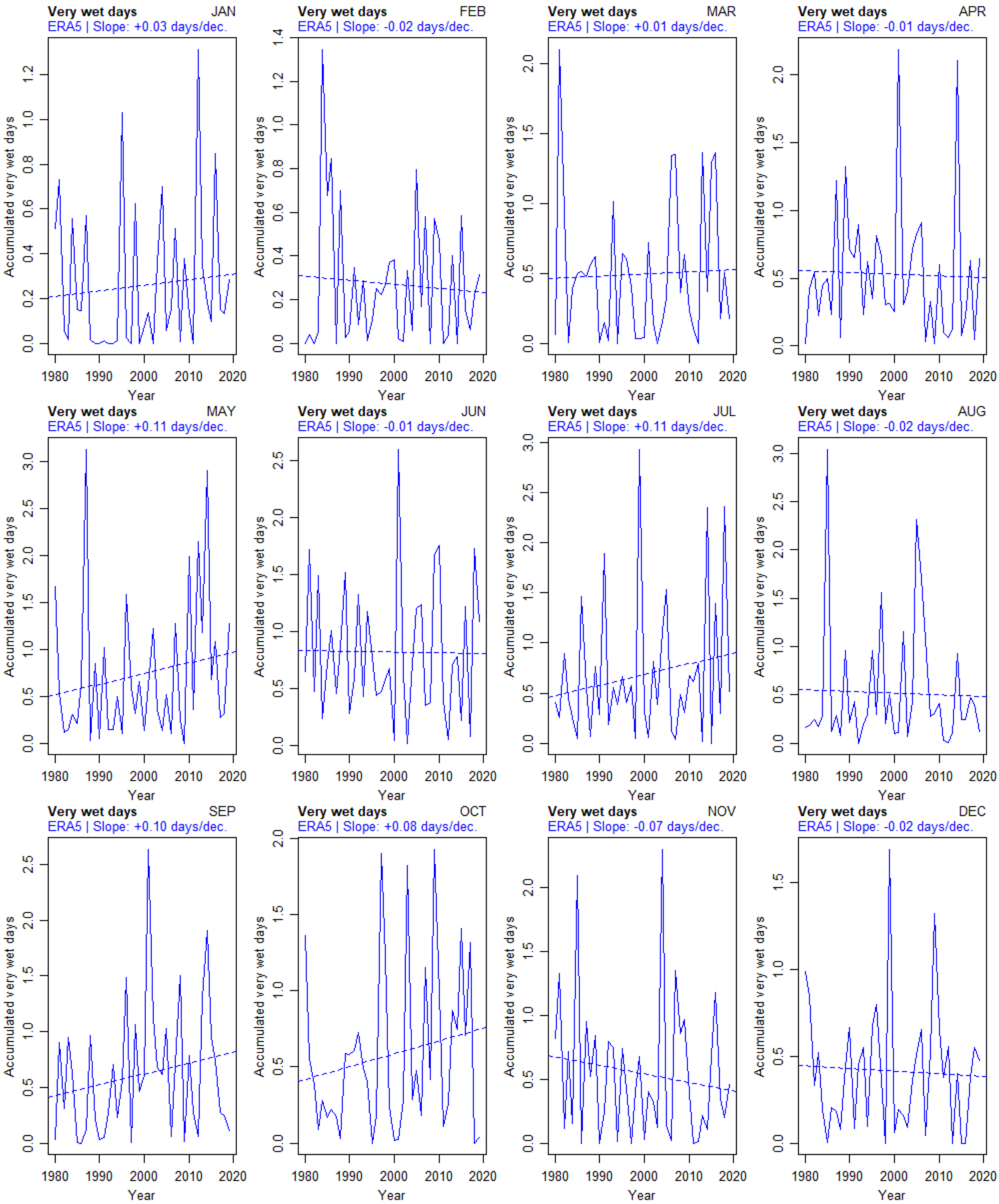

Figure 52 – Historic time series of the duration of the longest dry spell of the month
Time series over 1980-2019 period. <u>Data source:</u> ERA5, ECMWF / Copernicus Climate Change Service (Muñoz Sabater, 2019), Republic Hydrometeorological Service of Serbia.

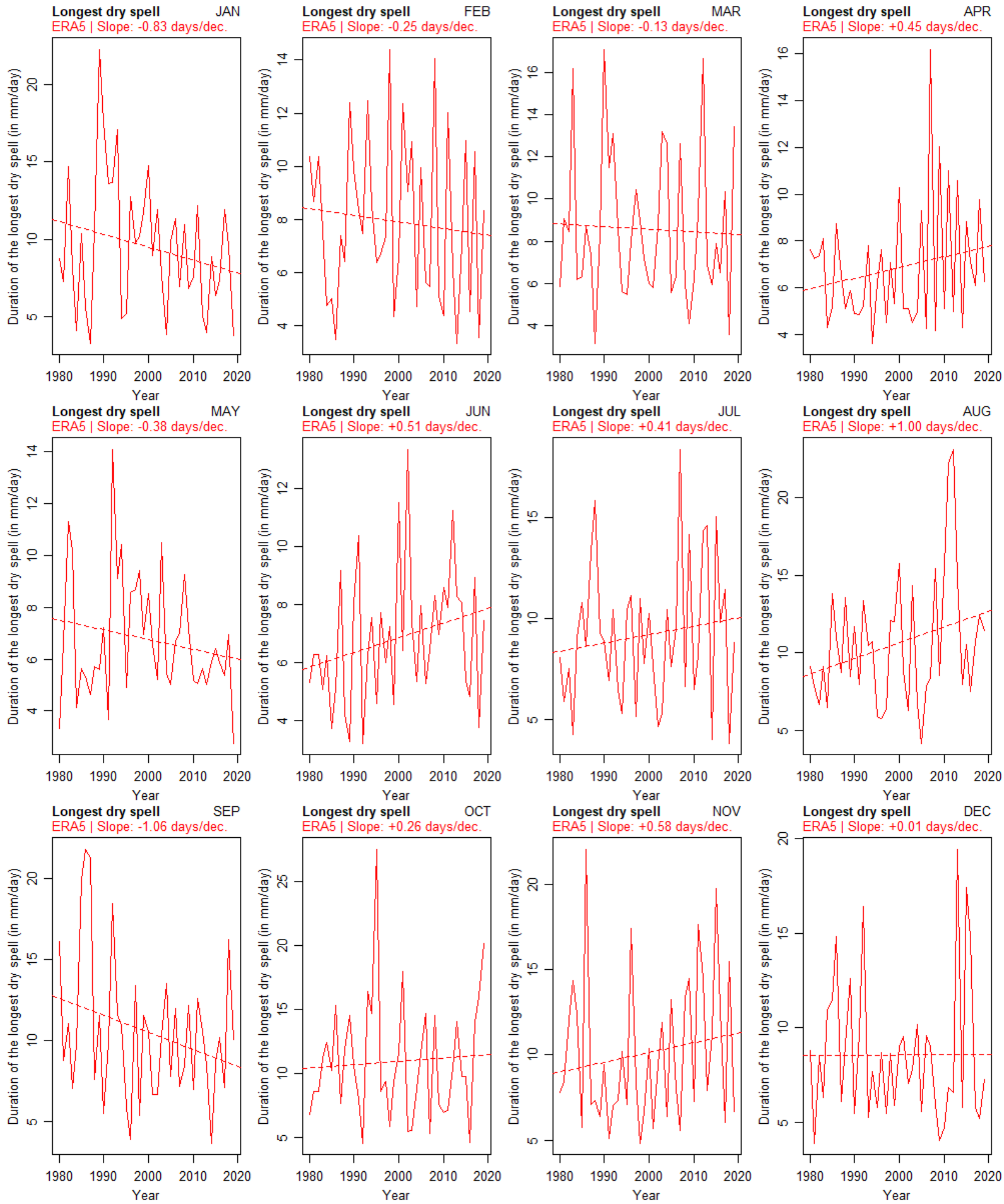

Table 13 - Characteristics of the trends from the historical time series of the monthly accumulated wet days, very wet days, and the duration of the longest dry spell of the month (linear models)
***In green**: Monthly accumulated wet days. **In blue:** monthly accumulated very wet days. **In red:** duration of the longest dry spell of the month. Data source: ERA5, ECMWF / Copernicus Climate Change Service (Muñoz Sabater, 2019), Republic Hydrometeorological Service of Serbia.*

Variable	Month	Slope	p-value	Adjusted R^2	Average value in 1980	Average value in 2019
WD_m	January	+0.67 days/dec.	0.23	0.01	9.53 days	12.13 days
WD_m	February	+0.65 days/dec.	0.20	0.02	9.20 days	11.75 days
WD_m	March	+0.11 days/dec.	0.82	-0.02	11.45 days	11.89 days
WD_m	April	-0.64 days/dec.	0.14	0.03	13.90 days	11.39 days
WD_m	May	+0.33 days/dec.	0.41	-0.01	13.00 days	14.28 days
WD_m	June	-0.01 days/dec.	0.99	-0.03	13.03 days	13.00 days
WD_m	July	+0.14 days/dec.	0.79	-0.02	10.42 days	10.97 days
WD_m	August	-0.53 days/dec.	0.31	0.00	10.04 days	7.99 days
WD_m	September	+0.51 days/dec.	0.34	0.00	7.61 days	9.61 days
WD_m	October	+0.40 days/dec.	0.36	0.00	7.32 days	8.88 days
WD_m	November	-0.30 days/dec.	0.49	-0.01	10.17 days	9.01 days
WD_m	December	-0.09 days/dec.	0.85	-0.03	11.38 days	11.01 days
VWD_m	January	+0.03 days/dec.	0.56	-0.02	0.21 days	0.31 days
VWD_m	February	-0.02 days/dec.	0.66	-0.02	0.31 days	0.23 days
VWD_m	March	+0.01 days/dec.	0.83	-0.03	0.46 days	0.52 days
VWD_m	April	-0.01 days/dec.	0.86	-0.03	0.55 days	0.50 days
VWD_m	May	+0.11 days/dec.	0.28	0.00	0.51 days	0.96 days
VWD_m	June	-0.01 days/dec.	0.94	-0.03	0.83 days	0.81 days
VWD_m	July	+0.11 days/dec.	0.28	0.01	0.47 days	0.89 days
VWD_m	August	-0.02 days/dec.	0.85	-0.03	0.55 days	0.48 days
VWD_m	September	+0.10 days/dec.	0.24	0.01	0.43 days	0.80 days
VWD_m	October	+0.08 days/dec.	0.26	0.01	0.42 days	0.75 days
VWD_m	November	-0.07 days/dec.	0.38	-0.01	0.67 days	0.41 days
VWD_m	December	-0.02 days/dec.	0.77	-0.02	0.44 days	0.38 days
DS_m	January	-0.83 days/dec.	0.15	0.03	11.16 days	7.92 days
DS_m	February	-0.25 days/dec.	0.56	-0.02	8.41 days	7.45 days
DS_m	March	-0.13 days/dec.	0.79	-0.02	8.84 days	8.33 days
DS_m	April	+0.45 days/dec.	0.21	0.02	5.94 days	7.71 days
DS_m	May	-0.38 days/dec.	0.26	0.01	7.51 days	6.05 days
DS_m	June	+0.51 days/dec.	0.11	0.04	5.85 days	7.82 days
DS_m	July	+0.41 days/dec.	0.40	-0.01	8.38 days	9.99 days
DS_m	August	+1.00 days/dec.	0.08	0.06	8.65 days	12.56 days
DS_m	September	-1.06 days/dec.	0.08	0.05	12.61 days	8.49 days
DS_m	October	+0.26 days/dec.	0.69	-0.02	10.44 days	11.45 days
DS_m	November	+0.58 days/dec.	0.33	0.00	8.98 days	11.25 days
DS_m	December	+0.01 days/dec.	0.99	-0.03	8.56 days	8.59 days

Historical annual trends

Historical annual trends on accumulated wet days, accumulated very wet days, and the duration of the longest dry spell can be observed in Figure 53 and Table 14.

As for precipitation, WD_y, VWD_y and DS_y present very large historical inter annual variations (between 100 and 150 days for WD_y, between 2 and 12 days for VWD_y and between 15 and 35 days for DS_y). The trends presented here are thus not very marked and should be observed with circumspection.

WD_y and VWD_y seemed to present a very slight increase during the last 40 years, (+1.25 days/decade for WD_y, +0.31 days/decade for VWD_y) bringing from 127 wet days in 1980 to 132 wet days in 2019, and 6 very wet days in 1980 to 7 wet days in 2019. DS_y on its part stayed stable on average, maintaining its level around 21 days.

Figure 53 – Historical annual time series of the accumulated wet days, accumulated very wet days, and duration of the longest dry spell of the year

Time series over 1980-2019 period. ***In green:*** *annually accumulated wet days.* ***In blue:*** *annually accumulated very wet days.* ***In red:*** *duration of the longest dry spell of the year. Data source: ERA5, ECMWF / Copernicus Climate Change Service (Muñoz Sabater, 2019)*

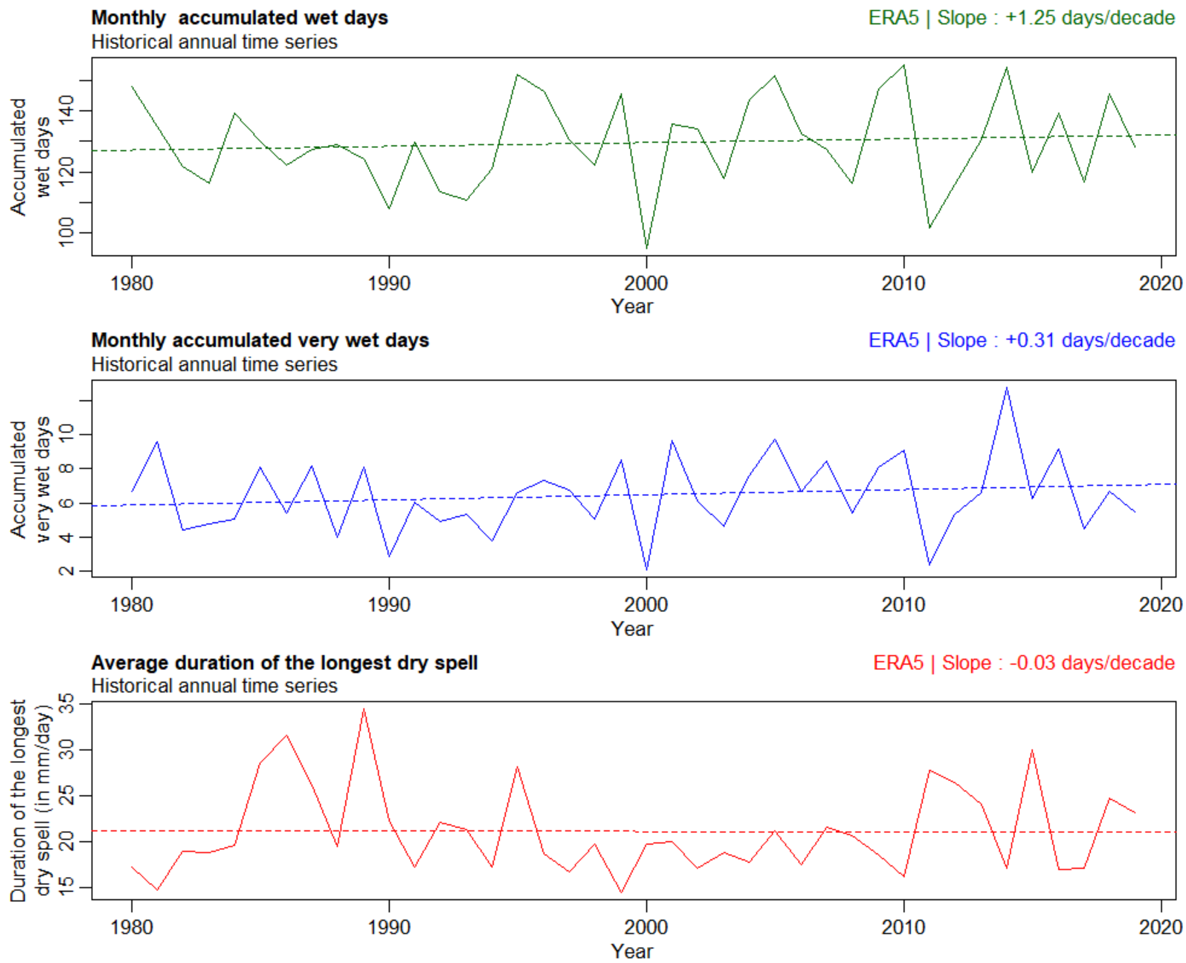

Table 14 – Characteristics of the trend from historical annual time series of the accumulated wet days, accumulated very wet days, and duration of the longest dry spell of the year (linear models)
Data source: ERA5, ECMWF / Copernicus Climate Change Service (Muñoz Sabater, 2019)

Variable	Slope	p-value	Adj. R^2	Average value in 1980	Average value in 2019
WD_y	+1.25 days/dec.	0.54	-0.02	127 days	132 days
VWD_y	+0.31 days/dec.	0.32	0.00	5.86 days	7.06 days
DS_y	-0.03 days/dec.	0.97	-0.03	21.16 days	21.05 days

Spatial distribution

The spatial distribution of the trends on accumulated wet days, accumulated very wet days, and the duration of the longest dry spell throughout Serbia can be observed in Figure 54.

Figure 54 – Historical decadal spatial distribution of annually accumulated wet days, very wet days, and the duration of the longest dry spell of the year
Data averaged over the 1980-2059 period, by decade. Data source: ERA5, ECMWF / Copernicus Climate Change Service (Muñoz Sabater, 2019)

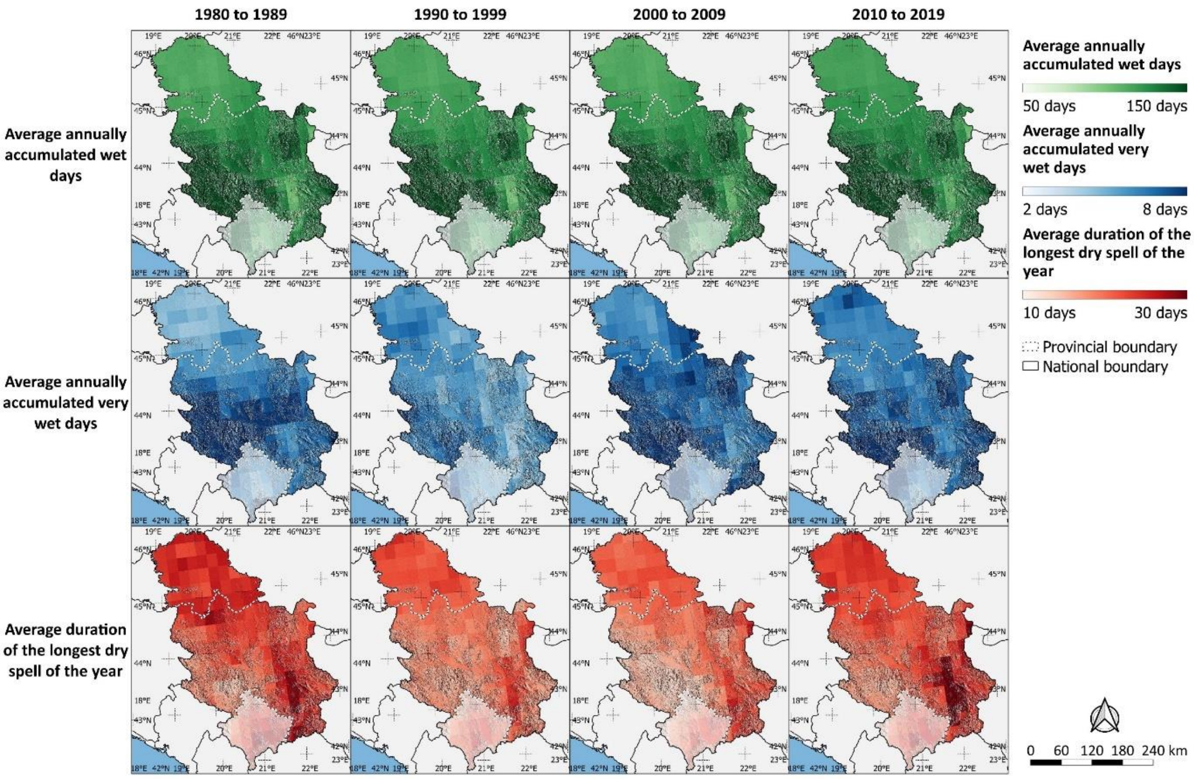

As for precipitation, the spatial distribution seems to be constant for WD_y and VWD_y, with higher in the high lands of the south especially on mountain tops, and lower in the plains of the North and valleys of the South. DS_y shows an inverse distribution: lower values in the high lands of the south, and higher values in the plains of the North and valleys of the South.

Projected monthly trends

The monthly project trends on accumulated wet days, accumulated very wet days and the duration of the longest dry spell at a monthly scale can be observed in Figure 55, Figure 56 and Figure 57, Table 15 and Table 16.

Figure 55 – Projected time series of the monthly accumulated wet days

Time series over 2020-2060 period. ***Pink dotted line****: variable value for each model separately under the RCP4.5 scenario.* ***grey dotted line****: variable value for each model separately under the RCP8.5 scenario.* ***Purple full line:*** *median value of the variable under RCP4.5 scenario.* ***Black full line:*** *median value of the variable under RCP8.5 scenario.* *<u>Data source:</u> NASA Earth Exchange - Global Daily Downscaled Climate Projections (NEX – GDDP) (Thrasher et al., 2012).*

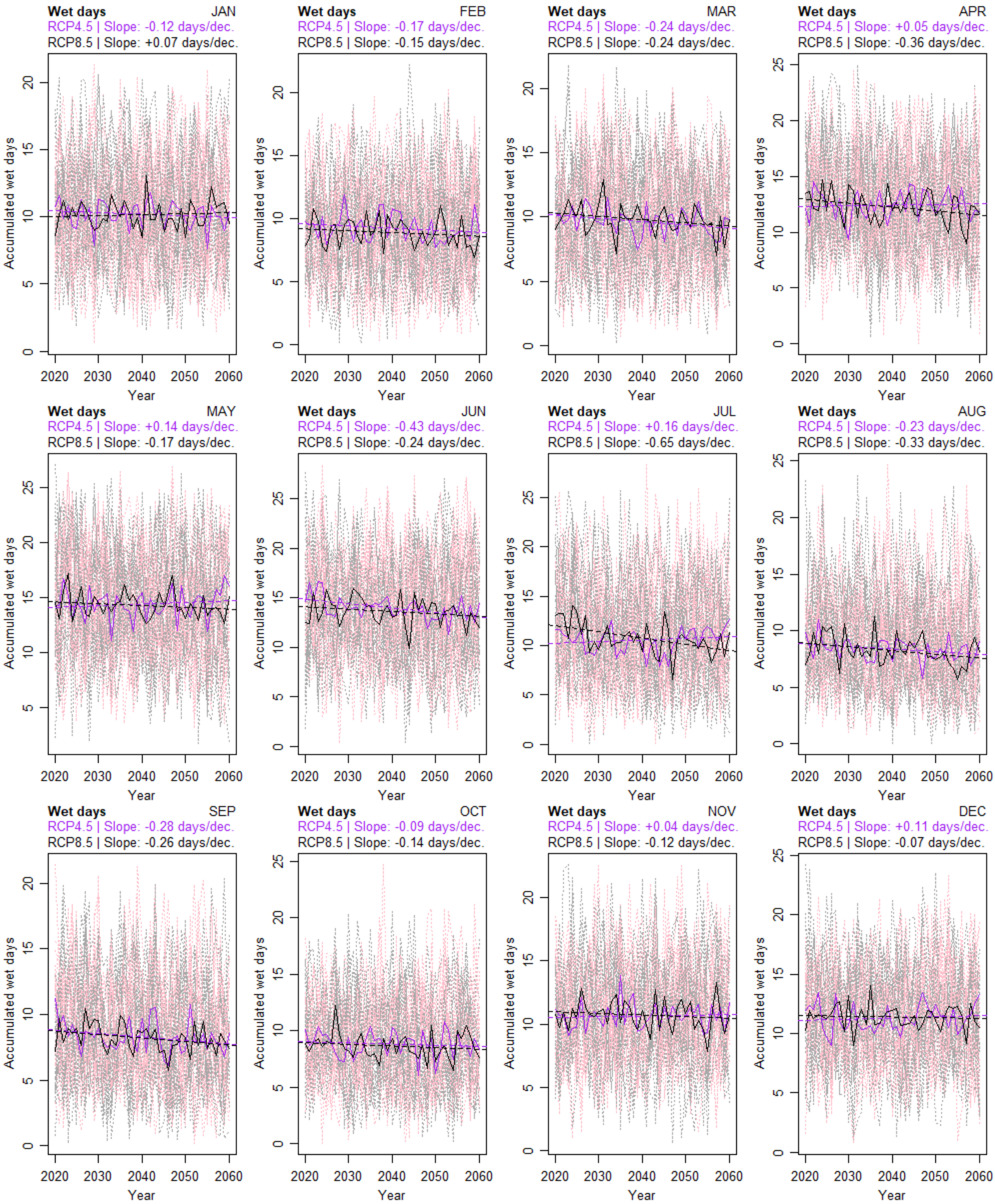

Figure 56 – Projected time series of the monthly accumulated very wet days

*Time series over 2020-2060 period. **Pink dotted line**: variable value for each model separately under the RCP4.5 scenario. **grey dotted line**: variable value for each model separately under the RCP8.5 scenario. **Purple full line:** median value of the variable under RCP4.5 scenario. **Black full line:** median value of the variable under RCP8.5 scenario. Data source: NASA Earth Exchange - Global Daily Downscaled Climate Projections (NEX – GDDP) (Thrasher et al., 2012).*

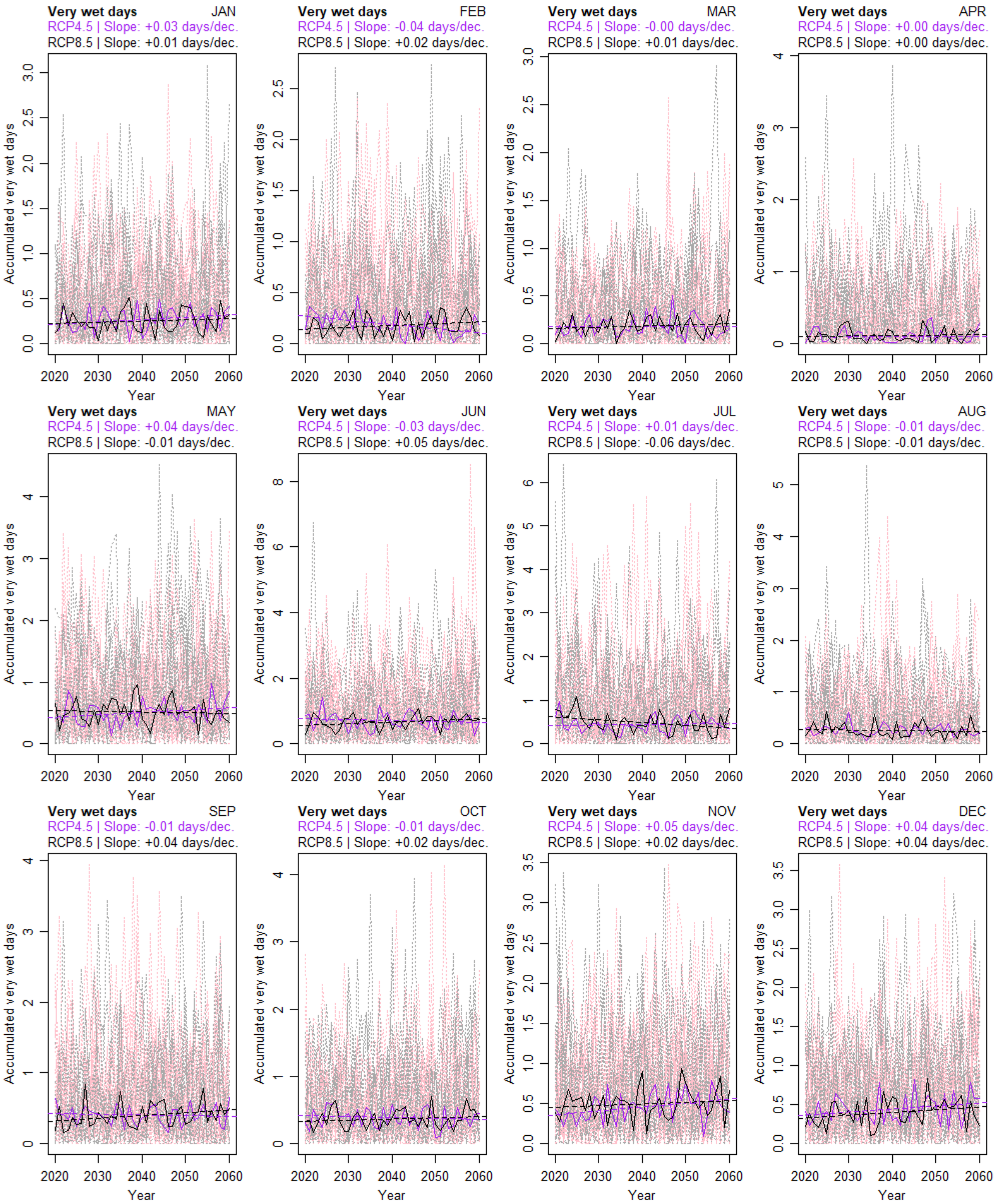

Figure 57 – Historic time series of the duration of the longest dry spell of the month

*Time series over 2020-2060 period. **Pink dotted line**: variable value for each model separately under the RCP4.5 scenario. **grey dotted line**: variable value for each model separately under the RCP8.5 scenario. **Purple full line:** median value of the variable under RCP4.5 scenario. **Black full line:** median value of the variable under RCP8.5 scenario. Data source: NASA Earth Exchange - Global Daily Downscaled Climate Projections (NEX – GDDP) (Thrasher et al., 2012).*

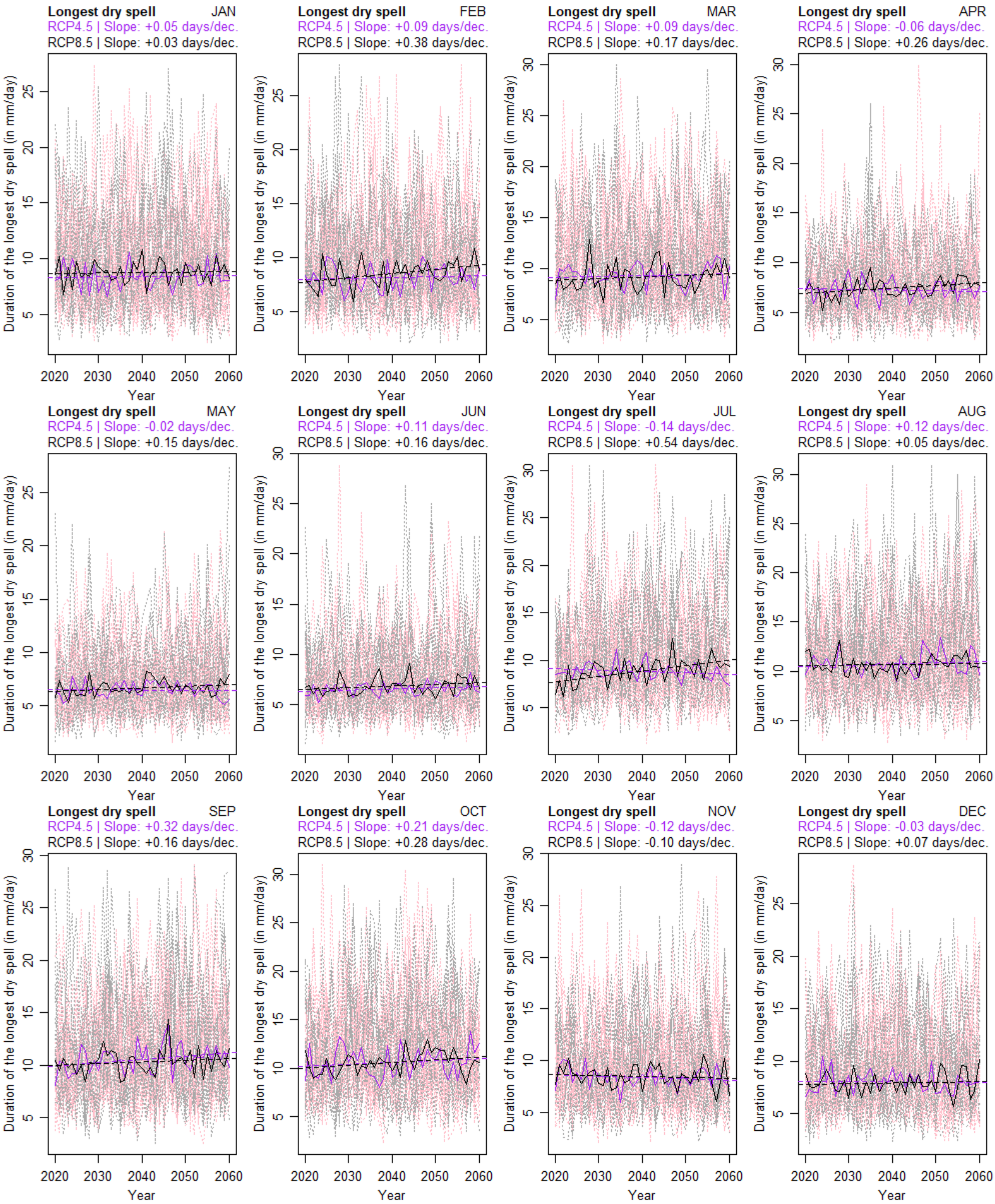

Table 15 – Characteristics of the trend from projected time series of monthly accumulated wet days, very wet days, and the duration of the longest dry spell of the month under the RCP4.5 scenario (linear models)
Data source: NASA Earth Exchange - Global Daily Downscaled Climate Projections (NEX – GDDP) (Thrasher et al., 2012).

RCP4.5						
Variable	**Month**	**Slope**	**p-value**	**R^2**	**Average value in 2040**	**Average value in 2060**
WD_m	January	-0.12 days/dec.	0.33	0.00	10.19 days	9.94 days
WD_m	February	-0.17 days/dec.	0.21	0.01	9.28 days	8.94 days
WD_m	March	-0.24 days/dec.	0.07	0.06	9.65 days	9.17 days
WD_m	April	+0.05 days/dec.	0.75	-0.02	12.44 days	12.54 days
WD_m	May	+0.14 days/dec.	0.44	-0.01	14.38 days	14.66 days
WD_m	June	-0.43 days/dec.	0.00	0.19	13.97 days	13.10 days
WD_m	July	+0.16 days/dec.	0.33	0.00	10.54 days	10.86 days
WD_m	August	-0.23 days/dec.	0.07	0.06	8.35 days	7.89 days
WD_m	September	-0.28 days/dec.	0.07	0.06	8.30 days	7.74 days
WD_m	October	-0.09 days/dec.	0.54	-0.02	8.82 days	8.64 days
WD_m	November	+0.04 days/dec.	0.78	-0.02	10.64 days	10.71 days
WD_m	December	+0.11 days/dec.	0.45	-0.01	11.30 days	11.53 days
VWD_m	January	+0.03 days/dec.	0.12	0.04	0.27 days	0.32 days
VWD_m	February	-0.04 days/dec.	0.00	0.18	0.19 days	0.11 days
VWD_m	March	-0.00 days/dec.	0.92	-0.03	0.18 days	0.18 days
VWD_m	April	+0.00 days/dec.	0.99	-0.03	0.11 days	0.11 days
VWD_m	May	+0.04 days/dec.	0.11	0.04	0.51 days	0.58 days
VWD_m	June	-0.03 days/dec.	0.42	-0.01	0.70 days	0.64 days
VWD_m	July	+0.01 days/dec.	0.73	-0.02	0.44 days	0.46 days
VWD_m	August	-0.01 days/dec.	0.53	-0.02	0.26 days	0.24 days
VWD_m	September	-0.01 days/dec.	0.65	-0.02	0.40 days	0.39 days
VWD_m	October	-0.01 days/dec.	0.50	-0.01	0.39 days	0.36 days
VWD_m	November	+0.05 days/dec.	0.04	0.08	0.46 days	0.55 days
VWD_m	December	+0.04 days/dec.	0.10	0.04	0.44 days	0.52 days
DS_m	January	+0.05 days/dec.	0.74	-0.02	8.39 days	8.48 days
DS_m	February	+0.09 days/dec.	0.56	-0.02	8.12 days	8.30 days
DS_m	March	+0.09 days/dec.	0.55	-0.02	9.31 days	9.48 days
DS_m	April	-0.06 days/dec.	0.62	-0.02	7.25 days	7.12 days
DS_m	May	-0.02 days/dec.	0.82	-0.02	6.49 days	6.45 days
DS_m	June	+0.11 days/dec.	0.17	0.02	6.54 days	6.77 days
DS_m	July	-0.14 days/dec.	0.21	0.02	8.81 days	8.53 days
DS_m	August	+0.12 days/dec.	0.41	-0.01	10.75 days	10.99 days
DS_m	September	+0.40°C/dec.	0.00	0.57	8.30 days	9.11 days
DS_m	October	+0.37°C/dec.	0.00	0.29	1.97 days	2.71 days
DS_m	November	+0.23°C/dec.	0.00	0.24	-3.55 days	-3.09 days
DS_m	December	+0.26°C/dec.	0.00	0.23	-6.25 days	-5.72 days

Table 16 – Characteristics of the trend from projected time series of monthly accumulated wet days, very wet days, and the duration of the longest dry spell of the month under the RCP8.5 scenario (linear models)
Data source: NASA Earth Exchange - Global Daily Downscaled Climate Projections (NEX – GDDP) (Thrasher et al., 2012).

RCP8.5						
Variable	**Month**	**Slope**	**p-value**	**R^2**	**Average value in 2040**	**Average value in 2060**
WD_m	January	+0.07 days/dec.	0.62	-0.02	10.18 days	10.31 days
WD_m	February	-0.15 days/dec.	0.29	0.00	8.90 days	8.59 days
WD_m	March	-0.24 days/dec.	0.10	0.04	9.78 days	9.29 days
WD_m	April	-0.36 days/dec.	0.04	0.08	12.26 days	11.53 days
WD_m	May	-0.17 days/dec.	0.26	0.01	14.29 days	13.95 days
WD_m	June	-0.24 days/dec.	0.18	0.02	13.62 days	13.15 days
WD_m	July	-0.65 days/dec.	0.00	0.22	10.79 days	9.50 days
WD_m	August	-0.33 days/dec.	0.05	0.07	8.24 days	7.58 days
WD_m	September	-0.26 days/dec.	0.06	0.06	8.22 days	7.71 days
WD_m	October	-0.14 days/dec.	0.36	0.00	8.64 days	8.37 days
WD_m	November	-0.12 days/dec.	0.42	-0.01	10.70 days	10.45 days
WD_m	December	-0.07 days/dec.	0.59	-0.02	11.38 days	11.24 days
VWD_m	January	+0.01 days/dec.	0.46	-0.01	0.25 days	0.27 days
VWD_m	February	+0.02 days/dec.	0.17	0.02	0.18 days	0.21 days
VWD_m	March	+0.01 days/dec.	0.32	0.00	0.18 days	0.21 days
VWD_m	April	+0.00 days/dec.	0.75	-0.02	0.11 days	0.12 days
VWD_m	May	-0.01 days/dec.	0.69	-0.02	0.52 days	0.50 days
VWD_m	June	+0.05 days/dec.	0.07	0.06	0.67 days	0.76 days
VWD_m	July	-0.06 days/dec.	0.03	0.10	0.49 days	0.36 days
VWD_m	August	-0.01 days/dec.	0.51	-0.01	0.25 days	0.23 days
VWD_m	September	+0.04 days/dec.	0.10	0.05	0.40 days	0.47 days
VWD_m	October	+0.02 days/dec.	0.41	-0.01	0.37 days	0.40 days
VWD_m	November	+0.02 days/dec.	0.38	0.00	0.50 days	0.54 days
VWD_m	December	+0.04 days/dec.	0.10	0.04	0.40 days	0.47 days
DS_m	January	+0.03 days/dec.	0.83	-0.02	8.77 days	8.82 days
DS_m	February	+0.38 days/dec.	0.01	0.14	8.52 days	9.28 days
DS_m	March	+0.17 days/dec.	0.35	0.00	9.15 days	9.48 days
DS_m	April	+0.26 days/dec.	0.03	0.10	7.43 days	7.94 days
DS_m	May	+0.15 days/dec.	0.11	0.04	6.69 days	6.99 days
DS_m	June	+0.16 days/dec.	0.15	0.03	6.85 days	7.16 days
DS_m	July	+0.54 days/dec.	0.00	0.24	8.87 days	9.95 days
DS_m	August	+0.05 days/dec.	0.69	-0.02	10.63 days	10.73 days
DS_m	September	+0.16 days/dec.	0.31	0.00	10.32 days	10.64 days
DS_m	October	+0.28 days/dec.	0.05	0.07	10.59 days	11.15 days
DS_m	November	-0.10 days/dec.	0.46	-0.01	8.46 days	8.25 days
DS_m	December	+0.07 days/dec.	0.61	-0.02	7.92 days	8.06 days

Overall, although a large interannual variation, most of the monthly values remained stable on average under both scenarios. WD_m is predicted to vary between -0.6 days/decade to +0.2 days/decade, VWD_m between -0.1 days/decade and no variation, and DS_m a variation between -0.4 day/decade and +0.1 day/decade.

Projected annual trends

Projected annual trends on accumulated wet days, accumulated very wet days, and the duration of the longest dry spell can be observed in Figure 58 and Table 17.

Figure 58 – Projected annual time series of accumulated wet days, accumulated very wet days, and duration of the longest dry spell of the year

Time series over 2020-2060 period. Time series over 2020-2060 period. ***Pink dotted line****: variable value for each model separately under the RCP4.5 scenario.* ***grey dotted line****: variable value for each model separately under the RCP8.5 scenario.* ***Purple full line:*** *median value of the variable under RCP4.5 scenario.* ***Black full line:*** *median value of the variable under RCP8.5 scenario.* *Data source: NASA Earth Exchange - Global Daily Downscaled Climate Projections (NEX – GDDP) (Thrasher et al., 2012).*

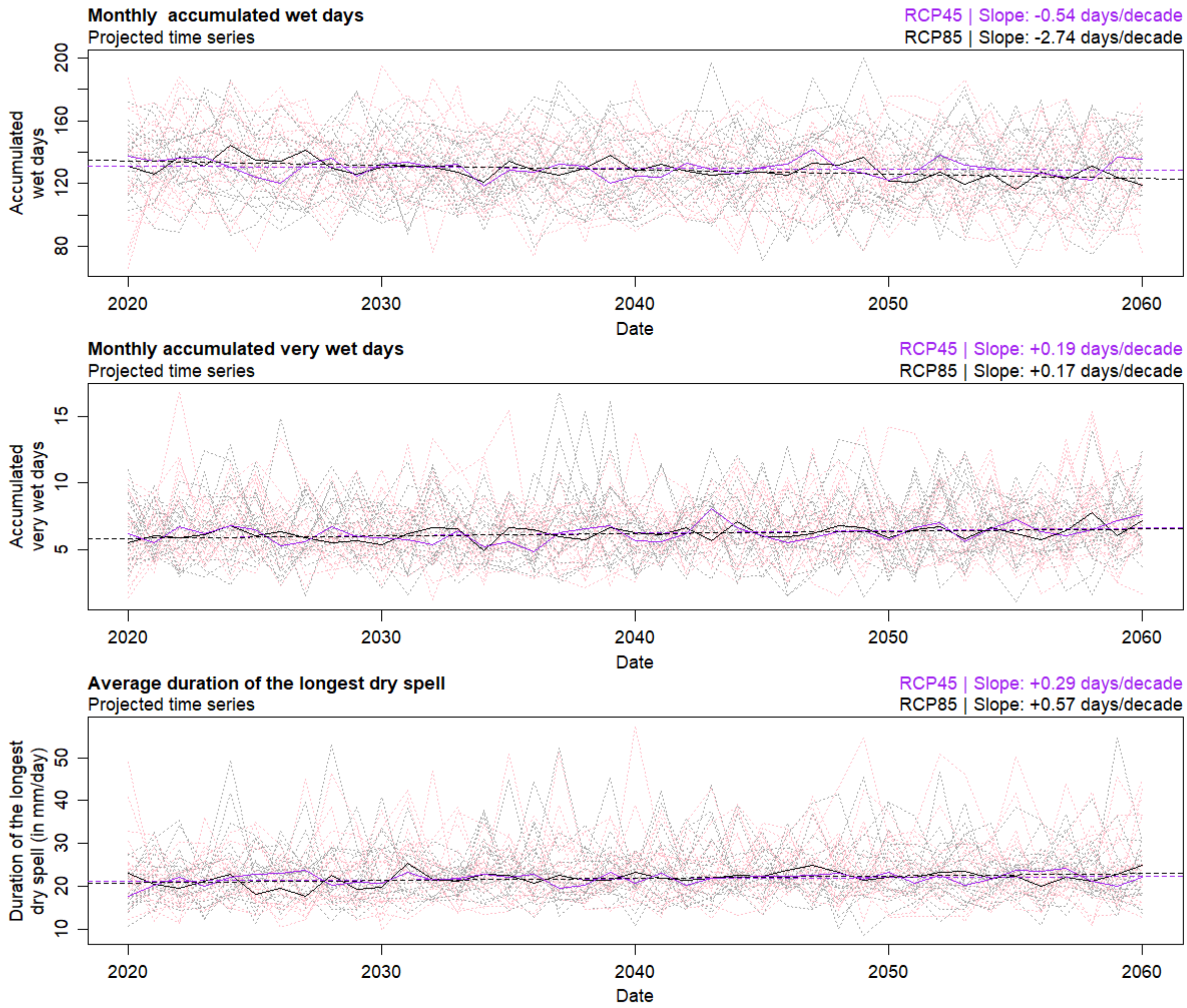

As for precipitation, WD_y, VWD_y and DS_y present very large projected inter annual variations (between 80 and 200 days for WD_y, between 4 and 15 days for VWD_y and between 10 and 50 days for DS_y). The trends presented here are thus not very clear and should be observed with circumspection.

NEX database expects WD_y, VWD_y and DS_y to remain stable for the next 40 years under both scenarios, with a value around 130 days for WD_y, 6 days for VWD_y, and 22 days for DS_y. The only exception to this general trend is WD_y under the RCP8.5 scenario, where a small decrease is noticeable: +3 days/decade, bringing WD_y from 129 days on average in 2040 to 123 days on average in 2060. This trends thus confirms the decrease of accumulated precipitation observed in Figure 46 under the RCP8.5 scenario.

Table 17 – Characteristics of the trend from projected data for accumulated wet days, accumulated very wet days, and duration of the longest dry spell of the year (linear models)
Data source: NASA Earth Exchange - Global Daily Downscaled Climate Projections (NEX – GDDP) (Thrasher et al., 2012).

RCP4.5					
Variable	**Slope**	**p-value**	**Adjusted R^2**	**Average value in 2040**	**Average value in 2060**
WD_y	-0.54 days/decade	0.46	-0.01	130 days	129 days
VWD_y	+0.19 days/decade	0.03	0.09	6.22 days	6.60 days
DS_y	+0.29 days/decade	0.12	0.04	22 days	22 days
RCP8.5					
Variable	**Slope**	**p-value**	**Adjusted R^2**	**Average value in 2040**	**Average value in 2060**
WD_y	-2.74 days/decade	0.00	0.28	129 days	123 days
VWD_y	+0.17 days/decade	0.02	0.12	6.22 days	6.57 days
DS_y	+0.57 days/decade	0.01	0.15	22 days	23 days

Conclusion

As for accumulated precipitation, wet days, very wet days, and the duration of the longest dry spell presented a very large interannual variation. The trends presented were thus not very clear and should be observed with circumspection.

Wet days and very wet days in Serbia follow a similar pattern to the accumulated precipitation pattern high during the wet season (May-June) and low during the dry season (November to April). During September and October, the rainy days are fewer but more intense. The longest dry spell presents an inverse pattern: higher during the dry season, and low during the wet season.

Although wet days and very wet days presented a very slight increase during the last 40 years, (+1.25 days/decade for WD_y, +0.31 days/decade for VWD_y) they are expected to stay stable for the next 40 years by the NEX projections under both RCP4.5 and RCP8.5 scenario. The duration of the longest dry spell stayed stable on average during the last 40 years and is expected to remain as such by the NEX database.

11. Frost days, ice days and chill hours

This section will present the variations of frost days, ice days, and chill hours in the Republic of Serbia, using the following variables:

- Annually **accumulated frost days** (FD_y) and monthly **accumulated frost days** (FD_m). Accumulated frost days are defined as the number of days over a given period, when the daily minimum temperature is below 0°C.
- Annually **accumulated ice days** (ID_y) and monthly **accumulated ice days** (ID_m). Accumulated ice days are defined as the number of days over a given period, when the daily maximum temperature is below 0°C.
- Annually **accumulated chill hours** (CH_y) and monthly **accumulated chill hours** (CH_m). Accumulated chill hours are define as the number of hours over a given period, when the daily average temperature is below 0°C.

Because frost days, ice days and chill hours are calculated at a daily or hourly scale, and because daily data from weather stations were not available, this section will only present variables calculated using ERA5 data for historical trends. Moreover, as no hourly predictions of average temperature were available, the projected chill hours were defined as the number of days where the average daily temperature was below 0°C, multiplied by 24.

Current seasonal variations

The current seasonal variation of frost days, ice days and chill hours in the Republic of Serbia are presented in Figure 59.

This chart presents FD_m, ID_m and CH_m, averaged over 30 years (1990 to 2019).

FD_m, ID_m, and CH_m follow the same general pattern. The three indices are peaking in January (around 22 days for FD_m, 8 days for ID_m and about 400h for CH_m). They then steadily decrease from January to April – May. On average, there is no more ice days after March, and no more chill hours and frost days after April. These indices reappear in September – October. On average the first frost days and chill hours appear in October while the first ice days appear in November. These three indices then increase back until January.

__Figure 59 – Current monthly variations of frost days, ice days, and chill hours__

*Data averaged over the 1990-2019 period. **In green:** monthly accumulated frost days. **In blue:** monthly accumulated ice days. **In red:** monthly accumulated chill hours. Data source: ERA5 - ECMWF / Copernicus Climate Change Service (Muñoz Sabater, 2019).*

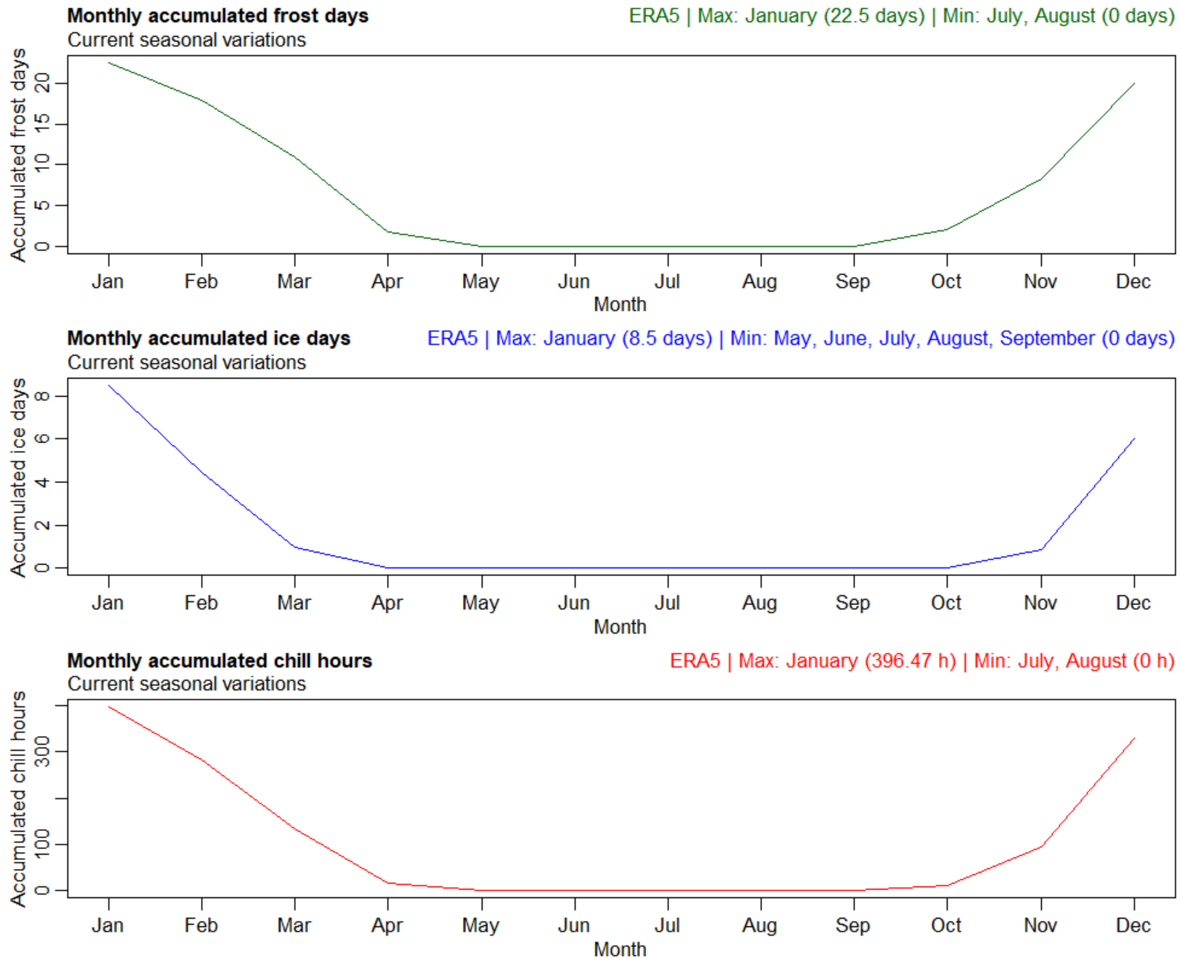

Spatial distribution

The monthly spatial distribution of frost days, ice days and chill hours throughout Serbia can be observed in Figure 60 and Figure 61.

As for minimum temperatures, frost days, ice days and chill hours tend to be more numerous and persist for a longer period on the higher altitude of the south of the country.

__Figure 60 – Current spatial distribution of monthly accumulated frost days and ice days__

*Data averaged over the 1990-2019 period. **In green:** monthly accumulated frost days. **In blue:** Monthly accumulated ice days. <u>Data source:</u> ERA5 - ECMWF / Copernicus Climate Change Service (Muñoz Sabater, 2019).*

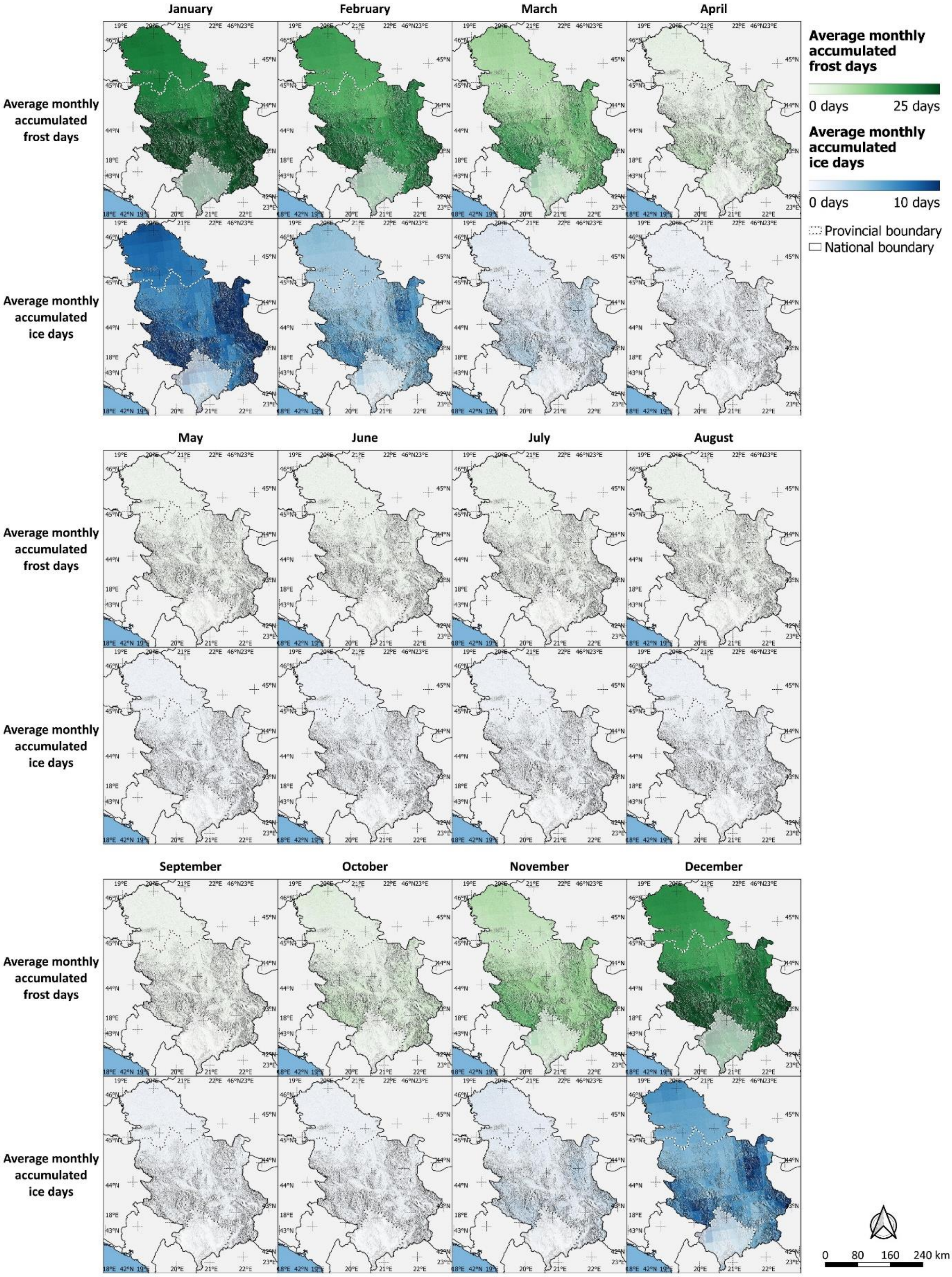

Figure 61 – Current spatial distribution of the monthly accumulated chill hours
Data averaged over the 1990-2019 period. Data source: ERA5 - ECMWF / Copernicus Climate Change Service (Muñoz Sabater, 2019).

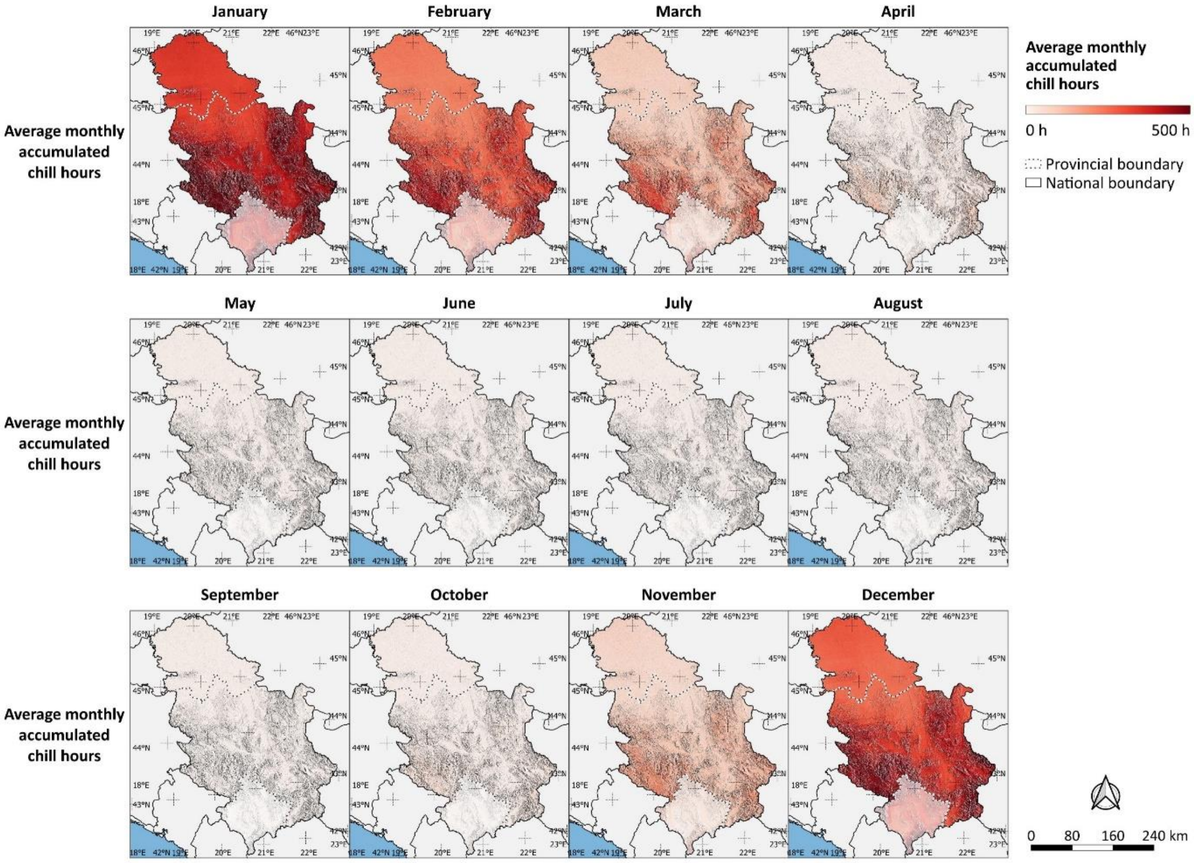

Historical monthly trends

The historical trends of monthly accumulated frost days, ice days and chill hours can be observed in Figure 62, Figure 63 and Figure 64 and Table 18.

Overall, most of the months shows a decrease in FD_m, ID_m and CH_m. In terms of critical months, the largest decrease in FD_m can be observed for the months of November (-2.1 days/decade), (-1.7 days/decade) and January (-1.2 days/decade). the largest decrease in IDm can be observed for the months of February (-1 days/decade), December (-0.6 days/decade) and January (-0.5 days/decade). Finally, the largest decrease in CH_m can be observed for the months of February (-34 h/decade), November (-30 h/decade) and January (-16 h/decade).

Figure 62 – Historical monthly time series of accumulated frost days

Time series over 1980-2019 period. Data source: ERA5, ECMWF / Copernicus Climate Change Service (Muñoz Sabater, 2019)

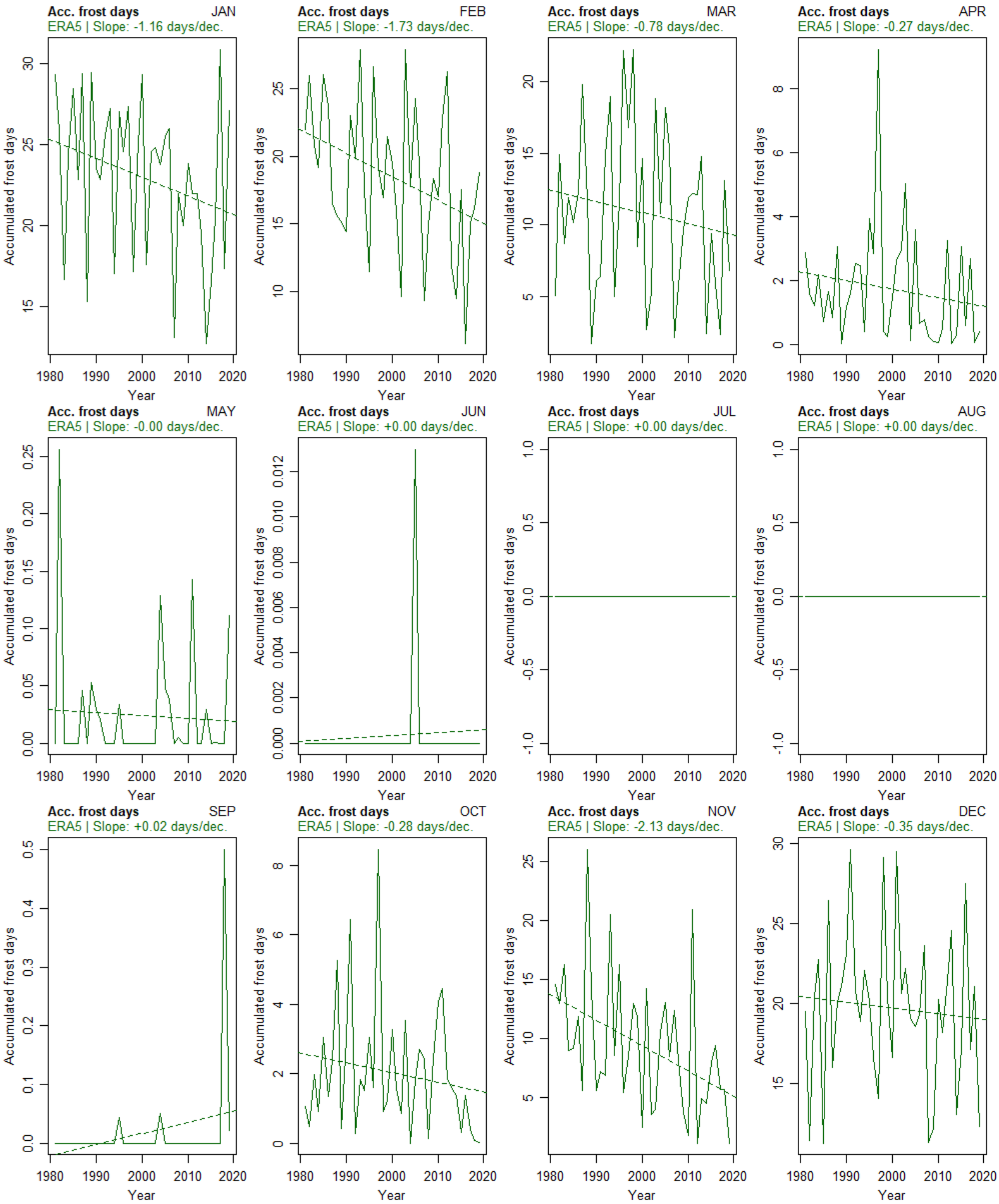

Figure 63 – Historical monthly time series of accumulated ice days

Time series over 1980-2019 period. <u>Data source:</u> ERA5, ECMWF / Copernicus Climate Change Service (Muñoz Sabater, 2019)

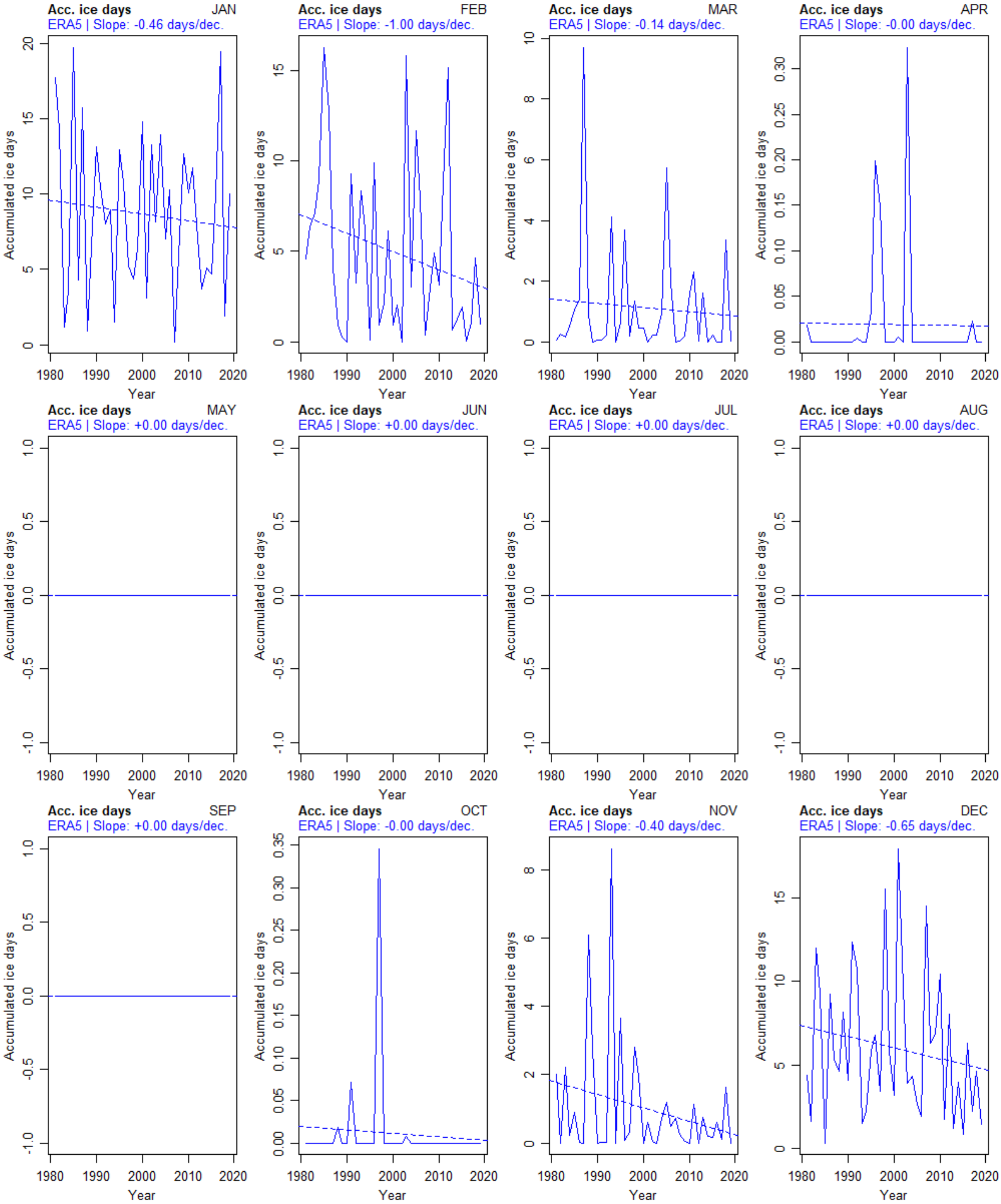

Figure 64 – Historical monthly time series of accumulated chill hours

Time series over 1980-2019 period. Data source: ERA5, ECMWF / Copernicus Climate Change Service (Muñoz Sabater, 2019)

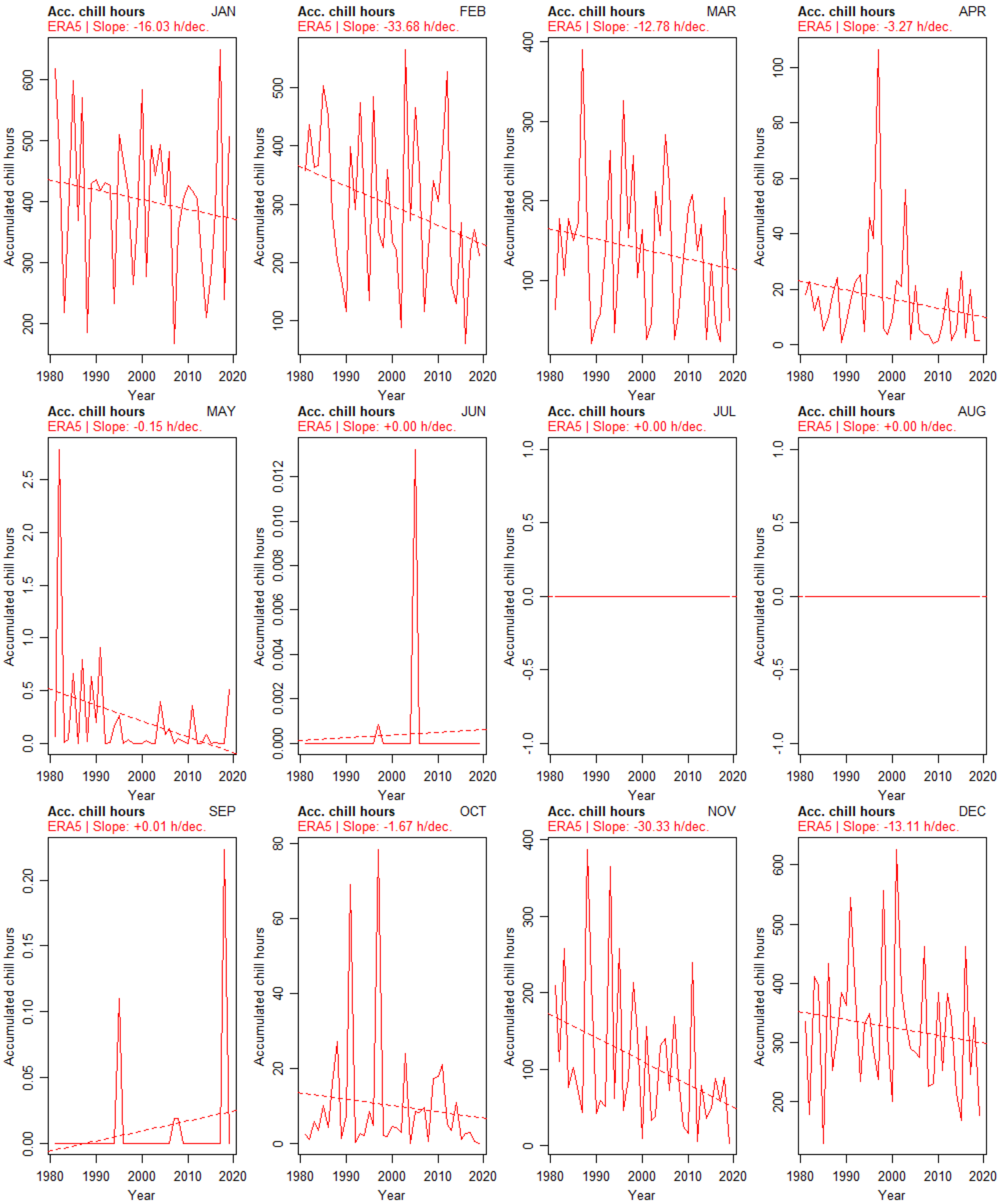

Table 18 – Characteristics of the trends from the historical time series of the monthly accumulated of frost days, ice days, and chill hours (linear models)

***In green**: Monthly accumulated frost days. **In blue:** monthly accumulated ice days. **In red:** monthly accumulated chill hours. Data source: ERA5, ECMWF / Copernicus Climate Change Service (Muñoz Sabater, 2019).*

Variable	Month	Slope	p-value	Adjusted R^2	Average value in 1980	Average value in 2019
FD_m	January	-1.16 days/dec.	0.09	0.05	25.30 days	20.79 days
FD_m	February	-1.73 days/dec.	0.02	0.11	21.97 days	15.22 days
FD_m	March	-0.78 days/dec.	0.34	0.00	12.42 days	9.37 days
FD_m	April	-0.27 days/dec.	0.30	0.00	2.26 days	1.20 days
FD_m	May	-0.00 days/dec.	0.72	-0.02	0.03 days	0.02 days
FD_m	June	+0.00 days/dec.	0.66	-0.02	0.00 days	0.00 days
FD_m	July	+0.00 days/dec.	NA	NA	0.00 days	0.00 days
FD_m	August	+0.00 days/dec.	NA	NA	0.00 days	0.00 days
FD_m	September	+0.02 days/dec.	0.10	0.05	-0.02 days	0.05 days
FD_m	October	-0.28 days/dec.	0.29	0.00	2.59 days	1.51 days
FD_m	November	-2.13 days/dec.	0.01	0.16	13.65 days	5.33 days
FD_m	December	-0.35 days/dec.	0.62	-0.02	20.45 days	19.09 days
ID_m	January	-0.46 days/dec.	0.55	-0.02	9.61 days	7.82 days
ID_m	February	-1.00 days/dec.	0.14	0.03	7.00 days	3.09 days
ID_m	March	-0.14 days/dec.	0.62	-0.02	1.40 days	0.86 days
ID_m	April	-0.00 days/dec.	0.93	-0.03	0.02 days	0.02 days
ID_m	May	+0.00 days/dec.	NA	NA	0.00 days	0.00 days
ID_m	June	+0.00 days/dec.	NA	NA	0.00 days	0.00 days
ID_m	July	+0.00 days/dec.	NA	NA	0.00 days	0.00 days
ID_m	August	+0.00 days/dec.	NA	NA	0.00 days	0.00 days
ID_m	September	+0.00 days/dec.	NA	NA	0.00 days	0.00 days
ID_m	October	-0.00 days/dec.	0.64	-0.02	0.02 days	0.00 days
ID_m	November	-0.40 days/dec.	0.12	0.04	1.83 days	0.28 days
ID_m	December	-0.65 days/dec.	0.30	0.00	7.33 days	4.79 days
CH_m	January	-16.03 h/dec.	0.36	0.00	435.60 h	373.10 h
CH_m	February	-33.68 h/dec.	0.07	0.06	364.36 h	233.03 h
CH_m	March	-12.78 h/dec.	0.33	0.00	164.63 h	114.78 h
CH_m	April	-3.27 h/dec.	0.25	0.01	22.98 h	10.23 h
CH_m	May	-0.15 h/dec.	0.03	0.10	0.51 h	-0.07 h
CH_m	June	+0.00 h/dec.	0.68	-0.02	0.00 h	0.00 h
CH_m	July	+0.00 h/dec.	NA	NA	0.00 h	0.00 h
CH_m	August	+0.00 h/dec.	NA	NA	0.00 h	0.00 h
CH_m	September	+0.01 h/dec.	0.18	0.02	-0.01 h	0.02 h
CH_m	October	-1.67 h/dec.	0.49	-0.01	13.39 h	6.87 h
CH_m	November	-30.33 h/dec.	0.02	0.11	171.85 h	53.57 h
CH_m	December	-13.11 h/dec.	0.41	-0.01	352.54 h	301.41 h

Historical annual trends

Historical annual trends on accumulated frost days, ice days and chill hours can be observed in Figure 65 and Table 19.

Figure 65 – Historical annual time series of accumulated frost days, ice days and chill hours
Time series over 1980-2019 period. ***In green:*** *annually accumulated frost days.* ***In blue:*** *annually accumulated ice days.* ***In red:*** *annually accumulated chill hours. Data source: ERA5, ECMWF / Copernicus Climate Change Service (Muñoz Sabater, 2019)*

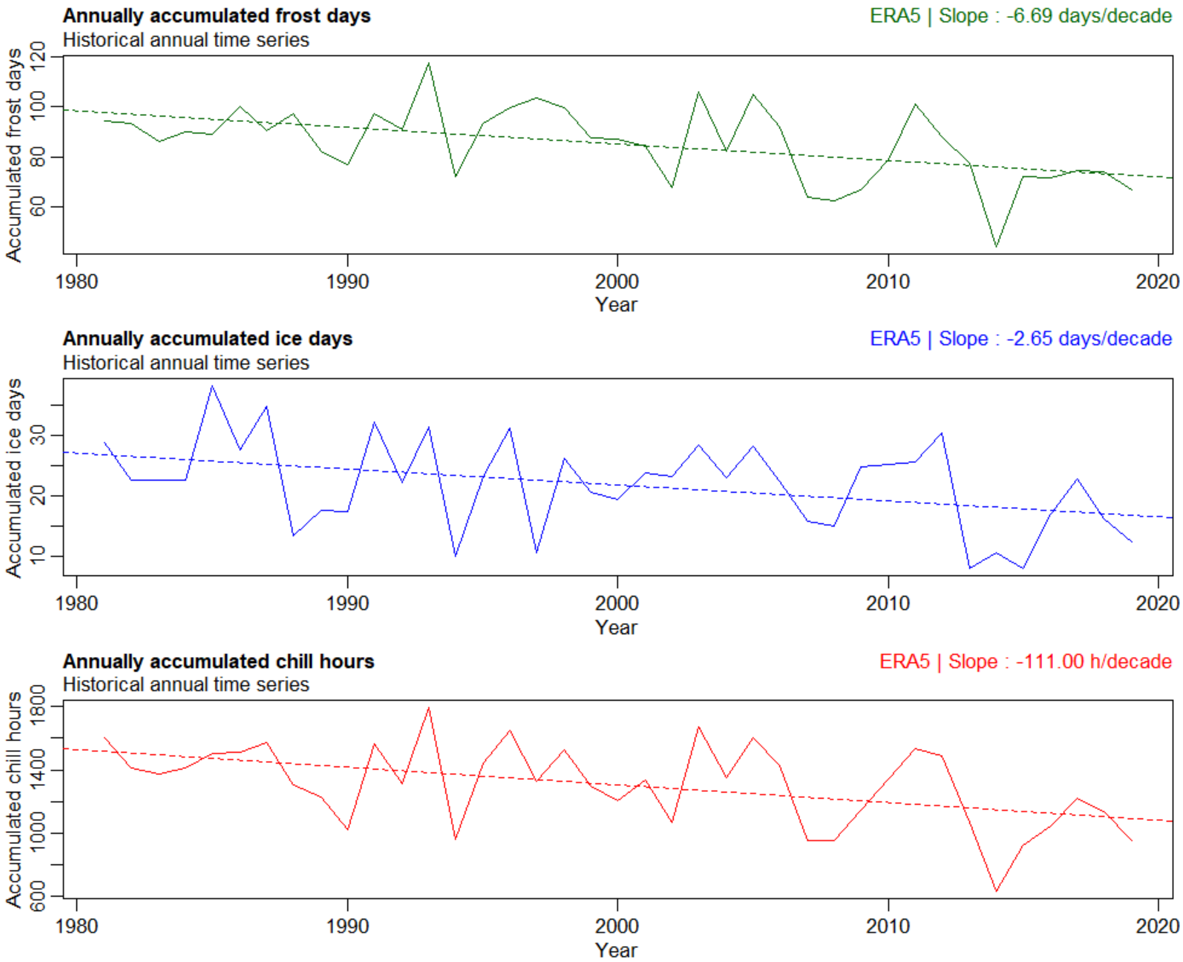

Table 19 – Characteristics of the trend from historical annual times series of accumulated frost days, ice days and chill hours (linear models)
Data source: ERA5, ECMWF / Copernicus Climate Change Service (Muñoz Sabater, 2019)

Variable	Slope	p-value	Adj. R^2	Average value in 1980	Average value in 2019
FD_y	*-6.69 days*	*0.00*	*0.24*	*99 days*	*73 days*
ID_y	*-2.65 days*	*0.01*	*0.14*	*27 days*	*17 days*
CH_y	*-111.00 h*	*0.00*	*0.22*	*1526 h*	*1093 h*

FD_y, ID_y and CH_y in Serbia presented a general decrease for the last 40 years (FD_y: -7.7 days/decade, ID_y: -2.6 days/decade and CH_y: -111 hours/decade). This decrease brought FD_y from 99 days on average in 1980 to 73 days on average in 2019, ID_y from 27 days on average in 1980 to 17 days on average in 2019, and CH_y from 1526 h on average in 1980 to 1093 h on average in 2019.

Spatial distribution

The spatial distribution of the trends on annually accumulated frost days, ice days and Chill Hours throughout Serbia can be observed in Figure 66.

The spatial distribution is constant for all the indices: frost days, ice days and chill hours tend to be more numerous on the higher altitude of the south of the country.

Figure 66 – Historical and projected decadal spatial distribution of annually accumulated frost days, ice days and chill hours

*Data averaged over the 1980-2019 period, by decade. **In green:** annually accumulated frost days. **In blue:** annually accumulated ice days. **In red:** annually accumulated chill hours. Data source: ERA5, ECMWF / Copernicus Climate Change Service (Muñoz Sabater, 2019)*

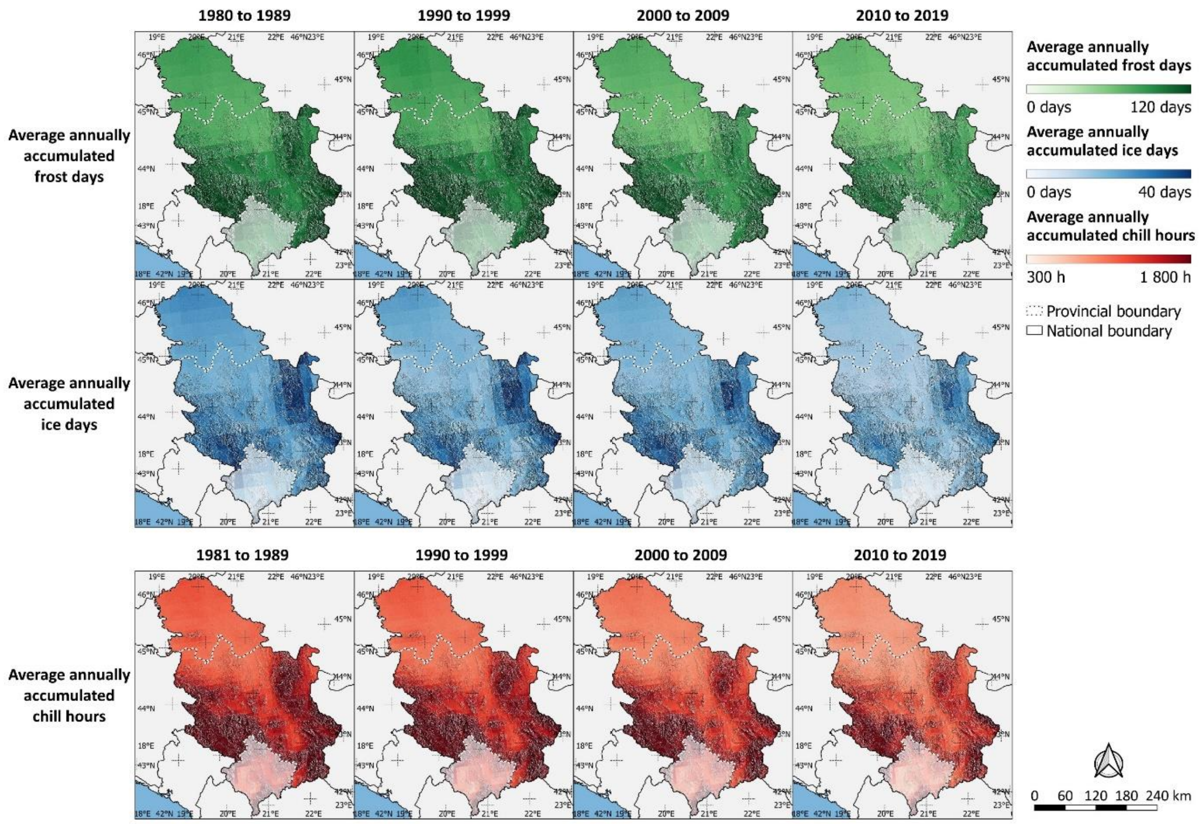

Projected monthly trends

The projected trends of monthly accumulated frost days, ice days and chill hours can be observed in Figure 67, Figure 68, Figure 69, Table 20 and Table 21.

Figure 67 – Projected time series of the monthly accumulated frost days

Time series over 2020-2060 period. ***Pink dotted line****: variable value for each model separately under the RCP4.5 scenario.* ***grey dotted line****: variable value for each model separately under the RCP8.5 scenario.* ***Purple full line:*** *median value of the variable under RCP4.5 scenario.* ***Black full line:*** *median value of the variable under RCP8.5 scenario. <u>Data source:</u> NASA Earth Exchange - Global Daily Downscaled Climate Projections (NEX – GDDP) (Thrasher et al., 2012).*

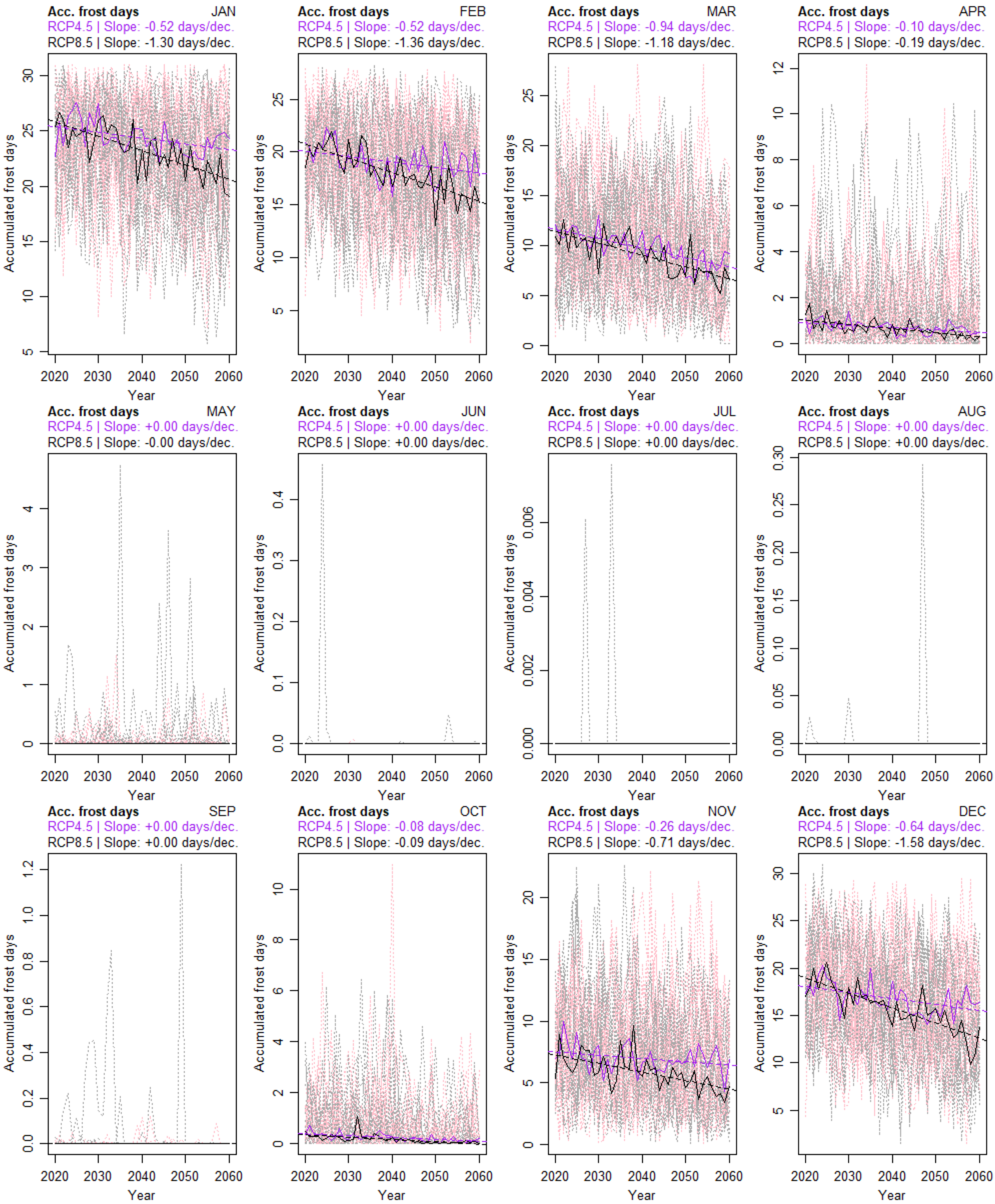

Figure 68 – Projected time series of the monthly accumulated ice days

Time series over 2020-2060 period. ***Pink dotted line****: variable value for each model separately under the RCP4.5 scenario.* ***grey dotted line****: variable value for each model separately under the RCP8.5 scenario.* ***Purple full line:*** *median value of the variable under RCP4.5 scenario.* ***Black full line:*** *median value of the variable under RCP8.5 scenario. <u>Data source:</u> NASA Earth Exchange - Global Daily Downscaled Climate Projections (NEX – GDDP) (Thrasher et al., 2012).*

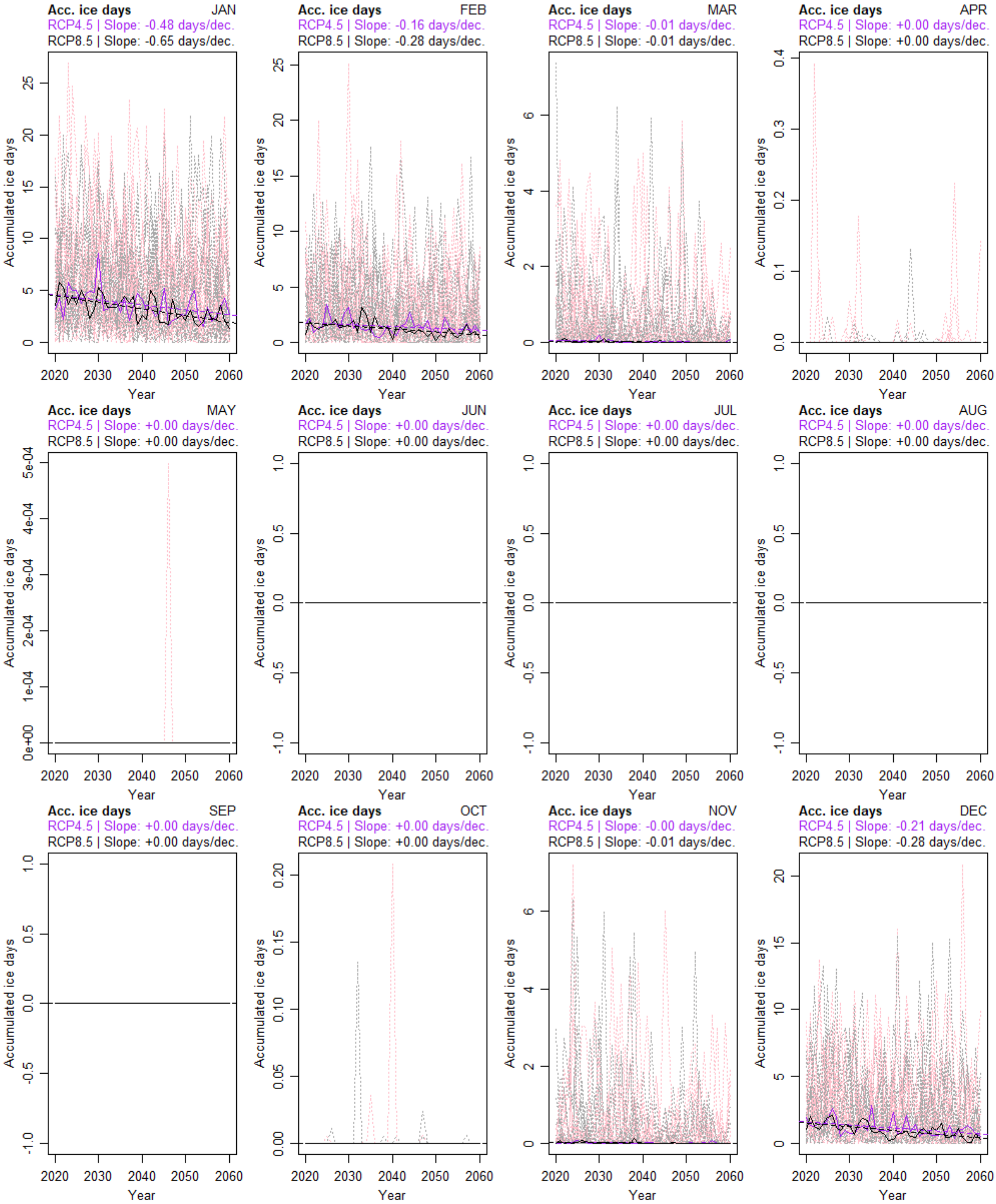

Figure 69 – Projected time series of the monthly accumulated chill hours

*Time series over 2020-2060 period. **Pink dotted line**: variable value for each model separately under the RCP4.5 scenario. **grey dotted line**: variable value for each model separately under the RCP8.5 scenario. **Purple full line:** median value of the variable under RCP4.5 scenario. **Black full line:** median value of the variable under RCP8.5 scenario. Data source: NASA Earth Exchange - Global Daily Downscaled Climate Projections (NEX – GDDP) (Thrasher et al., 2012).*

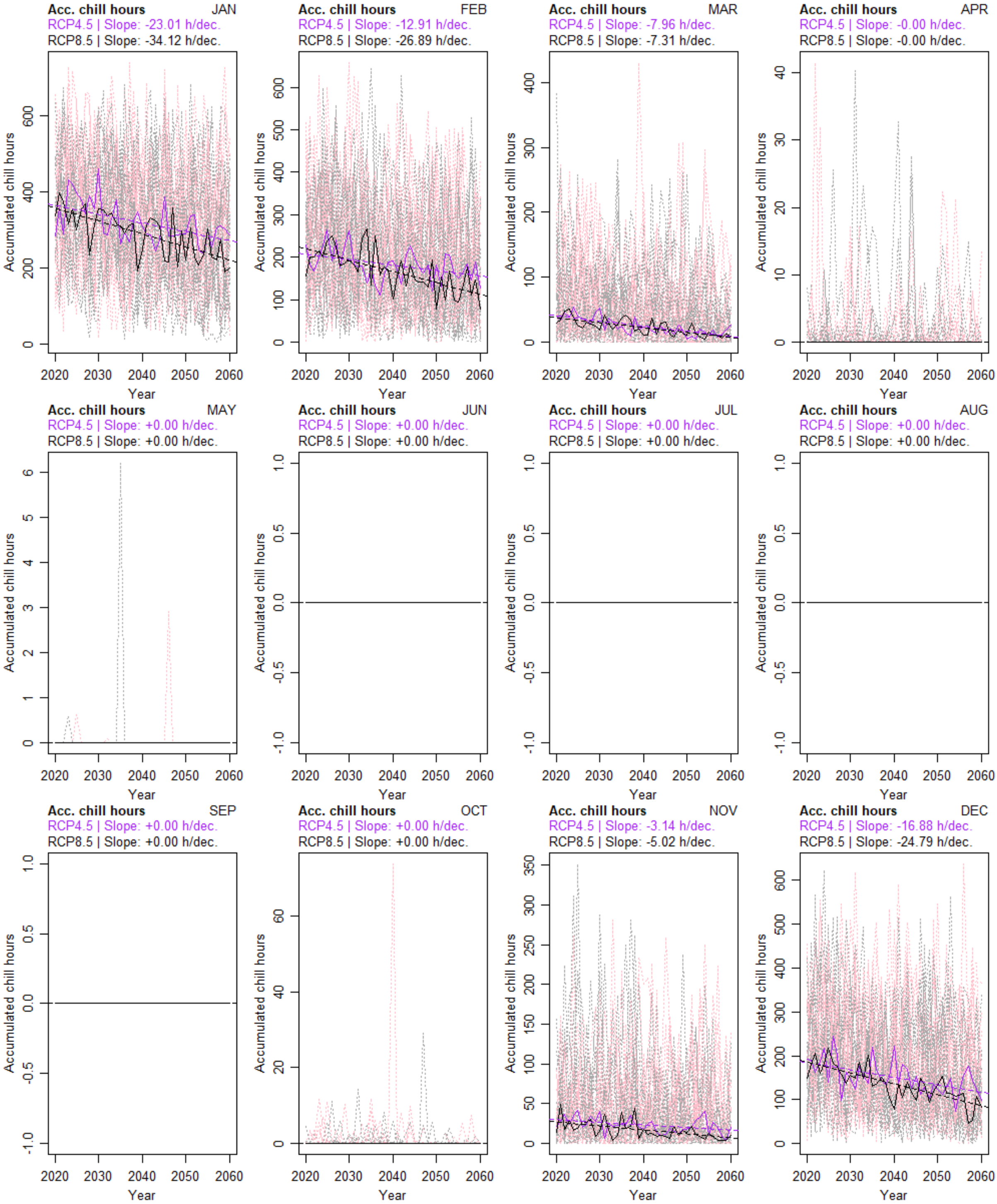

Table 20 – Characteristics of the trend from projected time series of monthly accumulated wet days, very wet days, and the duration of the longest dry spell of the month under the RCP4.5 scenario (linear models)
Data source: NASA Earth Exchange - Global Daily Downscaled Climate Projections (NEX – GDDP) (Thrasher et al., 2012).

RCP4.5						
Variable	**Month**	**Slope**	**p-value**	**R^2**	**Average value in 2040**	**Average value in 2060**
FD_m	January	-0.52 days/dec.	0.00	0.18	24.32 days	23.28 days
FD_m	February	-0.52 days/dec.	0.01	0.13	19.06 days	18.03 days
FD_m	March	-0.94 days/dec.	0.00	0.49	9.73 days	7.85 days
FD_m	April	-0.10 days/dec.	0.00	0.17	0.71 days	0.51 days
FD_m	May	+0.00 days/dec.	0.33	0.00	0.00 days	0.00 days
FD_m	June	+0.00 days/dec.	NA	NA	0.00 days	0.00 days
FD_m	July	+0.00 days/dec.	NA	NA	0.00 days	0.00 days
FD_m	August	+0.00 days/dec.	NA	NA	0.00 days	0.00 days
FD_m	September	+0.00 days/dec.	NA	NA	0.00 days	0.00 days
FD_m	October	-0.08 days/dec.	0.00	0.36	0.25 days	0.09 days
FD_m	November	-0.26 days/dec.	0.06	0.06	6.94 days	6.41 days
FD_m	December	-0.64 days/dec.	0.00	0.23	16.76 days	15.48 days
ID_m	January	-0.48 days/dec.	0.01	0.16	3.61 days	2.66 days
ID_m	February	-0.16 days/dec.	0.06	0.06	1.47 days	1.14 days
ID_m	March	-0.01 days/dec.	0.01	0.13	0.02 days	0.00 days
ID_m	April	+0.00 days/dec.	NA	NA	0.00 days	0.00 days
ID_m	May	+0.00 days/dec.	NA	NA	0.00 days	0.00 days
ID_m	June	+0.00 days/dec.	NA	NA	0.00 days	0.00 days
ID_m	July	+0.00 days/dec.	NA	NA	0.00 days	0.00 days
ID_m	August	+0.00 days/dec.	NA	NA	0.00 days	0.00 days
ID_m	September	+0.00 days/dec.	NA	NA	0.00 days	0.00 days
ID_m	October	+0.00 days/dec.	NA	NA	0.00 days	0.00 days
ID_m	November	-0.00 days/dec.	0.17	0.02	0.02 days	0.01 days
ID_m	December	-0.21 days/dec.	0.00	0.17	1.16 days	0.74 days
CH_m	January	-23.01 h/dec.	0.00	0.25	317.98 h	271.97 h
CH_m	February	-12.91 h/dec.	0.01	0.16	181.46 h	155.64 h
CH_m	March	-7.96 h/dec.	0.00	0.54	24.92 h	9.01 h
CH_m	April	-0.00 h/dec.	0.05	0.07	0.00 h	0.00 h
CH_m	May	+0.00 h/dec.	NA	NA	0.00 h	0.00 h
CH_m	June	+0.00 h/dec.	NA	NA	0.00 h	0.00 h
CH_m	July	+0.00 h/dec.	NA	NA	0.00 h	0.00 h
CH_m	August	+0.00 h/dec.	NA	NA	0.00 h	0.00 h
CH_m	September	+0.00 h/dec.	NA	NA	0.00 h	0.00 h
CH_m	October	+0.00 h/dec.	NA	NA	0.00 h	0.00 h
CH_m	November	-3.14 h/dec.	0.01	0.14	23.11 h	16.84 h
CH_m	December	-16.88 h/dec.	0.00	0.27	151.86 h	118.10 h

Table 21 – Characteristics of the trend from projected time series of monthly accumulated wet days, very wet days, and the duration of the longest dry spell of the month under the RCP8.5 scenario (linear models)
Data source: NASA Earth Exchange - Global Daily Downscaled Climate Projections (NEX – GDDP) (Thrasher et al., 2012).

RCP8.5						
Variable	**Month**	**Slope**	**p-value**	**R^2**	**Average value in 2040**	**Average value in 2060**
FD_m	January	-1.30 days/dec.	0.00	0.55	23.22 days	20.61 days
FD_m	February	-1.36 days/dec.	0.00	0.58	18.05 days	15.33 days
FD_m	March	-1.18 days/dec.	0.00	0.54	9.03 days	6.67 days
FD_m	April	-0.19 days/dec.	0.00	0.41	0.66 days	0.28 days
FD_m	May	-0.00 days/dec.	0.11	0.04	0.00 days	0.00 days
FD_m	June	+0.00 days/dec.	NA	NA	0.00 days	0.00 days
FD_m	July	+0.00 days/dec.	NA	NA	0.00 days	0.00 days
FD_m	August	+0.00 days/dec.	NA	NA	0.00 days	0.00 days
FD_m	September	+0.00 days/dec.	NA	NA	0.00 days	0.00 days
FD_m	October	-0.09 days/dec.	0.00	0.30	0.18 days	0.00 days
FD_m	November	-0.71 days/dec.	0.00	0.36	5.86 days	4.44 days
FD_m	December	-1.58 days/dec.	0.00	0.65	15.78 days	12.62 days
ID_m	January	-0.65 days/dec.	0.00	0.41	3.28 days	1.98 days
ID_m	February	-0.28 days/dec.	0.00	0.27	1.22 days	0.67 days
ID_m	March	-0.01 days/dec.	0.00	0.20	0.02 days	0.00 days
ID_m	April	+0.00 days/dec.	NA	NA	0.00 days	0.00 days
ID_m	May	+0.00 days/dec.	NA	NA	0.00 days	0.00 days
ID_m	June	+0.00 days/dec.	NA	NA	0.00 days	0.00 days
ID_m	July	+0.00 days/dec.	NA	NA	0.00 days	0.00 days
ID_m	August	+0.00 days/dec.	NA	NA	0.00 days	0.00 days
ID_m	September	+0.00 days/dec.	NA	NA	0.00 days	0.00 days
ID_m	October	+0.00 days/dec.	NA	NA	0.00 days	0.00 days
ID_m	November	-0.01 days/dec.	0.01	0.14	0.01 days	0.00 days
ID_m	December	-0.28 days/dec.	0.00	0.39	0.98 days	0.42 days
CH_m	January	-34.12 h/dec.	0.00	0.47	290.68 days	222.44 days
CH_m	February	-26.89 h/dec.	0.00	0.43	167.23 days	113.45 days
CH_m	March	-7.31 h/dec.	0.00	0.49	23.00 days	8.37 days
CH_m	April	-0.00 h/dec.	0.13	0.03	0.00 days	0.00 days
CH_m	May	+0.00 h/dec.	NA	NA	0.00 days	0.00 days
CH_m	June	+0.00 h/dec.	NA	NA	0.00 days	0.00 days
CH_m	July	+0.00 h/dec.	NA	NA	0.00 days	0.00 days
CH_m	August	+0.00 h/dec.	NA	NA	0.00 days	0.00 days
CH_m	September	+0.00 h/dec.	NA	NA	0.00 days	0.00 days
CH_m	October	+0.00 h/dec.	NA	NA	0.00 days	0.00 days
CH_m	November	-5.02 h/dec.	0.00	0.27	16.79 days	6.75 days
CH_m	December	+0.07 days/dec.	0.61	-0.02	7.92 days	8.06 days

Overall, under both scenario, most of the months shows a decrease in FD_m, ID_m and CH_m.

For NEX median model under the RCP4.5 scenario the largest decrease in FD_m can be observed for the months of March (-0.9 days/decade), December (-0.6 days/decade) and January (-0.4 days/decade). For NEX median model under the RCP8.5 scenario the largest decrease in FD_m can be observed for the months of December (-1.6 days/decade), February (-1.4 days/decade) and January (-1.3 days/decade).

For NEX median model under the RCP4.5 scenario the largest decrease in ID_m can be observed for the months of January (-0.5 days/decade), December (-0.2 days/decade) and February (-0.2 days/decade). For NEX median model under the RCP8.5 scenario the largest decrease in ID_m can be observed for the months of January (-0.6 days/decade), February (-0.3 days/decade) and December (-0.3 days/decade).

For NEX median model under the RCP4.5 scenario, the largest decrease in CH_m can be observed for the months of January (-23 h/decade), December (-17 h/decade) and February (-13 h/decade). For NEX median model under the RCP4.5 scenario, the largest decrease in CH_m can be observed for the months of January (-34 h/decade), February (-27 h/decade) and March (-7 h/decade).

Overall, the critical months for FD_m, ID_m, and CH_m are the coldest months, from December to March.

Projected annual trends

Projected annual trends on annually accumulated frost days, ice days and chill hours can be observed in

Figure 70and Table 22.

Table 22 – Characteristics of the trend from projected data for annually accumulated frost days, ice days and chill hours (linear models)
Data source: Second national communication of the Republic of Serbia under the United Nations framework convention on climate change (Rajkovic et al., 2013) and NASA Earth Exchange - Global Daily Downscaled Climate Projections (NEX – GDDP) (Thrasher et al., 2012).

RCP4.5					
Variable	**Slope**	**p-value**	**Adjusted R^2**	**Average value in 2040**	**Average value in 2060**
FD_y	-3.02 days/decade	0.00	0.59	78.90 days	72.86 days
ID_y	-0.89 days/decade	0.00	0.26	8.62 days	6.85 days
CH_y	-63.07 h/decade	0.00	0.53	769.19 h	643.05 h
RCP8.5					
Variable	**Slope**	**p-value**	**Adjusted R^2**	**Average value in 2040**	**Average value in 2060**
FD_y	-6.00 days/decade	0.00	0.83	74.15 days	62.15 days
ID_y	-1.34 days/decade	0.00	0.48	7.62 days	4.95 days
CH_y	-94.26 h/decade	0.00	0.71	696.99 h	508.47 h

Frost days, ice days and chill hours are expected under both scenarios to continue their decrease during the next 40 years.

The NEX median model under the RCP4.5 scenario expects FD_y to decrease by about -3 days/decade, from 79 days on average in 2040 to 73 days on average in 2060. ID_y is expected to decrease by about -0.9 days/decade, from 8.6 days on average in 2040 to 6.8 days on average in 2060. Finally, CH_y is expected to decrease by about -63 h/decade, from 769 h on average in 2040 to 643 h on average in 2060.

The NEX median model under the RCP8.5 scenario expects FD_y to decrease by about -6 days/decade, from 74 days on average in 2040 to 62 days on average in 2060. ID_y is expected to decrease by about -1.3 days/decade, from 7.6 days on average in 2040 to 4.9 days on average in 2060. Finally, CH_y is expected to decrease by about -94 h/decade, from 697 h on average in 2040 to 508 h on average in 2060.

Figure 70 – Projected annual time series of accumulated frost days, ice days, and chill hours
*Time series over 2020-2060 period. Time series over 2020-2060 period. **Pink dotted line**: variable value for each model separately under the RCP4.5 scenario. **grey dotted line**: variable value for each model separately under the RCP8.5 scenario. **Purple full line:** median value of the variable under RCP4.5 scenario. **Black full line:** median value of the variable under RCP8.5 scenario. Data source: NASA Earth Exchange - Global Daily Downscaled Climate Projections (NEX – GDDP) (Thrasher et al., 2012).*

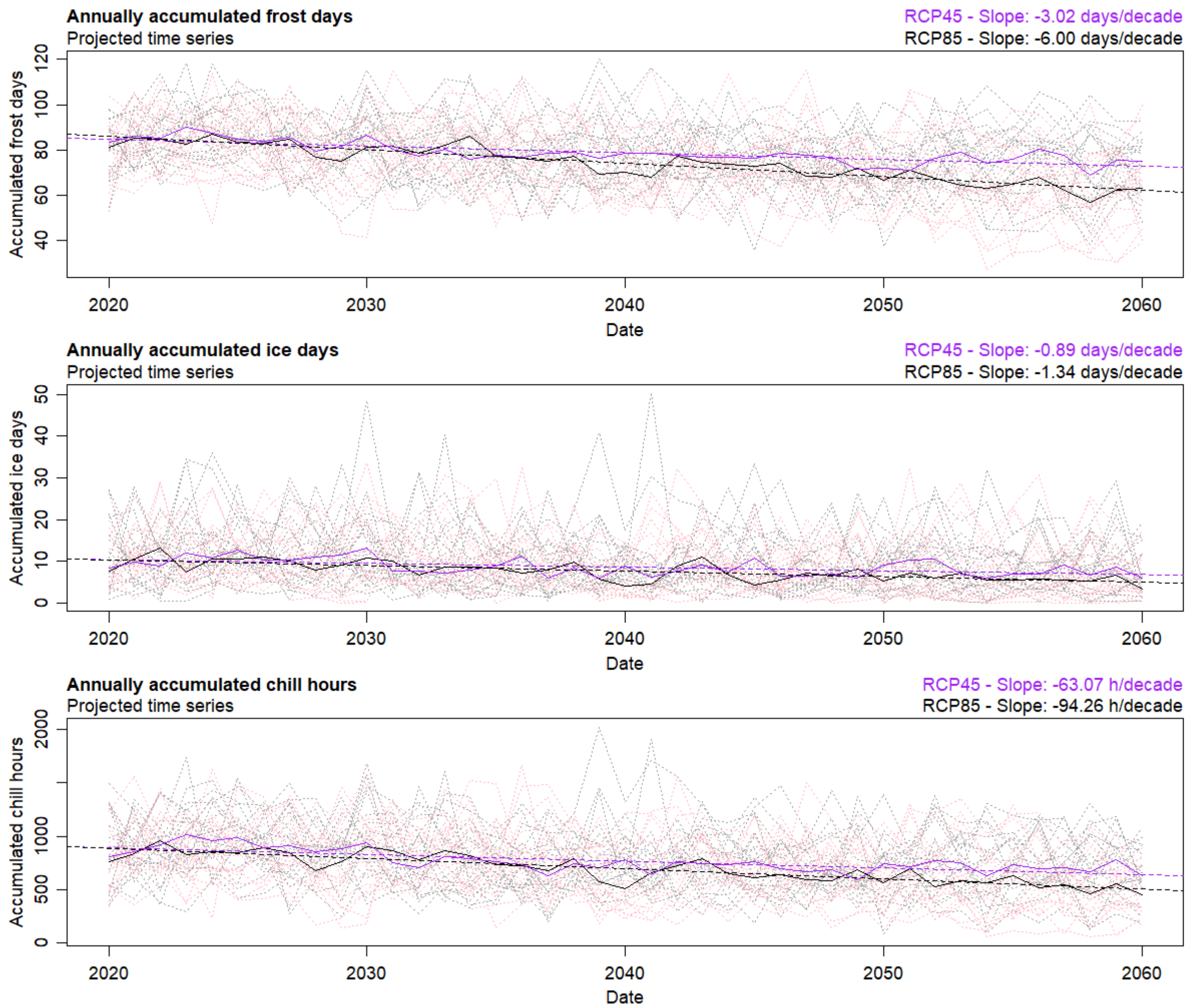

Conclusion

Frost days, ice days and chill hours appears in the coldest months of the year in Serbia, from September to April, peaking during the month of January (around 22 days for FD_m, 8 days for ID_m and about 400h for CH_m). These 3 cold temperature variables are steadily decreasing in Serbia and are expected to continue their decrease. These decreases are expected to be more acute during the coldest month of the year, from December to March.

12. Summer days and tropical nights

This section will present the variations of summer days and tropical nights in the Republic of Serbia, using the following variables:

- Annually **accumulated summer days** (SD_y) and monthly **accumulated summer days** (SD_m). Accumulated summer days are defined as the number of days over a given period, when the daily maximum temperature is above 25°C.
- Annually **accumulated tropical nights** (TrN_y) and monthly **accumulated tropical nights** (TrN_m). Accumulated tropical nights are defined as the number of days over a given period, when the daily minimum temperature is above 20°C.

Because summer days and tropical nights are calculated at a daily or hourly level, and because daily data from weather stations were not available, this section will only present variables calculated using ERA5 data for historical trends.

Current seasonal variations

The current seasonal variation of summer days and tropical nights in the Republic of Serbia are presented in Figure 71. This chart presents SD_m and TrN_m, averaged over 30 years (1990 to 2019). This analysis was conducted using ERA5 data.

Figure 71 – Current monthly variations of summer days and tropical nights
Data averaged over the 1990-2019 period. ***In green:*** *monthly accumulated summer days.* ***In red:*** *monthly accumulated tropical night. <u>Data source:</u> ERA5 - ECMWF / Copernicus Climate Change Service (Muñoz Sabater, 2019).*

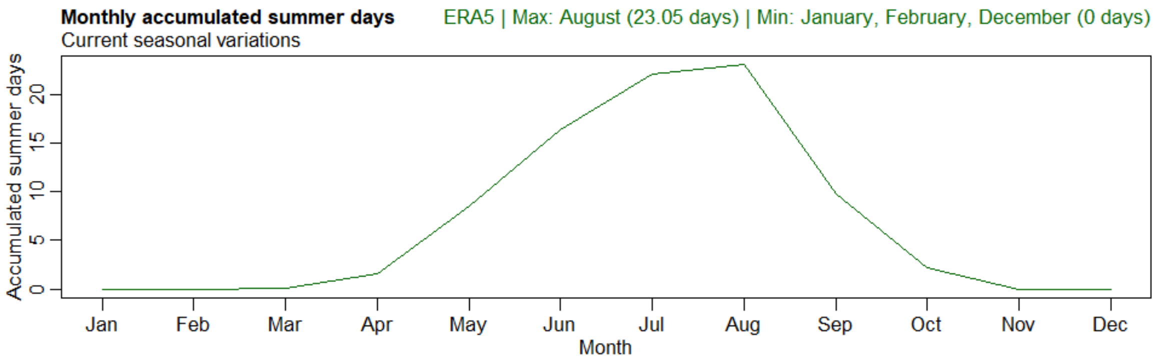

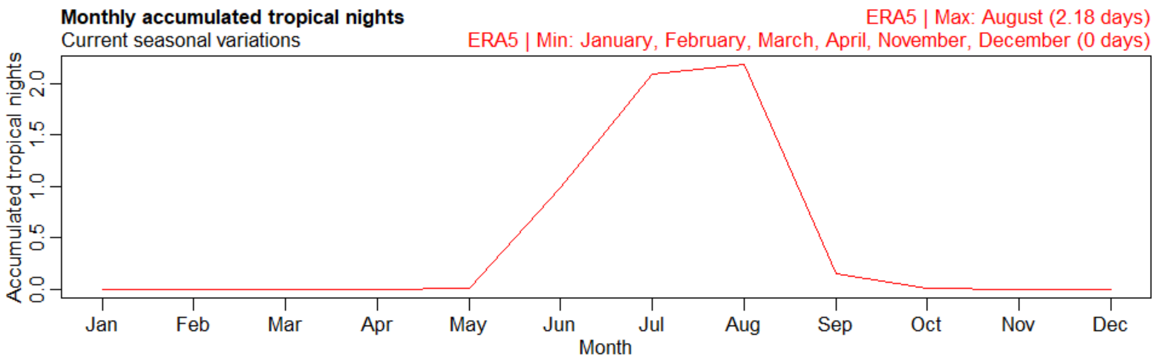

Summer days and tropical nights are peaking in august (23 days for summer days, and 2.2 days for tropical nights) before steadily decreasing. Past October there are no more tropical nights on average, while past November there is no more summer days on average. Summer days reappear in March and proceed to a steady increase until August. Tropical Nights reappear in May and also steadily increase until August. It is worth noting that there are very few tropical nights in Serbia: up to a maximum of 2.2 monthly in august.

Spatial distribution

The monthly spatial distribution of summer days and tropical nights throughout Serbia can be observed in Figure 72.

Summer days and tropical nights tend to be more numerous and persist during a longer period in the flat lands of the North of the country and in the valleys of the south, where altitude is lower.

Notably, tropical nights are more numerous during the peak months (July and August) in the Belgrade region. This is probably due to the high albedo and heat absorption capacity of large number of artificial surfaces present in the area (see Land cover and land use).

Figure 72 – Current spatial distribution of monthly accumulated summer days and tropical nights.
Data averaged over the 1990-2019 period. ***In green:*** *summer days.* ***In red:*** *tropical nights. Data source: ERA5 - ECMWF / Copernicus Climate Change Service (Muñoz Sabater, 2019).*

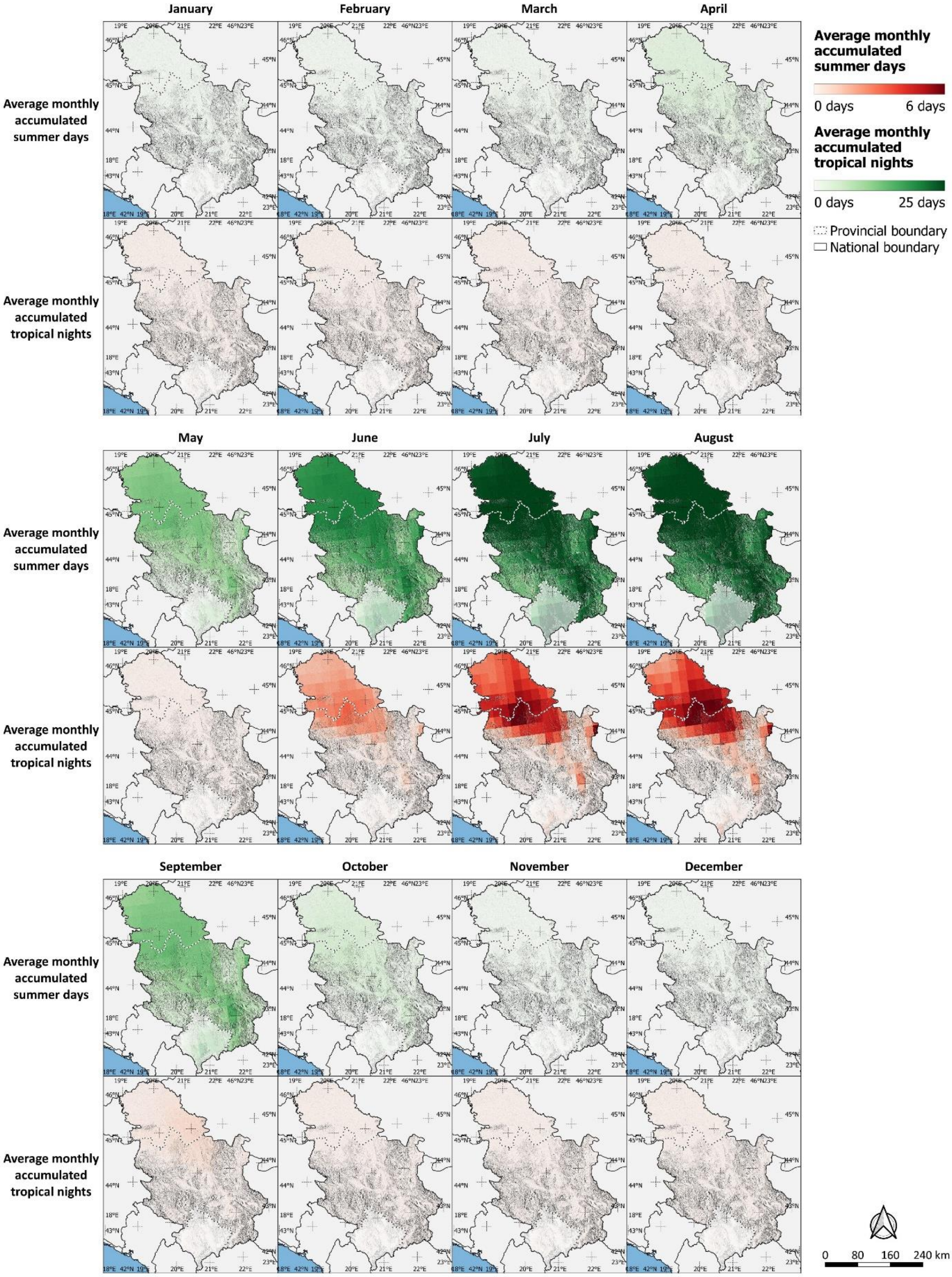

Historical monthly trends

The historical trends of monthly accumulated summer days and tropical nights can be observed in Figure 73, Figure 74 and Table 23.

Figure 73 – Historical monthly time series of accumulated summer days

Time series over 1980-2019 period. Data source: ERA5, ECMWF / Copernicus Climate Change Service (Muñoz Sabater, 2019)

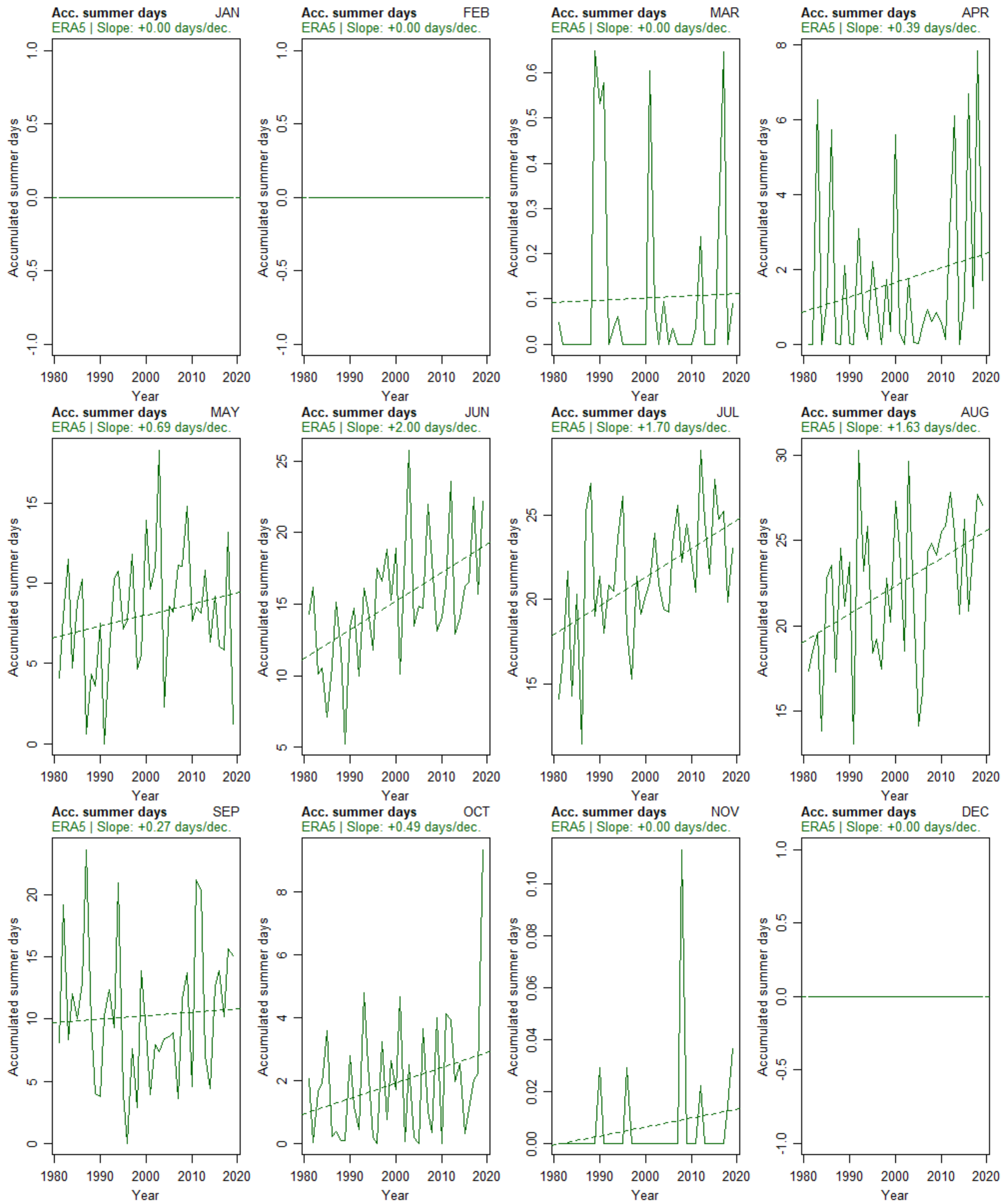

Figure 74 – Historical monthly time series of accumulated tropical nights

Time series over 1980-2019 period. Data source: ERA5, ECMWF / Copernicus Climate Change Service (Muñoz Sabater, 2019)

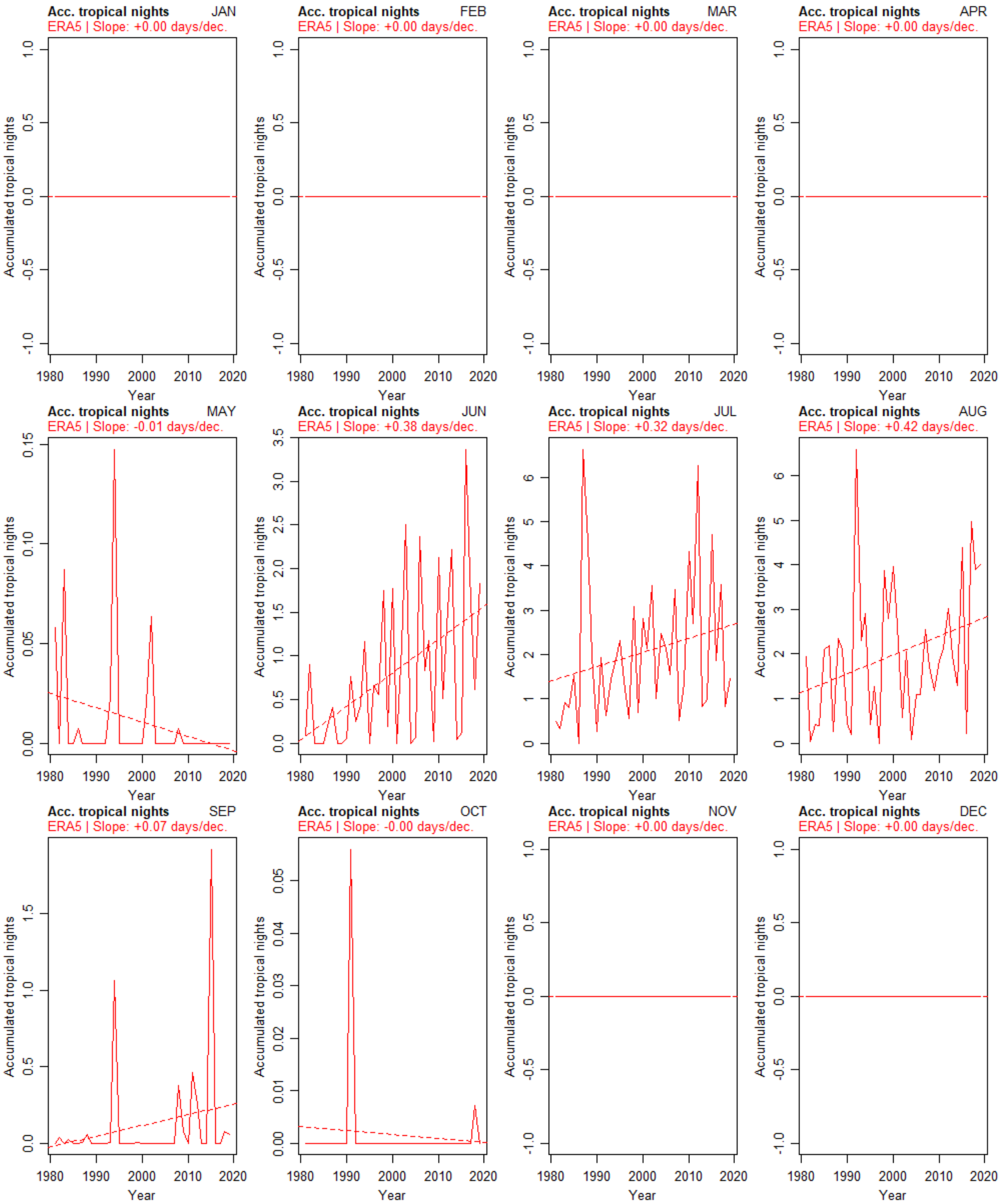

Overall, most of the months shows an increase of SD_m and TrN_m. In terms of critical months, the largest increases in SD_m can be observed for the months of June (+2.0 days/decade), July (+1.7 days/decade) and August (+1.6 days/decade). the largest increase in TrN_m can be observed for the months of August (+0.4 days/decade), June (+0.4 days/decade) and July (+0.3 days/decade).

Table 23 – Characteristics of the trends from the historical time series of the monthly accumulated of summer days and tropical nights (linear models)
***In green**: Monthly accumulated summer days. **In red:** monthly accumulated tropical nights. Data source: ERA5, ECMWF / Copernicus Climate Change Service (Muñoz Sabater, 2019).*

Variable	Month	Slope	p-value	Adjusted R^2	Average value in 1980	Average value in 2019
SD_m	January	+0.00 days/dec.	NA	NA	0.00 days	0.00 days
SD_m	February	+0.00 days/dec.	NA	NA	0.00 days	0.00 days
SD_m	March	+0.00 days/dec.	0.87	-0.03	0.09 days	0.11 days
SD_m	April	+0.39 days/dec.	0.23	0.01	0.86 days	2.39 days
SD_m	May	+0.69 days/dec.	0.23	0.01	6.64 days	9.32 days
SD_m	June	+2.00 days/dec.	0.00	0.25	11.21 days	19.00 days
SD_m	July	+1.70 days/dec.	0.00	0.24	17.94 days	24.56 days
SD_m	August	+1.63 days/dec.	0.01	0.16	19.05 days	25.40 days
SD_m	September	+0.27 days/dec.	0.74	-0.02	9.74 days	10.77 days
SD_m	October	+0.49 days/dec.	0.07	0.06	0.92 days	2.83 days
SD_m	November	+0.00 days/dec.	0.22	0.01	0.00 days	0.01 days
SD_m	December	+0.00 days/dec.	NA	NA	0.00 days	0.00 days
TrN_m	January	+0.00 days/dec.	NA	NA	0.00 days	0.00 days
TrN_m	February	+0.00 days/dec.	NA	NA	0.00 days	0.00 days
TrN_m	March	+0.00 days/dec.	NA	NA	0.00 days	0.00 days
TrN_m	April	+0.00 days/dec.	NA	NA	0.00 days	0.00 days
TrN_m	May	-0.01 days/dec.	0.09	0.05	0.02 days	0.00 days
TrN_m	June	+0.38 days/dec.	0.00	0.22	0.04 days	1.53 days
TrN_m	July	+0.32 days/dec.	0.16	0.03	1.41 days	2.65 days
TrN_m	August	+0.42 days/dec.	0.05	0.07	1.14 days	2.78 days
TrN_m	September	+0.07 days/dec.	0.16	0.03	-0.03 days	0.25 days
TrN_m	October	-0.00 days/dec.	0.56	-0.02	0.00 days	0.00 days
TrN_m	November	+0.00 days/dec.	NA	NA	0.00 days	0.00 days
TrN_m	December	+0.00 days/dec.	NA	NA	0.00 days	0.00 days

Historical annual trends

Historical annual trends on accumulated summer days and tropical nights can be observed in Figure 75 and Table 24.

SD_y and TrN_y, in Serbia presented a general increase during the last 40 years (SD_y: +7.2 days/decade, TrN_y: +1.2 days/decade). This decrease brought SD_y from 66 days on average in 1980 to 94 days on average in 2019 and TrN_y from 3 days on average in 1980 to 7 days on average in 2019.

Figure 75 – Historical annual time series of accumulated summer days and tropical nights
*Time series over 1980-2019 period. **In green:** annually accumulated summer days. **In red:** annually accumulated tropical nights. Data source: ERA5, ECMWF / Copernicus Climate Change Service (Muñoz Sabater, 2019)*

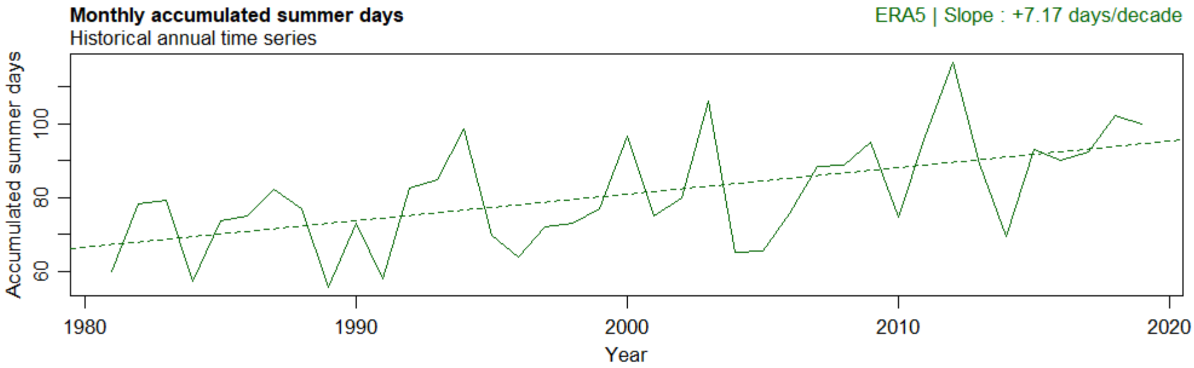

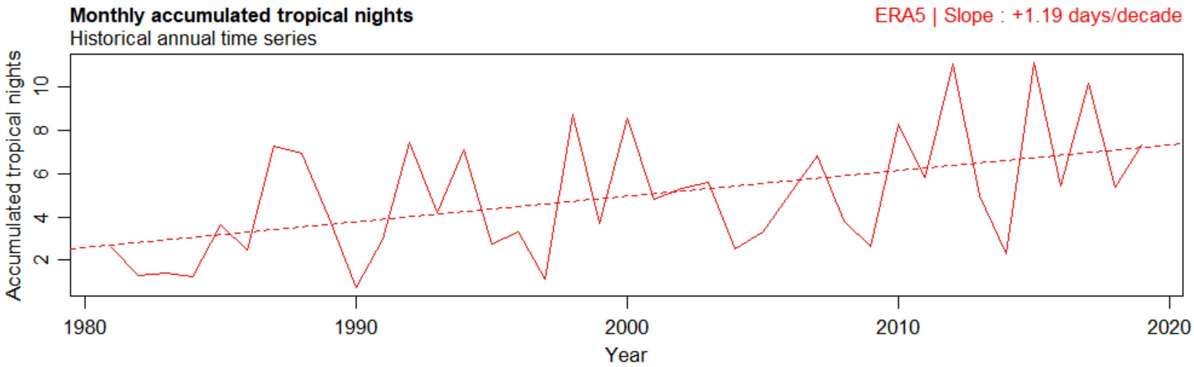

Table 24 – Characteristics of the trend from historical annual times series of accumulated frost days, ice days and chill hours (linear models)
Data source: ERA5, ECMWF / Copernicus Climate Change Service (Muñoz Sabater, 2019)

Variable	Slope	p-value	Adj. R^2	Average value in 1980	Average value in 2019
SD_y	+7.17 days/decade	0.00	0.30	66.45 days	94.40 days
TrN_y	+1.19 days/decade	0.00	0.22	2.58 days	7.21 days

Spatial distribution

The spatial distribution of annually accumulated summer days and tropical nights throughout Serbia can be observed in Figure 76.

Summer days and tropical nights presented a consistent distribution during the last 40 years: the two variables tend to be more numerous and persist for longer period in the flat lands of the North of the country and in the valleys of the south, where altitude is lower. Notably, tropical nights are more numerous in the Belgrade region. This is probably due to the high albedo and heat absorption capacity of the large number of artificial surfaces present in the area (see Land cover and land use).

Figure 76 – Historical and projected decadal spatial distribution of annually accumulated frost days, ice days and chill hours

*Data averaged over the 1980-2019 period, by decade**. In green:** annually accumulated frost days. **In blue:** annually accumulated ice days. **In red:** annually accumulated chill hours. <u>Data source:</u> ERA5, ECMWF / Copernicus Climate Change Service (Muñoz Sabater, 2019)*

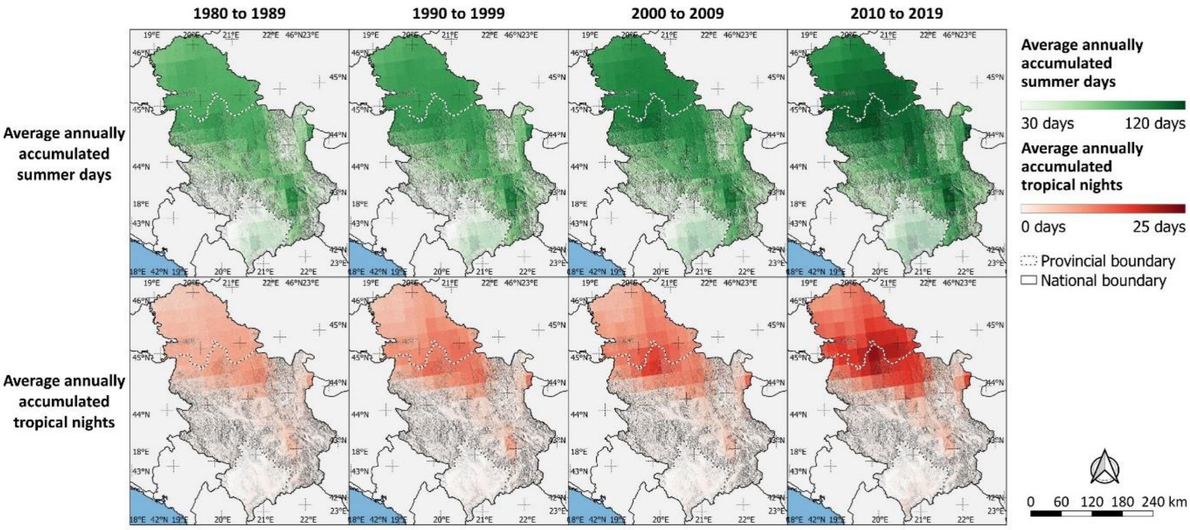

Projected monthly trends

The projected trends of monthly accumulated summer days and tropical nights can be observed in Figure 77, Figure 78, Table 25 and Table 26.

Overall, most of the months shows an increase of SD_m and TrN_m.

Under the RCP4.5 scenario, the NEX median model shows the largest increases in SD_m during the months of <u>September</u> (+1.2 days/decade), <u>June</u> (+0.8 days/decade) and <u>July</u> (+0.6 days/decade). Under the RCP8.5 scenario, the largest increase in SD_m can be observed for the months of <u>September</u> (+2.1 days/decade), <u>June</u> (+1.6 days/decade) and <u>May</u> (+1.3 days/decade).

Under the RCP4.5 scenario, the NEX median model shows the largest increase in TrN_m during the months of <u>August</u> (+1.5 days/decade), <u>July</u> (+1.3 days/decade) and <u>June</u> (+0.1 days/decade). Under the RCP8.5 scenario the largest increase in TrN_m can be observed for the months of <u>August</u> (+2.6 days/decade), J<u>uly</u> (+2.5 days/decade) and <u>June</u> (+0.6 days/decade).

Overall, the critical months for SD_m and TrN_m are the hottest months, from June to September.

Figure 77 – Historical monthly time series of accumulated summer days

Time series over 2020-2060 period. ***Pink dotted line****: variable value for each model separately under the RCP4.5 scenario.* ***grey dotted line****: variable value for each model separately under the RCP8.5 scenario.* ***Purple full line:*** *median value of the variable under RCP4.5 scenario.* ***Black full line:*** *median value of the variable under RCP8.5 scenario. Data source: NASA Earth Exchange - Global Daily Downscaled Climate Projections (NEX – GDDP) (Thrasher et al., 2012).*

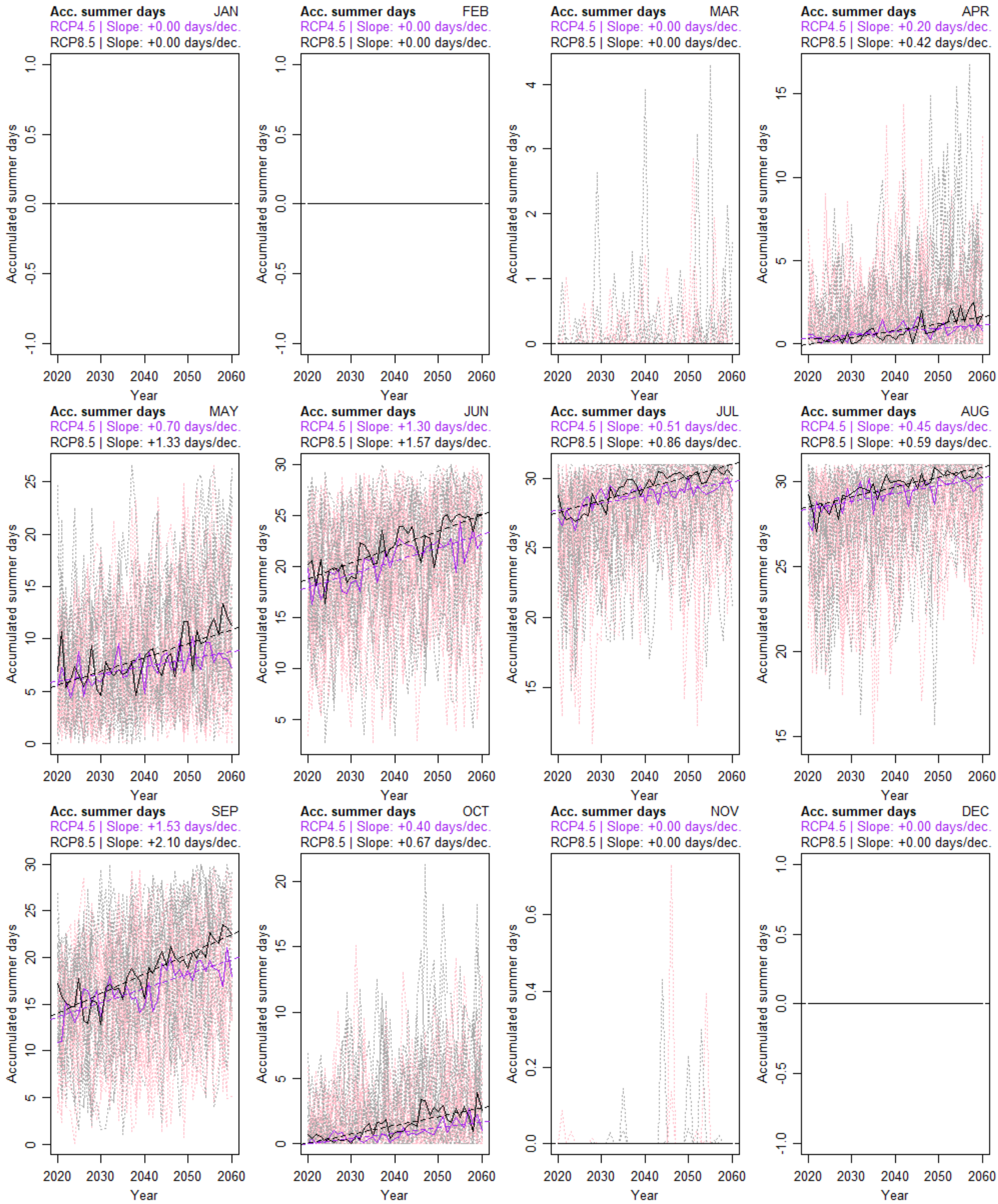

Figure 78 – Historical monthly time series of accumulated tropical nights

Time series over 2020-2060 period. ***Pink dotted line****: variable value for each model separately under the RCP4.5 scenario.* ***grey dotted line****: variable value for each model separately under the RCP8.5 scenario.* ***Purple full line:*** *median value of the variable under RCP4.5 scenario.* ***Black full line:*** *median value of the variable under RCP8.5 scenario. Data source: NASA Earth Exchange - Global Daily Downscaled Climate Projections (NEX – GDDP) (Thrasher et al., 2012).*

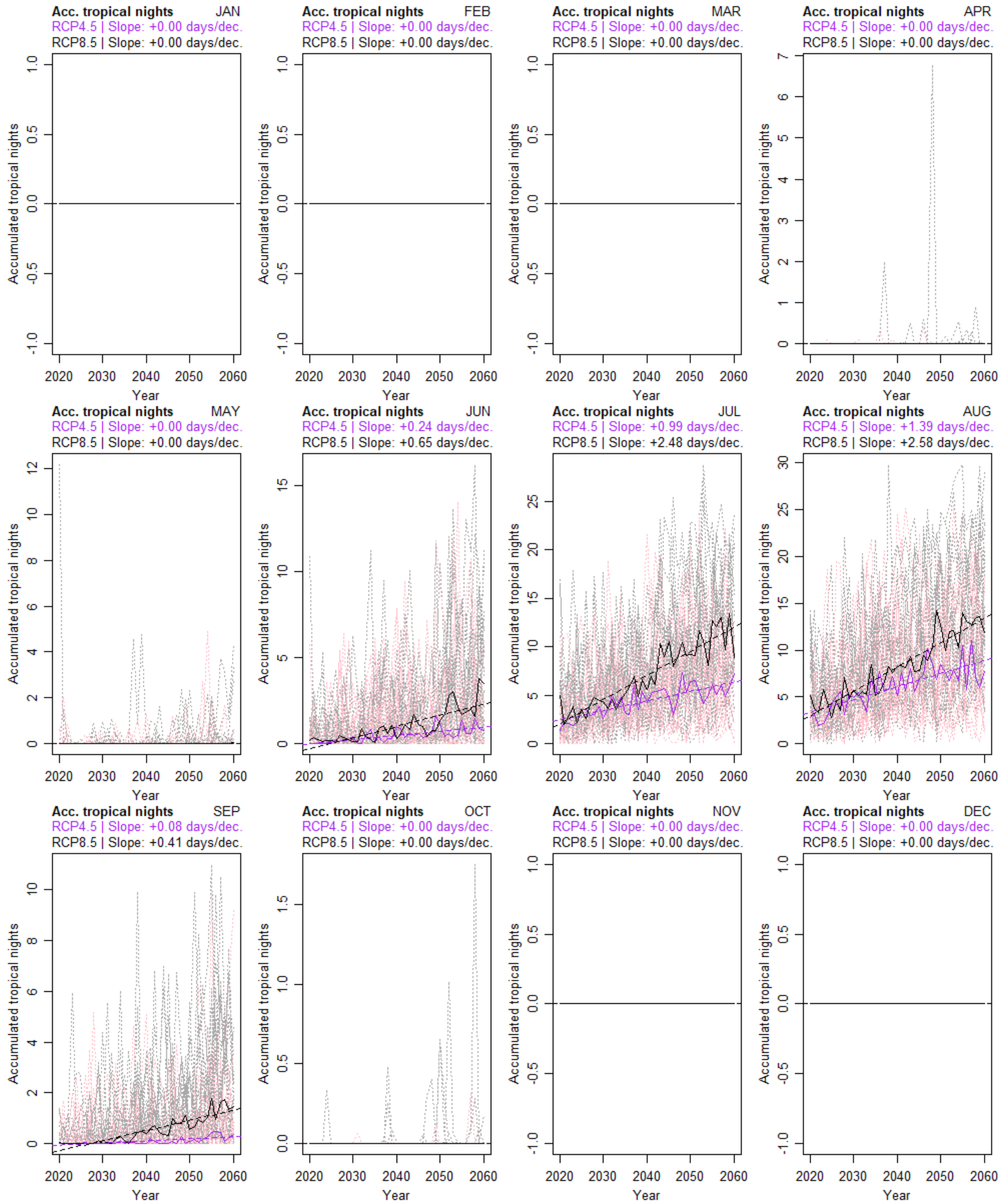

Table 25 – Characteristics of the trend from projected time series of monthly accumulated summer days and tropical nights days under the RCP4.5 scenario (linear models)
Data source: NASA Earth Exchange - Global Daily Downscaled Climate Projections (NEX – GDDP) (Thrasher et al., 2012).

RCP4.5						
Variable	**Month**	**Slope**	**p-value**	**R^2**	**Average value in 2040**	**Average value in 2060**
SD_m	January	+0.00 days/dec.	NA	NA	0.00 days	0.00 days
SD_m	February	+0.00 days/dec.	NA	NA	0.00 days	0.00 days
SD_m	March	+0.00 days/dec.	NA	NA	0.00 days	0.00 days
SD_m	April	+0.20 days/dec.	0.00	0.33	0.73 days	1.13 days
SD_m	May	+0.70 days/dec.	0.00	0.32	7.35 days	8.75 days
SD_m	June	+1.30 days/dec.	0.00	0.60	20.49 days	23.09 days
SD_m	July	+0.51 days/dec.	0.00	0.48	28.74 days	29.76 days
SD_m	August	+0.45 days/dec.	0.00	0.48	29.28 days	30.18 days
SD_m	September	+1.53 days/dec.	0.00	0.60	16.65 days	19.71 days
SD_m	October	+0.40 days/dec.	0.00	0.56	0.81 days	1.61 days
SD_m	November	+0.00 days/dec.	NA	NA	0.00 days	0.00 days
SD_m	December	+0.00 days/dec.	NA	NA	0.00 days	0.00 days
TrN_m	January	+0.00 days/dec.	NA	NA	0.00 days	0.00 days
TrN_m	February	+0.00 days/dec.	NA	NA	0.00 days	0.00 days
TrN_m	March	+0.00 days/dec.	NA	NA	0.00 days	0.00 days
TrN_m	April	+0.00 days/dec.	NA	NA	0.00 days	0.00 days
TrN_m	May	+0.00 days/dec.	NA	NA	0.00 days	0.00 days
TrN_m	June	+0.24 days/dec.	0.00	0.47	0.48 days	0.96 days
TrN_m	July	+0.99 days/dec.	0.00	0.61	4.42 days	6.41 days
TrN_m	August	+1.39 days/dec.	0.00	0.59	6.10 days	8.88 days
TrN_m	September	+0.08 days/dec.	0.00	0.45	0.09 days	0.26 days
TrN_m	October	+0.00 days/dec.	NA	NA	0.00 days	0.00 days
TrN_m	November	+0.00 days/dec.	NA	NA	0.00 days	0.00 days
TrN_m	December	+0.00 days/dec.	NA	NA	0.00 days	0.00 days

Table 26 – Characteristics of the trend from projected time series of monthly accumulated summer days and tropical nights days under the RCP8.5 scenario (linear models)
Data source: NASA Earth Exchange - Global Daily Downscaled Climate Projections (NEX – GDDP) (Thrasher et al., 2012).

RCP8.5						
Variable	**Month**	**Slope**	**p-value**	**R^2**	**Average value in 2040**	**Average value in 2060**
SD_m	January	+0.00 days/dec.	NA	NA	0.00 days	0.00 days
SD_m	February	+0.00 days/dec.	NA	NA	0.00 days	0.00 days
SD_m	March	+0.00 days/dec.	NA	NA	0.00 days	0.00 days
SD_m	April	+0.42 days/dec.	0.00	0.56	0.80 days	1.64 days
SD_m	May	+1.33 days/dec.	0.00	0.47	8.24 days	10.90 days
SD_m	June	+1.57 days/dec.	0.00	0.65	21.88 days	25.03 days
SD_m	July	+0.86 days/dec.	0.00	0.73	29.27 days	30.98 days
SD_m	August	+0.59 days/dec.	0.00	0.67	29.65 days	30.83 days
SD_m	September	+2.10 days/dec.	0.00	0.77	18.25 days	22.44 days
SD_m	October	+0.67 days/dec.	0.00	0.60	1.41 days	2.76 days
SD_m	November	+0.00 days/dec.	NA	NA	0.00 days	0.00 days
SD_m	December	+0.00 days/dec.	NA	NA	0.00 days	0.00 days
TrN_m	January	+0.00 days/dec.	NA	NA	0.00 days	0.00 days
TrN_m	February	+0.00 days/dec.	NA	NA	0.00 days	0.00 days
TrN_m	March	+0.00 days/dec.	NA	NA	0.00 days	0.00 days
TrN_m	April	+0.00 days/dec.	NA	NA	0.00 days	0.00 days
TrN_m	May	+0.00 days/dec.	0.06	0.06	0.00 days	0.01 days
TrN_m	June	+0.65 days/dec.	0.00	0.65	1.02 days	2.32 days
TrN_m	July	+2.48 days/dec.	0.00	0.82	7.04 days	12.00 days
TrN_m	August	+2.58 days/dec.	0.00	0.85	8.20 days	13.37 days
TrN_m	September	+0.41 days/dec.	0.00	0.81	0.53 days	1.34 days
TrN_m	October	+0.00 days/dec.	NA	NA	0.00 days	0.00 days
TrN_m	November	+0.00 days/dec.	NA	NA	0.00 days	0.00 days
TrN_m	December	+0.00 days/dec.	NA	NA	0.00 days	0.00 days

Projected annual trends

Projected annual trends on annually accumulated summer days and tropical nights can be observed in Figure 79 and Table 27.

Figure 79 – Projected time series of annually accumulated summer days and tropical nights
Time series over 2020-2060 period. Time series over 2020-2060 period. ***Pink dotted line****: variable value for each model separately under the RCP4.5 scenario.* ***grey dotted line****: variable value for each model separately under the RCP8.5 scenario.* ***Purple full line:*** *median value of the variable under RCP4.5 scenario.* ***Black full line:*** *median value of the variable under RCP8.5 scenario. Data source: NASA Earth Exchange - Global Daily Downscaled Climate Projections (NEX – GDDP) (Thrasher et al., 2012).*

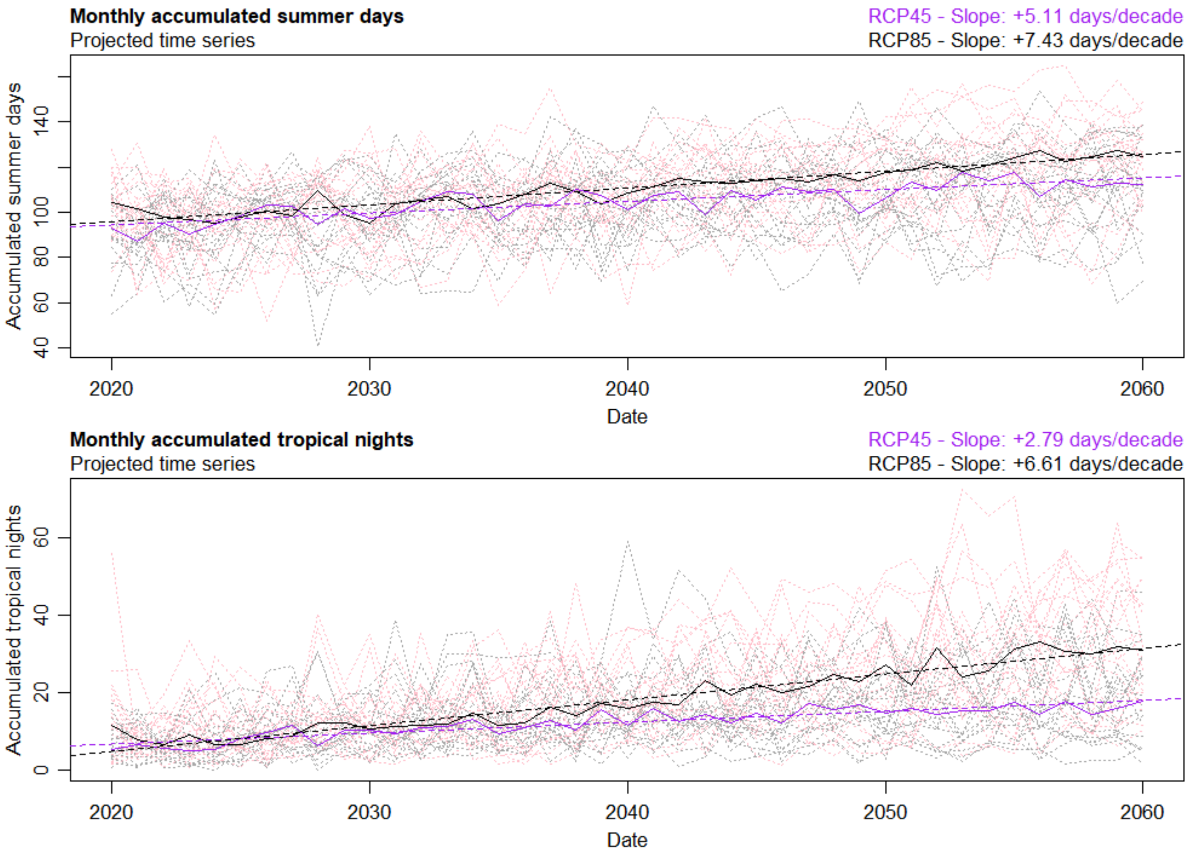

Summer days and tropical nights are expected, by both NEX and EBU-POM, to continue their increase during the next 40 years.

Under the RCP4.5 scenario, the NEX median model expects SD_y to increase by about -5.1 days/decade, from 105 days in 2040 to 115 days in 2060, and TrN_y is expected to increase by about 2.7 days/decade, from 12 days in 2040 to 18 days in 2060.

Under the RCP8.5 scenario, the NEX median model expects a steeper increase of the two variables. SD_y is expected to increase by about +7.4 days/decade, from 111 days in 2040 to 115 days in 2060, and TrN_y is expected to increase by about +6.6 days/decade, from 18 days in 2040 to 31 days in 2060.

Table 27 – Characteristics of the trend from projected data for annually accumulated summer days and tropical nights (linear models)
<u>Data source:</u> Second national communication of the Republic of Serbia under the United Nations framework convention on climate change (Rajkovic et al., 2013) and NASA Earth Exchange - Global Daily Downscaled Climate Projections (NEX – GDDP) (Thrasher et al., 2012).

RCP4.5					
Variable	**Slope**	**p-value**	**Adjusted R^2**	**Average value in 2040**	**Average value in 2060**
SD_y	+5.11 days/decade	0.00	0.66	104.84 days	115.06 days
TrN_y	+2.79 days/decade	0.00	0.78	12.21 days	17.79 days
RCP8.5					
Variable	**Slope**	**p-value**	**Adjusted R^2**	**Average value in 2040**	**Average value in 2060**
FD_y	+7.43 days/decade	0.00	0.88	110.59 days	125.46 days
ID_y	+6.61 days/decade	0.00	0.92	18.01 days	31.23 days

Conclusion

Summer days and tropical nights appears during the hottest months of the year in Serbia, from March to November, peaking during the month of August (around 23 days for SD_m and 2.2 days for TrN_m). These 2 hot temperature variables are steadily increasing in Serbia and are expected to continue their increase. These increases are expected to be more acute during the hottest month of the year, from June to September.

13. Degree days and hardiness zones

This section will present the accumulated degree days and hardiness zone in the Republic of Serbia. These variables are defined as follow:

- **Degree days** are defined as the daily accumulated degree above 10°C. It is calculated based on the daily mean temperature and represents the amount of heat accumulated through the day. For this variable we will considerer **monthly accumulated degree days (DD_m)** and **annually accumulated degree days (DD_y).**
  Because degree days are calculated at a daily level, and because daily data from weather stations were not available, this section will only present degree days calculated using ERA5 data for historical trends.
- **Hardiness zones (HZ)** represent the area where the annual minimum temperature is contained in a predefined range. These range are defined by the USDA (USDA, March-19-2021). Hardiness zones are only defined annually. Therefore, only the variation of the **average (annual) hardiness zone of Serbia** will be observed in the following section.

Because degree days are calculated at a daily scale, and because daily data from weather stations were not available, this section will only present degree days calculated using ERA5 data for historical trends.

Current seasonal variations

The current seasonal variation of monthly accumulated degree days in the Republic of Serbia are presented in Figure 80. This chart presents DD_m, averaged over 30 years (1990 to 2019).

Figure 80 – Current monthly variations of degree days
Data averaged over the 1990-2019 period. Data source: ERA5 - ECMWF / Copernicus Climate Change Service (Muñoz Sabater, 2019)

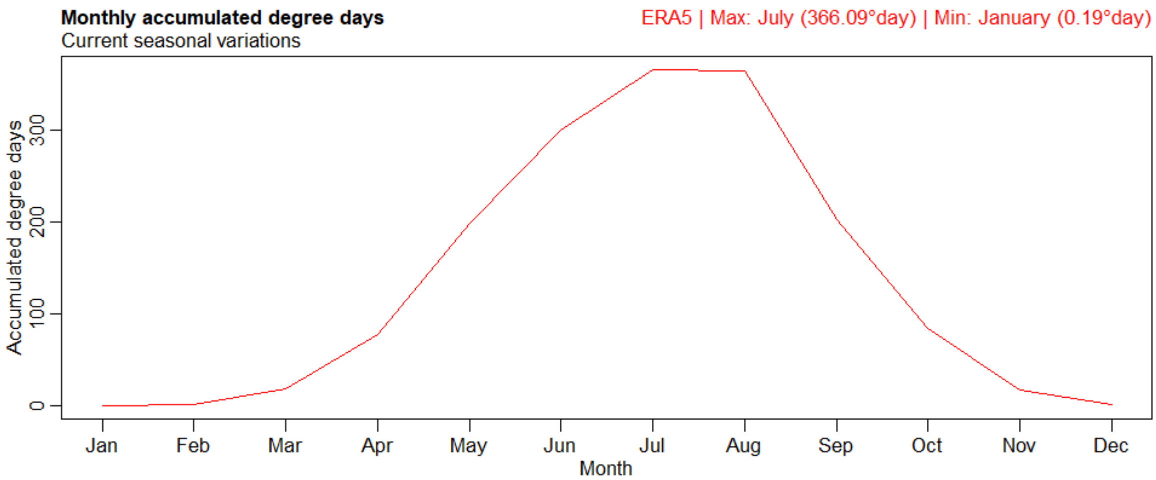

The first monthly accumulated degree days appear in March, when the daily mean temperature start to reach 10 °C. it steadily increases from March to July, when it reaches close to 400-degree days. Degree days are stable through July and August, and then decreases sharply until December, when degree days disappear entirely.

Spatial distribution

The monthly spatial distribution of degree days throughout Serbia can be observed in Figure 81.

Figure 81 – Current spatial distribution of monthly accumulated degree days
Data averaged over the 1990-2019 period. <u>Data source:</u> ERA5 - ECMWF / Copernicus Climate Change Service (Muñoz Sabater, 2019).

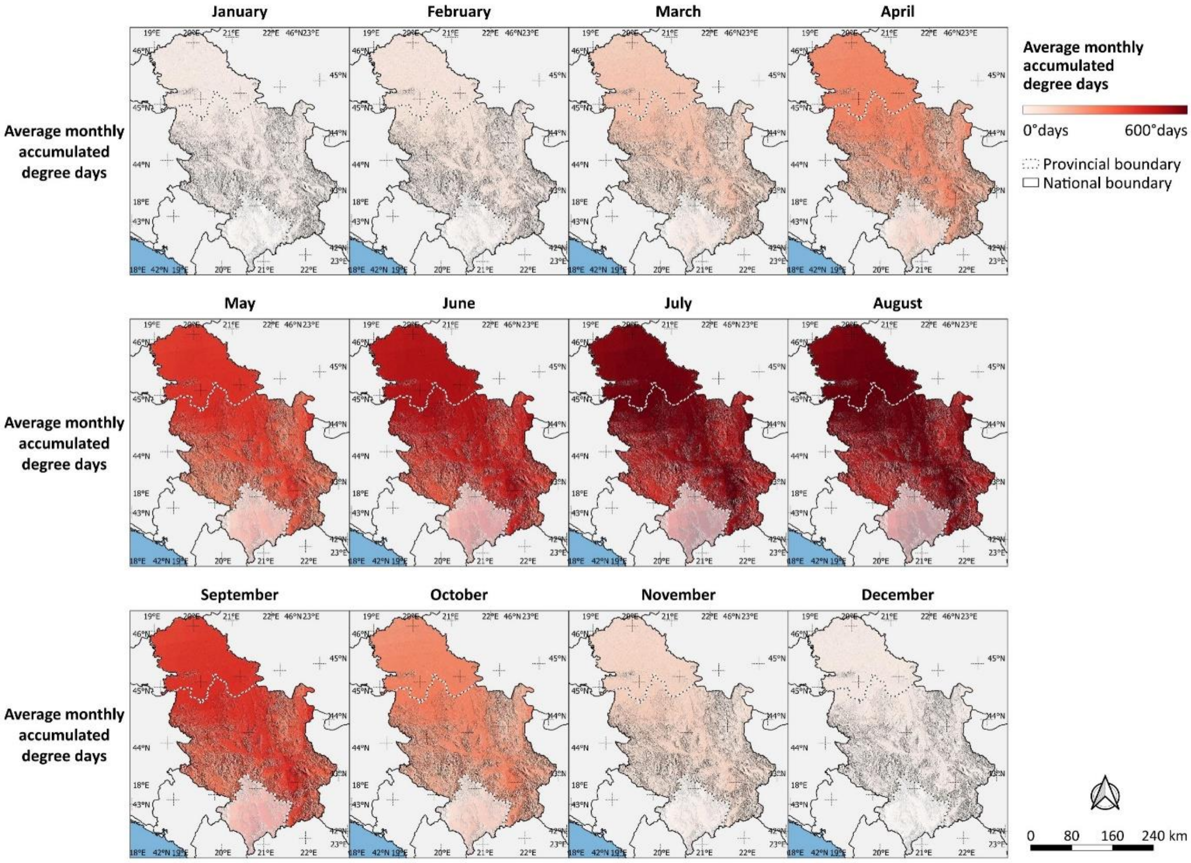

The distribution of degree days throughout Serbia is strongly related to the topography. High values of degree days are visible at low altitude, in the flat land of the North and in the valley of the South of the country. This distribution stays constant throughout the year.

Historical monthly trends

The historical trends of monthly accumulated degree days can be observed in Figure 82 and Table 28.

Overall, most of the months shows an increase of DD_m. In terms of critical months, the largest increases in DD_m can be observed for the months of <u>June</u> (+18.6°days/decade), <u>August</u> (+18.4°days/decade) and <u>July</u> (+16.0°days/decade).

Figure 82 – Historical monthly time series of accumulated degree days

Time series over 1980-2019 period. Data source: ERA5, ECMWF / Copernicus Climate Change Service (Muñoz Sabater, 2019)

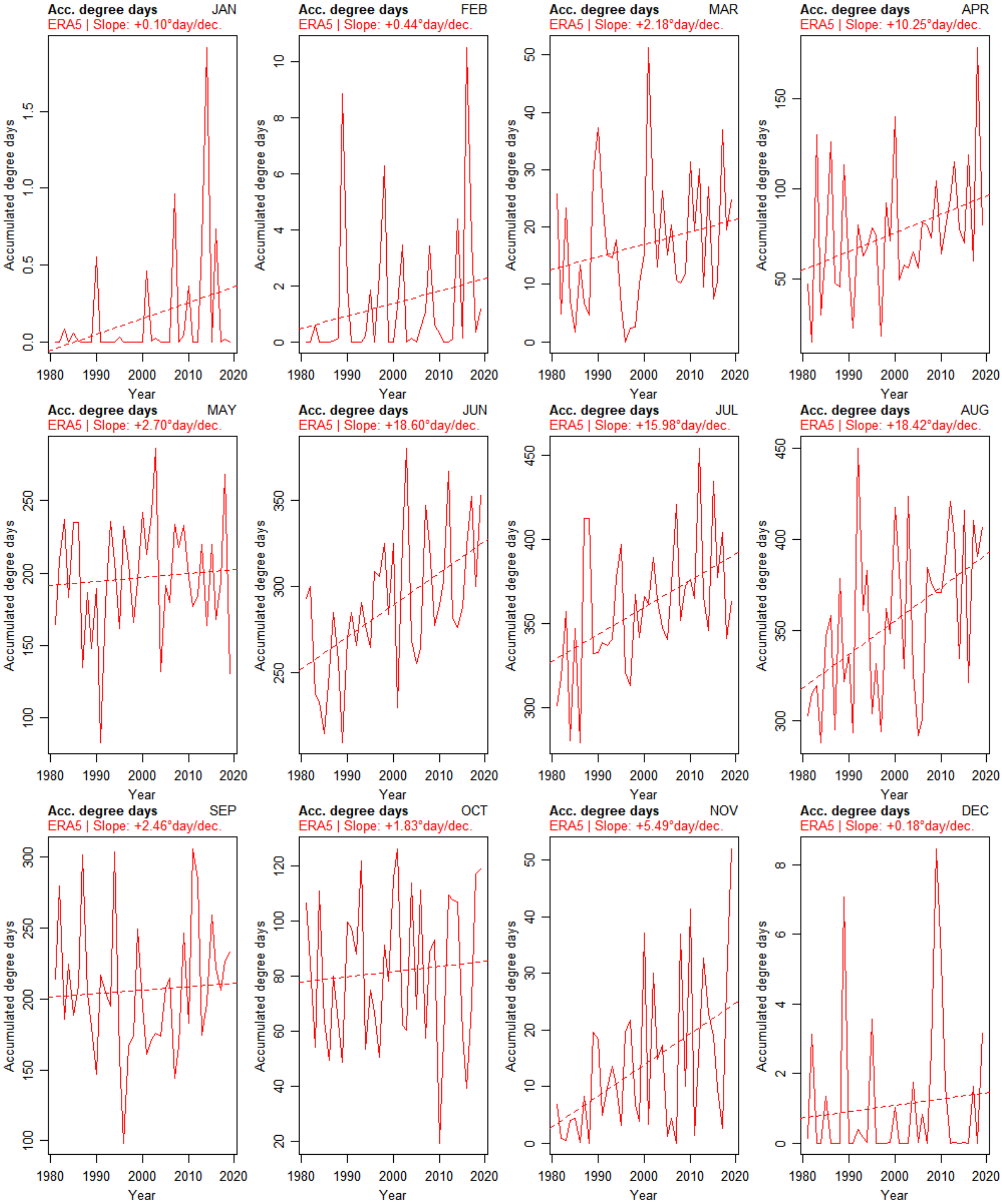

Table 28 – Characteristics of the trends from the historical time series of the monthly accumulated degree days (linear models)
Data source: ERA5, ECMWF / Copernicus Climate Change Service (Muñoz Sabater, 2019).

Variable	Month	Slope	p-value	Adjusted R^2	Average value in 1980	Average value in 2019
DD_m	January	+0.10°days/dec.	0.05	0.07	-0.05°days	0.35°days
DD_m	February	+0.44°days/dec.	0.21	0.02	0.49°days	2.21°days
DD_m	March	+2.18°days/dec.	0.19	0.02	12.65°days	21.14°days
DD_m	April	+10.25°days/dec.	0.03	0.09	55.11°days	95.10°days
DD_m	May	+2.70°days/dec.	0.65	-0.02	191.50°days	202.04°days
DD_m	June	+18.60°days/dec.	0.00	0.26	252.02°days	324.54°days
DD_m	July	+15.98°days/dec.	0.00	0.21	327.60°days	389.93°days
DD_m	August	+18.42°days/dec.	0.00	0.20	318.45°days	390.27°days
DD_m	September	+2.46°days/dec.	0.72	-0.02	201.52°days	211.09°days
DD_m	October	+1.83°days/dec.	0.64	-0.02	77.96°days	85.10°days
DD_m	November	+5.49°days/dec.	0.00	0.20	2.83°days	24.26°days
DD_m	December	+0.18°days/dec.	0.54	-0.02	0.72°days	1.43°days

Historical annual trends

Historical annual trends of accumulated degree days and average hardiness zone can be observed in Figure 83 and Table 29.

Figure 83 – Historical time series of the annual accumulated degree days and average hardiness zone
Time series over 1980-2019 period. ***In red:*** *ERA5.* ***In light blue:*** *variable from each weather stations.* ***In dark blue, full line:*** *annual median value over the weather stations data.* ***In dark blue, dashed line:*** *minimum and maximum value (respectively) over the weather stations data. Data source: ERA5, ECMWF / Copernicus Climate Change Service (Muñoz Sabater, 2019)*

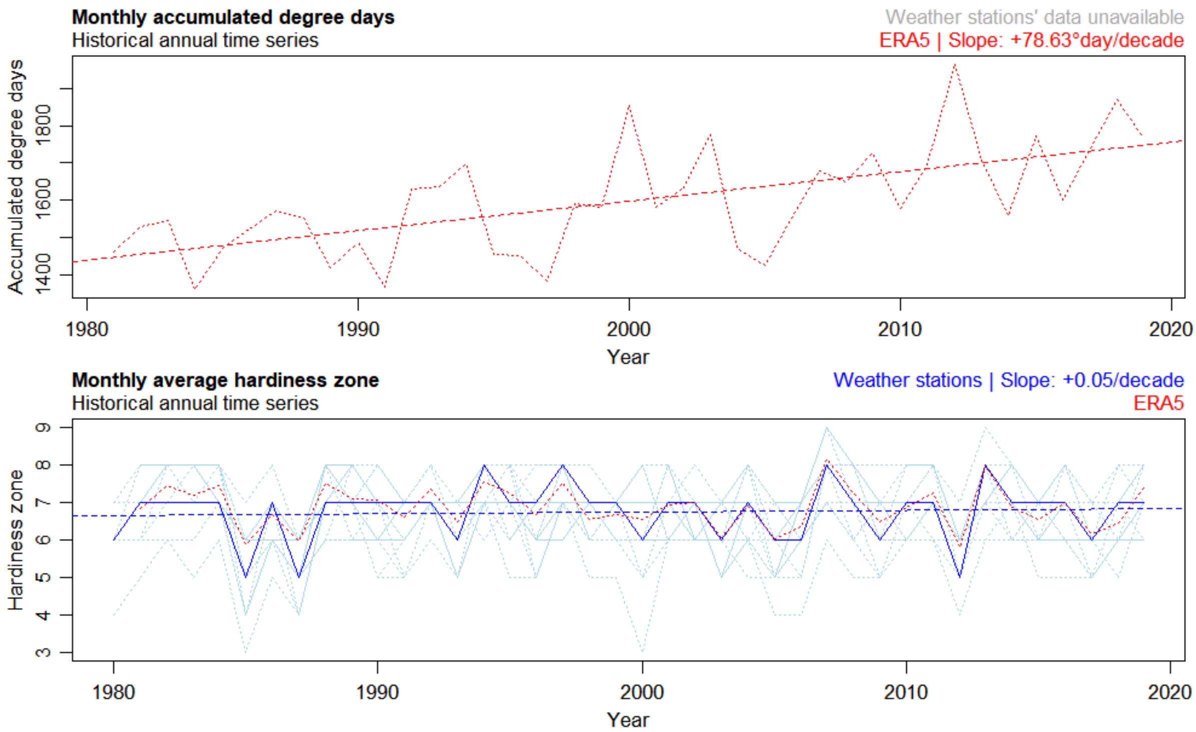

Annually accumulated degree days in Serbia presented a general increase for the last 40 years (+79°days/decade). This increase, due to the increase of the average temperature in Serbia, brought DD_y from 1441°days on average in 1980 to 1747°days on average in 2019.

Because annual minimum temperature stayed roughly stable in Serbia during the last 40 years (see Figure 32) the average hardiness zone in Serbia did not change during the last 40 years, maintaining itself around 7. This stability was confirmed by both local weather station data and ERA5 data.

Table 29 – Characteristics of the trend from historical data for annually accumulated degree days and average hardiness zone (linear models)
Data source: ERA5, ECMWF / Copernicus Climate Change Service (Muñoz Sabater, 2019)

Variable	Slope	p-value	Adj. R^2	Average value in 1980	Average value in 2019
DD_y	+78.63°days/decade	0.00	0.37	1440.79°days	1747.46°days
HZ	+0.05/decade	0.65	-0.02	6.66	6.84

Spatial distribution

The spatial distribution of the trends on annually accumulated degree days, and average hardiness zones can be observed in Figure 84.

The distribution of the annually accumulated degree days is constant through the period and is similar to the seasonal distribution: strongly related to the topography, high values are visible at low altitudes, where low values are visible at high altitudes.

The hardiness zones follow the minimum temperature distribution pattern, with lower hardiness zones at high altitudes, and higher hardiness zones at low altitude. Interestingly, the hardiness zone seems to be the highest in a 100 km wide band, oriented East-West, just South of the Sava Danube River axis.

Figure 84 – Historical and projected decadal spatial distribution of annually accumulated degree days and Hardiness zone
*Data averaged over the 1980-2059 period, by decade. **In red:** degree days. **In color gradient (blue to red):** Hardiness zone. Data source: ERA5, ECMWF / Copernicus Climate Change Service (Muñoz Sabater, 2019) and Second national communication of the Republic of Serbia under the United Nations framework convention on climate change (Rajkovic et al., 2013)*

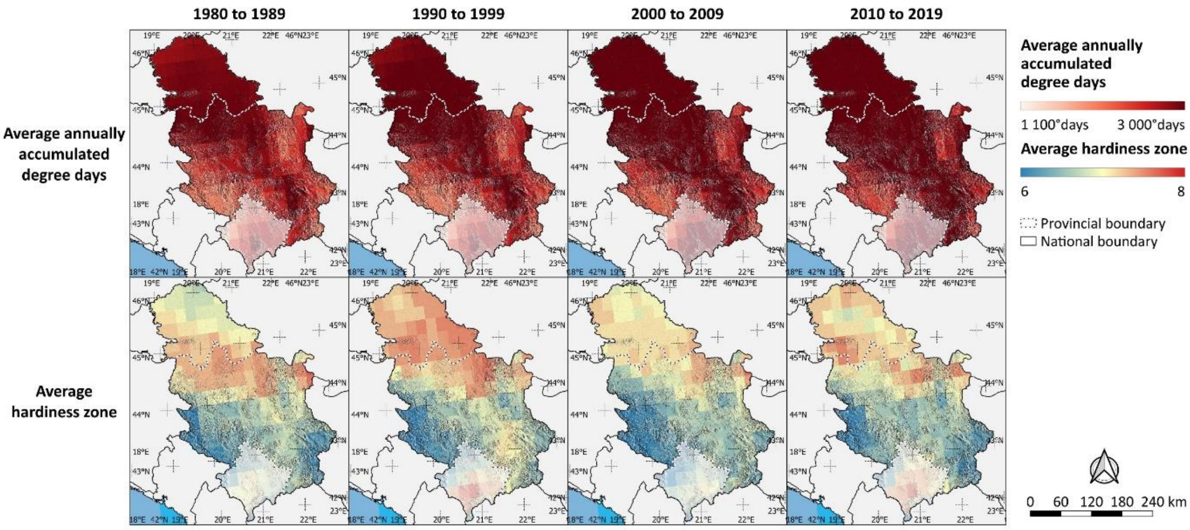

Projected monthly trends

The projected trends of monthly accumulated degree days can be observed in Figure 85 and Table 30.

Figure 85 – Projected monthly time series of accumulated degree days
Time series over 2020-2060 period. ***Pink dotted line****: variable value for each model separately under the RCP4.5 scenario.* ***grey dotted line****: variable value for each model separately under the RCP8.5 scenario.* ***Purple full line:*** *median value of the variable under RCP4.5 scenario.* ***Black full line:*** *median value of the variable under RCP8.5 scenario. <u>Data source:</u> NASA Earth Exchange - Global Daily Downscaled Climate Projections (NEX – GDDP) (Thrasher et al., 2012).*

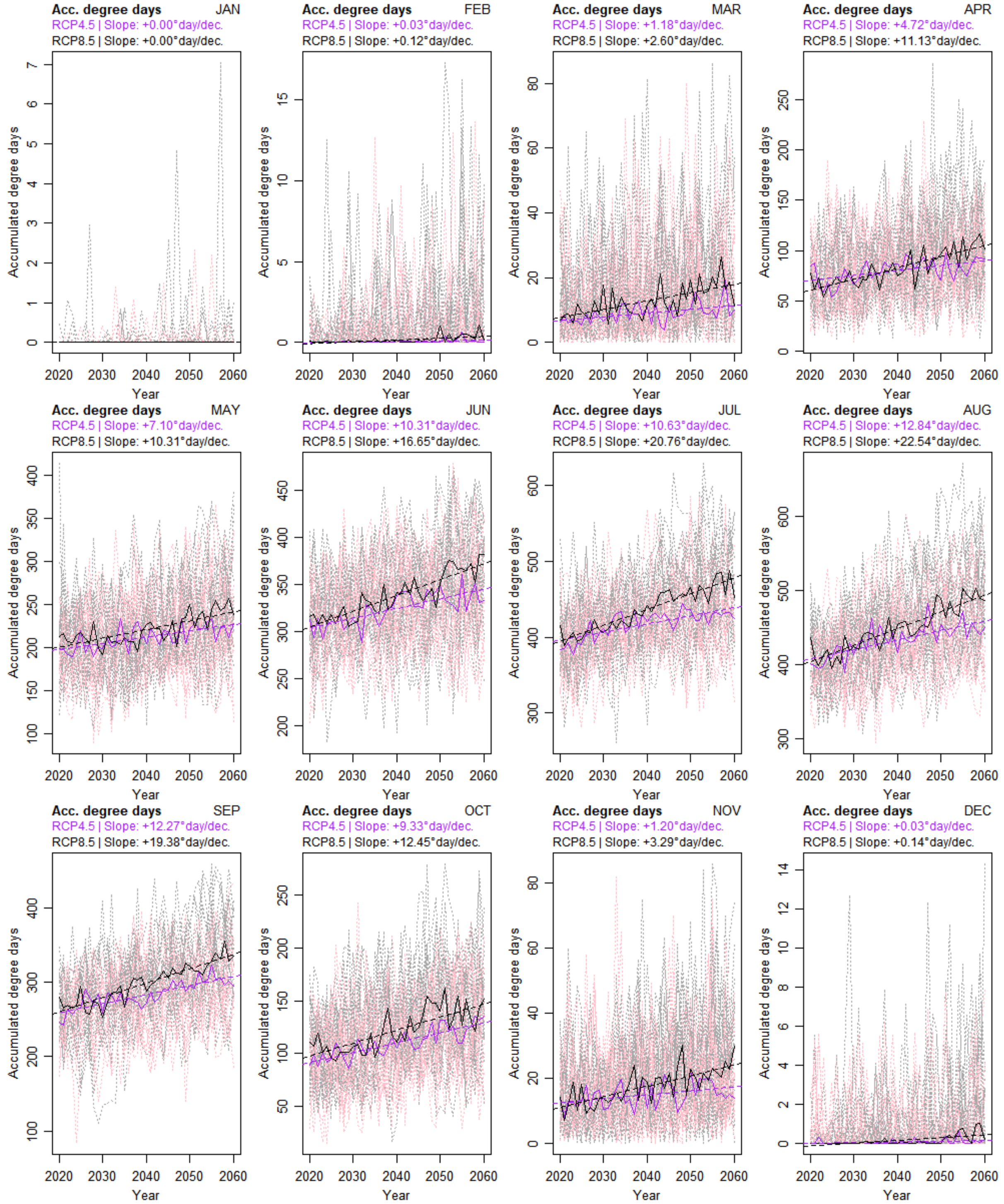

Table 30 – Characteristics of the trend from projected time series of monthly accumulated summer days and tropical nights days under both RCP4.5 and RCP8.5 scenario (linear models)
Data source: NASA Earth Exchange - Global Daily Downscaled Climate Projections (NEX – GDDP) (Thrasher et al., 2012).

RCP4.5						
Variable	**Month**	**Slope**	**p-value**	**R^2**	**Average value in 2040**	**Average value in 2060**
DD_m	January	+0.00°days/dec.	NA	NA	0.00°days	0.00°days
DD_m	February	+0.03°days/dec.	0.03	0.09	0.05°days	0.11°days
DD_m	March	+1.18°days/dec.	0.00	0.19	9.08°days	11.44°days
DD_m	April	+4.72°days/dec.	0.00	0.25	80.25°days	89.69°days
DD_m	May	+7.10°days/dec.	0.00	0.40	211.97°days	226.17°days
DD_m	June	+10.31°days/dec.	0.00	0.54	324.37°days	344.98°days
DD_m	July	+10.63°days/dec.	0.00	0.55	417.65°days	438.91°days
DD_m	August	+12.84°days/dec.	0.00	0.53	433.54°days	459.22°days
DD_m	September	+12.27°days/dec.	0.00	0.66	283.54°days	308.08°days
DD_m	October	+9.33°days/dec.	0.00	0.68	110.28°days	128.94°days
DD_m	November	+1.20°days/dec.	0.01	0.13	14.88°days	17.28°days
DD_m	December	+0.03°days/dec.	0.05	0.07	0.08°days	0.15°days
RCP8.5						
Variable	**Month**	**Slope**	**p-value**	**R^2**	**Average value in 2040**	**Average value in 2060**
DD_m	January	+0.00°days/dec.	NA	NA	0.00°days	0.00°days
DD_m	February	+0.12°days/dec.	0.00	0.32	0.16°days	0.40°days
DD_m	March	+2.60°days/dec.	0.00	0.39	12.71°days	17.91°days
DD_m	April	+11.13°days/dec.	0.00	0.65	82.96°days	105.23°days
DD_m	May	+10.31°days/dec.	0.00	0.53	220.98°days	241.60°days
DD_m	June	+16.65°days/dec.	0.00	0.76	338.74°days	372.05°days
DD_m	July	+20.76°days/dec.	0.00	0.84	435.88°days	477.39°days
DD_m	August	+22.54°days/dec.	0.00	0.81	448.91°days	493.98°days
DD_m	September	+19.38°days/dec.	0.00	0.82	299.09°days	337.84°days
DD_m	October	+12.45°days/dec.	0.00	0.58	122.08°days	146.99°days
DD_m	November	+3.29°days/dec.	0.00	0.52	17.57°days	24.16°days
DD_m	December	+0.14°days/dec.	0.00	0.36	0.15°days	0.43°days

Overall, most of the months shows an increase of DD_m.

Under the RCP4.5 scenario, the NEX median model shows the largest increases in DD_m during the months of August (+12.8°days/decade), September (+12.3°days/decade) and July (+10.6°days/decade). Under the RCP8.5 scenario, the largest increase in DD_m can be observed for the months of August (+22.5°days/decade), July (+20.8°days/decade) and September (+19.4°days/decade).

Projected annual trends

Projected annual trends on annually accumulated degree days and average hardiness zone can be observed in Figure 86 and Table 31.**Error! Reference source not found.**.

Figure 86 – Projected annual time series of accumulated degree days and average hardiness zone
*Time series over 2020-2060 period. Time series over 2020-2060 period. **Pink dotted line**: variable value for each model separately under the RCP4.5 scenario. **grey dotted line**: variable value for each model separately under the RCP8.5 scenario. **Purple full line:** median value of the variable under RCP4.5 scenario. **Black full line:** median value of the variable under RCP8.5 scenario. Data source: NASA Earth Exchange - Global Daily Downscaled Climate Projections (NEX – GDDP) (Thrasher et al., 2012).*

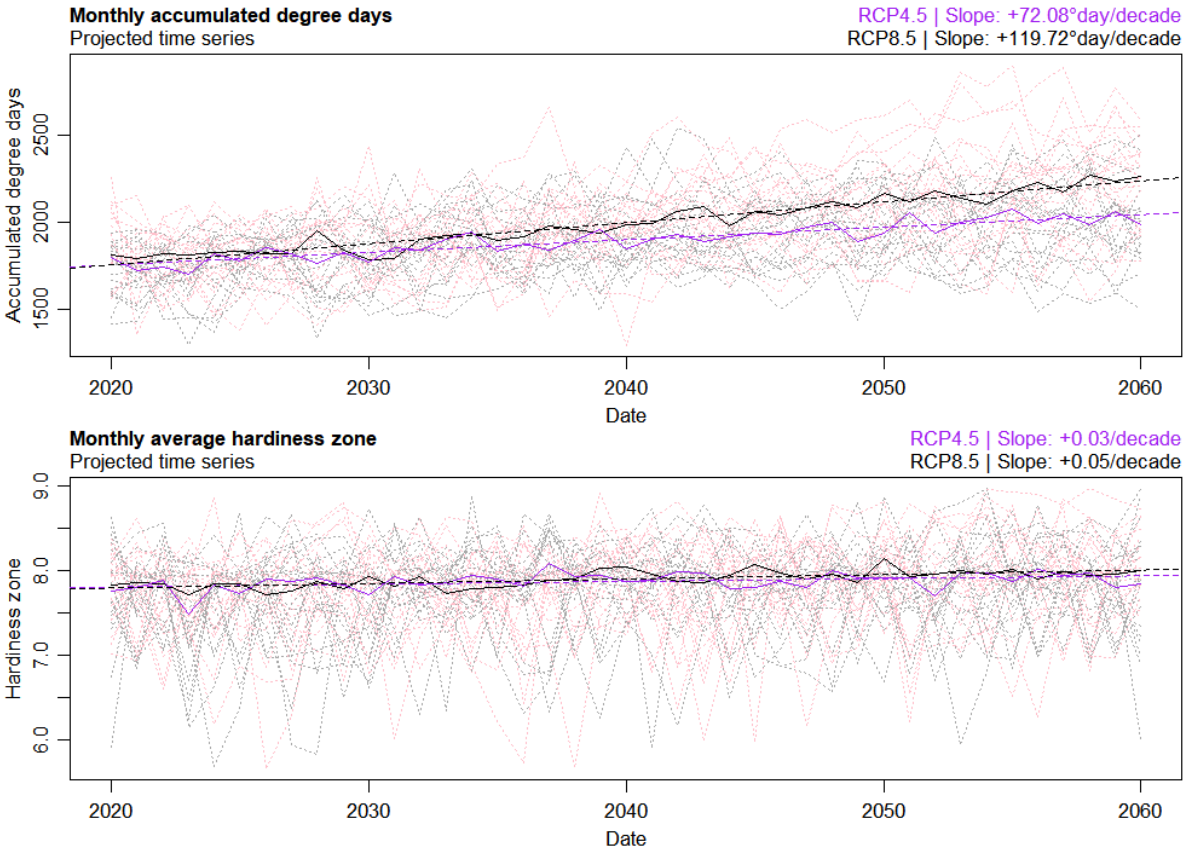

Table 31 – Characteristics of the trend from projected data for annually accumulated frost days, ice days and chill hours (linear models)
Data source: Second national communication of the Republic of Serbia under the United Nations framework convention on climate change (Rajkovic et al., 2013) and NASA Earth Exchange - Global Daily Downscaled Climate Projections (NEX – GDDP) (Thrasher et al., 2012).

RCP4.5					
Variable	**Slope**	**p-value**	**Adjusted R²**	**Average value in 2040**	**Average value in 2060**
DD_y	+72.08°days/decade	0.00	0.80	1900.21°days	2044.38°days
HZ	+0.03/decade	0.02	0.11	7.88	7.94
RCP8.5					
Variable	**Slope**	**p-value**	**Adjusted R²**	**Average value in 2040**	**Average value in 2060**
DD_y	+119.72°days/decade	0.00	0.92	1998.51°days	2237.94°days
HZ	+0.05/decade	0.00	0.43	7.90	8.01

The annually accumulated degree days is expected by scenario to maintain its increase for the next 40 years (RCP4.5: +72°days/decade, RCP8.5: +120°days/decade). This increase is expected to bring DD_y from 1900°days on average in 2040 to 2044°days on average in 2060 under the RCP4.5 scenario, and from 1999°days in 2040 to 2238°days in 2060 under the RCP8.5 scenario.

Regarding the average Hardiness zone, it is expected to stay stable for the next 40 years in Serbia

Conclusion

Degree days are present in Serbia from march to December, peaking in July and August. Annual and monthly accumulated degree days increased during the last 40 years, and are expected to continue increasing, to a rate between + 72-degree days per decade to +120 degree days per decade. These increases are expected to be more acute during the hottest month of the year, from July to September.

The average hardiness zone of Serbia did not change significatively during the last 40 years and is expected to stay stable during the next 40 years.

14. Water deficit

This section will present the **accumulated water deficit** in the Republic of Serbia. The water deficit is calculated here as the difference between measured evapotranspiration (ET), and potential evapotranspiration (PET). In this section we will focus on **monthly accumulated water deficit** ($Wdef_m$), and **annually accumulated water deficit** ($Wdef_y$).

ET and PET were not available in the weather stations dataset. Therefore, this section will only present degree days calculated using Terra Net Evapotranspiration.

Current seasonal variations

The seasonal variation of the monthly accumulated water deficit in the Republic of Serbia is presented in Figure 87.

Figure 87 – Current seasonal variation or monthly accumulated water deficit
Data averaged over the 2001-2019 period. Data source: NASA LP DAAC - EBMOD16A2.006: Terra Net Evapotranspiration (Running et al., 2021).

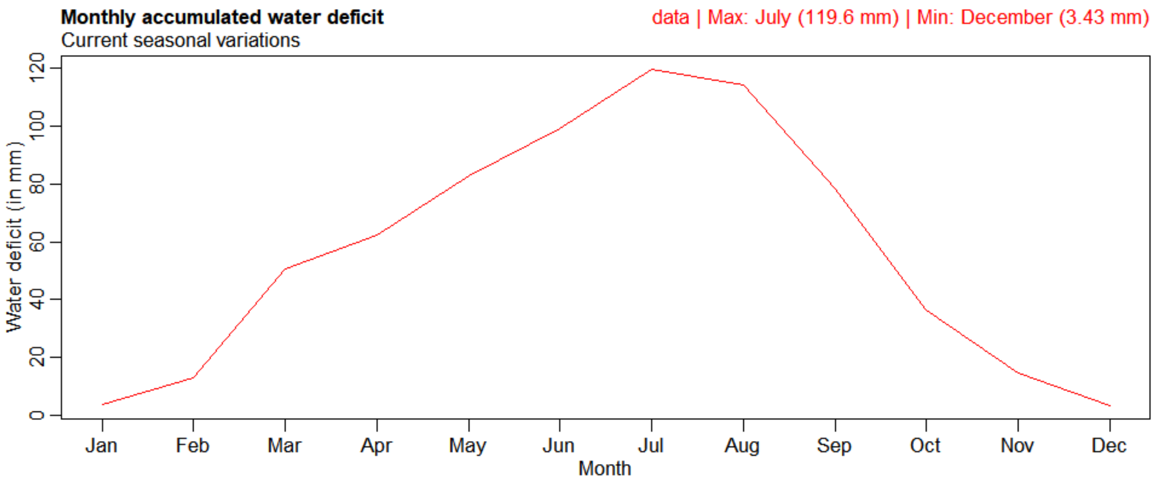

Monthly accumulated water deficit is peaking during the month of July and August (around 150 mm). It then steadily decreases until December-January, where $Wdef_m$ is close to 0 mm. It then increases steadily back to its maximum July-August. The decrease period (August to December) is steeper than the increase period (January to July).

Spatial distribution

The current seasonal spatial distribution of the monthly accumulated water deficit throughout the Republic of Serbia can be observed in Figure 88.

The seasonal water deficit distribution is strongly related to the topography. High water deficit values are visible in the low altitude area, in the flat land of the North and in the valley of the South of the country. This distribution stays constant through the year.

Figure 88 – Spatial distribution of the monthly accumulated water deficit in the Republic of Serbia.
Data averaged over the 2001-2019 period. Data source: NASA LP DAAC - EBMOD16A2.006: Terra Net Evapotranspiration (Running et al., 2021).

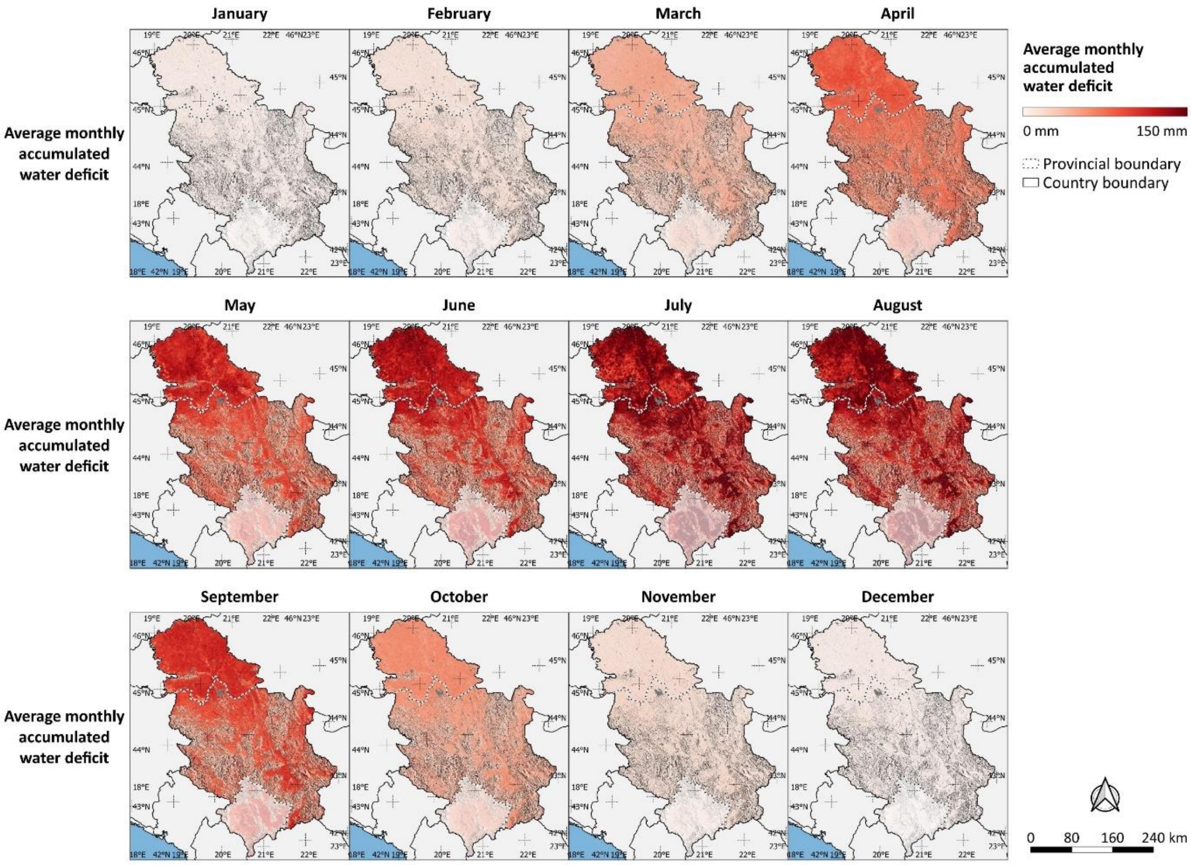

Historical monthly trends

The historical trends of monthly accumulated water deficit can be observed in Figure 89 and Table 32.

The analysis of the historical trends on accumulated frost days at a monthly scale are consistent with the annual analysis. Overall, most of the months shows an increase in **Wdef$_m$**.

In terms of critical months, the largest decrease in **Wdef$_m$** can be observed for the months of September (+11.9 mm/decade), August (+8.2 mm/decade) and April (+8.3 mm/decade). There are however 2 notable exceptions to this trend: May (-13.8 mm/decade) and July ((-5.4 mm/decade) seems to show a decrease in **Wdef$_m$**.

Figure 89 – Historical monthly time series of accumulated water deficit

Time series over 2001-2019 period. <u>Data source:</u> NASA LP DAAC - EBMOD16A2.006: Terra Net Evapotranspiration (Running et al., 2021)

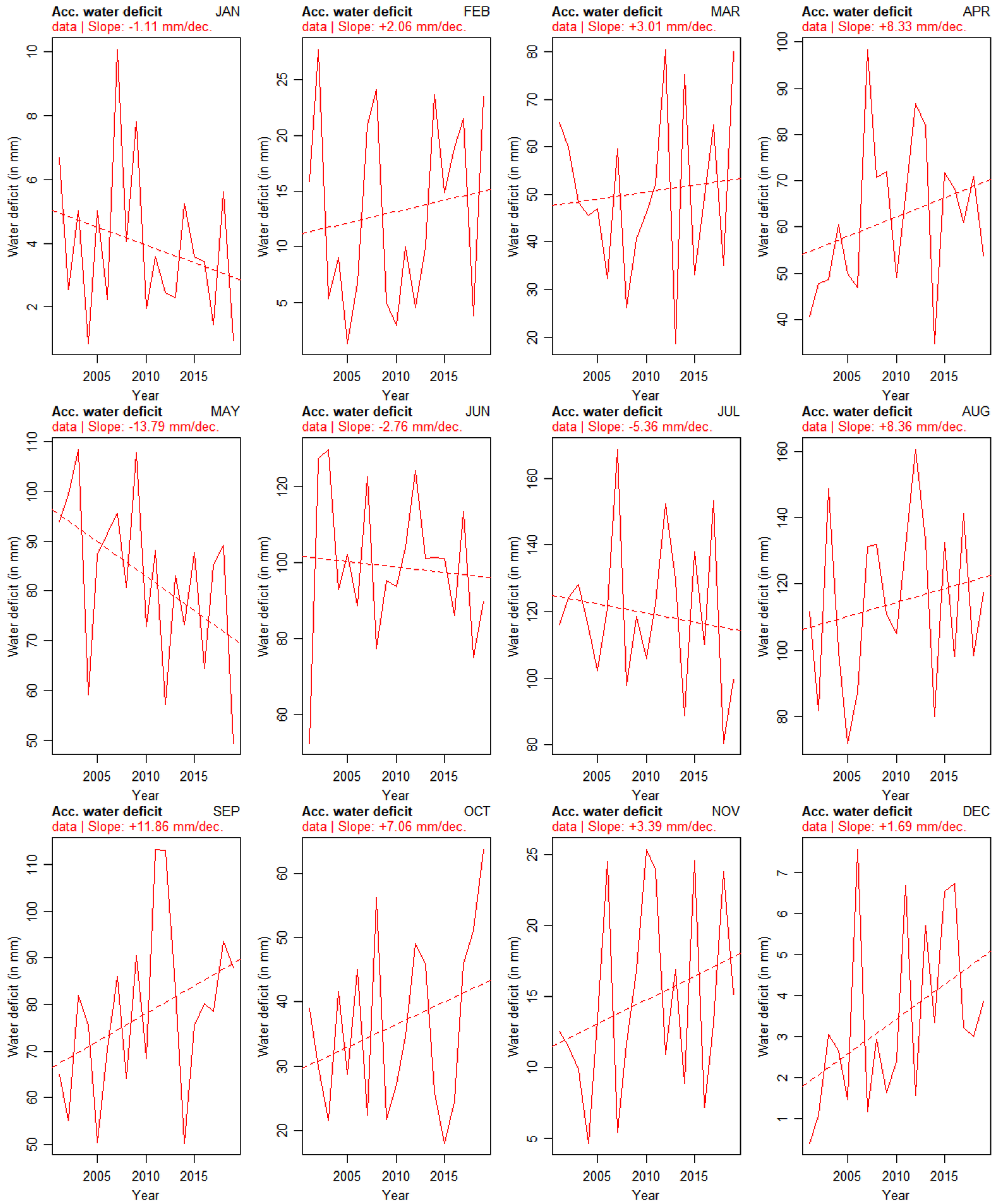

Table 32 – Characteristics of the trends from the historical time series of the monthly accumulated water deficit (linear models)
Data source: NASA LP DAAC - EBMOD16A2.006: Terra Net Evapotranspiration (Running et al., 2021)

Variable	Month	Slope	p-value	Adjusted R^2	Average value in 1980	Average value in 2019
$WDef_m$	January	-1.11 mm/dec.	0.29	0.01	7.26 mm	2.94 mm
$WDef_m$	February	+2.06 mm/dec.	0.58	-0.04	6.96 mm	15.01 mm
$WDef_m$	March	+3.01 mm/dec.	0.70	-0.05	41.46 mm	53.22 mm
$WDef_m$	April	+8.33 mm/dec.	0.24	0.03	37.17 mm	69.65 mm
$WDef_m$	May	-13.79 mm/dec.	0.04	0.18	124.26 mm	70.48 mm
$WDef_m$	June	-2.76 mm/dec.	0.75	-0.05	107.15 mm	96.41 mm
$WDef_m$	July	-5.36 mm/dec.	0.58	-0.04	135.69 mm	114.78 mm
$WDef_m$	August	+8.36 mm/dec.	0.44	-0.02	89.23 mm	121.84 mm
$WDef_m$	September	+11.86 mm/dec.	0.11	0.09	42.49 mm	88.75 mm
$WDef_m$	October	+7.06 mm/dec.	0.22	0.03	15.27 mm	42.78 mm
$WDef_m$	November	+3.39 mm/dec.	0.24	0.02	4.56 mm	17.79 mm
$WDef_m$	December	+1.69 mm/dec.	0.06	0.14	-1.65 mm	4.95 mm

Historical annual trends

Historical nthly accumulated water deficit can be observed in Figure 90 and Table 33.

Figure 90 – Historical time series of annually accumulated water deficit
Time series over 2001-2019 period. Data source: NASA LP DAAC - EBMOD16A2.006: Terra Net Evapotranspiration (Running et al., 2021).

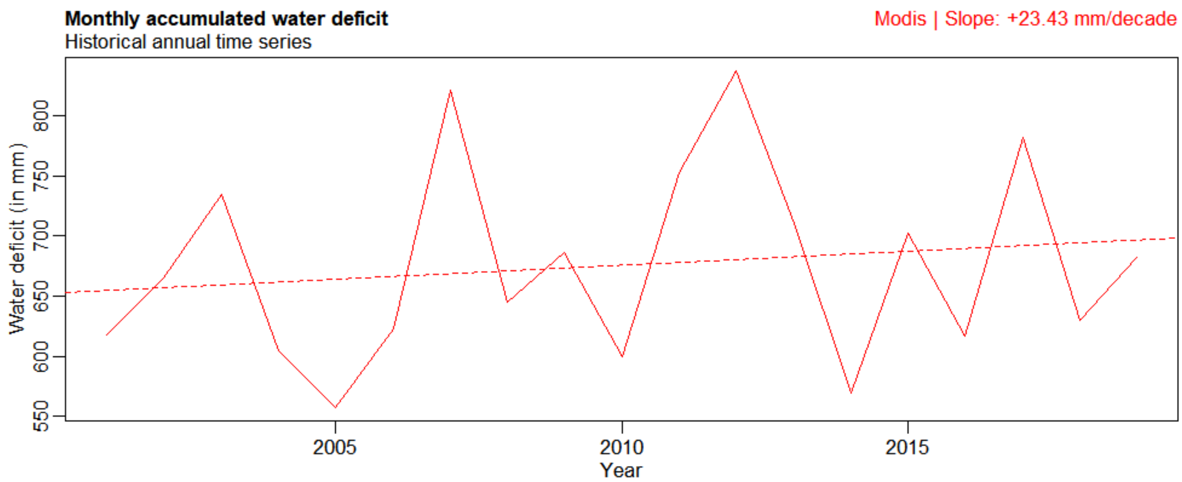

Table 33 – Characteristics of the trend from historical data for annually accumulated degree days and average hardiness zone (linear models)
Data source: ERA5, ECMWF / Copernicus Climate Change Service (Muñoz Sabater, 2019)

Variable	Slope	p-value	Adj. R^2	Average value in 1980	Average value in 2019
$Wdef_y$	+23.43 mm/decade	0.51	-0.03	605.35 mm	696.71 mm

Although a large interannual variation (from 550 mm to 850 mm), the annually accumulated water deficit of Serbia has increased on average for the last 19 years (+23 mm /decade). This increase lead $\mathbf{Wdef_y}$ from 665 mm on average in 2001 to 697 mm on average in 2019.

Spatial distribution

The historical decadal spatial distribution of the annually accumulated water deficit over the period 2001-2019 throughout the Republic of Serbia can be observed in Figure 91.

Figure 91 – Historical decadal spatial distribution of annually accumulated water deficit
Data averaged over the 2001-2019 period, by decade. Data source: NASA LP DAAC - EBMOD16A2.006: Terra Net Evapotranspiration (Running et al., 2021).

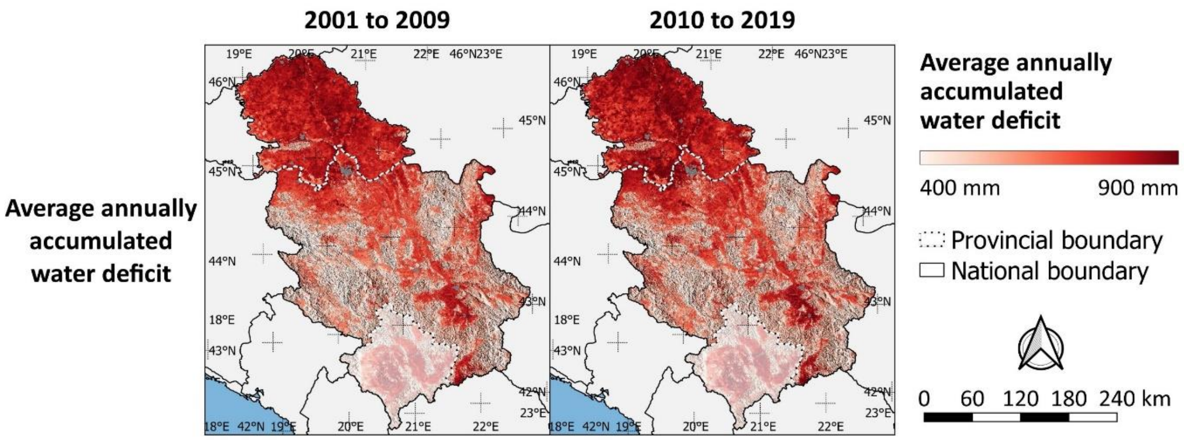

The distribution of the annually accumulated water deficit in the republic of Serbia remained constant through the last 19 years, presenting higher values at lower altitude.

Conclusion

Accumulated water deficit is peaking during the month of July and August, and steadily decreases until December-January, where $Wdef_m$ is close to 0 mm. It then increases steadily back to its maximum July-August. Historically, the water deficit increased in Serbia for the last 19 years. This trend was particularly marked at the end of the summer month (August and September).

15. Snowfall and snow depth

This section will present two snow variables in the Republic of Serbia. These variables are:

- **Accumulated snowfall:** This variable represents the accumulated snowfall in mm of water equivalent. In this section we will focus on **monthly accumulated snowfall** (SnF_m) and **annually accumulated snowfall** (SnF_y).
- **Average snow depth:** This variable represents the average snow depth in mm of water equivalent. In this section we will focus on **monthly average snow depth** (SnD_m) and **annual average snow depth** (SnD_y).

Snowfall and snow depth were not available in the weather stations dataset. Therefore, this section will only present data calculated using GLDAS data.

Current seasonal variations

The seasonal variation of the snowfall and snow depth in the Republic of Serbia are presented in Figure 92.

Figure 92 – Current seasonal variation of accumulated snowfall and average snow depth
*Data averaged over the 2000-2019 period. **In blue:** monthly accumulated snowfall. **In green:** monthly averaged snow depth. <u>Data source:</u> NASA GES DISC - GLDAS-2.1: Global Land Data Assimilation System (Rodell et al., 2004).*

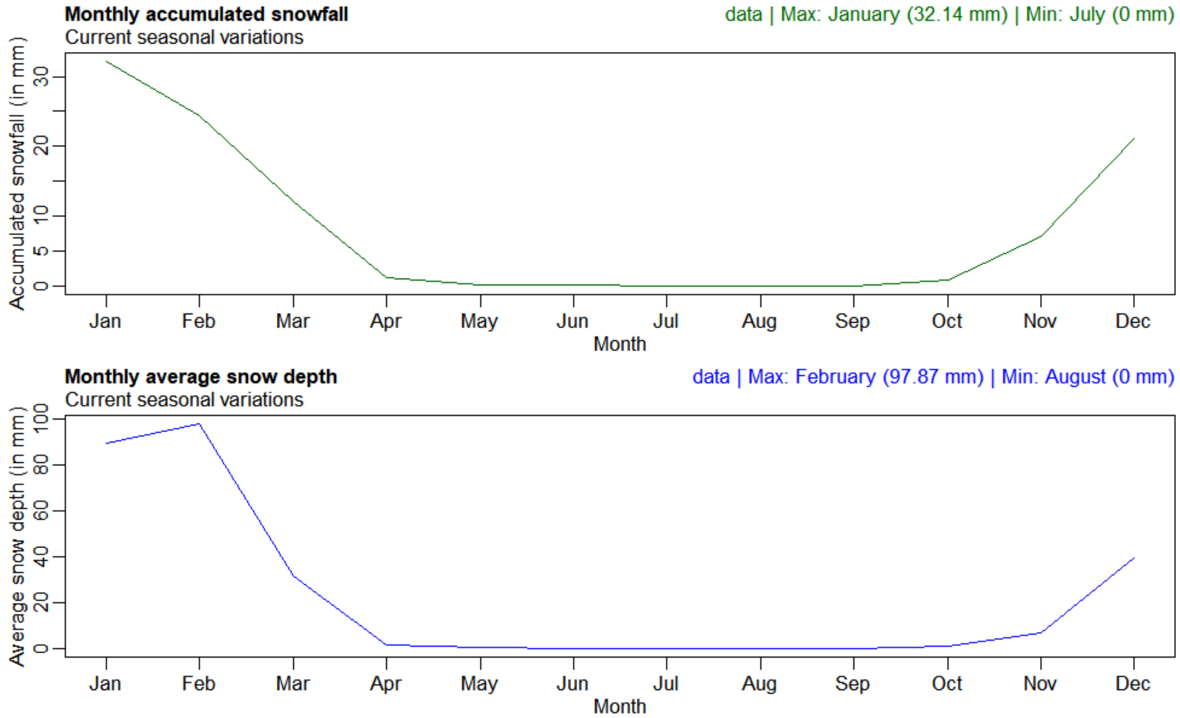

Currently, snowfall starts on October in the Republic of Serbia, and gradually increases until January when it reaches slightly more than 30 mm of water equivalent per month. It then steadily decreases until May, when no more snowfall is observed. Snow depth follows the same general trend. Snow cover appears in Serbia with the first snowfall of October, and, from there, increases until February, when it reaches slightly more than 30 mm of water equivalent. It then sharply decreases until May, when no more snow cover can be found.

Spatial distribution

Figure 93 – Spatial distribution of the current variation of accumulated snowfall and average snow depth
*Data averaged over the 2000-2019 period**. In blue:** monthly accumulated snowfall. **In green:** monthly averaged snow depth. Data source: NASA GES DISC - GLDAS-2.1: Global Land Data Assimilation System (Rodell et al., 2004).*

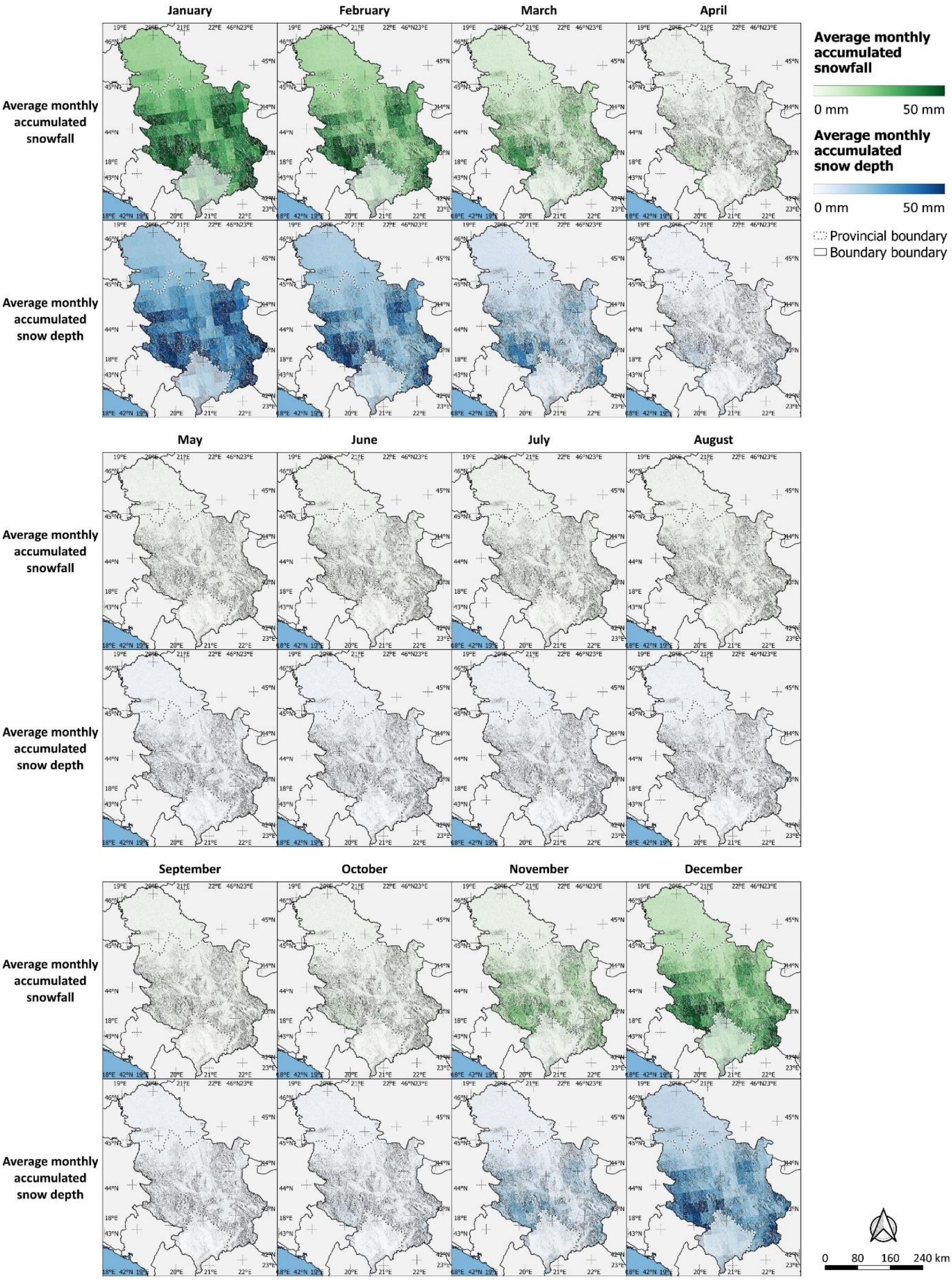

The current seasonal spatial distribution of the snowfall and snow depth throughout the Republic of Serbia can be observed in Figure 99. As can be expected, the distribution of snow cover and snowfall is, during the snow month, centered on the highest altitude of the Southeast and Southwest. There is almost no snowfall or snow depth to the North of the Sava-Danube axis, to the exception of the top of the Fruška Gora range, during the month of January and February.

Historical monthly trends

The historical monthly trends of the snowfall and snow depth in the Republic of Serbia can be observed in Figure 94, Figure 95 and Table 34.

Table 34 – Characteristics of the trends from the historical time series of the monthly accumulated of frost days, ice days, and chill hours (linear models)

***In green**: Monthly accumulated frost days. **In blue:** monthly accumulated ice days. **In red:** monthly accumulated chill hours. Data source: ERA5, ECMWF / Copernicus Climate Change Service (Muñoz Sabater, 2019).*

Variable	Month	Slope	p-value	Adjusted R^2	Average value in 1980	Average value in 2019
SnF_m	January	+2.22 mm/dec.	0.76	-0.05	25.59 mm	34.25 mm
SnF_m	February	-2.60 mm/dec.	0.77	-0.05	32.05 mm	21.89 mm
SnF_m	March	+2.07 mm/dec.	0.68	-0.05	5.95 mm	14.02 mm
SnF_m	April	-0.00 mm/dec.	1.00	-0.06	1.22 mm	1.22 mm
SnF_m	May	-0.02 mm/dec.	0.37	-0.01	0.07 mm	0.00 mm
SnF_m	June	-0.04 mm/dec.	0.43	-0.02	0.14 mm	-0.01 mm
SnF_m	July	+0.00 mm/dec.	NA	NA	0.00 mm	0.00 mm
SnF_m	August	-0.00 mm/dec.	0.56	-0.04	0.00 mm	0.00 mm
SnF_m	September	-0.00 mm/dec.	0.65	-0.04	0.01 mm	0.00 mm
SnF_m	October	-0.63 mm/dec.	0.33	0.00	2.72 mm	0.26 mm
SnF_m	November	-3.28 mm/dec.	0.25	0.02	16.70 mm	3.92 mm
SnF_m	December	-0.85 mm/dec.	0.88	-0.05	23.53 mm	20.20 mm
SnD_m	January	+2.53 mm/dec.	0.90	-0.05	82.13 mm	91.99 mm
SnD_m	February	-19.53 mm/dec.	0.70	-0.05	155.50 mm	79.31 mm
SnD_m	March	-7.97 mm/dec.	0.59	-0.04	55.12 mm	24.05 mm
SnD_m	April	-0.91 mm/dec.	0.11	0.09	4.26 mm	0.71 mm
SnD_m	May	-0.05 mm/dec.	0.01	0.27	0.23 mm	0.02 mm
SnD_m	June	-0.02 mm/dec.	0.30	0.01	0.10 mm	0.01 mm
SnD_m	July	+0.00 mm/dec.	0.42	-0.02	0.00 mm	0.01 mm
SnD_m	August	+0.00 mm/dec.	0.28	0.01	0.00 mm	0.01 mm
SnD_m	September	-0.01 mm/dec.	0.43	-0.02	0.05 mm	0.01 mm
SnD_m	October	-0.37 mm/dec.	0.33	0.00	1.70 mm	0.27 mm
SnD_m	November	-4.08 mm/dec.	0.18	0.05	18.77 mm	2.86 mm
SnD_m	December	-7.54 mm/dec.	0.58	-0.04	61.87 mm	32.46 mm

Figure 94 – Historical time series of the monthly average NDVI

Time series over 2001-2019 period. <u>Data source:</u> MODIS - NASA LP DAAC (Myneni et al., 2015).

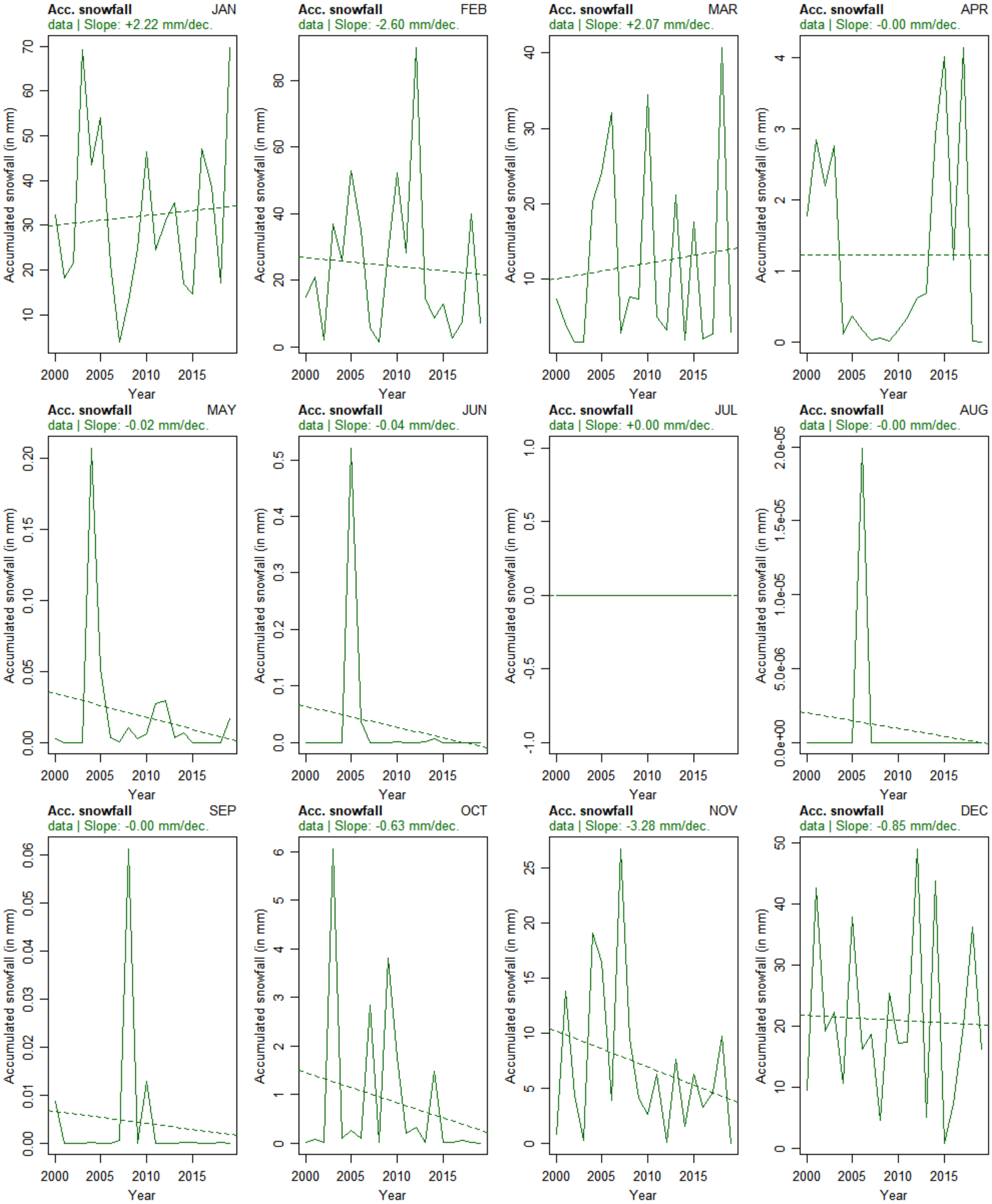

Figure 95 – Historical time series of the monthly average NDVI
Time series over 2001-2019 period. Data source: MODIS - NASA LP DAAC (Myneni et al., 2015).

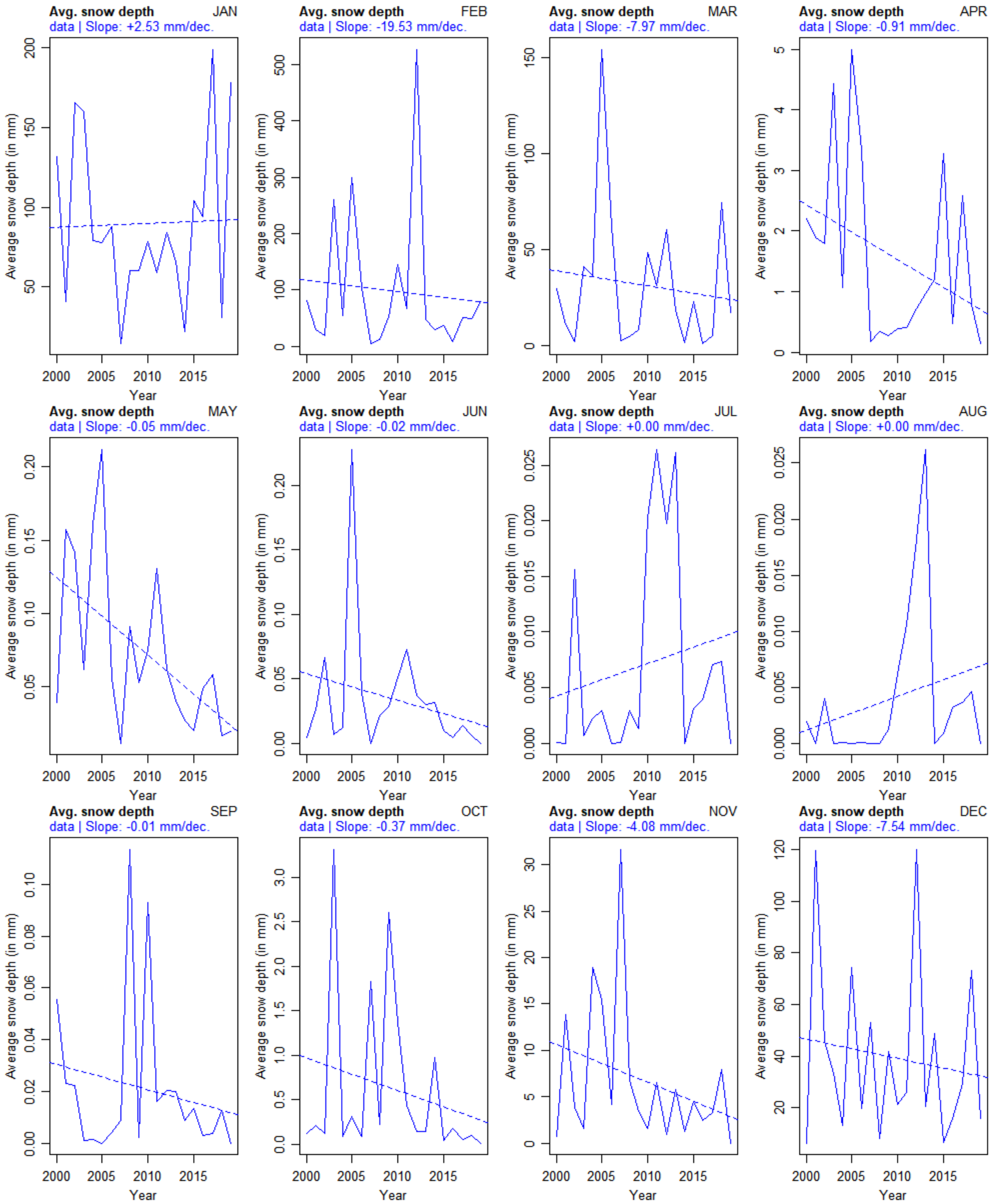

Overall, most of the months shows a decrease in SnF_m. In terms of critical months, the largest decrease in SnF_m can be observed for the months of November (-3.3 mm/decade), February (-2.6 mm/decade) and December (-0.9 mm/decade). There are however 2 notable exceptions to this trend: January (+2.2 mm/decade) and March (+2.1 mm/decade) show an increase in SnF_m.

Overall, most of the months shows a decrease in SnD_m. In terms of critical months, the largest decrease in SnD_m can be observed for the months of February (-19.5 mm/decade), March (-8 mm/decade) and

December (-7.5 mm/decade). There are however one notable exceptions to this trend: January (+2.5 mm/decade) show an increase in SnD_m.

Historical annual trends

Historical annual trends on snow indices can be observed in Figure 96 and Table 35.

SnF_y and SnD_y in Serbia presented a very mild decrease for the last 20 years (SnF_y: -3.1 mm/decade, SnD_y: -3 mm/decade). This decrease brought SnF_y from 102 mm on average in 2000 to 96 mm on average in 2019 and SnD_y from 25 mm on average in 2000 to 19 mm on average in 2019.

Figure 96 – Historical time series of annually accumulated snowfall and annually average snow depth
Data averaged over the 2000-2019 period. ***In blue:*** *annually accumulated snowfall.* ***In green:*** *annual average snow depth. Data source: NASA GES DISC - GLDAS-2.1: Global Land Data Assimilation System (Rodell et al., 2004).*

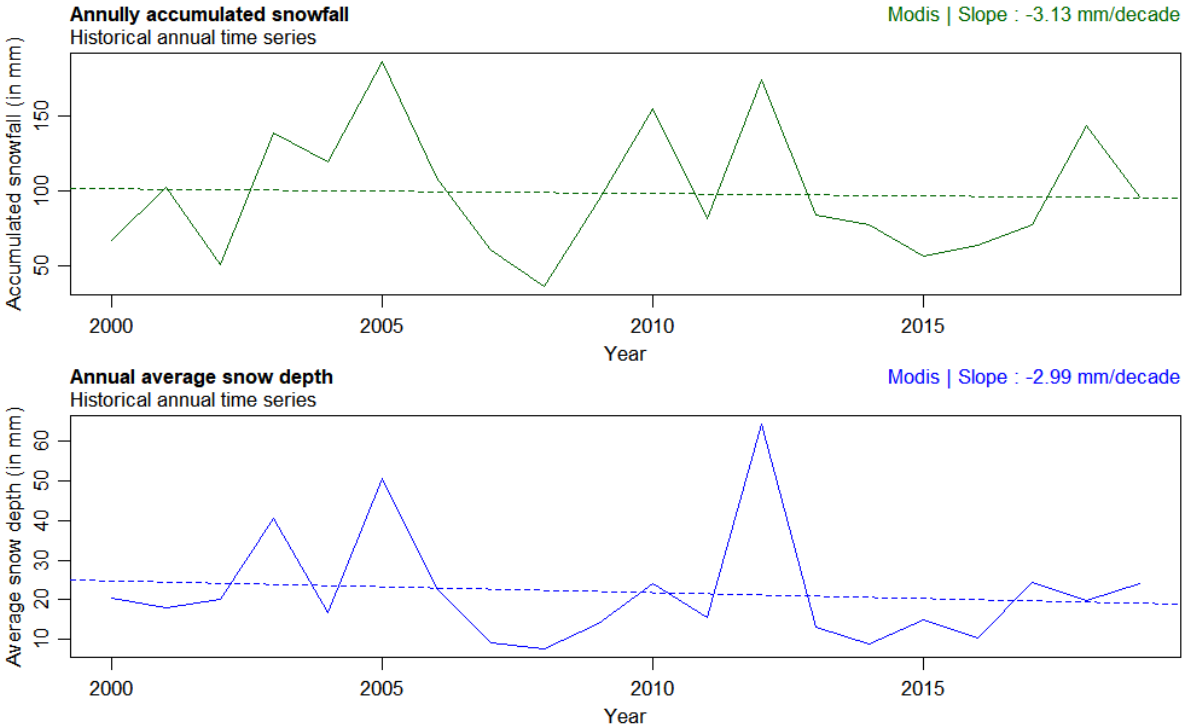

Table 35 – Characteristics of the trend from historical annual times series of accumulated frost days, ice days and chill hours (linear models)
Data source: ERA5, ECMWF / Copernicus Climate Change Service (Muñoz Sabater, 2019)

Variable	Slope	p-value	Adj. R^2	Average value in 1980	Average value in 2019
SnF_y	-3.13 mm/decade	0.85	-0.05	107.98 mm	95.75 mm
SnD_y	-2.99 mm/decade	0.61	-0.04	30.80 mm	19.14 mm

Spatial distribution

The historical decadal spatial distribution of the snow indices over the period 2000-2019 throughout the Republic of Serbia can be observed in Figure 97.

As for their yearly values, the distribution of snow cover and snowfall remained the same since 2000, each centered on the highest altitude of the Southeast and Southwest with a small quantity of snowfall and snow depth on the Fruška Gora range.

__Figure 97 – Historical decadal spatial distribution of annual average NDVI, LAI and vegetation productivity.__ Data averaged over the 2000-2019 period, by decade__. In blue:__ annually accumulated snowfall. __In green:__ annual average snow depth. <u>Data source:</u> NASA GES DISC - GLDAS-2.1: Global Land Data Assimilation System (Rodell et al., 2004).

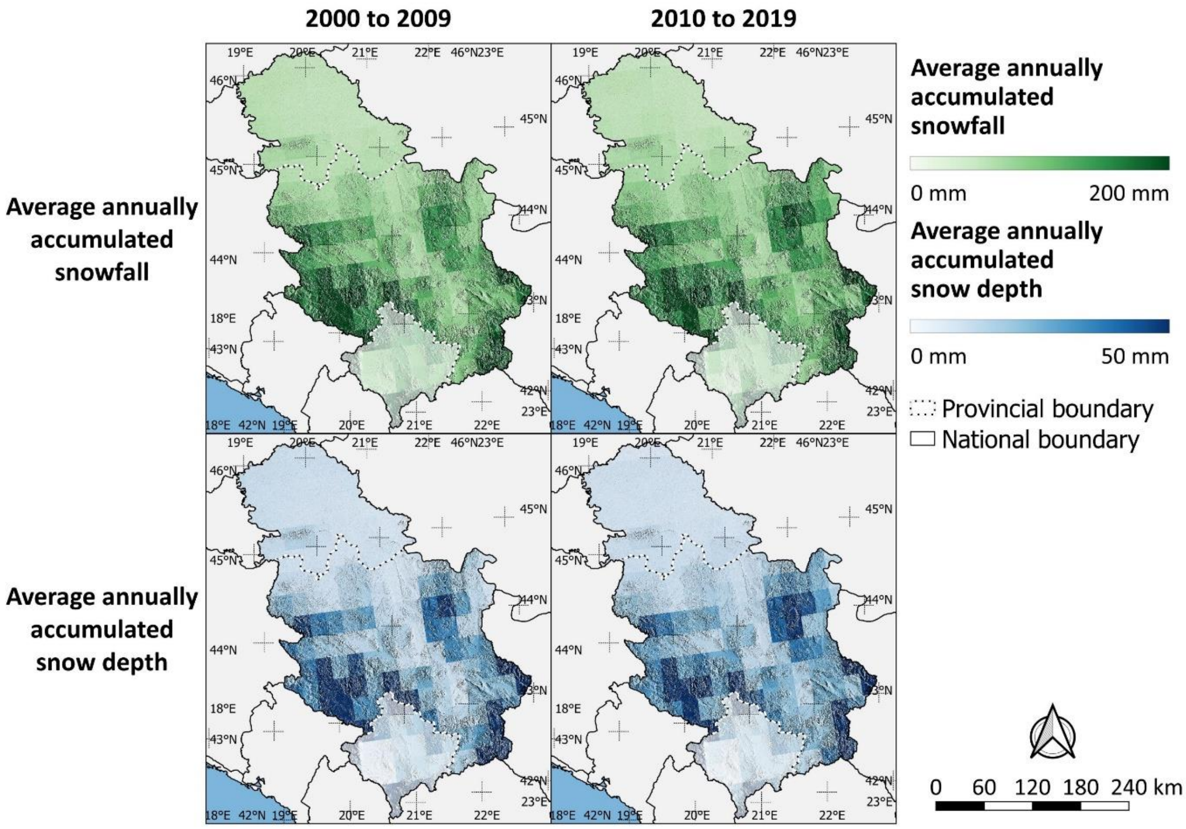

Conclusion

Snowfall and snow depth appears in October in the republic of Serbia and peak during the month of January. Both indices then steadily decrease and disappear in May. These two indices have decreased for the last 20 years. This trend was particularly marked during the months of February and December.

16. NDVI, LAI and Vegetation Productivity

This section will present the variation of three vegetation indices in the Republic of Serbia. These indices are:

- **Leaf Area Index:** It is a dimensionless index representing the ratio of canopy area to total area. The higher the index, the larger the canopy. In this section we will focus on **monthly average Leaf Area Index** (LAI_m) and **annual average leaf area index** (LAI_y). These indices were calculated using MODIS database.
- **Normalize Difference Vegetation Index:** It is dimensionless spectral index representing the amount of live green vegetation. The higher the index the greener the area. In this section we will focus on **monthly average normalize difference vegetation Index** ($NDVI_m$) and **annual average normalize difference vegetation index** ($NDVI_y$) These indices were calculated using MODIS database.
- **Vegetation Productivity:** This index indicates the spatial distribution and change of the vegetation cover. It is produced by the European Environment Agency (EEA) and is derived from remote sensing observed time series of vegetation indices (European Environment Agency, March-20-2021). Because only annual data was available, we will only discuss the **annual average vegetation productivity** (VP). These indices were calculated using MODIS database.

Current seasonal variations

The monthly variation of the $NDVI_m$ and LAI_m is represented in Figure 98.

Current $NDVI_m$ and LAI_m reaches their minimum in January (2700 for NDVI and 2.3 for LAI). Both indices then slowly increase, following a sigmoid shape, reaching the annual maximum in June for $NDVI_m$ (7300), and July for LAI_m (30). $NDVI_m$ and LAI_m then decrease toward their respective January level. However, where LAI_m decrease in a sigmoid shape, $NDVI_m$ decrease is constant.

Figure 98 – Current seasonal variation of NDVI and LAI

Data averaged over the 2001-2019 period. ***In red:*** *NDVI$_m$.* ***In green:*** *LAI$_m$. Data source: NASA LP DAAC (Didan, 2015; Myneni et al., 2015).*

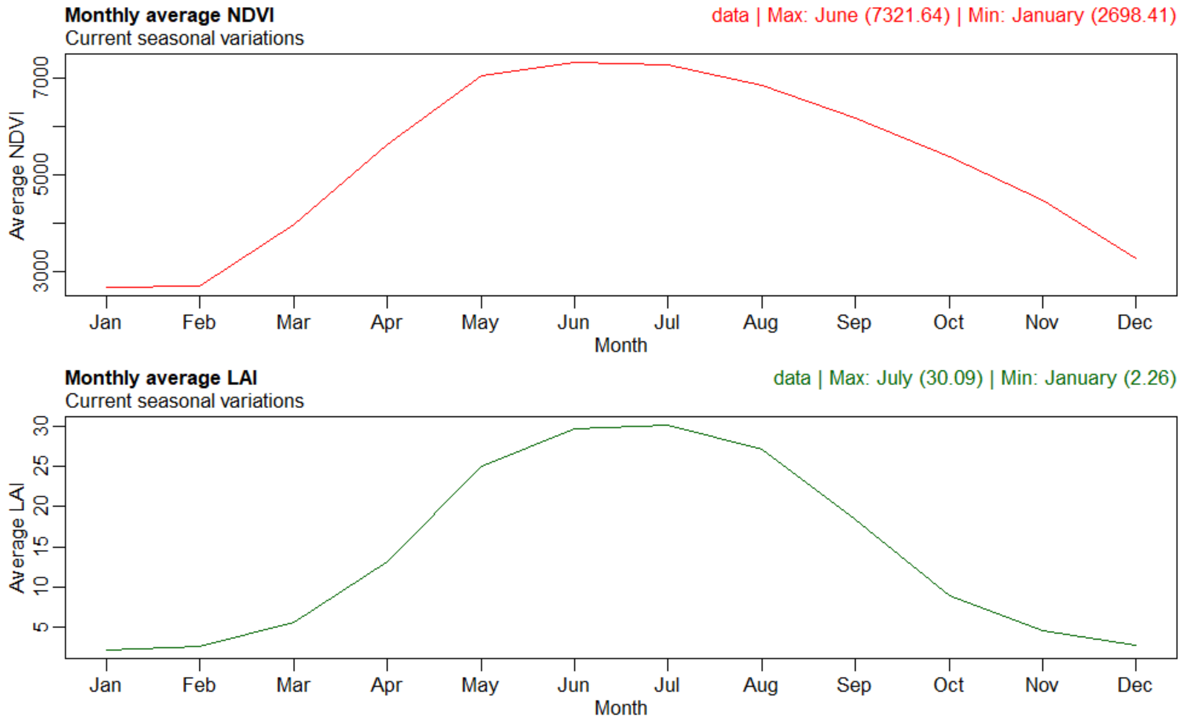

Spatial distribution

The seasonal spatial distribution of the LAI$_m$ and NDVI$_m$ throughout the Republic of Serbia can be observed in Figure 99.

LAI$_m$ and NDVI$_m$ stays higher on higher altitudes, where agriculture is less practical. At these altitudes, the presence of forest increases the two indexes. In terms of regionality, there is a clear difference between the North and the South of the Sava-Danube axis. To the South, the high altitudes and the presence of forests pushes the LAI$_m$ and NDVI$_m$ to higher values. There, the Morava rivers valleys are well defined as NDVI$_m$ and LAI$_m$ cold spots. To the North of the Sava-Danube axis, the NDVI$_m$ and LAI$_m$ stays low an evenly distributed, except in large urban centers such as the Belgrade area, where NDVI$_m$ and LAI$_m$ stays lower than elsewhere until June, and on top of the Fruška Gora range, where both Index are higher. From June to September, the harvesting is noticeable as patches of sharp decreases of NDVI$_m$ and LAI$_m$, starting from the Northeast.

Figure 99 – Spatial distribution of the current monthly average NDVI and LAI
Data averaged over the 2001-2019 period. <u>Data source:</u> NASA LP DAAC (Didan, 2015; Myneni et al., 2015).

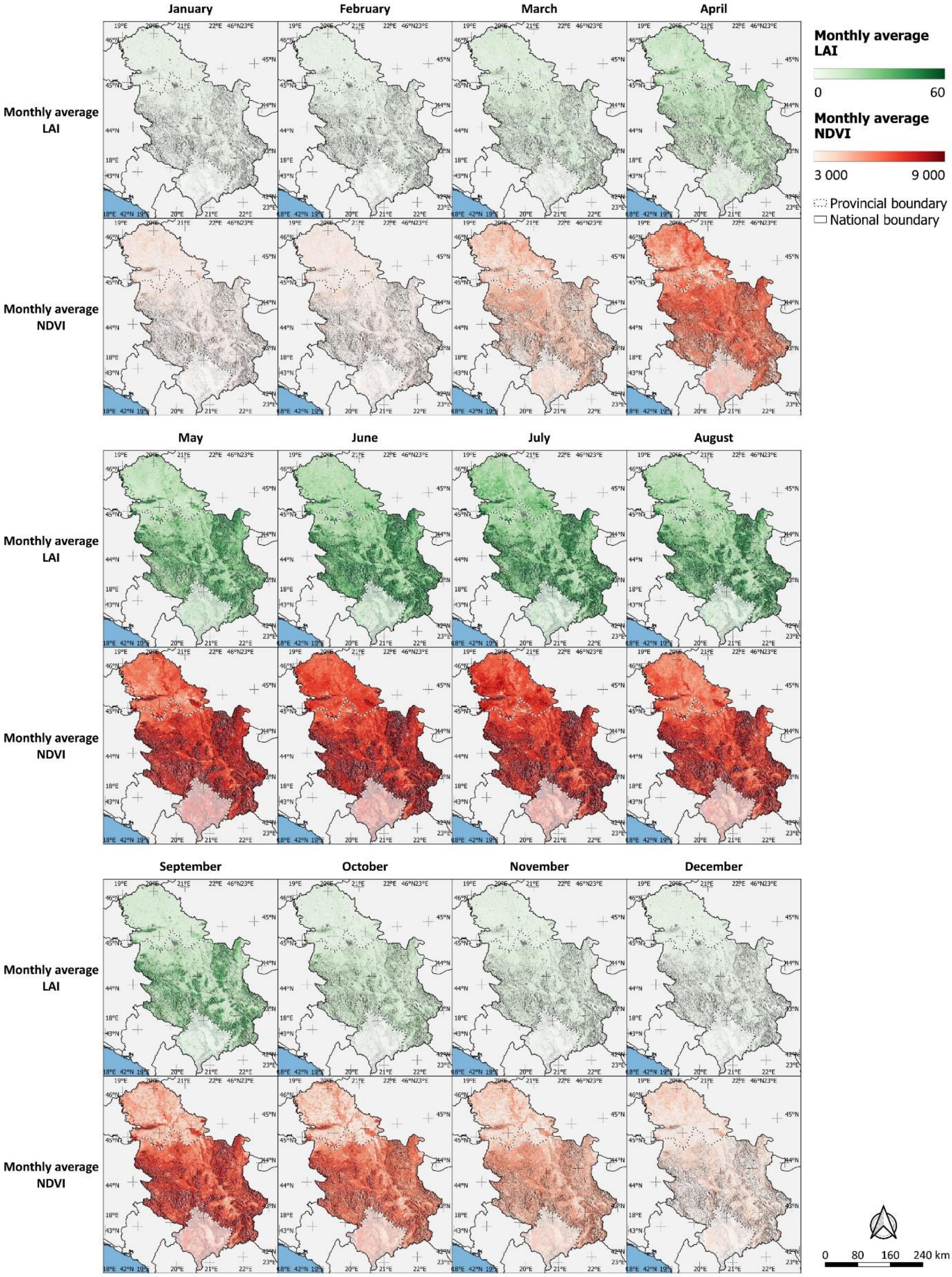

Historical monthly trends

The monthly past trends of $NDVI_m$ and LAI_m in the Republic of Serbia can be observed in Figure 100, Figure 101 and Table 36.

Figure 100 – Historical time series of the monthly average NDVI
Time series over 2001-2019 period. <u>Data source:</u> MODIS - NASA LP DAAC (Myneni et al., 2015).

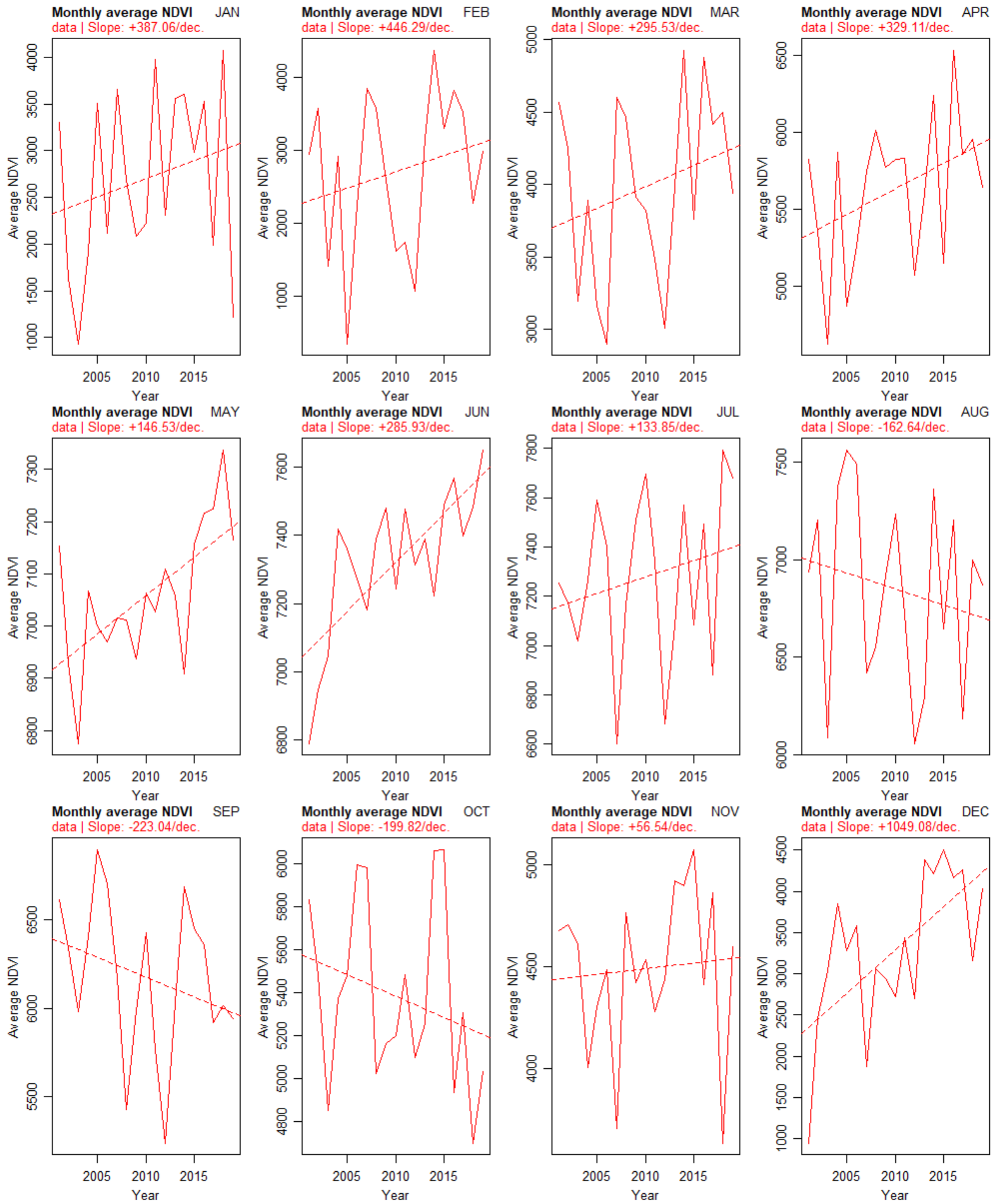

Figure 101 – Historical time series of the monthly average LAI

Time series over 2001-2019 period. Data source: MODIS - NASA LP DAAC (Didan, 2015).

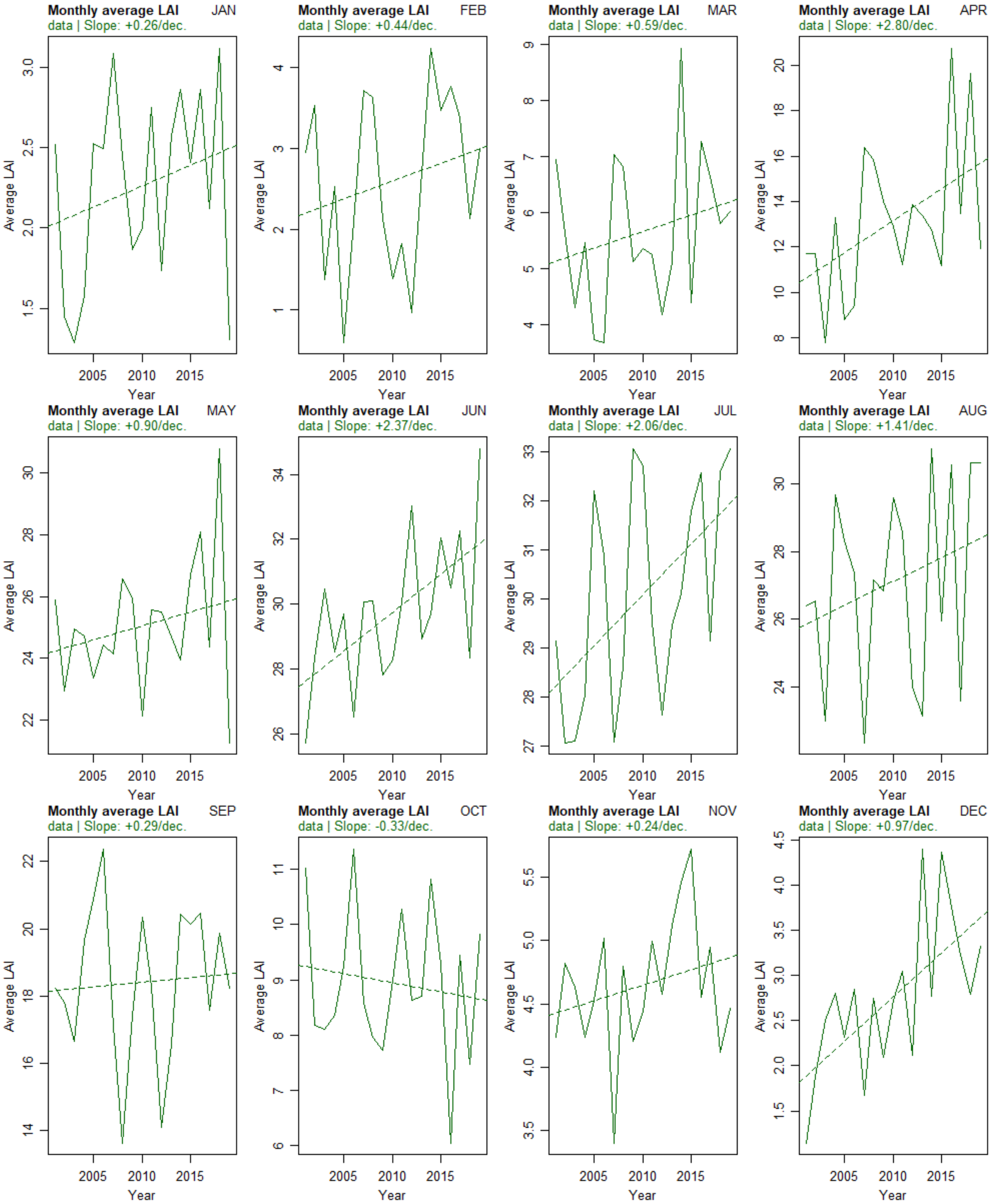

Table 36 – Characteristics of the trends from the historical time series of the monthly accumulated of frost days, ice days, and chill hours (linear models)

In green: *Monthly accumulated frost days.* ***In blue:*** *monthly accumulated ice days.* ***In red:*** *monthly accumulated chill hours. Data source: ERA5, ECMWF / Copernicus Climate Change Service (Muñoz Sabater, 2019).*

Variable	Month	Slope	p-value	Adjusted R^2	Average value in 1980	Average value in 2019
$NDVI_m$	January	+387.06/dec.	0.35	0.00	1537.23	3046.76
$NDVI_m$	February	+446.29/dec.	0.33	0.00	1365.71	3106.23
$NDVI_m$	March	+295.53/dec.	0.27	0.02	3095.84	4248.39
$NDVI_m$	April	+329.11/dec.	0.10	0.10	4649.23	5932.74
$NDVI_m$	May	+146.53/dec.	0.00	0.36	6619.71	7191.18
$NDVI_m$	June	+285.93/dec.	0.00	0.53	6463.84	7578.98
$NDVI_m$	July	+133.85/dec.	0.36	-0.01	6876.48	7398.51
$NDVI_m$	August	-162.64/dec.	0.44	-0.02	7337.28	6702.98
$NDVI_m$	September	-223.04/dec.	0.23	0.03	6846.12	5976.26
$NDVI_m$	October	-199.82/dec.	0.28	0.01	5984.04	5204.74
$NDVI_m$	November	+56.54/dec.	0.74	-0.05	4321.91	4542.43
$NDVI_m$	December	+1049.08/dec.	0.00	0.37	148.03	4239.45
LAI_m	January	+0.26/dec.	0.31	0.01	1.48	2.50
LAI_m	February	+0.44/dec.	0.33	0.00	1.28	3.00
LAI_m	March	+0.59/dec.	0.32	0.00	3.91	6.20
LAI_m	April	+2.80/dec.	0.04	0.18	4.77	15.68
LAI_m	May	+0.90/dec.	0.33	0.00	22.35	25.87
LAI_m	June	+2.37/dec.	0.01	0.33	22.64	31.88
LAI_m	July	+2.06/dec.	0.02	0.24	23.92	31.95
LAI_m	August	+1.41/dec.	0.25	0.02	22.88	28.39
LAI_m	September	+0.29/dec.	0.77	-0.05	17.55	18.67
LAI_m	October	-0.33/dec.	0.57	-0.04	9.93	8.65
LAI_m	November	+0.24/dec.	0.28	0.01	3.92	4.87
LAI_m	December	+0.97/dec.	0.00	0.39	-0.15	3.64

$NDVI_m$ present a clear temporal dichotomy in terms of temporal evolution.

During the months of November to July, $NDVI_m$ seem to increase. In terms of critical months, the largest increase in $NDVI_m$ can be observed for the months of December (+1049/decade), February (+446/decade) and January (+387/decade). However, at the end of summer, August to October, the NDVI seem to decrease. This decrease in the $NDVI_m$ of the end of the summer could be explained by water stress at the end of the growth season.

LAI_m on its part present a more constant variation. Overall, most of the months shows an increase in LAI_m. In terms of critical months, the largest increase in LAI_m can be observed for the months of April (+2.8/decade), June +2.4/decade) and July +2.0/decade).

Historical annual trends

Historical annual trends on NDVI, LAI and vegetation productivity can be observed in Figure 102 and Table 37.

Figure 102 – Historical time series of the annual average NDVI, LAI and vegetation productivity
Time series over 2001-2019 period. ***In red:*** *$NDVI_y$.* ***In green:*** *LAI_y.* ***In blue:*** *VPy. Data source: MODIS - NASA LP DAAC (Didan, 2015; Myneni et al., 2015) and European Environment Agency (EEA) (European Environment Agency (EEA), March-21-2021).*

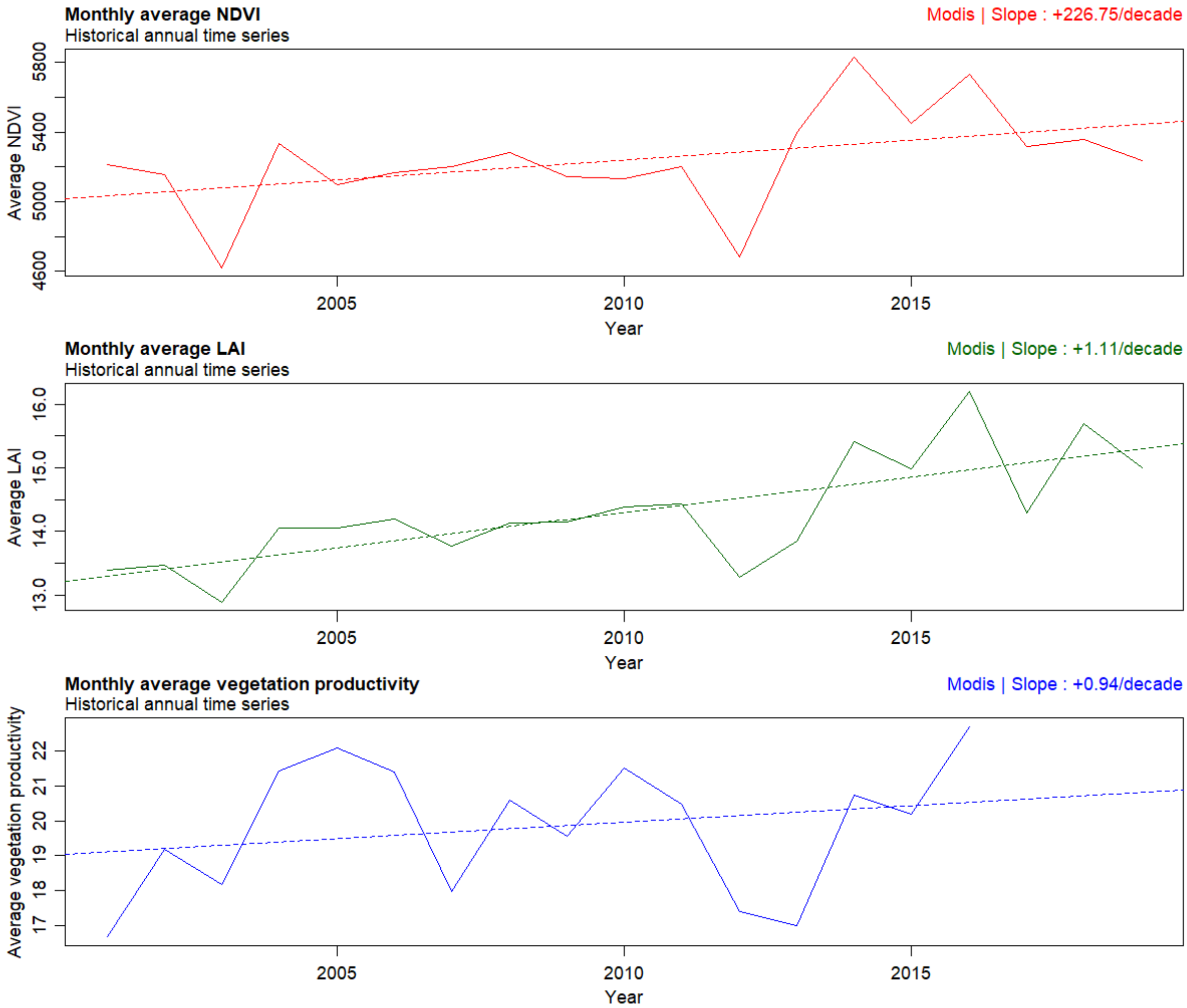

Overall, all the vegetation indices show a steady increase since 2001 ($NDVI_y$: +227/decade, LAI_y: +1.1/decade, VP: +1.0/decade). It is worth noticing that the very dry year of 2012 is very noticeable on every index's time series as a brutal decrease of the index on that year.

Table 37 – Characteristics of the trend from historical data for annual average NDVI, LAI, and vegetation productivity (linear models)
Data source: MODIS - NASA LP DAAC (Didan, 2015; Myneni et al., 2015) and European Environment Agency (EEA) (European Environment Agency (EEA), March-21-2021).

Variable	Slope	p-value	Adj. R^2	Average value in 1980	Average value in 2019
$NDVI_y$	+226.75/decade	0.05	0.16	4559.58	5443.92
LAI_y	+1.11/decade	0.00	0.51	10.98	15.29
VP	+0.94/decade	0.38	-0.01	17.14	20.80

Spatial distribution

The historical decadal spatial distribution of $NDVI_y$, LAI_y and VP over the period 2001-2019 throughout the Republic of Serbia can be observed in Figure 103.

Figure 103 – Historical decadal spatial distribution of annual average NDVI, LAI and vegetation productivity
Data averaged over the 2001-2019 period, by decade. Data source: MODIS - NASA LP DAAC (Didan, 2015; Myneni et al., 2015) and European Environment Agency (EEA) (European Environment Agency (EEA), March-21-2021)

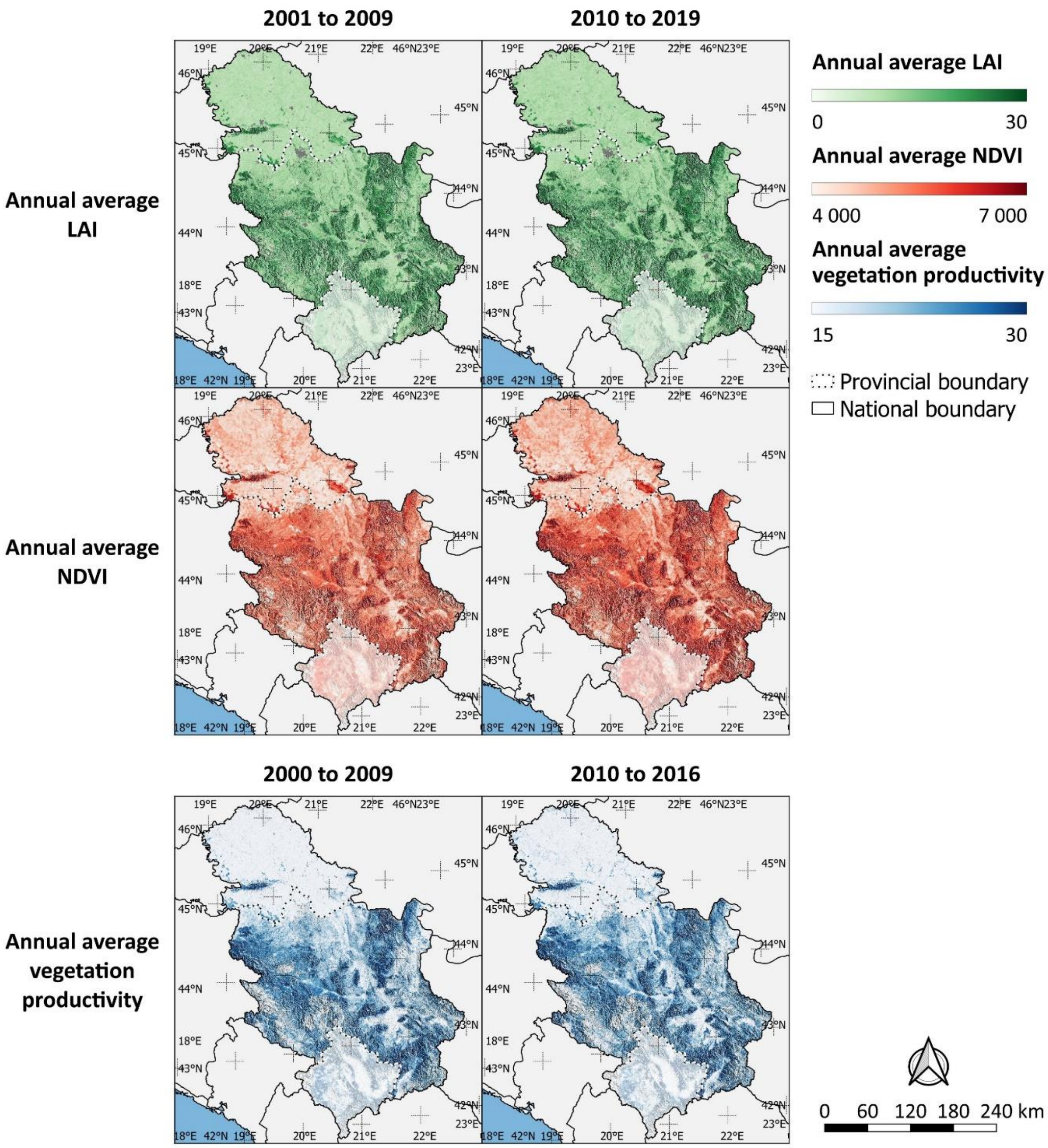

The distribution of the selected vegetation indices stayed constant during the study period, with higher values on the higher altitudes, and lower values at lower altitudes.

Conclusion

Current $NDVI_m$ and LAI_m reaches their minimum in January, and slowly increase to June and July, before decreasing again. Historically $NDVI_y$, LAI_y and VP increased steadily during the last 40 years. This overall increase seems to be constant throughout the year for LAI_m. For $NDVI_m$ the increase is shown to be more seasonal, with an increase from November to July, and a decrease from August to October.

17. Start and length of the growing season

This section will present two growth season variables in the Republic of Serbia. These variables are:

- **Start date of the growing season** (GS): Day of the year when vegetation starts to grow (calculated by the European Environment Agency based on the Plant Phenology Index (European Environment Agency (EEA), March-21-2021)).
- **Length of the growing season** (GL): Timespan between the start of the growing season and the end of the growing season (calculated by the European Environment Agency based on the Plant Phenology Index (European Environment Agency (EEA), March-21-2021)).

These two variables are only defined annually. Therefore, the trend analysis will only be conducted at a yearly scale.

Historical annual trends

Historical annual trends on growing season variables can be observed in Figure 104 and Table 38.

Figure 104 – Historical time series of start date and length of the growing season
Time series over 2001-2016 period. ***In red:*** *start date of growing season.* ***In green:*** *length of the growing season.*
Data source: European Environment Agency (EEA) (European Environment Agency (EEA), March-21-2021).

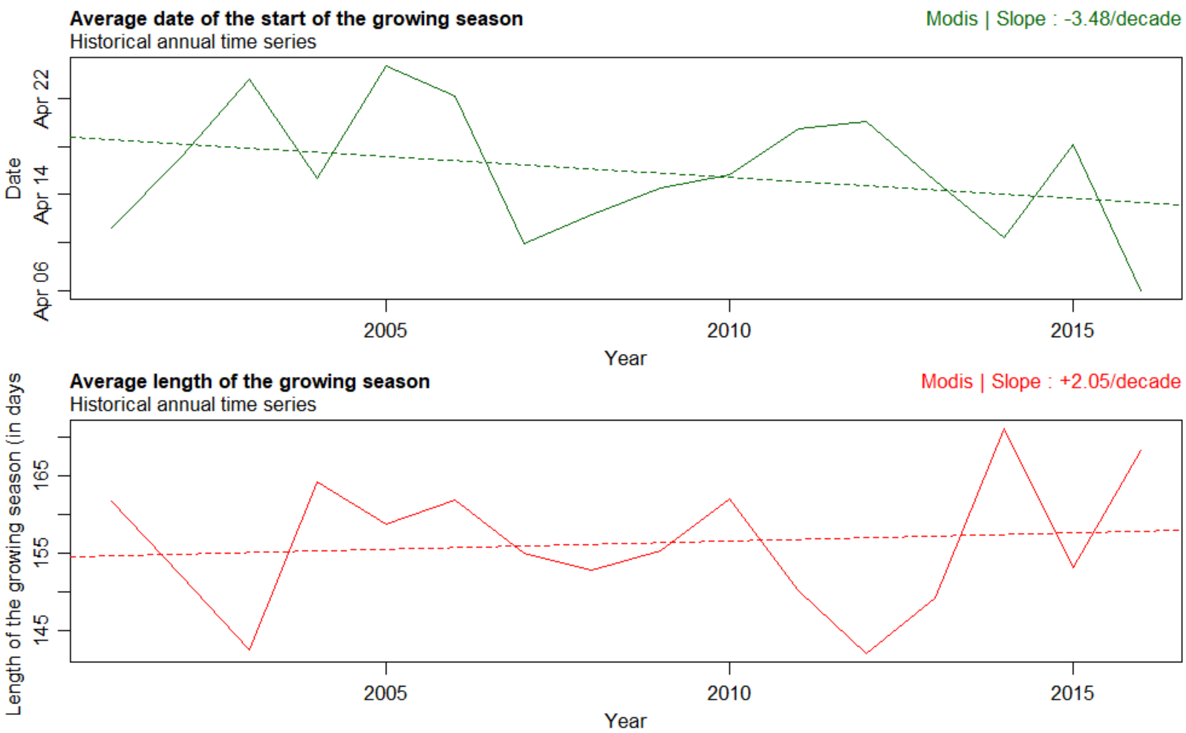

Although a slow decrease in the start date of growing season (around -3 days/decade) and a slow increase in the length of growing season (about +2 days/decade) can be observed, the very high year to year variability of both index makes these trends debatable (p>>0.05; adj. R^2 close to 0). The growing season in the Republic of Serbia Starts on average around the 14th of April, and last for about 155 days.

Table 38 – Historical trends characteristics for start date and length of the growing season (linear models)
Time series over 2001-2016 period. Data source: European Environment Agency (EEA) (European Environment Agency (EEA), March-21-2021).

Variable	Slope	p-value	Adj. R^2	Average value in 1980	Average value in 2019
GS	-3.48/decade	0.24	0.03	115.26	101.67
GL	+2.05/decade	0.67	-0.06	150.44	158.46

Spatial distribution

The historical decadal spatial distribution of GS, and GL over the period 2001-2016 throughout the Republic of Serbia can be observed in Figure 105.

Figure 105 – Historical spatial distribution of start date and length of the growing season
Data averaged over the 2001-2010 and 2010-2016 periods. Data source: European Environment Agency (EEA) (European Environment Agency (EEA), March-21-2021).

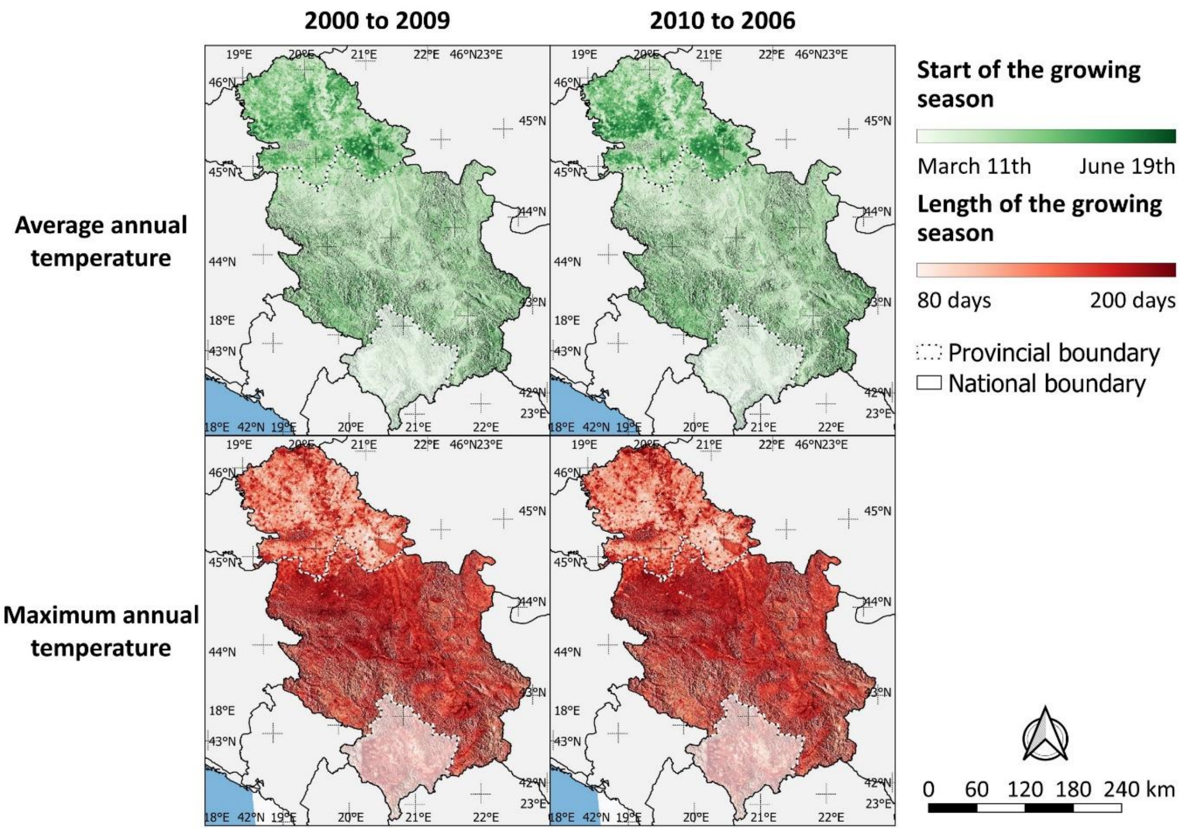

There is a clear dichotomy between the North and the South of the country. To the South of the Sava-Danube axis, both variables are evenly distributed, with a slight later start (a shorter length) of growing season at higher altitude. To the North of the country, the land is mainly dedicated to agriculture and thus the growing season is strongly related to the crop calendar. Hence, depending on the type of agriculture or the agricultural methods, the start and length of growing season can vary from parcel to parcel. Therefore, the distribution of the two variables is aggregated in patches of different values, depending on the type of agricultural practices. Finally, the distribution of the growing season variable didn't change noticeably between the two periods observed.

Conclusion

The growing season in the Republic of Serbia Starts on average around the 14th of April, and last for about 155 days. Between 2001 and 2016, these values didn’t change significatively. The Growing season starts later and last for a shorter period of time in the North of the Sava-Danube axis, where most of the agriculture is concentrated.

BIBLIOGRAPHY

Center for International Earth Science Information Network - CIESIN - Columbia University, 2018. Gridded Population of the World, Version 4 (GPWv4): Population Density Adjusted to Match 2015 Revision UN WPP Country Totals, Revision 11.

Didan K., 2015. MOD13A1 MODIS/Terra Vegetation Indices 16-Day L3 Global 500m SIN Grid V006. *Distrib. by NASA EOSDIS L. Process. DAAC*. https://doi.org/10.5067/MODIS/MOD13A1.006. Accessed 2021-06-24, (21/03/2021).

Duscher K., Günther A., Richts A., Clos P., Philipp U. & Struckmeier W., 2015. The GIS layers of the "International Hydrogeological Map of Europe 1:1,500,000" in a vector format. *Hydrogeol. J.* **23**(8).

European Commission Joint Research Centre, March-21-2021. European Soil Data Centre (ESDAC). esdac.jrc.ec.europa.eu, (21/03/2021).

European Environment Agency, March-20-2021. Vegetation Productivity. https://www.eea.europa.eu/ds_resolveuid/IND-480-en, (20/03/2021).

European Environment Agency (EEA), March-21-2021. Vegetation growing season variables. https://www.eea.europa.eu/data-and-maps/data/annual-start-of-vegetation-growing, (21/03/2021).

European Environmnet Agency (EEA), 2020. Copernicus Land Monitoring Service 2020. https://land.copernicus.eu/global/

Farr T.G., Rosen P.A., Caro E., Crippen R., Duren R., Hensley S., Kobrick M., Paller M., Rodriguez E., Roth L., Seal D., Shaffer S., Shimada J., Umland J., Werner M., Oskin M., Burbank D. & Alsdorf D.E., 2007. The shuttle radar topography mission. *Rev. Geophys.* **45**(2).

Hengl T., 2018. Sand content in % (kg / kg) at 6 standard depths (0, 10, 30, 60, 100 and 200 cm) at 250 m resolution.

Hengl T. & Gupta S., 2019. Soil water content (volumetric %) for 33kPa and 1500kPa suctions predicted at 6 standard depths (0, 10, 30, 60, 100 and 200 cm) at 250 m resolution.

Muñoz Sabater J., 2019. ERA5-Land hourly data from 1981 to present. *Copernicus Clim. Chang. Serv. Clim. Data Store*.

Myneni R., Knyazikhin Y. & Park T., 2015. MCD15A2H MODIS/Terra+Aqua Leaf Area Index/FPAR 8-day L4 Global 500m SIN Grid V006. 2015. *Distrib. by NASA EOSDIS L. Process. DAAC*. https://doi.org/10.5067/MODIS/MCD15A2H.006, (21/03/2021).

Nachtergaele F., Van Velthuizen H., Verelst L., Batjes N., Dijkshoorn K., Van Engelen V., Fischer G., Jones A., Montanarella L., Petri M., Prieler S., Shi X., Teixeira E. & Wiberg D., 2010. The harmonized world soil database (August), 34–37.

OpenStreetMap Contributors, 2020. OpenStreetMap (OSM). *OpenStreetMap Found.*

Panagos P., Van Liedekerke M., Jones A. & Montanarella L., 2012. European Soil Data Centre: Response to European policy support and public data requirements. *Land use policy* **29**(2), 329–338.

Pekel J.-F., Cottam A., Gorelick N. & Belward A.S., 2016. High-resolution mapping of global surface water and its long-term changes. *Nature* **540**(7633), 418–422.

Rajkovic B., Vujadinovic M. & Vukovic A., 2013. Report on revisited climate change scenarios including review on applied statistical method for removing of systematic model errors, with maps of temperature, precipitation and required climate indices changes, MERZ, Belgrade, Serbia.

Republic Hydrometeorological Service of Serbia, 2020. Meteorological yearbooks. *Meteorol. Yearb.*

http://www.hidmet.gov.rs/ciril/meteorologija/klimatologija_godisnjaci.php%0A

Rodell M., Houser P.R., Jambor U., Gottschalck J., Mitchell K., Meng C.J., Arsenault K., Cosgrove B., Radakovich J., Bosilovich M., Entin J.K., Walker J.P., Lohmann D. & Toll D., 2004. The Global Land Data Assimilation System. *Bull. Am. Meteorol. Soc.* **85**(3), 381–394.

Running S., Mu Q. & Zhao M., 2021. MODIS/Terra Net Evapotranspiration 8-Day L4 Global 500m SIN Grid V061 [Data set]. *NASA EOSDIS L. Process. DAAC*. https://doi.org/10.5067/MODIS/MOD16A2.061%0A, (21/03/2021).

Srbijavode, 2020. Srbijavode GIS Portal. https://geoportal.srbijavode.rs/visios/Portal

Statistical Office of the Republic of Serbia, 2012. Census of Agriculture. https://www.stat.gov.rs/en-us/

Statistical Office of the Republic of Serbia, 2018. Farm Structures Survey. https://www.stat.gov.rs/en-us/

Statistical Office of the Republic of Serbia, 2020. Statistical Office of the Republic of Serbia. https://www.stat.gov.rs/

Taylor K.E., Stouffer R.J. & Meehl G.A., 2012. An overview of CMIP5 and the experiment design. *Bull. Am. Meteorol. Soc.* **93**(4), 485–498.

Thrasher B., Maurer E.P., McKellar C. & Duffy P.B., 2012. Technical Note: Bias correcting climate model simulated daily temperature extremes with quantile mapping. *Hydrol. Earth Syst. Sci.* **16**(9), 3309–3314.

USDA, March-19-2021. Hardiness Zones. https://planthardiness.ars.usda.gov/PHZMWeb/, (19/03/2021).

World Bank, 2020. World Bank Data: Population. *World Bank Data Website*.

ANNEXES

Municipality ID reference table

Municipality Name	ID number	Municipality Name	ID number	Municipality Name	ID number
Ivanjica	1	Ub	58	Belgrade - Rakovica	115
Kladovo	2	Crna Trava	59	Belgrade - Savski venac	116
Knić	3	Čajetina	60	Belgrade - Sopot	117
Knjaževac	4	Čačak	61	Belgrade - Stari grad	118
Kosjerić	5	Šabac	62	Belgrade - Čukarica	119
Koceljeva	6	Lapovo	63	Blace	120
Kragujevac	7	Niš - Niška Banja	64	Bogatić	121
Kraljevo	8	Belgrade - Surčin	65	Bojnik	122
Krupanj	9	Niš - Pantelej	66	Temerin	123
Kruševac	10	Niš - Crveni Krst	67	Titel	124
Kuršumlija	11	Niš - Palilula	68	Vrbas	125
Kučevo	12	Niš - Medijana	69	Čoka	126
Lajkovac	13	Kostolac	70	Šid	127
Lebane	14	Vranjska Banja	71	Petrovaradin	128
Leskovac	15	Sevojno	72	Boljevac	129
Loznica	16	Ada	73	Bor	130
Lučani	17	Alibunar	74	Bosilegrad	131
Ljig	18	Apatin	75	Brus	132
Ljubovija	19	Bač	76	Bujanovac	133
Majdanpek	20	Bačka Palanka	77	Valjevo	134
Mali Zvornik	21	Bačka Topola	78	Varvarin	135
Malo Crniće	22	Bački Petrovac	79	Velika Plana	136
Medveđa	23	Bela Crkva	80	Veliko Gradište	137
Merošina	24	Beočin	81	Vladimirci	138
Mionica	25	Bečej	82	Vladičin Han	139
Negotin	26	Vršac	83	Vlasotince	140
Nova Varoš	27	Žabalj	84	Vranje	141
Novi Pazar	28	Žitište	85	Vrnjačka Banja	142
Osečina	29	Zrenjanin	86	Gadžin Han	143
Paraćin	30	Inđija	87	Golubac	144
Petrovac na Mlavi	31	Irig	88	Gornji Milanovac	145
Pirot	32	Kanjiža	89	Despotovac	146
Požarevac	33	Kikinda	90	Dimitrovgrad	147
Požega	34	Kovačica	91	Doljevac	148
Preševo	35	Kovin	92	Žabari	149
Priboj	36	Kula	93	Žagubica	150
Prijepolje	37	Mali Iđoš	94	Žitorađa	151
Prokuplje	38	Nova Crnja	95	Zaječar	152
Ražanj	39	Novi Bečej	96	Aleksandrovac	153
Rača	40	Novi Kneževac	97	Aleksinac	154
Raška	41	Novi Sad	98	Arandjelovac	155
Rekovac	42	Opovo	99	Arilje	156
Jagodina	43	Odžaci	100	Babušnica	157
Svilajnac	44	Pančevo	101	Bajina Bašta	158
Svrljig	45	Pećinci	102	Batočina	159
Sjenica	46	Plandište	103	Bela Palanka	160
Smederevo	47	Ruma	104	Belgrade - Barajevo	161
Smederevska Palanka	48	Senta	105	Belgrade - Voždovac	162
Sokobanja	49	Sečanj	106	Belgrade - Vračar	163
Surdulica	50	Sombor	107	Belgrade - Grocka	164
Užice	51	Srbobran	108	Belgrade - Zvezdara	165
Topola	52	Sremska Mitrovica	109	Belgrade - Zemun	166
Trgovište	53	Sremski Karlovci	110	Belgrade - Lazarevac	167
Trstenik	54	Stara Pazova	111	Belgrade - Mladenovac	168
Tutin	55	Subotica	112	Belgrade - Novi Beograd	169
Ćićevac	56	Belgrade - Obrenovac	113		
Ćuprija	57	Belgrade - Palilula	114		

Definition of variables

Variable	Acronym	Definition	Unit	Chapter
Daily minimum temperature	TN	Daily minimum temperature within the selected area	°C	8
Daily maximum temperature	TN	Daily maximum temperature within the selected area	°C	8
Daily accumulated precipitation	RR	Daily accumulated precipitation within the selected area	mm	8
Monthly minimum of the daily minimum temperature	TNn	Minimum of the daily minimum temperature during the considered month	°C	8
Monthly minimum of the daily maximum temperature	TXn	Minimum of the daily maximum temperature during the considered month	°C	8
Monthly maximum of the daily minimum temperature	TNx	Maximum of the daily minimum temperature during the considered month	°C	8
Monthly maximum of the daily maximum temperature	TXx	Maximum of the daily maximum temperature during the considered month	°C	8
Frost Days	FD	Let TN_{ij} be the minimum temperature on day i of the period j. Count the number of days where $TN_{ij} < 0°C$	Days	9
Ice Days	ID	Let TX_{ij} be the maximum temperature on day i of the period j. Count the number of days where $TX_{ij} < 0°C$	Days	9
Summer Days	SD	Let TX_{ij} be the maximum temperature on day i of the period j. Count the number of days where $TX_{ij} > 25°C$	Days	9
Tropical Nights	TrN	Let TN_{ij} be the minimum temperature on day i of the period j. Count the number of days where $TN_{ij} > 20°C$	Days	9
Chill hours	CH	Let TH_{ij} be the average temperature on hour i of the period j. Count the number of days where $TH_{ij} < 0°C$	Days	9
Daily precipitation intensity	RRx	Let be Pwj be the daily precipitation amount on wet days (P>= 1mm) in the period j. if WD represents the number wet days in j, then: $$Pint = \sum_{W=1}^{W} P_{wj}/W$$	mm	10

Variable	Acronym	Definition	Unit	Chapter
Wet day	WD	Let P_{ij} be the daily precipitation amount on day i in period j. Count the number of days where $P_{ij} > 1mm$	days	10
Very wet day	VWD	Let P_{ij} be the daily precipitation amount on a wet day w (P≥1mm) in period i and $P_{wT}95$ be the 95th percentile of daily precipitation during the 1980-2020 period. If W represents the number of wet days in the period, then: $$VWD = \sum_{W=1}^{W} P_{Wi}, where\ P_{Wi} > P_{WT}95$$	days	10
Longest dry spell	DS	Let Rij be the daily precipitation amount on day i in period j. Count the largest number of consecutive dayys where P_{ij}<1mm.	days	10
Accumulated snow fall	SnF	Daily accumulated snow precipitation within the selected area, in mm of water equivalent.	mm	11
Average snow depth	SnD	Daily mean depth of the layer of snow in a selected area, in mm of water equivalent.	mm	11
Water Deficit	Wdef	Difference between the measured evapotranspiration (ET), and potential evapotranspiration (PET).	mm	12
Degree days	DD	Let TG_{ij} be the daily average temperature of the day i period j. Then: $$DD = \sum_{i=1}^{i} (TG_{ij} - 10)\ where\ TG_{ij} > 10$$	Days	13
Hardiness Zones	HZ	Let TNn_i the annual minimum temperature of the year i. Then Hardiness level of the zone for the year i is the range corresponding to Tnni. The ranges are defined in (USDA, March-19-2021)	No unit	14
Leaf Area Index	LAI	Ratio of canopy cover area to area of the zone	No unit	15
Normalize Difference Vegetation Index	NDVI	Let be R and NIR the spectral reflectance measurements acquired in the red and near-infrared regions, respectively. Then: $$NDVI = \frac{NIR - R}{NIR + R}$$	No unit	15
Vegetation Productivity	VP	The vegetation productivity as defined in (European Environment Agency, March-20-2021)	No unit	15

Variable	Acronym	Definition	Unit	Chapter
Start of the growing season	GS	The start of the growing season as defined in (European Environment Agency (EEA), March-21-2021)	Date	16
Length of the growing season	GL	The length of the growing season as defined in (European Environment Agency (EEA), March-21-2021)	Days	16